BETWEEN DESTINY AND DISEASE: GENETICS AND MOLECULAR PATHWAYS OF CENTRAL NERVOUS SYSTEM AGING

By

Christin Ann Glorioso

B.S., University of Michigan, 2002

Submitted to the Graduate Faculty of

The Center for Neuroscience in partial fulfillment

of the requirements for the degree of Doctor of Philosophy

University of Pittsburgh

2010

UNIVERSITY OF PITTSBURGH

SCHOOL OF MEDICINE

This thesis was presented

by

Christin Ann Glorioso

It was defended on

March 17, 2010

and approved by

Dr. Michael Zigmond, Professor, Neurology and psychiatry

Dr. Charles Bradberry, Associate professor, Psychiatry

Dr. Gonzalo Torres, Assistant professor, Neurobiology

Dr. Peter Gianaros, Assistant professor, psychiatry and psychology

Dr. Stuart Kim, Professor, Developmental biology and genetics

Thesis Advisor: Dr. Etienne Sibille, Associate professor, Psychiatry

BETWEEN DESTINY AND DISEASE: GENETICS AND MOLECULAR PATHWAYS OF CNS AGING

Christin Ann Glorioso, Ph.D.

University of Pittsburgh, 2010

Human brain aging is associated with robust “normal” functional, structural, and molecular changes that underlie changes in cognition, memory, mood and motor function, amongst other processes. Normal aging is also a requirement for onset of many neurological diseases, ranging from later onset neurodegenerative diseases such as Alzheimer’s(AD) and Parkinson’s diseases(PD), to earlier onset psychiatric disorders such as bipolar disorder(BPD) and schizophrenia(SCHZ). Understanding the molecular mechanisms and genetic underpinnings of normal age-related brain changes would have profound consequences for prevention and treatment of age-related impairments and disease. Here I introduce current knowledge of these functional changes, their structural and molecular underpinnings, their genetic modulators, and the contribution of normal aging to age-related neurological disease. I then present my contribution to this field in the form of three papers on genetic modulation of mammalian brain molecular aging. These studies demonstrate and investigate mechanisms underlying the causal modulation of molecular brain aging rates by Brain Derived Neurotrophic Factor (BDNF) and Serotonin (5-HT) in knock-out (KO) mice, and associative modulation by the putative longevity gene, Sirtuin 5, in humans (novel low-expressing promoter polymorphism ($Sirt5_{prom2}$)). In humans we additionally investigate the potential mechanism(s) underlying neurological disease gating by normal aging, providing supporting evidence for molecular aging being a genetically controlled “transcriptional program” that progressively promotes age-regulated neurological diseases. In the discussion, I place these studies in a broader context within the field, detailing their implications and future directions.

TABLE OF CONTENTS

LIST OF TABLES

LIST OF FIGURES

PREFACE

I would like to express my gratitude to everyone who has supported and inspired me in my scientific training. First I would like to thank my thesis advisor, Dr. Etienne Sibille, who not only allowed me the freedom to pursue my own ideas but met them with enthusiasm. Additionally, he patiently guided me through the process of learning to write and present scientifically, which are invaluable contributions to my future career. The Sibille lab is uniquely forward-thinking and cutting edge, combining techniques and expertise from a variety of disciplines from genomics to computer modeling to behavior. I believe this type of approach is necessary to understand the complex polygenic processes and diseases that are our focus. I am excited to see the important discoveries that will inevitably arise from the lab in the future.

I would next like to thank the University of Pittsburgh Medical Scientist Training Program for giving me the opportunity to train to become a physician-scientist in such a high quality and enjoyable environment. In addition to the program's rigor and richness for both clinical and scientific training, some of my favorite people to interact with are Pitt MSTP students and faculty.

I would next like to thank the members of my committee, Drs. Charlie Bradberry, Pete Gianaros, Michael Zigmond, Gonazalo Torres, and Stuart Kim for offering helpful advice and being extremely supportive. I am particularly grateful for the mentorship of my committee chair and NRSA co-sponsor, Dr. Michael Zigmond, whose emphasis on polish and professionalism has improved my grantsmanship and presentations. Additionally, his enthusiastic interest in my project has helped to shape my scientific thinking and encouraged me to be confident in my work.

Additionally, I would like to offer special thanks to my outside examiner, Dr. Stuart Kim, who has already been a big influence and source of encouragement in my short career. I first met Dr. Kim when I was invited to give a short presentation following his keynote presentation at the 2008 "molecular mechanisms of aging and age related disease" conference. As I sat on the edge of my seat during his talk, I quickly realized

that his ideas were similar in nature to my own. While his data were in the worm and mine in human, we were both convinced that aging is a program extending from development. While currently this paradigm is not popular, I am convinced that it will be widely accepted in the future. I am grateful to Dr. Kim for his support and guidance and for taking time out of his busy schedule to come to Pittsburgh for my defense.

Importantly, I have been very fortunate to have a loving family who has always believed in and encouraged me. Most obviously, my father has been an immeasurable influence on my scientific career, from asking me to consider scientific questions as a child, to taking me to conferences, to believing in my abilities and expecting me to be courageous and succeed. His belief in having big goals, perseverance, and independent thinking have shaped my outlook and been a large part of my successes. My mother has also been a large influence in my life. She has been an important role model of a successful professional woman and has always been supportive of my career. She is one of my biggest champions, tirelessly helping me through worst times as well as celebrating the best times. I am additionally very grateful to my sister and best friend, Alexandra 'Boo' Glorioso, who has been a sounding board for and invaluable help in working through problems big and small, and is one of my favorite people to celebrate life's victories with. I couldn't imagine doing this without her. Additionally, I want to thank the newest members of my immediate family, Paola and Leo, for making my world brighter and helping me to celebrate.

I also want to thank all of my friends who have been an essential part of my experience in graduate school. I always look forward to free nights spent reflecting on and enjoying life with them; great times. Lastly, I want to thank my boyfriend, Ben Musher, who has been wonderful and made these last few months probably the most fun ever had writing a thesis.

INTRODUCTION

"Normal" brain aging is understudied compared with peripheral aging and has many fundamentally different mechanisms and modulators, which are intrinsic to the onset and progression of age-related declines and neurological diseases. Some mechanisms, such as those related to insulin signaling and cellular insult are shared between the periphery and brain; however, mechanisms related to cellular turnover and depletion, such as telomere shortening and senescence, are not as pertinent in the largely non-dividing brain. Instead, progressive morphological and molecular changes within life-long existing neurons and glia likely underlie age-related cognitive, motor, and mood changes and disease susceptibility (see Figure 1). Brain aging also has many unique genetic modulators such as neurotransmitters, neurotrophins, and neurological disease-related genes (see Figure 1). Here I introduce current knowledge of functional correlates of brain aging and then progressively discuss their putative underpinnings, starting with gross structural and functional, then cellular, then molecular and finally genetic modulators. Lastly, I introduce the overlap between and contribution of normal brain aging to age-gated neurological disease.

Figure 1. Overarching schema. "Normal" age-related molecular changes in neurons and glia: putative modulators, mediators and consequences.

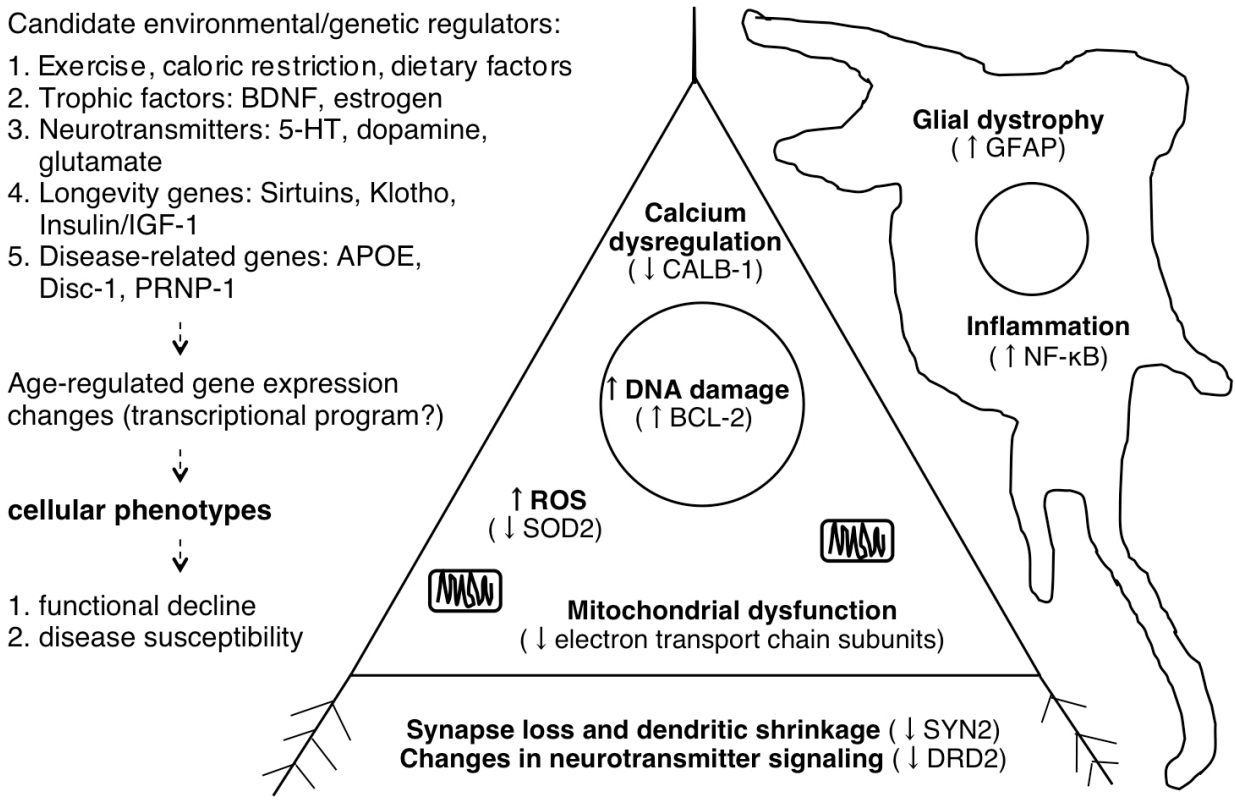

Figure 1. Known age-related cellular phenotypes are in bold in neurons (left) and glia (right). Many neuronal phenotypes (such as DNA damage) also occur in glia but are not depicted here for clarity. In parentheses are single representative examples (amongst many) of age-regulated gene expression changes seen by human brain microarray that may contribute to/underlie a particular cellular phenotype.

I.A.i Normal age-related changes in cognition, motor function, and affect.

Normal age-related declines in neurological functioning have been extensively studied and are robust and consistent. Meta-analysis of cross-sectional and longitudinal datasets have demonstrated a 40-60% decline in cognitive speed at age 80 from age 20 in non-demented adults (1, 2). Aging differentially affects aspects of neurological functioning (1, 3-5). “Fluid abilities” or those reliant on processing speed, problem solving, inhibitory function, working memory, long-term memory and spatial ability, decline with age (see Figure 2 (1, 2, 6)). In fact, performance IQ (reliant primarily on fluid abilities) measured by the Welchsler test drops on average 30 points from age 20 to age 70 (2, 7). In contrast, so-called “crystallized abilities” related to knowledge or expertise such as vocabulary, world knowledge, general knowledge, implicit memory, understanding proverbs, and occupational expertise do not decline or even show improvement over the lifespan (see Figure 2, reviewed in (1, 4, 6)). Consistent with this, verbal IQ measured in WAIS-R standardization sample only drops on average only 5 points from age 20 to age 70 (2, 8). Importantly, selectively affected cognitive changes follow the same continuous and progressive pattern starting in the 20s and continuing through old age as grey matter volume loss and molecular changes, which may underlie these functional changes (9).

Figure 2. Differential effects of aging on cognitive processes.
(adapted from Park DC, Reuter Lorenz P. 2009 (6))

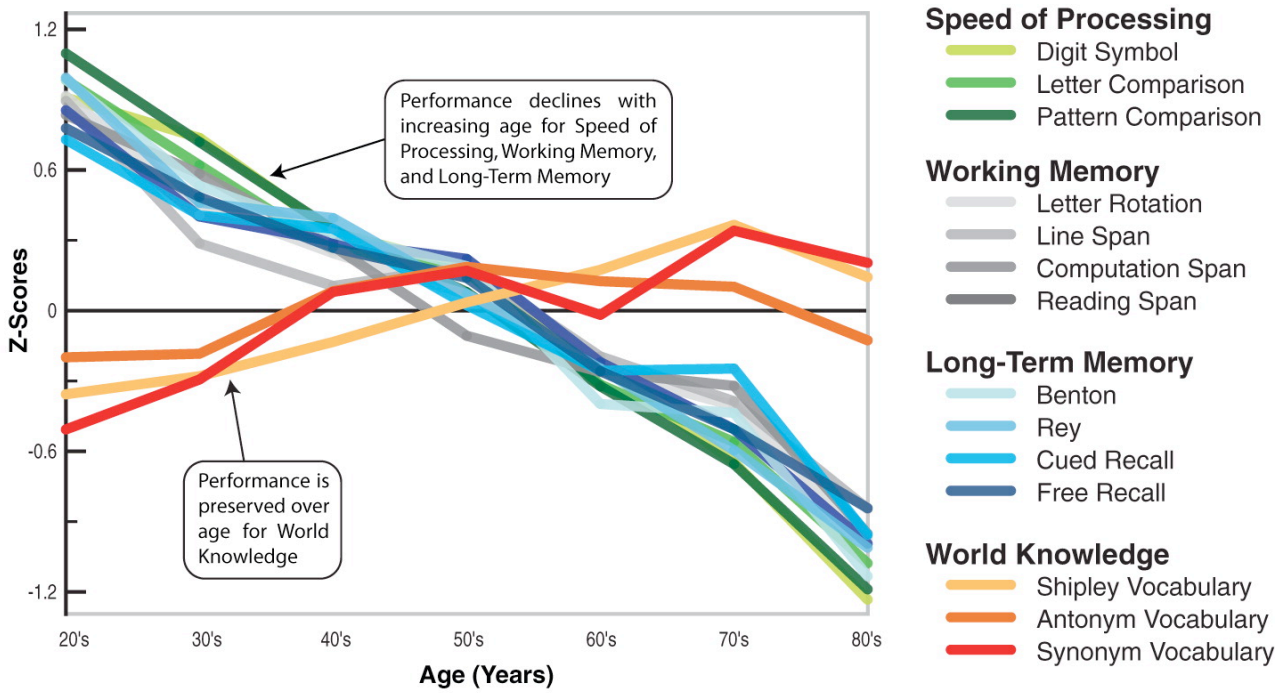

Figure 2. Z-score (y-axis) is a measure of distance from the mean in standard deviations ((value- mean)/stdev).

A variety of motor functions, including reaction time, speed of movement, and hand and foot coordination have also been shown to consistently slow with age (10-12). This is likely mediated by aging of the central nervous system as cortical Dopamine D2 receptor level, which declines with age (13, 14), correlates with motor speed as well as cognitive function (14). Like cognitive aging, these changes follow a continuous and progressive pattern, as exemplified in the Baltimore longitudinal study, which demonstrated that simple and disjunctive (i.e. go no go task) reaction times increased by 0.5 (~4.0%/decade) and 1.6 msec/year (3.9%/decade), respectively, starting at age 20 and continuing through the oldest ages (90+ years) (10).

Meta-analyses have shown that changes in mood and affective perception also exist with age. Older adults are worse at recognizing sad or angry emotions than younger adults, which can not be accounted for by general cognitive decline as they perform equally as well in recognition of happiness and better in recognition of disgust (5). Generally, older adults show a positivity-bias in attention and memory, recover from negative events faster, and are less likely to engage in destructive interpersonal interactions such as shouting during conflict (reviewed in (15)). Consistent with this and contrary to popular belief, older adults have less risk of major depression, with average onset of major depression at age 30.5 with declining risk beginning in the early 40s (16). This seems counterintuitive given that suicide rates are greatly increased in people over 65 versus the general population (14.2 and 10.2 per 100,000 respectively), with even greater rates in non-hispanic white males over 85 (48 per 100,000) (http://www.nimh.nih.gov/health/publications/suicide-in-the-us-statistics-and-prevention/index.shtml#CDC-Web-Tool). However, this is not due to increasing rates of major depression but higher ratios of completion to attempts largely in men, especially those living alone, widowed, and/or terminally ill (17, 18). Additionally, the lower rates of depression seen in older adults seems counterintuitive because the same frontal brain areas required for cognition, which decline functionally with age, are required for emotional control, which does not decline with age. However, it has been shown that adults with poorer performance on cognitive tests also show less positivity-bias, suggesting they have less emotional control (15). There is also very high co-morbidity of depression with neurodegenerative and dementia-related diseases such as Alzheimer's and Parkinson's disease, in people with poorer cardiovascular health, and especially in stroke patients (19). Combined, this suggests that people adaptively learn and become more proficient at maintaining a positive affect with age, but that control of this declines with declining cognition and in degenerative states. Thus, age-related loss of emotional regulation in people with more rapidly declining cognition may be an important factor for risk of depression in old age and disease.

It is important to note that there is large individual variability in the rates of age-related cognitive decline, ranging from little or no decline in cognition to more rapid decline (see Figure 3 (20)). A potential caveat to many cross-sectional studies on this topic is that the largest predictor of cognitive capacity in old age is cognitive capacity in youth, accounting for ~50% of the variance (21). With this in mind, there is good longitudinal evidence for both genetic and environmental contributors to rates of cognitive decline. The APOE-ε4 allele, for example, which increases risk for and lowers onset age of Alzheimer's disease, has been extensively studied and has substantial evidence for association with accelerated cognitive decline (21-24). There is also some evidence for genetic contribution of COMT, BDNF, Klotho, PRNP, and DISC-1 although neither non-candidate high-throughput approaches or meta-analyses of candidate genes have been performed (see also genetics section (21, 22, 25)). Environmental factors that have been associated with slower cognitive decline include exercise, healthy body mass index, higher education level, good cardiovascular health, being a non-smoker, caloric restriction, and there is some evidence for nutritional factors such as antioxidant, omega-3 fatty acids, and red wine consumption (21, 24, 26-29).

Figure 3. Individual differences in rates of cognitive decline. (From Wilson et. al. 2002 (20)).

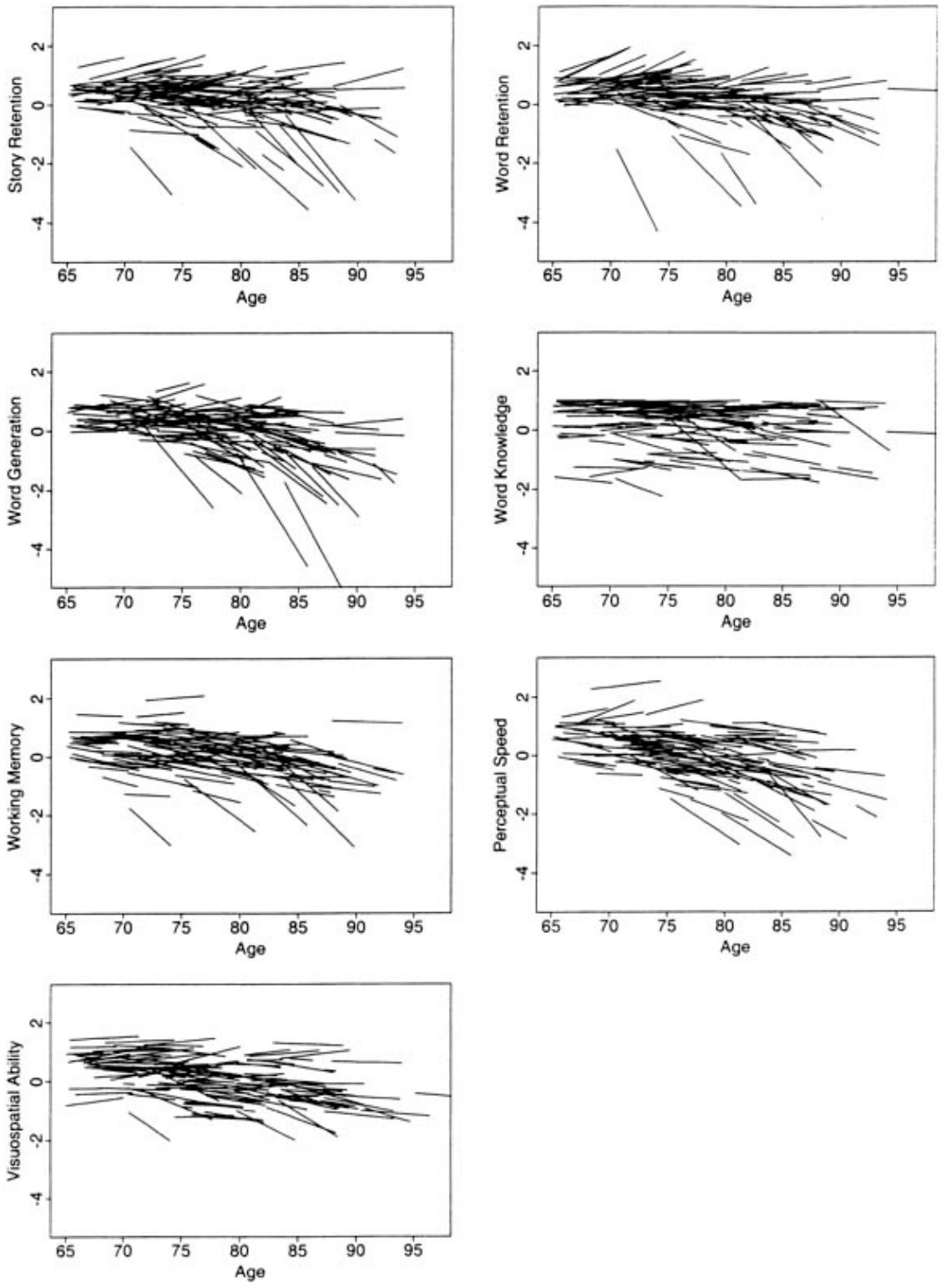

I.A.ii Normal age-related changes in brain structure/function.

What structural and functional changes potentially underlie these changes in cognition, motor function, and affect? Longitudinal and cross-sectional MRI studies have demonstrated significant grey matter loss with age at rates of (3.2-5.3 ml/year) or approximately 0.5%/year (See Figure 3)(30-33).

Figure 4. Grey-matter volume decreases linearly with age throughout adulthood. (Adapted from Good et. al 2001 (33))

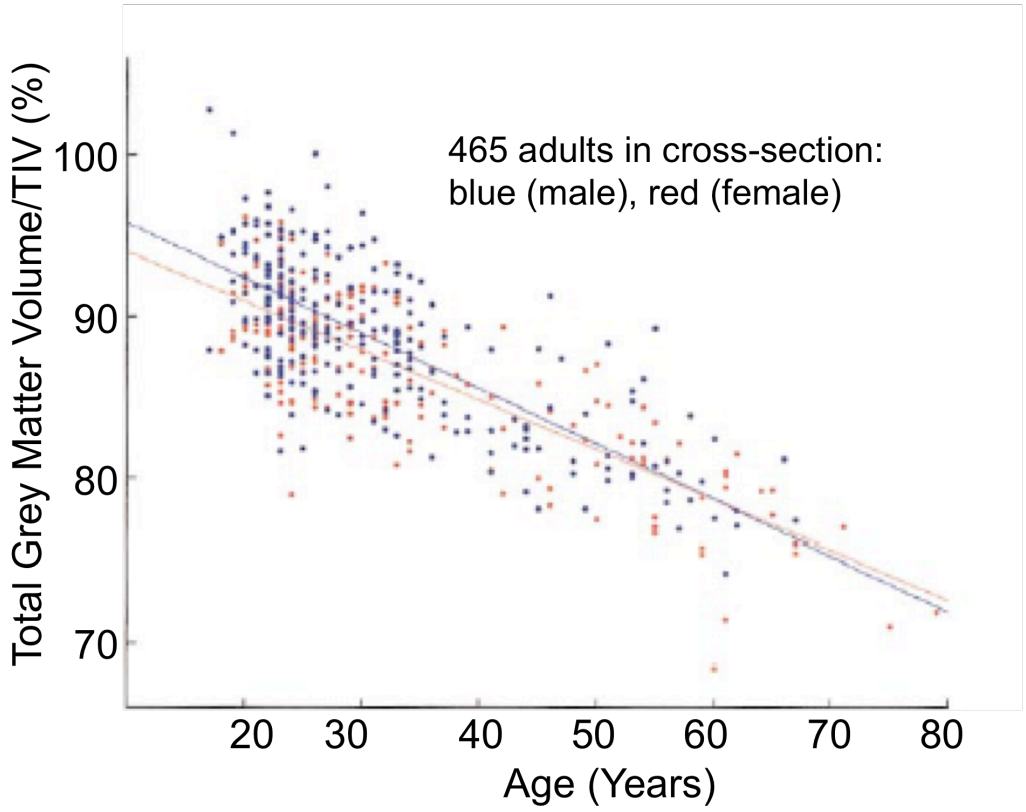

Figure 4. Total grey matter volumes are corrected for total intracranial volume (TIV) to correct for differences in head size.

A striking example of this was conducted by Resnick et. al in 2003 , which followed longitudinally 92 non-demented adults (ages 59-85) at baseline, 2, and 4 years out and found significant ($p<.001$) decreases in total grey matter at each time point within individuals (34). These changes are area-specific as frontal areas such as anterior cingulate cortex, prefrontal cortex, left and right insula, and left inferior frontal cortex have the most consistent decreases in volume with age in the literature whereas hippocampus and amygdala were unchanged or variable between studies (30, 31, 33-36). The area-specificity of these changes is consistent with age-related cognitive changes, i.e. the most robust changes are seen in frontal areas required for cognitive processing and working memory. Additionally, losses of white matter integrity and changes in brain activity in response to tasks on fMRI, such as hippocampal hypo-responsiveness and greater frontal bi-laterality in memory tasks, are seen with age (reviewed in (6)). There is also a fair amount of evidence that these gross structural and functional changes correlate with changes in cognition (reviewed in (6)).

I.A.iii Normal age-related changes in cellular morphology.

What underlies changes in grey-matter/white matter volumes? It was previously thought that neuronal death occurs in the brain with age. However, better stereotactic techniques and careful exclusion of subjects with neurodegenerative disease has shown that little or no neuronal death occurs during normal aging (37-39). Instead grey-matter volume losses are the result of dendritic arbor shrinkage and synaptic losses in individual neurons (37-39). Duan et. al demonstrated a ~43% and 27% loss of apical and basal cortical neuron dendritic spines in aged versus young macaque monkeys (see Figure 5 (40)). These reductions in synapse density may underlie cognitive deficits, as they correlate with prefrontal cortex activity reduction in executive processing tasks (37).

Figure 5. Age-related loss of dendritic spine density (from Dickstein et. al, 2007 (39))

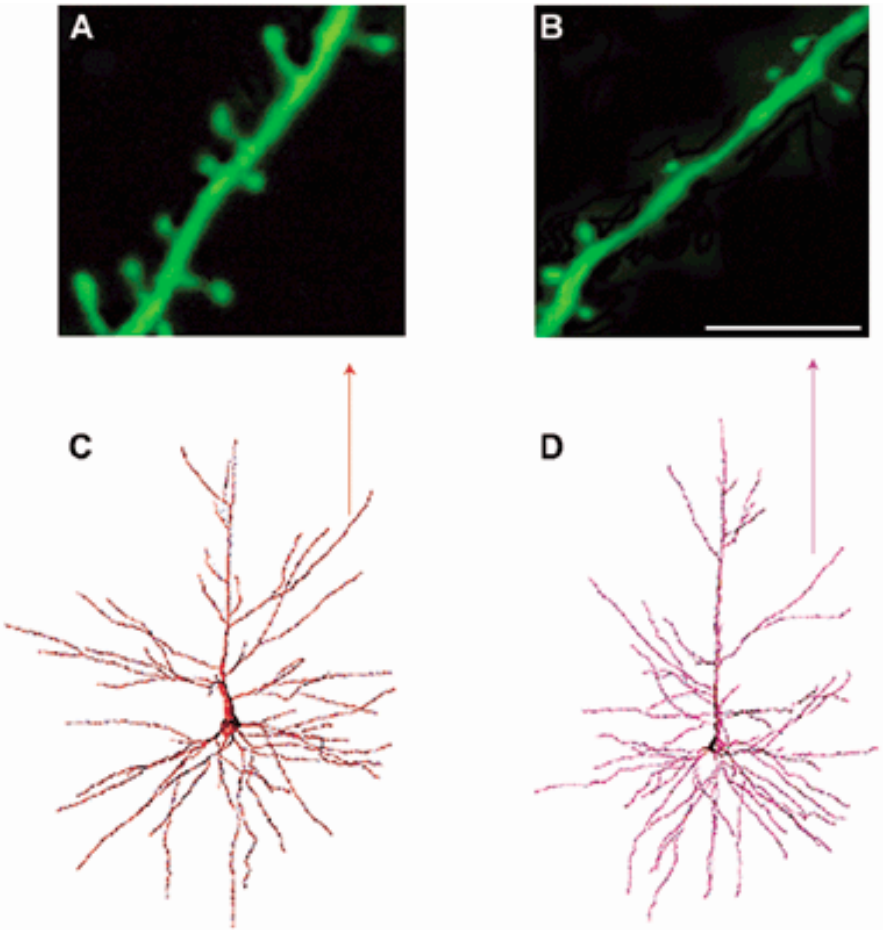

Figure 5. Spine densities on neocortical pyramidal neurons from young and aged rhesus monkeys. Panels A and B show confocal laser scanning images of apical dendritic segments in a young (10-12 yrs) (A) and aged (24-25 yrs) (B) rhesus monkey (scale bar = 8 μm). Note the increased spine density in the young monkey compared to the old monkey. Panels C and D show examples of a retrogradely traced neuron, filled with Lucifer Yellow, and reconstructed in 3-dimensions using NeuroZoom and NeuroGL software applications. The neuron in (C) is from a young animal and the neuron in (D) is from an aged animal. The arrow points to the dendritic segments analyzed in A and B. (Adapted from Duan et al., 2003).

Similarly, for glia, older studies concluded that astrocytic gliosis and microgliosis, as visualized by MHC-II or GFAP (glial markers) staining in brain slices, was caused by increasing glial numbers with age, which has also been shown to be false with more careful stereological techniques (41-43). Instead, glial processes thicken with age (and thus show greater glial marker staining), termed “glial dystrophy”, perhaps to preserve correct distances from shrinking neuronal processes for glial-neuronal exchange (41-43).

I.B. Molecular pathways of brain aging.

In addition to cellular morphological changes, within neurons there is increasing DNA damage, reactive oxygen species, calcium dysregulation, mitochondrial dysfunction and inflammatory processes (reviewed in (37)). Underlying these cellular phenotypes, central nervous system (CNS) molecular aging both shares and has unique molecular pathways from the periphery. Shared pathways include those related to metabolism and caloric restriction, as well as those related to cellular insult, including DNA damage, inflammation, and reactive oxygen species (ROS) (see below; reviewed in (37)). In peripheral tissues, aging is additionally driven by senescence-related mechanisms such as telomere shortening and depletion of precursor cells, which are not as pertinent in CNS because cellular turnover is limited. There are also nervous system-predominant molecular mechanisms, including those driven by neurotrophins (BDNF) and neurotransmitters (serotonin, dopamine, glutamate)(see below (44-47)).

I.B.i. Molecular pathways of brain aging: metabolic.

Caloric restriction (CR) is one of the most studied mechanisms of increasing longevity across species from yeast to primates (48). Relevant to brain aging specifically, a primate CR model demonstrated delayed brain atrophy (49) and in older humans short-term CR is associated with improved memory prospectively (50). This may be an evolutionarily conserved means of sensing poor nutritional

environments and thus increasing reproductive lifespan to wait for richer environments. It is tied into and shares signaling with ROS-related mechanisms, as CR-driven metabolic slowing results in fewer mitochondrial produced ROS and thus less DNA damage (reviewed in (51)). Mediators of CR, Growth Hormone, Insulin, IGF-1, and the circulating longevity hormone, Klotho, which binds to the IGF-1 receptor, as well as the Sirtuin family of longevity genes, have been shown to modulate both organismal lifespan and healthspan across species (48, 52, 53). There is emerging evidence that these are key players in brain aging, including causal studies in model organisms and some genetic association of human polymorphisms in these genes with brain aging (see genetics section). The Sirtuin family of longevity genes, encompassing seven homologous NAD-dependent histone and protein deacetylases, is the target of resveratrol, the putative lifespan extending compound in red wine and grapes. These genes are particularly promising targets for key brain aging modulators. Related to their varied subcellular localizations, they have pleitropic anti-aging effects in neurons and glia, including abrogation of protein aggregates and accumulating misfolded proteins, enhancing stress response and improving DNA repair, prevention of cell death pathways and mitochondrial dysfunction, and preventing inflammatory processes in glia (reviewed in (54)). Additionally Sirt1 has been shown to prevent Wallerian-type axonal degeneration after injury (55) and to be a key player in neurogenesis (56). Other players in this pathway, elucidated predominantly from studies of peripheral tissues in the model organism literature, include FOXO, Daf16, p66, PTEN, m-TOR, and CLOCK-1 amongst many others (48). Mechanisms of metabolic pathway control of brain aging have only begun to be understood.

I.B.ii. Molecular pathways of brain aging: cellular insult.

Nuclear and mitochondrial DNA damage, predominantly single base mutations, such as 8-oxoguanine, steadily accumulate in the aging brain across species (reviewed in (37, 57)). There is considerable support for pathways downstream of increasing DNA damage and ROS directing brain aging, including

accelerated brain aging and neurodegeneration, in many people with progeria syndromes caused by DNA repair gene mutations (37). Additionally, severity of age-related memory impairment is correlated with brain and plasma levels of antioxidants (reviewed in (57)). Besides genes mutated in progeria syndromes there is also a role specifically for P53 in brain aging and centrally driven lifespan regulation, as selective brain knock-down of P53 in drosophila results in increased longevity and resistance to oxidative stress (37, 58). However, the specific pathways linking DNA damage to age-related neuronal/glial morphological changes remain poorly understood.

I.B.iii. Molecular pathways of brain aging: neurotrophins.

While there is a large literature relating neurotrophins such as GDNF, NGF and bFGF to treatment and prevention of neurodegenerative disease such as AD and PD, Brain Derived Neurotrophic Factor (BDNF) is the most well studied modulator of normal brain aging (reviewed in (59)). Particularly, there is a large literature connecting the human BDNF val66met (secretion deficient) polymorphism to brain aging in mice and humans (see genetics section below). Additionally, it is a logical modulator of molecular aging, as it is an activity-dependent secreted growth factor, which declines steadily with age in the brain (60), is neuroprotective against a variety of insults, and is required for changes in spine density underlying learning and memory systems that decline with age (reviewed in (59)). Indeed, infusion of BDNF can restore age-related impairment in Long Term Potentiation (LTP) in middle-aged rats (61). BDNF is also required for neurogenesis in mice and it's expression is induced by exercise and caloric restriction, which are known to be modulators of normal brain aging (reviewed in (59)). How pathways downstream of BDNF specifically modulate cellular age-related molecular changes remains unclear. We begin to explore this here by investigating the effects of BDNF ablation both embryonically and conditionally in adulthood by microarray in frontal cortex (paper 1 (62)).

I.B.iv. Molecular pathways of brain aging: neurotransmitters.

There is increasing evidence for a role for neurotransmitters, particularly serotonin, glutamate and dopamine, in modulating normal brain aging. This has important implications for public health and also new treatment strategies for aging and age-related disease because so many current psychiatric and neurological drugs target neurotransmitter receptors. Serotonin has been hypothesized to play a role in normal brain aging by us and others because it and its receptors have age-regulated levels and share many signaling pathways with other age-regulatory molecules such as BDNF and IGF-1, and because SSRIs can modulate neurogenesis (reviewed in (44, 45), see also paper 2 (63)). Additionally, serotonin blocking drugs and serotonin synthesis (tph-1) and receptor mutants (ser-1, ser-4) delay age-related phenotypes and/or extend longevity in c. elegans (64-67). However, causal studies specific to the brain and in higher order model organisms, as well as prospective studies of human age-related phenotypes in relation to serotonergic drugs, are still lacking. In paper 2 (63), we demonstrate the first causal evidence linking genetic disruption of serotonergic signaling with anticipated molecular brain aging in mice.

Glutamate, the brain's predominant excitatory neurotransmitter, is also a probable candidate for modulating brain aging because it facilitates release of BDNF and is essential for LTP and synaptic plasticity, as well as neurogenesis, activity-dependent neuronal survival, and neural outgrowth during development (reviewed in (46)). Through elevation of intracellular Ca^{2+} and effects on CREB and NFκB mediated signaling, glutamate effects both rapid changes in dendritic architecture and long term transcriptional effects on a variety of genes, including neurotrophins, through which it likely exerts it's effects on age-related morphological changes (reviewed in (46)). Glutamate is also an important player because of its role in both protection in the context of ischemic preconditioning, and facilitation of excitotoxic neuronal injury and death (46).

Dopamine has strong correlative and causative evidence for modulation of brain aging (47) as well as being implicated in several age-gated diseases, including PD, HD, SCHZ, and BPD. Components of the dopamine system also decline with

age, including the dopamine transporter (DAT), and the D1 and D2 receptors (reviewed in (47)). Mice fed the dopamine precursor, Levodopa, have extended longevity by 50% and improved fertility, perhaps through the caloric restriction pathway, as they showed reduced growth despite the same amount of food intake as controls (68, 69). This cross-talk with caloric restriction pathways is corroborated by D2 receptor knock-out (ko) mice, which have decreased levels of GH and IGF-1 (70). In humans, pharmacological studies in healthy volunteers have shown that D-amphetamine enhances performance on a variety of tasks and that found that the D2 receptor agonist, Bromocriptine, facilitates spatial working memory, suggesting that D2 receptor down-regulation with age may play a role in age-related memory and cognitive decline (47). Additionally, PET studies have demonstrated that in healthy adults striatal D2 receptor binding correlates with executive and motor functioning as well as perceptual speed (both of which correlated with subject age) even when controlling for chronological age (14, 47, 71), suggesting that D2 levels may be partially responsible for the effects of molecular aging on cognitive function. In addition to declining dopamine signaling having cross-talk with caloric restriction pathways and directly mediating age-related cognitive decline, dopamine pathways also have cross-talk with ROS age-related pathways. For example, Monoamine oxidase B, which acts to inactivate robustly increases with age (60), generates large numbers of free radicals and thus may contribute to increasing ROS with age (reviewed in (72)). Dopamine also regulates glial dystrophy-related pathways by regulating NFκB and GFAP levels (reviewed in (72)) and interacts with calcium-related pathways and circadian-rhythm pathways through interaction with Clock amongst other genes (reviewed in (73)).

I.C. Molecular underpinnings (gene expression correlates) of normal human brain aging.

Several groups, including our own, have characterized the gene expression underpinnings of these age-related changes using human post-mortem brain microarray (60, 74, 75). Consistently a selective portion of the genome (~5-10%) has

been shown to have age-regulated changes in expression levels in the brain (60, 74). The most affected genes are consistent with the age-related cellular phenotypes they likely underlie, i.e. decreasing neurotrophic factors (BDNF, IGF-1), calcium-related proteins (Calbindin), markers of synaptic density (SYN2), and neurotransmitter receptors (HTR2A, DRD2), and increasing markers of DNA damage (BCL-2), and glial dystrophy (GFAP, NFk-B). The mechanism(s) driving these selective age-regulated expression changes is largely unknown. Lu et. al in their seminal 2004 paper, postulated a clock mechanism whereby accumulating DNA damage with age could selectively alter promoter regions of age-regulated genes(74). In support of this theory, they demonstrated that genes with age-regulated expression levels in human Prefrontal cortex had promoter regions that were more vulnerable to DNA damage than genes that were not age-regulated(74).

At the same time, our group demonstrated that age-regulated gene expression changes were highly conserved across two areas of prefrontal cortex. Fitting with these expression changes underlying shrinking neuronal processes and glial dystrophy, we demonstrated that age down-regulated transcripts were predominantly of neuronal origin, whereas age up-regulated transcripts were predominantly of glial origin ((60) see Figure 4). These changes were so robust and consistent that molecular age (calculated from a composite score of age-regulated gene transcript levels) could be used to predict subject chronological age (See Figure 6 (60)). Consistent with the large individual variability seen in rates of age-related cognitive decline, we saw individual variability in rates of molecular brain aging, which could not be attributed to cohort characteristics such as body mass index (see Figure 7 (60)).

Figure 6. Molecular aging is conserved in the prefrontal cortex. (From L. Erraji-Benchekroun et. al 2005 (60)).

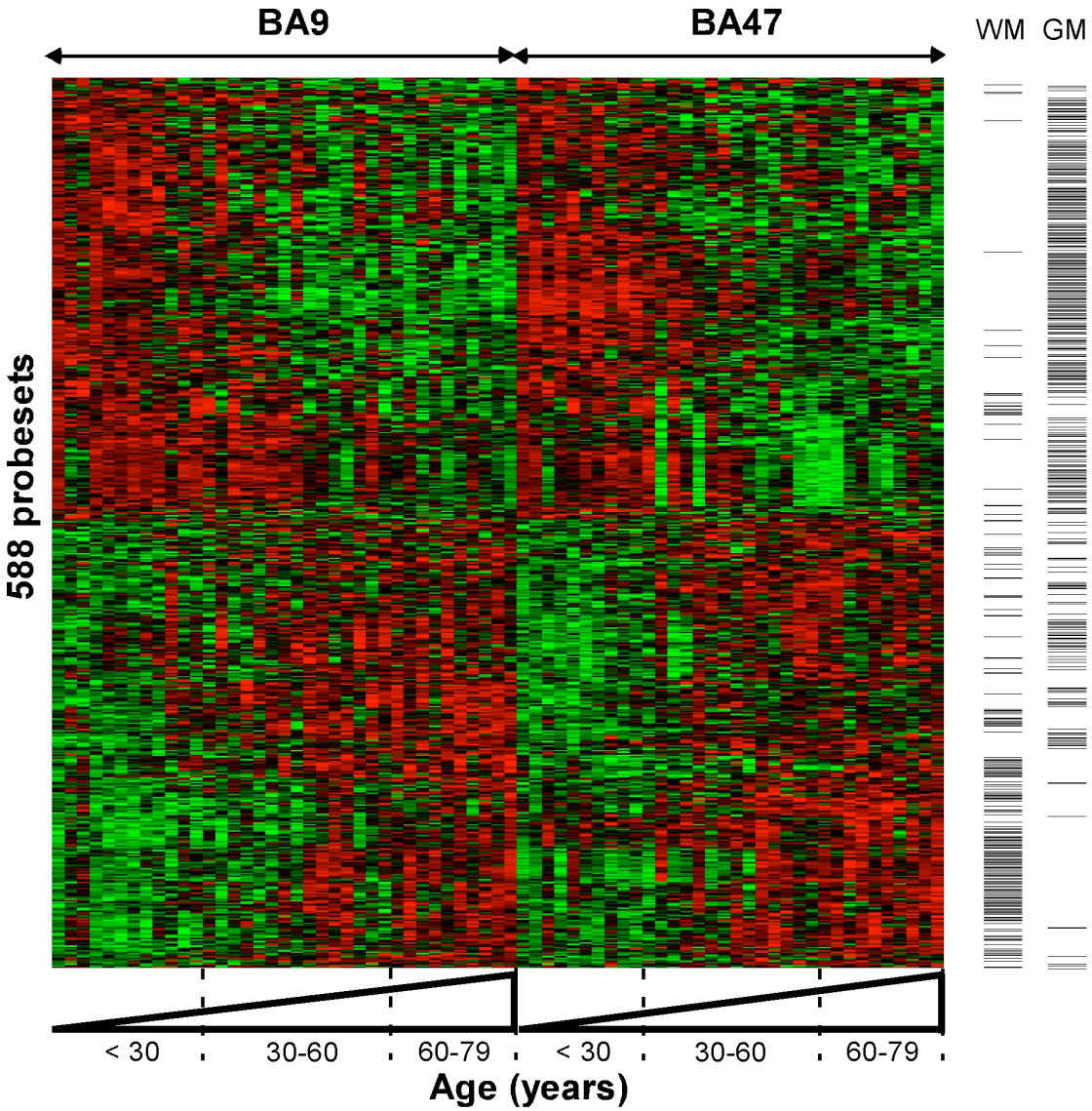

Figure 6. Expression levels for 588 age-affected probesets are presented together for BA9 and BA47. Each probeset is represented by a row, each array, or brain area per subject by a column. Samples are organized left to right by brain area and increasing age. Green and red bars indicate decreased and increased gene expression, respectively, versus the averaged signal for these genes across all samples. For example, a horizontal row going from red to green indicates a gene whose expression decreases with age in that brain area. Along the Y-axis, probesets are clustered according to similarities in expression profiles across age. A similar number of probesets were downregulated (n=291, upper panel) and upregulated (n=297, lower panel) throughout lifetime. Columns to the right indicate the distribution of genes with glial-(WM) or neuronal-enriched (GM) signals. Notice the high concentration of glial-enriched genes with increased expression with age, while most, but not all, neuronal-enriched genes appeared to be downregulated with age.

Figure 7. Molecular age predicts chronological age.
(From L. Erraji-Benchekroun et. al 2005(60)).

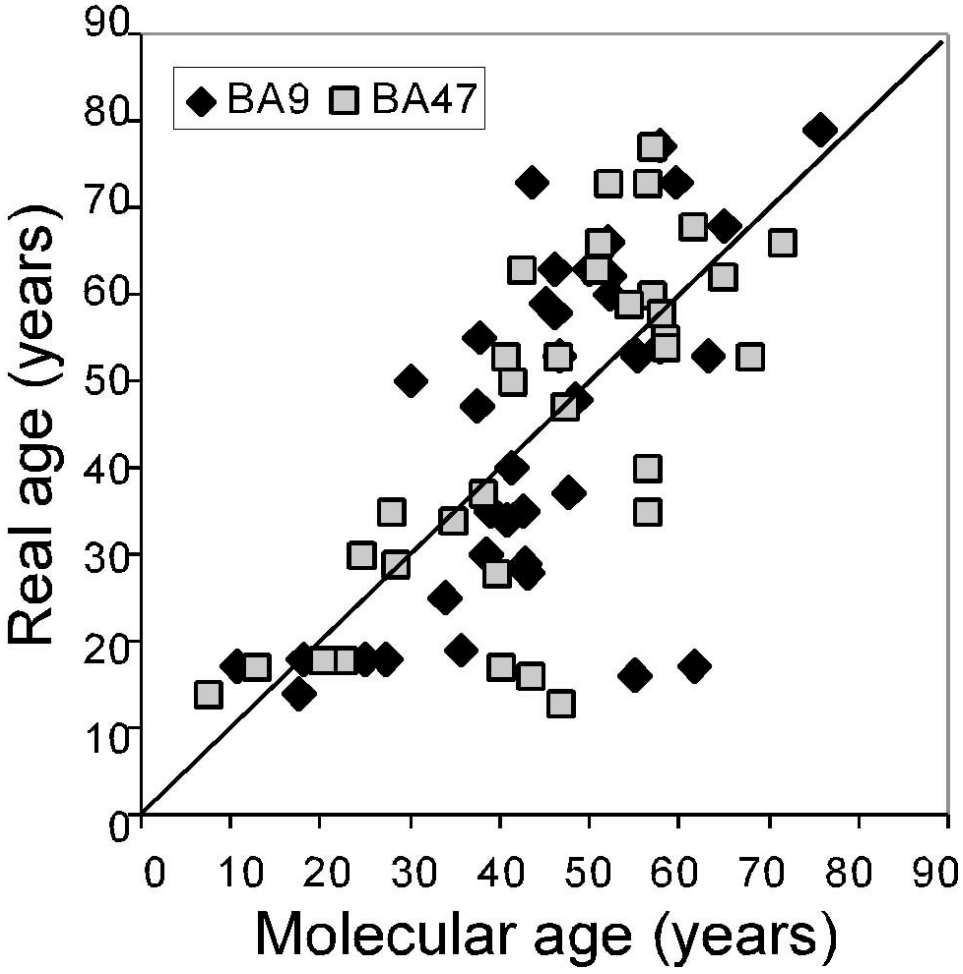

Figure 7. The "Molecular" age, or age as defined by gene expression levels, represents a summary number for each sample that depicts the average deviation in gene expression within this sample when compared to age-affected transcripts in all other subjects (See Methods). Overall, there was a high correlation between "molecular" and chronological ages (BA9: r=0.65; BA57, r=0.73). A few samples demonstrated larger deviation than average at both young and older ages. These subjects did not correspond to any identifiable clinical, demographic or experimental parameters.

The consistency of age-related gene expression changes suggested to us that they are likely under control of a biological “program”, similar to peripheral aging of somatic tissue and perhaps analogous to genetically controlled transcriptional programs occurring during development. This led us to hypothesize that individual differences in molecular brain aging rates can be partially accounted for by genetic variation (see paper 3). These studies have opened up leads to understanding what the master molecular driving forces are behind age-regulated molecular changes underlying structural and functional brain aging. A better understanding of the mechanism behind these changes and their genetic regulation may be key to creating new therapies for treatment of age-related declines and disease. In the three papers presented here, we begin to address these questions. Next I will discuss what is known about genetic regulation of “normal” brain aging.

I.D. Genetics of normal brain aging.

The genetics of normal brain aging has a vast associated literature. Here I present candidate genes with the most evidence for association. They can be organized into three broad categories: genes related to molecular pathways of aging, longevity genes, and genes associated with age-gated neurological disease, although substantial overlap occurs between these categories.

I.D.i.a. Genes related to molecular pathways of aging: BDNF.

One of the most well studied polymorphisms in relation to brain aging is the BDNF val66met single amino acid substitution polymorphism, which results in decreased activity-dependent secretion of BDNF in neuronal cultures (76). The Met allele is associated with poorer episodic memory, and abnormal fMRI-assessed hippocampal function, accelerated age-related loss in verbal reasoning, and anticipated age-related grey matter volume losses by structural MRI (76-79).

I.D.i.b. Genes related to molecular pathways of aging: serotonergic genes.

The short allele of the Serotonin transporter promoter polymorphism (SERT SLC6A4), most famous for association with depression in the context of stressful life events (80), associated with worse delayed recall and smaller hippocampal volumes in older adults (81). Consistent with this, the long allele of this polymorphism was shown to be overrepresented in Japanese centenarians (82). Another study linked the other well-studied SERT polymorphism (VNTR2) with rates of cognitive decline but not baseline cognition on a variety of measures, but failed to find association with SLC6A4 (83). A Serotonin 2A receptor polymorphism has also been linked with longitudinal decrease in delayed recall (84). These results are encouraging for a role of Serotonin polymorphisms in brain aging, but most require replication. Additionally, causal studies in model organisms linking these genes to brain aging are lacking, and the mechanism behind the contribution of these polymorphisms to altered rates of brain aging remain unknown. In paper 2, we present the first causal evidence linking a serotonergic gene to brain aging, demonstrating that HTR1B receptor KO mice display anticipated molecular brain aging.

I.D.i.c Genes related to molecular pathways of aging: dopaminergic genes.

Among dopaminergic polymorphisms, Catechol-O-methyl transferase (COMT) Val158Met Val allele, which is associated with decreased prefrontal cortex dopamine levels, has been most studied in relation to brain aging. It is consistently associated with accelerated rates age-related cognitive decline (85-87) and differences in longitudinal loss of grey matter(88). However, KO or knock-down studies of COMT establishing causation in model organisms are still lacking. Other than COMT in the dopaminergic system, one study has linked the Tyrosine hydroxylase locus to human longevity (89).

I.D.ii.a. Longevity genes: Klotho.

Klotho (KL),named after the Greek goddess who spun the thread of life, was first identified as a longevity gene in 1997 by analysis of a strain of short-lived mice (lifespan around 2 months) who had early onset of age-related disorders (ectopic calcification, osteopenia, arteriosclerosis, emphysema, and insulin resistance) (52, 90). They were subsequently shown to have accelerated age-related neuronal pathology (91) and premature cognitive aging (92). KL is expressed in the distal tubule cells of the kidney and the choroid plexus of the brain and codes for a circulating hormone that binds to the insulin-like growth factor (IGF-1) receptor and represses intracellular insulin signaling (52). KL-hypermorphs, conversely, have an approximate 20% increase in longevity and delayed age-related disorders (52). The human KL-VS polymorphism results in a two amino acid change in the protein (93) and is associated with a heterozygous advantage for increased life span, increased risk for cardiovascular disease, osteoporosis, and stroke, as well as decreased IQ at age 79, however this was not significant after controlling for baseline IQ at age 11(93-98). In paper 3, we investigate the effects of this polymorphism on rates of molecular aging in the human brain.

I.D.ii.b. Longevity genes: insulin signaling genes.

In C. elegans and Drosophila, insulin-signaling genes, which when mutated can increase lifespan up to sixfold, are the most extensively studied longevity genes (99, 100). Specific to the brain, knock-out of daf-2 (orthologue to the human IGF-I receptor (IGF-IR)) in only a small subset of neurons significantly extends lifespan (reviewed in (100)). One study examined the effects of human polymorphisms in the IGF-I receptor (IGF-IR), PIK3CB (phosphoinositol 3-kinase; C. elegans AGE-1 orthologue), IRS-1 (D. melanogaster CHICO gene orthologue), FOXO1A (C. elegans DAF-16 orthologue) on human lifespan, and found a significant association with IGF-IR G/A 1013 polymorphism (99). Also, polymorphisms in AKT-1 and FOXO3A (101) have subsequently been associated with human longevity, even in meta-analysis

(102). The large literature and extensive evidence linking insulin signaling polymorphisms and human lifespan is reviewed in (103), however, the relation of these polymorphisms specifically to brain aging has not been investigated.

I.D.ii.c. Longevity genes: P53.

Reduced expression of Cep-1 (P53 orthologue) extends lifespan in C. elegans and overexpression of P53 reduces lifespan in mice (reviewed in (103)). An human arginine/proline polymorphism in codon 72 of P53 has some (albeit conflicting) evidence for association with human lifespan (reviewed in (103)), which has not been investigated in relation to brain aging.

I.D.ii.d. Longevity genes: Sirtuins.

Overexpression of Sirtuins extends longevity in C. Elegans and drosophila (104). Additionally, Sirtuin KO mouse models show decreased longevity and accelerated age-related phenotypes (reviewed in (105)). In humans, an association between two Sirt3 polymorphisms and longevity has been found (106, 107) as well as between a Sirt1 polymorphism and cognitive function in old age (108). However, the link between sirtuins and brain aging remains largely unexplored. In paper 2 (63), we demonstrate altered Sirt5 expression in brains of an HTR1B KO mouse model of anticipated brain aging and in paper three, we go on to demonstrate accelerated molecular brain aging in association with a novel low-expressing Sirt5 polymorphism.

I.D.iii.a. Age-gated neurological disease-related genes: APOE.

APOE is a lipoprotein that binds to the LDL receptor family and has three human variants, (E2, E3, and E4) that each differ by a single amino acid. The E4 allele is consistently associated with greater risk and earlier onset of cardiovascular

disease, stroke, and Alzheimer's disease in a dose dependent manner, while the E2 allele has been shown to be protective (reviewed in (25)). Carriers of the E4 allele also show greater age-related decline in cognition (reviewed in (25)), as demonstrated by lower IQ at age 70 but not at age 11(23). The molecular mechanism behind the E4 allele's association with more rapid cognitive aging and greater risk of age-related disease appears to be threefold: an association with increased subject cholesterol levels, greater Aβ accumulation, and less ability for dendritic sprouting in E4 carriers, which has been causally related to E4 in models (reviewed in (109)).

I.D.iii.b. Age-gated neurological disease-related genes: PRNP

A prion protein gene (PRNP) variant met129val, is associated with risk of Creutzfeldt-Jakob disease, Alzheimer's disease, cognitive impairment, dementia, and brain morphology, and normal cognitive aging which interacts with the Klotho KL-VS polymorphism ((110-112) see also genetics: Klotho). The mechanism behind this likely relates to ROS pathways as PRNP functions neuroprotectively, likely as a super oxide dismutase (112).

I.D.iii.c. Age-gated neurological disease-related genes: DISC-1

Disrupted in schizophrenia 1 (DISC-1), most famous for its association with schizophrenia and bipolar disorder, likely functions by influencing neurite extension, signal transduction, neurotransmission, and the cytoskeleton, although these mechanisms have not been fully elucidated (92). A snp in this gene that results in a single amino acid substitution results in reduced hippocampal volume and accelerated age-related cognitive decline (92).

I.E. How normal brain aging may contribute to age-gated neurological disease

Aging is a requirement for onset of many neurological diseases ranging from late onset neurodegenerative diseases such as Alzheimer's and Parkinson's diseases (average onset 60 and 75 years respectively) (113) to earlier onset psychiatric disorders such as schizophrenia and bipolar disorder (average onset 25 years) (114). While many studies have focused on contrasting disease brains with chronologically age-matched controls, this strategy may be problematic as it is becoming increasingly evident that normal aging is an integral aspect and modulator of disease onset and progression. Evidence for this comes from the sheer prevalence of diseases with increasing age, such as Alzheimer's disease, for which prevalence increases exponentially from age 65 upward, reaching nearly 45% by age 95 (Figure 7 (113)).

Figure 8. Prevalence of AD by age (From Nussbaum et. al 2005 (113))

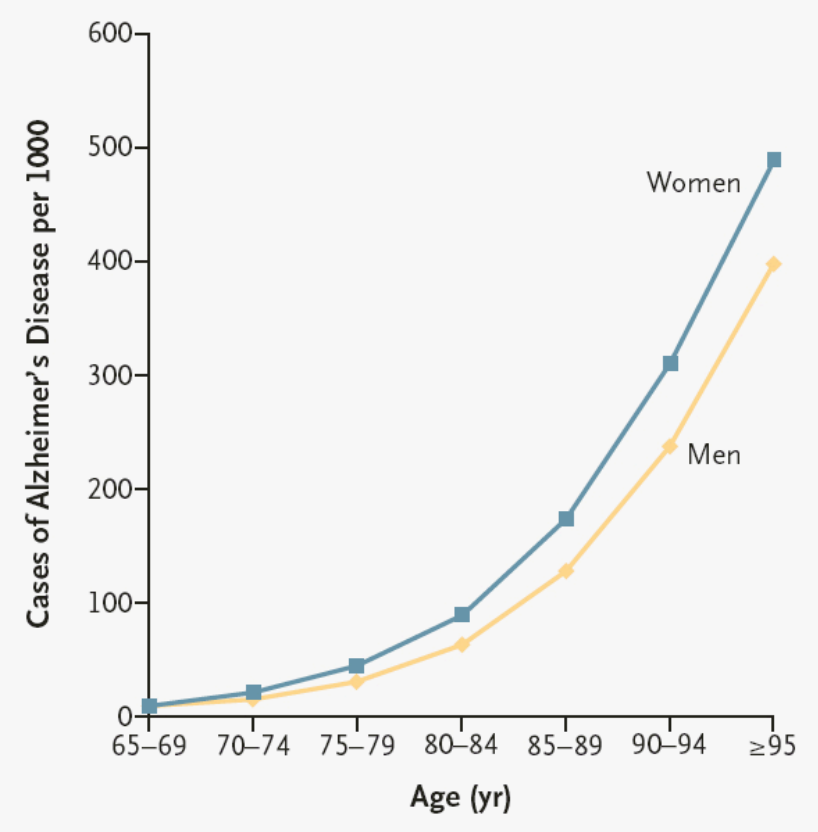

Also, genetic modulators and molecular pathways of normal brain aging share substantial overlap with those associated with age-gated neurological disease. For example, BDNF val66met, COMT val158met, APOE4 and PRNP met129val have all been associated with risk for AD and PD (22, 115, 116) and the BDNF val66met has additionally been associated with age of onset schizophrenia (117). Epidemiological studies have shown that low calorie diets are associated with decreased risk of AD and PD (reviewed in (27)) and CR delays Aβ deposition in squirrel monkeys (118) and improves functional outcome in a monkey model of PD (119). Additionally, BDNF administration can delay neurodegeneration in animal models of Huntington's disease (HD) (reviewed in (46)) and AD (reviewed in (120)). Sirt1 is also implicated in disease, as overexpression has been shown to be protective against neurodegeneration in both AD and ALS model organisms (reviewed in (121)).

Additional evidence for normal aging modulating onset of age-gated disease comes from genetic models of increased longevity, which have been associated with delay in age-related disorders. For example, mice hypermorphic for the longevity gene, Klotho, not only live ~20% longer but also have a corresponding delay in onset of ectopic calcification, osteopenia, arteriosclerosis, emphysema, and insulin resistance (52, 122). This also has increasing evidence for age-gated neurological diseases specifically, as lifespan extension via reduction of insulin/insulin growth factor signaling (IIS pathway) resulted in delayed proteotoxicity in both C. elegans and mouse Alzheimer's disease models (123, 124).

While normal aging appears to modulate disease, it is important to point out that the converse does not hold, ie. not all disease susceptibility genes modulate aging. For example, the familial AD genes, PSEN1, PSEN2, and APP appear to have no association with cognitive aging (22, 25). Also, neuronal loss is a key feature of neurodegenerative disease, which as previously discussed, does not occur during normal aging.

The modulation of a variety of neurological diseases by normal aging is promising for the creation of novel magic-bullet type anti-aging therapeutics for treatment of disease and age-related decline. However, how aging gates neurological

diseases and what contributes to individual variability in age of onset is essential to this and still remains largely unknown. In paper 3, we postulate and demonstrate evidence for a gene-expression level gating mechanism behind this. We show that neurological disease-related genes are overrepresented amongst those with age-regulated expression levels and change almost unanimously in pro-disease directions and that rates of these changes are associated with a novel longevity gene polymorphism ($Sirt5_{prom2}$). The studies presented here contribute to knowledge of genetic and molecular pathways of normal brain aging and how they gate age-related neurological disease.

II. CHAPTER 1- PAPER 1

"Specificity and timing of neocortical transcriptome changes in response to BDNF gene ablation during embryogenesis or adulthood"

Molecular Psychiatry (2006) 11, 633–648. doi:10.1038/sj.mp.4001835; published online 9 May 2006

Christin Glorioso[1], Michael Sabatini[1,2], Travis Unger[1], Takanori Hashimoto[1], Lisa M. Monteggia[4], David A. Lewis[1,3] and Károly Mirnics[1,2,§]

[1]Department of Psychiatry, University of Pittsburgh School of Medicine, Pittsburgh, PA, USA

[2]Department of Neurobiology, University of Pittsburgh School of Medicine, Pittsburgh, PA, USA

[3]Department of Neuroscience, University of Pittsburgh School of Medicine, Pittsburgh, PA, USA

[4]Department of Psychiatry, University of Texas Southwestern Medical Center, Dallas, TX, USA

Correspondence: Dr K Mirnics, Department of Psychiatry, University of Pittsburgh School of Medicine, E1655 Biomed Sci Tower, Pittsburgh, PA 15261, USA. E-mail: karoly+@pitt.edu

ABSTRACT

Brain-derived neurotrophic factor (BDNF) has been reported to be critical for the development of cortical inhibitory neurons. However, the effect of BDNF on the expression of transcripts whose protein products are involved in GABA neurotransmission has not been assessed. In this study, gene expression profiling using oligonucleotide microarrays was performed in prefrontal cortical tissue from mice with inducible deletions of BDNF. Both embryonic and adulthood ablation of BDNF gave rise to many shared transcriptome changes. BDNF appeared to be required to maintain gene expression in the SST-NPY-TAC1 subclass of GABA neurons, although the absence of BDNF did not alter their general phenotype as inhibitory neurons. Furthermore, we observed expression alterations in genes encoding early-immediate genes (ARC, EGR1, EGR2, FOS, DUSP1, DUSP6) and critical cellular signaling systems (CDKN1c, CCND2, CAMK1g, RGS4). These BDNF-dependent gene expression changes may illuminate the biological basis for transcriptome changes observed in certain human brain disorders.

INTRODUCTION

Brain-derived neurotrophic factor (BDNF) is a critical regulator of neural development, promoting the survival of a variety of neurons in the CNS (for a review, see (125)). For example, the development of certain phenotypic features of cortical GABA neurons requires BDNF (126-130). In addition, BDNF is produced and released in an activity-dependent fashion by pyramidal neurons, a major target of GABA neurons. Together, these data suggest that BDNF is a target-derived trophic factor for GABA interneurons. In turn, GABA neurons might regulate BDNF synthesis and release from pyramidal cells in an activity-dependent manner (131, 132).

Cortical GABA neurons are heterogeneous and can be subdivided into a variety of subclasses based on their expression of different calcium binding proteins and neuropeptides (for a review, see (133, 134). These subclasses also differ in their laminar distribution, connectivity and physiological properties. However, the

dependence of different subclasses of GABA neurons on BDNF signaling remains to be determined. For example, the inducible deletion of BDNF (135) does not result in altered mRNA levels of the 67 kDa isoform of glutamic acid decarboxylase (GAD1) or parvalbumin (PARV) in adult mice (136).

Furthermore, the dependence of any given neuronal type on BDNF may differ as a function of developmental stage (137). For example, BDNF is a critical mediator of the maturation of glutamatergic synapses in developing mouse somatosensory cortex (138). Similarly, developing dorsal thalamus neurons need BDNF for survival from the cerebral cortex, and dorsal thalamic cell death can be regulated by increasing or blocking cortical levels of BDNF (139). In addition, behavioral deficits are more pronounced in mice with embryonic than adult ablation of BDNF (135). These data suggest that BDNF requirement of neurons may change from development to adulthood, and mice with embryonic and adult deletion of BDNF may exhibit markedly different neocortical transcriptome profiles.

To obtain comprehensive insight into the BDNF-dependent transcriptome changes and determine what aspects of interneuronal phenotypes are affected by reduced BDNF levels, we performed high-density oligonucleotide microarray profiling of the prefrontal cortex of mice with inducible deletion of BDNF. The goals of the current study were to: 1) establish transcriptome changes which are a result of embryonic deletion of BDNF, 2) identify transcriptome changes that are a result of adult deletion of BDNF, 3) describe the genes that are most influenced by the absence of BDNF across both conditions, 4) define the transcriptome differences between the embryonic and adult BDNF-deficient mice, and 5) identify neuronal cortical phenotypes that may be preferentially affected by the absence of BDNF.

MATERIALS AND METHODS

A. BDNF-deficient mice

All mice used in this experimental series were described previously (135, 136). To generate the animals for the current experimental series, two genetically-altered, independently-derived mouse strains were used. Reduction of BDNF expression was

achieved using an inducible knockout (KO) of the BDNF gene where two transgenes, the tetracycline transactivator (tTA) gene driven by neuron-specific enolase (NSE) promoter (nse-tTA) (140) and the Cre recombinase gene under the control of tTA-responsive tetO promoter (tetO-cre) (141, 142) regulate the deletion of floxed exon V of BNDF (143) in a tetracycline-dependent manner. The two mouse lines with NSE-tTA and tetO-cre transgenes were both maintained as homozygotes. Crossing of these lines resulted in bigenic mice (143). For the embryonic deletion of BDNF, mice were bred in the absence of the tetracycline analogue doxycycline; this resulted in late embryonic ablation of BDNF (140). For the adulthood deletion of BDNF, mice were bred in the presence of doxycycline (1 mg/ml) in drinking water and maintained on this until 3 months of age. At that time doxycycline was removed from the drinking water, thus inducing recombination. Maximum recombination was achieved 4 weeks after doxycycline removal (135) resulting in a >70% reduction in BDNF transcript and protein levels (135, 136). Littermates with NSE-tTA and tetO-cre transgenes were used as controls. These mice expressed similar levels of BDNF as wild type mice (135).

Mice with BDNF deletion induced from embryogenesis or in adulthood, together with the corresponding control animals, were sacrificed between 5 and 6 months of age. The experimental series consisted of frontal cortices from a total of 38 animals with different animals used for each method of gene expression analysis. For the microarray experiments, the adulthood and embryonic BDNF ablation groups consisted of 4 animals each, and these animals were compared to 3 control animals for each of the experimental groups (14 animals in total). For qPCR experiments, we used 3 animals for each experimental and control group (12 animals in total). For the in situ hybridization experiments, an additional 3 animals per group were assessed (12 animals in total).

B. Microarray experiments

Frontal cortices were rapidly dissected, frozen on dry ice, and stored at –80°C until RNA extraction. Total RNA was isolated using the Trizol reagent. RNA quality was assessed using the Agilent Bioanalyzer. Reverse transcription, in vitro

transcription and fragmentation were performed according to manufacturer's recommendation (Affymetrix, Sunnyvale, CA). Samples were hybridized onto MOE430A mouse Affymetrix GeneChips which contained >22,000 probesets using the Affymetrix hybridization station. To avoid microarray batch variation only microarrays from a single lot were used. Microarrays were considered for use only if the average 3':5' ratio for GAPDH and actin did not exceed 1:1.2. Segmentation of scanned microarray images was performed by Microarray Analysis Suite 5.0 (MAS5). Determination of expression levels and scaling were performed using Robust Multi-array Average (RMA) (144, 145). The resulting dataset was filtered for genes that reported <30% present calls based on MAS5 analysis. For scale linearity, the data were log2 transformed, and differential expression was established using average log2 ratio (ALR) between the studied cohorts (|ALR|=1 corresponds to a 2-fold increase or decrease, |ALR|= 0.585 represents a 50% change, while |ALR|= 0.263 depicts a 20% expression alteration).

C. Data analysis

Identification of differentially expressed genes across mice with adult and embryonic BDNF-deletion. We identified genes as differentially expressed between all wild type and all BDNF KO samples if they fulfilled the following 4 criteria: 1) reported > 0.263 |average $\log_2$ ratio| (|ALR|) in embryonic BDNF-deleted mice versus their matched wild-type controls, 2) a groupwise Student t-test reported $p< 0.05$ in the embryonic BDNF-deleted mice versus their matched wild-type controls, 3) reported > 0.263 |ALR| in adult BDNF-deleted mice versus their matched wild-type controls and 4) a groupwise Student t-test reported $p< 0.05$ in the adult BDNF-deleted mice versus their matched wild-type controls. These combined criteria were implemented to reduce false positive findings and eliminate significant, but very small, expression changes that may have a marginal biological effect (146). A gene was "definitively changed" if it met all 4 aforementioned criteria, while a gene was considered "putatively changed" if it met 3 of these 4 criteria.

Identification of differentially expressed genes showing a more robust expression change in mice with embryonic BDNF-deletion. A gene was considered to

show a more robust expression change in the comparison of mice with embryonic BDNF deletion and matching wild-type controls if it reported: 1) an |ALR| difference > 0.263 between the two BDNF-deleted mouse groups versus their own controls ($ALR_{DIF} = ALR_{ADULT\ KO\text{-}WT} - ALR_{EMBRYONIC\ KO\text{-}WT}$) and 2) Student t-test significance for the embryonic BDNF-ablated mice at $p < 0.05$ level in comparison to the control littermates.

Estimation of false discovery ratio (FDR). Estimation of FDR was performed for the genes that were commonly altered between the mice with embryonic and adult deletion of BDNF using a custom-designed permutation-based method (147-149). Briefly, microarrays were randomly mixed into two groups containing near equal numbers of experimental and control arrays (see Supplemental Figure 1). Six random permutations were performed with a blocking factor of mouse type (e.g., embryonic or adult deletion). For each permutation the two array groups were subjected to the same analysis that was used to determine the expression differences (see above). The discovered genes (false positive discovery) were averaged across the 6 comparisons and this value was expressed as a % of genes uncovered in the true experimental comparison, thus representing FDR in our experimental design.

Calculation of pooled significance. As we used independent samples with independent controls across the two groups of BDNF-ablated mice, expression levels were compared independently. Combined significance in all Tables was achieved by calculating the -2*(ln(pvalue embryonic BDNF KO comparison) + ln(pvalue for adult BDNF KO comparison)). The calculation was performed with four degrees of freedom.

Correlations: Correlations were calculated using Pearson r value for the $\log_2$ ratios between the two compared conditions. Clustering: Two-way clustering (sample and gene vectors) was performed on RMA generated log2-transformed expression levels using Euclidian distance measurement in Genes @ Work developed by IBM (150). Custom database: RMA normalized data and statistical measurements were imported into MS-Access. This database is searchable by significance, accession number, log ratio and gene name. The database displays individual RMA normalized data points across all experimental conditions. Data sharing: The MS-Access

database with all data points (~130 MB) is available upon request. All the raw microarray data has been deposited into GEO in a MIAME-MGED compliant format and is publicly available without any restrictions.

D. Transcript quantification by real-time quantitative polymerase chain reaction (qPCR)

For selected genes qPCR was performed on a new set of animals from each group (3 each for both experimental and control groups, 12 in total). Validation was performed on all samples, each originating from a single animal. After primer validation (primer efficiency 95-100%) the experiments were performed using standard delta Ct-Sybr Green measurement protocols with two independent reverse transcriptions and 4 replicates for each of the reverse transcriptions (151). Beta-actin was used as a standard normalizer. Statistical significance was calculated using a Student t-test using ΔCt measurements for each well. $\Delta\Delta$Ct was calculated as (average ΔCt experimental) – (average ΔCt control) between the tested groups. All primer sequences are available upon request.

E. In situ hybridization

Coronal sections of 20-μm thickness were cut from tissues containing the frontal cortex using a cryostat at -20°C, mounted on to gelatin-coated glass slides and stored at -80°C until use. cRNA [^{35}S]-labeled riboprobes were generated by PCR amplification of cDNA obtained from normal mouse brain. Approximately 3 ng (~2 X 10^6 DPM) of labeled probe was hybridized per each section. Methods used for hybridization were described previously (152, 153).

Slides were exposed to BioMax MR film (Kodak) for 8-22 h and then dipped and exposed to autoradiographic emulsion (NTB-2, Kodak) for 3-5 days at 4°C. Scion Image (version 4.0b) was used to obtain high-resolution scans of each film image for quantification. Darkfield images were captured from the developed slides. Slides were coded as to render the investigator performing the analysis blind to the condition of each specimen. KO and control sections were processed in parallel. Control hybridization with sense probe did not result in detecTable signal.

Quantification was performed by subtracting the average white matter optical density (OD) from the average signal measured across the neocortex (Scion Image). Relative expression differences were determined as a mean background-corrected OD differences of three animals per group, and significance was determined by Student t-test.

RESULTS

Transcriptome changes of mice with conditional ablation of BDNF during adult and embryonic life: similarities in expression patterns

Transcriptome analysis of BDNF-ablated mice at embryonic and adult age revealed a number of similarities. When compared to their respective control animals, 31 gene probesets reported significantly changed expression in both groups of BDNF-deficient mice (RMA measured $|ALR| > 0.263$ and $p<0.05$ in both groups of mice; Table 1). None of these probesets reported expression changes that were opposite in direction across the two BDNF KO groups. These expression data were part of a dataset with a low false discovery ratio (FDR<2%, Supplemental Figure 1). Of the genes with changed expression across both groups of mice, reductions in gene expression were more commonly observed than transcript inductions (24 probesets with a mean ALR= -0.59 and 7 probesets with a mean ALR= 0.39, respectively). In a two-way hierarchical clustering (Figure 1), both BDNF-deficient groups showed a clear separation of experimental and control animals, suggesting that this robust pattern is a clear consequence of BDNF deficiency. The expression ratios of the adult and embryonic BDNF-ablated mice versus their own controls showed a remarkable correlation for this set of genes ($r=0.96$, $p<0.001$; see Figure 2A for details).

Table 1 Gene expression differences observed in both embryonic and adult BDNF-deficient mice

Probesets	*Name*	*Symbol*	*Identifier*	*Adult KO*				*Embryonic KO*				*Comb pval*
				ExpAD	*CoAD*	*ALR*	*pval*	*ExpEM*	*CoEM*	*ALR*	*pval*	
1422168_a_at	brain-derived neurotrophic factor	Bdnf	NM_007540	5.84	7.01	−1.18	0.00042	5.26	6.46	−1.20	0.00060	0.000004
1418687_at	activity reg cytoskeletal-associated protein	Arc	NM_018790	9.42	10.33	−0.91	0.00232	8.15	9.31	−1.16	0.00687	0.000192
1455956_x_at	cyclin D2	Ccnd2	AV310588	6.70	7.55	−0.84	0.00370	5.65	6.39	−0.75	0.02427	0.000925
1424633_at	Ca/CaM-dependent protein kinase I gamma	Camk1g	AF428262	8.20	8.90	−0.69	0.00003	7.75	8.35	−0.60	0.00826	0.000004
1434745_at	cyclin D2	Ccnd2	BQ175880	7.61	8.28	−0.67	0.00672	6.54	7.28	−0.74	0.03152	0.002003
1417602_at	period homolog 2 (Drosophila)	Per2	NM_011066	6.06	6.73	−0.67	0.03908	5.00	5.35	−0.34	0.04550	0.013038
1416122_at	cyclin D2	Ccnd2	NM_009829	8.38	9.04	−0.66	0.01374	7.33	8.15	−0.82	0.03637	0.004299
1430127_a_at	cyclin D2	Ccnd2	AK007904	8.18	8.83	−0.65	0.04317	7.18	7.88	−0.70	0.00655	0.002594
1418025_at	basic helix-loop-helix domain, class B2	Bhlhb2	NM_011498	9.51	10.15	−0.64	0.01913	8.46	9.18	−0.72	0.01210	0.002169
1415834_at	dual specificity phosphatase 6	Dusp6	NM_026268	8.83	9.40	−0.58	0.03085	8.02	8.87	−0.85	0.00006	0.000025
1417065_at	early growth response 1	Egr1	NM_007913	11.28	11.83	−0.55	0.02152	10.09	10.97	−0.88	0.00109	0.000274
1450436_s_at	DnaJ (Hsp40) homolog, subfamily B, member 5	Dnajb5	AI664344	8.98	9.50	−0.52	0.01198	8.30	8.69	−0.39	0.02189	0.002424
1423853_at	RIKEN cDNA 6330527O06 gene	—	BC004791	10.38	10.89	−0.50	0.01238	9.83	10.46	−0.63	0.00361	0.000492
1417954_at	somatostatin	Sst	NM_009215	10.09	10.58	−0.49	0.00546	9.74	10.15	−0.41	0.02795	0.001495
1452094_at	proline 4-hydroxylase, alpha 1 polypeptide	P4ha1	AI314028	7.52	7.97	−0.45	0.02480	7.03	7.50	−0.46	0.02224	0.004691
1417251_at	palmdelphin	Palmd	NM_023245	5.71	6.14	−0.43	0.00451	5.31	5.64	−0.33	0.03197	0.001421
1422742_at	HIV type I enhancer binding protein 1	Hivep1	NM_007772	6.97	7.38	−0.41	0.01321	6.24	6.84	−0.59	0.00332	0.000483
1460711_at	RIKEN cDNA 9930116P15 gene	—	BG071611	6.90	7.30	−0.40	0.03642	6.01	6.69	−0.68	0.02830	0.008118
1419127_at	neuropeptide Y	Npy	NM_023456	9.71	10.11	−0.39	0.02543	9.27	9.65	−0.38	0.03483	0.007110
1426858_at	inhibin beta-B	Inhbb	BB353211	6.30	6.69	−0.39	0.00439	5.42	5.82	−0.40	0.04464	0.001869
1417403_at	Elongation of long chain fatty acids 6	Elovl6	AF480860	6.79	7.16	−0.37	0.04079	6.35	6.66	−0.31	0.00265	0.001095
1426640_s_at	tribbles homolog 2 (Drosophila)	Trib2	BC027159	7.78	8.15	−0.36	0.02039	6.93	7.55	−0.62	0.00540	0.001113
1417673_at	growth factor receptor bound protein 14	Grb14	NM_016719	6.60	6.95	−0.35	0.02909	5.98	6.35	−0.37	0.00620	0.001736
1426641_at	tribbles homolog 2 (Drosophila)	Trib2	BB354684	5.71	6.02	−0.31	0.03881	4.87	5.33	−0.46	0.01203	0.004047
1437185_s_at	thymosin, beta 10	Tmsb10	AV148480	12.24	11.97	0.27	0.01350	11.63	11.31	0.32	0.00388	0.000569
1426766_at	RIKEN cDNA 6330403K07 gene	—	AK018106	10.83	10.54	0.29	0.01077	10.05	9.73	0.32	0.02537	0.002515
1434109_at	RIKEN cDNA A930014C21 gene	—	AV291265	6.49	6.14	0.36	0.04088	5.78	5.51	0.27	0.01263	0.004423
1426510_at	RIKEN cDNA C330023F11 gene	—	AW537824	8.11	7.74	0.37	0.03926	7.58	7.19	0.39	0.00284	0.001127
1431946_a_at	amyloid beta (A4) precursor protein-binding, A1	Apba2bp	AK013520	8.24	7.86	0.38	0.03308	7.24	6.97	0.28	0.02993	0.007838
1425870_a_at	Kv channel-interacting protein 2	Kcnip2	AF439339	7.92	7.47	0.45	0.04324	7.59	7.26	0.33	0.01420	0.005155
1417649_at	cyclin-dependent kinase inhibitor 1C (P57)	Cdkn1c	NM_009876	8.36	7.57	0.80	0.00640	7.67	6.98	0.69	0.00328	0.000247

A differentially expressed gene had to show an $|ALR| > 0.263$ and a significance of $P > 0.05$ in both the embryonic and adult BDNF-ablated comparisons. Thirty-one gene probesets fulfilled these criteria. (Probeset – Affymetrix GeneChip identifier; ExpAD and ExpEM – RMA log2 expression level of adult and embryonic BDNF-deficient animals; CoAD and CoEM- RMA log2 expression level of corresponding control wild-type animals; ALR- average log2 ratio for the adult and embryonic BDNF-deficient comparisons; pval – Student's *T*-test *P*-value; Comp pval – *P*-value calculated across the two comparisons using Chi distribution).

Figure 9. Two-way clustering of the normalized expression levels of 31 genes showing common expression changes in adult and embryonic BDNF-ablated mice.

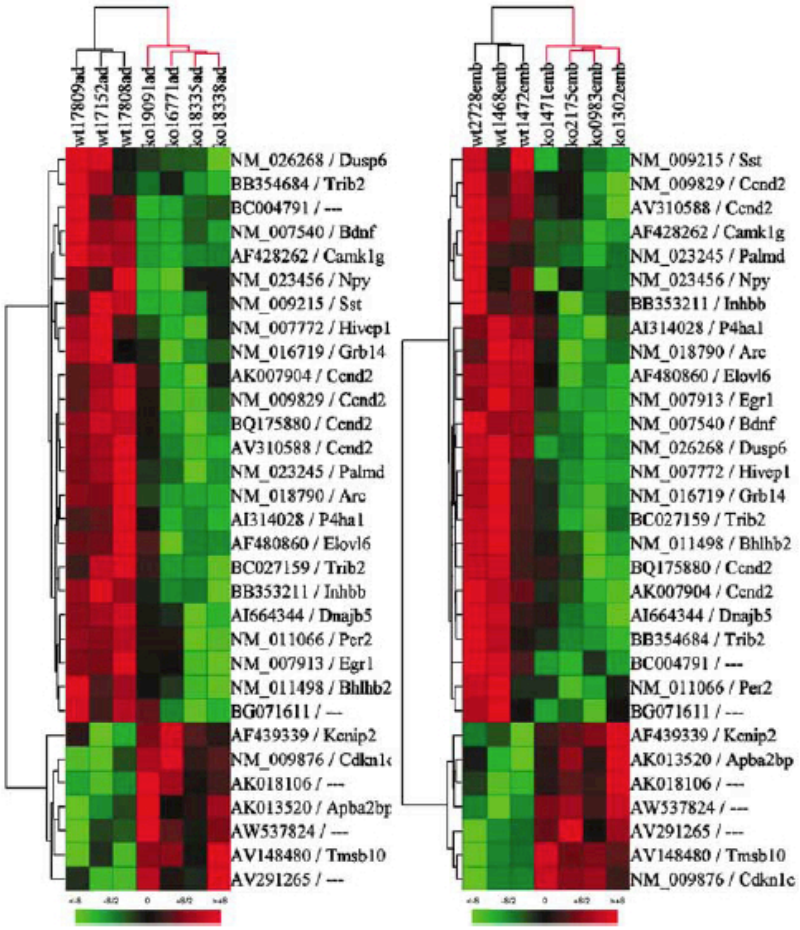

Figure 1 Two-way clustering of the normalized expression levels for 31 genes showing common expression changes in adult and embryonic brain-derived neurotrophic factor (BDNF)-ablated mice. In the vertical dendrogram each arm represents a single animal (red-cKO; black – wild-type control), rows denote gene probesets with NCBI accession numbers and gene symbols. Each pixel denotes a log2-normalized expression level in a single animal. Intensity of red is proportional to transcript increase, green intensity is proportional to transcript decrease. Dark boxes represent unchanged expression. Based on the expression levels of these 31 genes, the vertical dendrogram perfectly separated out the mouse genotypes both in the adult (left panel) and embryonic BDNF comparisons (right panel). Note that the clustering gave rise to an identical pattern in the two groups of the BDNF-deficient animals. For gene names and statistical parameters, see Table 1.

Figure 10. Correlation of expression changes between the adult and Embryonic BDNF-deficient animals.

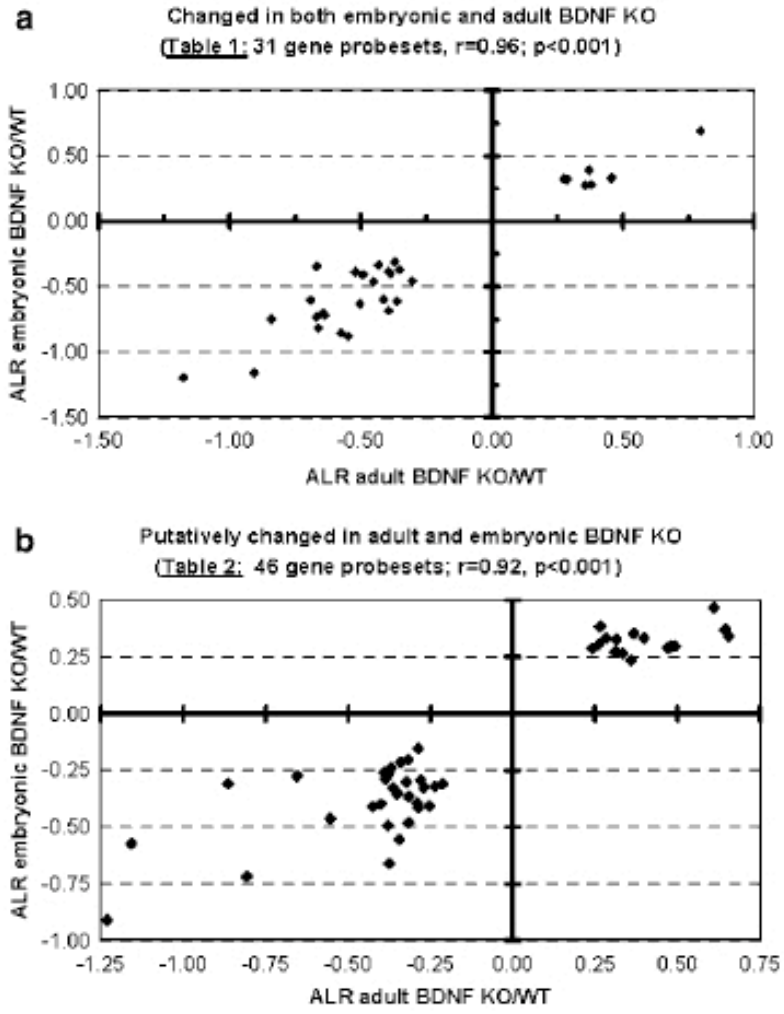

Figure 2 Correlation of expression changes between the adult and Embryonic brain-derived neurotrophic factor (BDNF)-deficient animals. *X* axis represents the average log2 ratio (ALR) in the adult BDNF-ablated – wild type comparison, while the *Y* axis represents the ALR in the embryonic BDNF-deficient – wild-type comparison. Each symbol represents a single gene. Both the definitively changed genes (**a**) and putatively changed genes (**b**) showed a very high correlation across the two models ($r = 0.96$, $P < 0.001$ and $r = 0.92$, $P < 0.001$, respectively). For ALR rations and other data see Tables 1 and 2.

We also identified a set of genes that showed a putative expression change across the two BDNF-ablated mouse groups (Table 2). When compared to their own controls, these genes showed a significant expression change for at least 3 of the 4 statistical criteria used in this study (ALR>0.263 and p<0.05 in both groups). Based on the following arguments, the majority of these 46 transcripts are very likely to represent true biological expression differences: 1) The FDR for this group was ~16 % (Supplemental Figure 1); 2) This group contained several duplicate microarray probe sets against genes that already reported a definitive expression change in Table 1; 3) Clustering with these genes perfectly separated out the KO and the WT animals in both the adult and embryonic BDNF ablation (Supplemental Figure 2); 4) For these genes, the expression levels between the two groups of BDNF-ablated mice were highly correlated (r=0.92; Figure 2B). 5) Selected transcript changes from this group were successfully verified by qPCR (see below).

Not surprisingly, the gene with the most reduced expression level was BDNF in both the adult and embryonic BDNF-ablated mice (ALR=-1.18 with p=0.0042 and ALR=-1.20 with p<0.0006, respectively), which further validates our findings and is consistent with previously published finding that these mice have a >70% expression deficit in BDNF expression (135, 136). The observed expression changes also involved 3 independent probesets of cyclin D2 (CCND2), as well as genes that interact with CCND2 (cyclin-dependent kinase inhibitor 1C - CDKn1c and Ca/CaM-dependent protein kinase I gamma - CAMK1g). Furthermore, the levels of the early immediate genes (IEG) activity reg cytoskeletal-associated protein (ARC), early growth response 1 (EGR1), early growth response 2 (EGR2), FBJ osteosarcoma oncogene (FOS), dual specificity phosphatase 1 (DUSP1) and dual specificity phosphatase 6 (DUSP6) were also robustly altered, suggesting that BDNF levels are critical for regulation of a complex IEG-dependent transcription network.

Furthermore, regulator of G-protein signaling 4 (RGS4) transcript was significantly decreased in the cortex of mice with the adulthood deletion of BDNF (ALR=-0.35; p=0.0046). A similar trend was observed in the mice with embryonic BDNF deletion (ALR=-0.35; p=0.0638), suggesting a causal relationship between BDNF expression and RGS4 transcript levels.

Table 2 Genes with putatively changed expression in both embryonic and adult BDNF-deficient mice

Probesets	*Name*	*Symbol*	*Identifier*	*Adult KO*				*Embryonic KO*				*Comb pval*
				ExpAD	*CoAD*	*ALR*	*pval*	*ExpEM*	*CoEM*	*ALR*	*pval*	
A. p < 0.05 and |ALR| > 0.263 in Ad KO and p < 0.05 or |ALR| > 0.263 in Em KO												
1448756_at	S100 calcium-binding protein A9 (calgranulin B)	S100a9	NM_009114	5.77	7.00	−1.23	0.04804	6.31	7.22	−0.91	0.43884	0.102452
1428301_at	RIKEN cDNA 2610042L04 gene	—	BM195235	7.81	8.97	−1.16	0.04744	6.27	6.84	−0.57	0.12880	0.037258
1416783_at	tachykinin 1	Tac1	NM_009311	5.58	6.45	−0.86	0.03929	4.79	5.10	−0.31	0.05258	0.014836
1422169_a_at	brain-derived neurotrophic factor	Bdnf	AY057913	7.08	7.74	−0.66	0.01110	6.55	6.83	−0.28	0.07254	0.006539
1423978_at	SH3-binding kinase	Sbk	BC025837	7.48	7.90	−0.43	0.04402	6.68	7.08	−0.41	0.11136	0.030971
1455439_a_at	lectin, galactose binding, soluble 1	Lgals1	AI642438	7.18	7.57	−0.39	0.00969	6.60	6.86	−0.26	0.01907	0.001774
1438370_x_at	—	—	BB357126	10.47	10.85	−0.39	0.00394	9.87	10.15	−0.29	0.07322	0.002637
1419573_a_at	lectin, galactose binding, soluble 1	Lgals1	NM_008495	7.29	7.66	−0.37	0.00974	6.90	7.14	−0.24	0.01056	0.001047
1451037_at	protein tyrosine phosphatase, non-receptor type 9	Ptpn9	BB224063	7.71	8.05	−0.34	0.02627	7.25	7.46	−0.21	0.02510	0.005489
1416514_a_at	fascin homolog 1, actin bundling protein	Fscn1	NM_007984	9.42	9.75	−0.32	0.02729	8.69	8.99	−0.30	0.12205	0.022328
1423427_at	adenylate cyclase activating polypeptide 1	Adcyap1	AI323434	7.99	8.31	−0.32	0.00169	7.35	7.56	−0.20	0.00926	0.000189
1450011_at	hydroxysteroid (17-beta) dehydrogenase 12	Hsd17b12	AK012103	8.85	9.14	−0.29	0.01448	8.25	8.40	−0.15	0.00025	0.000050
1425662_at	cytidine and dCMP deaminase domain 1	Cdadc1	AV348063	5.65	5.34	0.31	0.02739	5.02	4.75	0.27	0.10087	0.019042
1423630_at	cytoglobin	Cygb	BM899392	8.27	7.91	0.36	0.00421	7.87	7.64	0.23	0.02091	0.000911
1431569_a_at	RIKEN cDNA 2700050C12 gene	—	AK012406	8.44	7.96	0.48	0.00574	7.82	7.52	0.30	0.25971	0.011191
1460167_at	aldehyde dehydrogenase family 7, member A1	Aldh7a1	BC012407	8.21	7.72	0.49	0.04077	7.45	7.15	0.30	0.26359	0.059467
1449123_at	inter-alpha trypsin inhibitor, heavy chain 3	Itih3	NM_008407	8.31	7.67	0.64	0.00437	7.53	7.16	0.37	0.10354	0.003933
1419635_at	RIKEN cDNA 4833420G17 gene	—	NM_026127	5.56	4.91	0.66	0.03306	6.09	5.75	0.34	0.17292	0.035241

Probesets	*Name*	*Symbol*	*Identifier*	*Adult KO*				*Embryonic KO*				*Comb pval*
				ExpAD	*CoAD*	*ALR*	*pval*	*ExpEM*	*CoEM*	*ALR*	*pval*	
B. p < 0.05 and |ALR| > 0.263 in Em KO and p < 0.05 or |ALR| > 0.263 in Ad KO												
1427683_at	early growth response 2	Egr2	X06746	7.00	7.81	−0.81	0.07995	5.57	6.29	−0.72	0.00360	0.002637
1434403_at	sprouty protein with EVH-1 domain 2	Spred2	AV229054	8.81	9.19	−0.37	0.05799	7.90	8.56	−0.66	0.00903	0.004480
1423100_at	FBJ osteosarcoma oncogene	Fos	AV026617	9.95	10.30	−0.35	0.12465	8.51	9.06	−0.56	0.04597	0.035307
1438009_at	histone 1, H2ae	Hist1h2ae	W91024	5.99	6.37	−0.38	0.25208	5.95	6.44	−0.49	0.00212	0.004555
1448830_at	dual specificity phosphatase 1	Dusp1	NM_013642	9.20	9.52	−0.32	0.05770	8.25	8.73	−0.48	0.04194	0.016998
1416029_at	TGFB inducible early growth response 1	Tieg1	NM_013692	7.27	7.83	−0.55	0.09105	6.70	7.16	−0.46	0.01523	0.010515
1455812_x_at	Slit-like 2 (Drosophila)	Slitl2	BB530515	3.92	4.20	−0.29	0.18232	3.33	3.74	−0.42	0.02649	0.030585
1426519_at	proline 4-hydroxylase, alpha 1 polypeptide	P4ha1	BB253720	6.73	6.99	−0.25	0.03974	6.47	6.88	−0.41	0.01551	0.005172
1436584_at	sprouty homolog 2 (Drosophila)	Spry2	BB529691	8.24	8.64	−0.40	0.05828	7.64	8.04	−0.40	0.01948	0.008835
1455893_at	RIKEN cDNA 2610028F08 gene	—	BG067392	7.40	7.69	−0.29	0.10660	6.78	7.17	−0.39	0.01066	0.008840
1417930_at	Ngfi-A binding protein 2	Nab2	NM_008668	8.01	8.33	−0.32	0.05104	7.42	7.79	−0.37	0.03393	0.012744
1416286_at	regulator of G-protein signaling 4	Rgs4	BC003882	10.43	10.78	−0.35	0.06387	9.85	10.20	−0.35	0.00460	0.002682
1416432_at	6-p-fructo-2-kinase/fructose-2,6-biphosphatase 3	Pfkfb3	NM_133232	6.07	6.34	−0.27	0.07739	5.06	5.39	−0.33	0.03019	0.016493
1452160_at	TCDD-inducible poly(ADP-ribose) polymerase	Tiparp	BB762264	5.51	5.87	−0.36	0.12212	4.63	4.96	−0.33	0.00977	0.009226
1451046_at	zinc finger protein, multitype 1	Zfpm1	AA014267	7.56	7.80	−0.24	0.04611	7.04	7.36	−0.32	0.01008	0.004033
1421962_at	DnaJ (Hsp40) homolog B5	Dnajb5	AI664344	7.92	8.13	−0.21	0.00677	7.42	7.73	−0.31	0.00781	0.000574
1418587_at	Tnf receptor-associated factor 3	Traf3	NM_011632	8.55	8.84	−0.28	0.08660	8.00	8.29	−0.29	0.03449	0.020351

Table 2 Continued

Probesets	*Name*	*Symbol*	*Identifier*	*Adult KO*				*Embryonic KO*				*Comb pval*
				ExpAD	*CoAD*	*ALR*	*pval*	*ExpEM*	*CoEM*	*ALR*	*pval*	
1451264_at	RIKEN cDNA 4930488L10 gene	—	BC019939	8.11	8.48	−0.38	0.06498	7.60	7.86	−0.26	0.03320	0.015403
1449030_at	synapsin II	Syn2	BM936504	9.76	9.43	0.33	0.16956	9.68	9.42	0.27	0.00896	0.011375
1416996_at	TBC1 domain family, member 8	Tbc1d8	BC005421	8.12	7.88	0.24	0.02742	7.24	6.95	0.29	0.02031	0.004728
1422580_at	myosin, light polypeptide 4	Myl4	NM_010858	8.52	8.05	0.47	0.05170	7.47	7.17	0.29	0.01517	0.006391
1420388_at	protease, serine, 12 neurotrypsin (motopsin)	Prss12	NM_008939	9.22	8.96	0.26	0.04414	8.89	8.58	0.30	0.01920	0.006840
1419398_a_at	deleted in polyposis 1	Dp1	NM_007874	10.28	9.97	0.31	0.08339	9.76	9.43	0.33	0.00457	0.003383
1419687_at	RIKEN cDNA D930010J01 gene	—	NM_134147	7.71	7.43	0.28	0.07793	6.98	6.65	0.33	0.01220	0.007564
1448201_at	secreted frizzled-related sequence protein 2	Sfrp2	NM_009144	6.03	5.63	0.40	0.06491	5.38	5.05	0.33	0.01146	0.006104
1427038_at	preproenkephalin 1	Penk1	M13227	9.22	8.86	0.37	0.08052	8.83	8.47	0.35	0.01677	0.010273
1418149_at	chromogranin A	Chga	NM_007693	9.51	9.25	0.26	0.14020	8.93	8.54	0.39	0.01487	0.014950
1422552_at	RIKEN cDNA 2410012A13 gene	—	NM_023396	8.37	7.76	0.61	0.09098	7.15	6.69	0.47	0.04446	0.026332

For table layout and abbreviations, see Table 1. (A) Eighteen gene probesets showed $|ALR| > 0.263$ and $P < 0.05$ in the adult BDNF-ablated mice and a $|ALR| > 0.263$ or $P < 0.05$ in the embryonic comparison. (B) Twenty-eight gene probesets showed $|ALR| > 0.263$ and $P < 0.05$ in the embryonic BDNF-ablated mice and a $|ALR| > 0.263$ or $P < 0.05$ in the adult comparison. Note that across the two models the expression difference always reaches statistical significance (last column).

Somatostatin (SST), neuropeptide Y (NPY) and tachykinin 1 (TAC1) are all interneuronal peptide transcripts which are co-expressed to a large degree and define a subset of GABA-containing neocortical interneurons (154-156). All three transcripts were downregulated in both mice with embryonic (SST: ALR=-0.41; p=0.0279; NPY: ALR=-0.38; p=0.0348; TAC1: ALR=-0.31; p=0.0525) and adulthood (SST: ALR=-0.49; p=0.0054; NPY: ALR=-0.39; p=0.0254; TAC1: ALR=-0.86; p=0.0392) deletion of BDNF.

Transcriptome changes of mice with conditional ablation of BDNF during adult and embryonic life: differences in expression patterns

In addition to gene expression changes that were shared between the embryonic and adult KO animals, we also observed a number of gene expression changes that were specific to one of the BDNF-ablated groups. For the listing of all differentially expressed genes, see Supplemental Table 1 and Supplemental Table 2. From all these changes, one group of genes attracted our attention in particular. Namely, as the embryonic BDNF deletion creates a behavioral phenotype not observed in the adult BDNF-deficient animals (135), we hypothesized that the embryonic BDNF-deficient mice would show an expression phenotype not present in the adult KO animals. To identify this putative gene expression phenotype, we defined a set of genes that showed significant expression differences in the comparison of embryonic BDNF KO and control animals, but which were not observed (or not observed to the same degree) in the comparison of the adult BDNF KO mice and their matching wild-type controls (Table 3). Only 31 gene probesets matched these criteria. Of these expression changes, 11 were more upregulated in the embryonic comparison vis-à-vis the adult comparison, while 20 genes were more downregulated. Gene expression differences included alterations in critical developmental genes (HOMER1, neurogenic differentiation 6-NEUROD6/MATH2

neuronal pentraxin 2-NPTX2 and growth arrest specific 5-GAS5), RAN-RAP system

Table 3 More robust gene expression differences in the embryonic BDNF-ablated comparison than those observed in the adult BDNF-deficient comparison

Probesets	*Name*	*Symbol*	*Identifier*	*Adult KO*		*Embryonic KO*		*dALR*
				ALR	*pval*	*ALR*	*pval*	
1434216_a_at	DNA segment, Chr 7, Roswell Park 2 complex	D7Rp2e	BG070689	−0.41	0.39441	0.74	0.02101	1.16
1432332_a_at	DNA segment, Chr 7, Roswell Park 2 complex	D7Rp2e	AK008430	−0.22	0.43202	0.52	0.03422	0.74
1449410_a_at	growth arrest specific 5*	Gas5	NM_013525	−0.27	0.18080	0.28	0.03913	0.55
1419040_at	cytochrome P450, family 2, subfamily d, polypeptide 22	Cyp2d22	BF683039	−0.05	0.79526	0.45	0.01025	0.51
1428966_at	RIKEN cDNA 2610204K14 gene	—	AK018614	-0.09	0.27899	0.34	0.00323	0.43
1427011_a_at	LanC-like 1	Lancl1	AW107959	−0.11	0.45075	0.30	0.04989	0.41
1434292_at	RIKEN cDNA E130013N09 gene	—	BI731047	0.13	0.63777	0.53	0.04471	0.40
1420720_at	neuronal pentraxin 2*	Nptx2	BC026054	0.13	0.65458	0.49	0.04813	0.37
1449960_at	neuronal pentraxin 2*	Nptx2	NM_016789	0.07	0.64422	0.41	0.03622	0.34
1451092_a_at	RAN GTPase activating protein 1**	Rangap1	AV258722	0.00	0.93052	0.28	0.03613	0.29
1428282_at	tubulin-specific chaperone e	Tbce	AK011899	0.01	0.89171	0.28	0.00170	0.27
1450740_a_at	microtubule-associated protein, RP/EB family 1	Mapre1	BM228525	−0.06	0.84564	−0.32	0.02792	−0.27
1434403_at	sprouty protein with EVH-1 domain 2	Spred2	AV229054	−0.37	0.05799	−0.66	0.00903	−0.29
1418710_at	CD59a antigen	Cd59a	NM_007652	−0.10	0.41494	−0.39	0.00681	−0.29
1423150_at	neuroendocrine protein 1, 7B2 protein	Sgne1	AK019337	−0.26	0.49295	−0.57	0.00001	−0.31
1422621_at	RAN binding protein 2**	Ranbp2	NM_011240	−0.02	0.93664	−0.33	0.04852	−0.31
1417111_at	mannosidase 1, alpha	Man1a	BB070019	0.05	0.41337	−0.26	0.04823	−0.31
1425266_a_at	RAP1, GTP-GDP dissociation stimulator 1**	Rap1gds1	BC011279	0.04	0.80633	−0.28	0.04685	−0.32
1450227_at	ankyrin repeat domain 6	Ankrd6	BM199504	0.08	0.34436	−0.26	0.04695	−0.34
1425710_a_at	homer homolog 1 (Drosophila)*	Homer1	AB019479	−0.11	0.69813	−0.46	0.02194	−0.35
1423161_s_at	sprouty protein with EVH-1 domain 1	Spred1	AV295157	−0.19	0.30073	−0.55	0.02840	−0.35
1426980_s_at	RIKEN cDNA E130012A19 gene	—	BC006054	−0.25	0.14832	−0.61	0.04842	−0.36
1425263_a_at	myelin basic protein	Mbp	L07508	−0.04	0.83612	−0.40	0.03312	−0.36
1448117_at	kit ligand	Kitl	BB815530	−0.12	0.15542	−0.52	0.04354	−0.40
1456464_x_at	synaptotagmin 11	Syt11	BB129990	0.13	0.49334	−0.27	0.02610	−0.41
1421571_a_at	lymphocyte antigen 6 complex, locus C	Ly6c	NM_010741	0.02	0.80623	−0.41	0.00059	−0.43
1418047_at	neurogenic differentiation 6 - Math-2*	Neurod6	NM_009717	−0.15	0.63093	−0.60	0.00565	−0.45
1448850_a_at	DnaJ (Hsp40) homolog C5	Dnajc5	BC012268	0.13	0.28633	−0.33	0.01554	−0.47
1418835_at	pleckstrin homology-like domain, A1	Phlda1	NM_009344	−0.09	0.66440	−0.58	0.00723	−0.49
1424768_at	caldesmon 1	Cald1	BC019435	0.18	0.45841	−0.31	0.04908	−0.49
1424443_at	transmembrane 6 superfamily member 1	Tm6sf1	BC023123	0.20	0.48044	−0.42	0.03891	−0.63

Layout is similar to Table 1 with an addition of a last column (dALR) that describes the ALR difference seen between the embryonic and adult comparisons. Genes marked with * represent developmental genes while ** denotes RAN-RAP system genes.

genes (RAN GTPase activating protein 1-RANGAP1, RAN binding protein 2, RANBP2, RAP1 GTP-GDP dissociation stimulator 1-RAPGDS1) and a variety of other functional classes.

Interestingly, the two most upregulated gene probes encoded the same gene, D7RP2e (DNA segment, Chr 7, Roswell Park 2 complex), a gene with uncharacterized function. These 31 genes, using a two-way hierarchical clustering, separated correctly the animals with the embryonic deletion of BDNF from their matched controls (Figure 3, left panel). However, the same genes could not distinguish between the adult BDNF-ablated animals and their control littermates (Figure 3, right panel).

Validation of microarray findings

All of the 10 expression changes (SST, NPY, ARC, CCND2, EGR1, RGS4, CAMK1g, DUSP6, amyloid beta precursor protein-binding A1 - APBA2bp, Kv channel-interacting protein 2 - KCNIP2 and BDNF) tested were successfully verified by RT-qPCR on a new set of control and BDNF-ablated animals (Figure 4). When the microarray-reported groupwise ALR values were compared to the groupwise qPCR - $\Delta\Delta$Ct values for the 10 genes, the microarray and qPCR datasets showed a high concordance in both the embryonic and adult BDNF-ablated animals ($r=0.88$, $p<0.001$ and $r=0.83$, $p<0.001$, respectively). The magnitudes of observed expression changes were more prominent in the qPCR experiment than those reported by the GeneChips, confirming previous reports that RMA analysis may underestimate the expression differences in microarray experiments (144, 148).

Figure 11. Figure 3. Expression changes specific for mice with the embryonic deletion of BDNF.

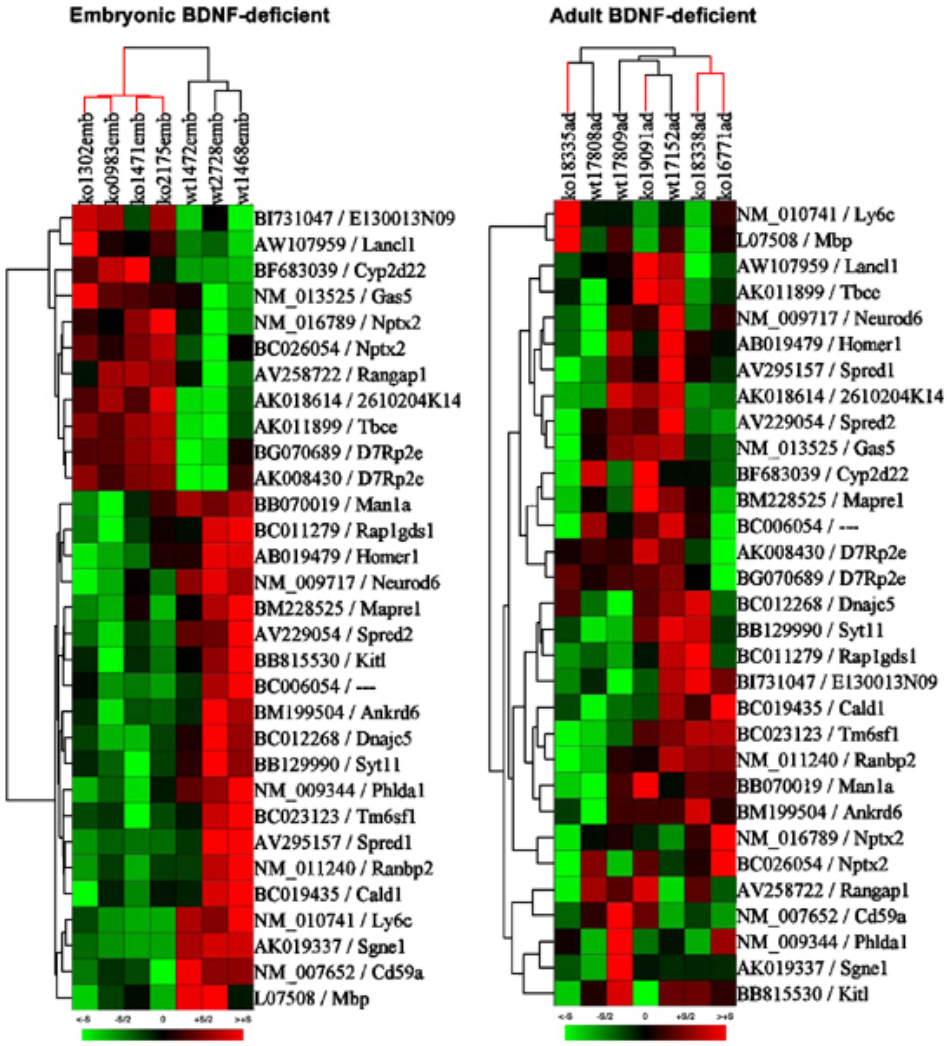

Figure 3. Expression changes specific for mice with the embryonic deletion of BDNF. A clustering of the 31 identified gene probes was performed and is presented similar to that seen in **Figure 1**. For source data and abbreviations see **Table 3**. Note that the wild-type and BDNF-ablated mice separate according to genotype (vertical dendrogram) in the mice with the embryonic deletion of BDNF (**left panel**), but not in mice with adult deletion of BDNF (**right panel**). Some of these expression changes may be responsible for behavioral differences between the two BDNF-deleted groups of mice.

Figure 12. Figure 4 Real-time qPCR and GeneChip microarray data are highly correlated.

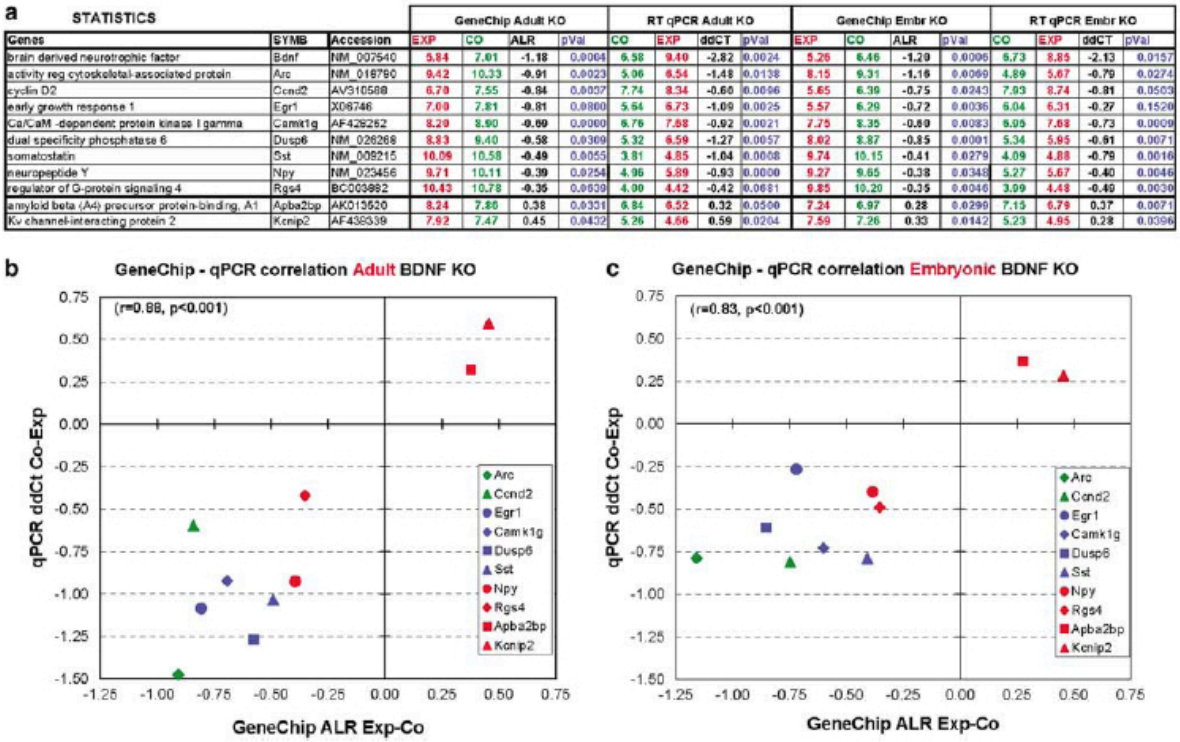

a STATISTICS

			GeneChip Adult KO				RT qPCR Adult KO				GeneChip Embr KO				RT qPCR Embr KO			
Genes	SYMB	Accession	EXP	CO	ALR	pVal	CO	EXP	ddCT	pVal	EXP	CO	ALR	pVal	CO	EXP	ddCT	pVal
brain derived neurotrophic factor	Bdnf	NM_007540	5.84	7.01	-1.18	0.0004	6.58	9.40	-2.82	0.0024	5.26	6.46	-1.20	0.0006	6.73	8.85	-2.13	0.0157
activity reg cytoskeletal-associated protein	Arc	NM_018790	9.42	10.33	-0.91	0.0023	5.06	6.54	-1.48	0.0138	8.15	9.31	-1.16	0.0069	4.89	5.67	-0.79	0.0274
cyclin D2	Ccnd2	AV310588	6.70	7.55	-0.84	0.0057	7.74	8.34	-0.60	0.0096	5.65	6.39	-0.75	0.0243	7.93	8.74	-0.81	0.0503
early growth response 1	Egr1	X06746	7.09	7.81	-0.81	0.0800	5.64	6.73	-1.09	0.0025	5.57	6.29	-0.72	0.0036	6.04	6.31	-0.27	0.1520
Ca/CaM -dependent protein kinase I gamma	Camk1g	AF429252	8.20	8.90	-0.69	0.0000	6.76	7.68	-0.92	0.0021	7.75	8.35	-0.60	0.0083	8.95	7.88	-0.73	0.0009
dual specificity phosphatase 6	Dusp6	NM_026268	8.83	9.40	-0.58	0.0309	5.32	6.59	-1.27	0.0057	8.02	8.87	-0.85	0.0001	5.34	5.95	-0.61	0.0071
somatostatin	Sst	NM_009215	10.09	10.58	-0.49	0.0055	3.81	4.85	-1.04	0.0008	9.74	10.15	-0.41	0.0279	4.09	4.88	-0.79	0.0016
neuropeptide Y	Npy	NM_023456	9.71	10.11	-0.39	0.0254	4.96	5.89	-0.93	0.0000	9.27	9.65	-0.38	0.0348	5.27	5.67	-0.40	0.0046
regulator of G-protein signaling 4	Rgs4	BC003982	10.43	10.78	-0.35	0.0639	4.00	4.42	-0.42	0.0681	9.85	10.20	-0.35	0.0046	3.09	4.48	-0.40	0.0030
amyloid beta (A4) precursor protein-binding, A1	Apba2bp	AK013520	8.24	7.86	0.38	0.0351	6.84	6.52	0.32	0.0500	7.24	6.97	0.28	0.0290	7.15	6.79	0.37	0.0071
Kv channel-interacting protein 2	Kcnip2	AF436039	7.92	7.47	0.45	0.0432	5.26	4.66	0.59	0.0204	7.59	7.26	0.33	0.0142	5.23	4.95	0.28	0.0396

Figure 4 Real-time qPCR and GeneChip microarray data are highly correlated. 10 genes were chosen for further verification based on their biological significance on new cohorts of brain-derived neurotrophic factor (BDNF)-deficient and control mice. The statistical data obtained with the two methods showed a high degree of similarity (**a**). The qPCR – microarray correlation was very high in both the animals with adult (**b**) and embryonic (**c**) BDNF deletion ($r = 0.88$, $P < 0.001$ and $r = 0.83$, $P < 0.001$, respectively).

Figure 4. Real-time qPCR and GeneChip microarray data are highly correlated

10 genes were chosen for further verification based on their biological significance on new cohorts of BDNF-deficient and control mice. The statistical data obtained with the two methods showed a high degree of similarity (**A**). The qPCR – microarray correlation was very high in both the animals with adult (**B**) and embryonic (**C**) BDNF deletion (r=0.88, p<0.001 and r=0.83, p<0.001, respectively).

BDNF is required for maintenance of SST-NPY interneuronal phenotype in the frontal cortex

BDNF is believed to be critical for the development of cortical interneurons (128, 130, 157-159), but the specificity of BDNF action for specific subclasses of interneurons is not known. Our previously published study suggested that the PARV containing interneuronal class is not affected in either one of these BDNF-ablated mice and that the overall GABA-ergic phenotype of the interneurons, judged by presence of GAD1 transcript levels, is preserved (136). However, both the microarray and qPCR datasets strongly suggested that BDNF expression has a critical effect on SST, NPY and TAC1-containing interneuronal populations. In addition, in situ hybridization (Figure 5) revealed a robust and significant downregulation of SST in the neocortex of both the adult and embryonic BDNF-ablated mice (1.7 and 1.9-fold, respectively) in another cohort of mice. Because SST, NPY and TAC1 are co-expressed to a large extent in a subset of GABA-ergic cortical cells (154-156, 160-163), we suggest that these transcripts are downregulated in the same interneuronal sub-population and most likely represent an interlinked, BDNF-dependent pathology.

Figure 13. Figure 5. Somatostatin (SST) and neuropeptide Y (NPY) mRNA expression is reduced I with embryonic and adulthood BDNF-deletion.

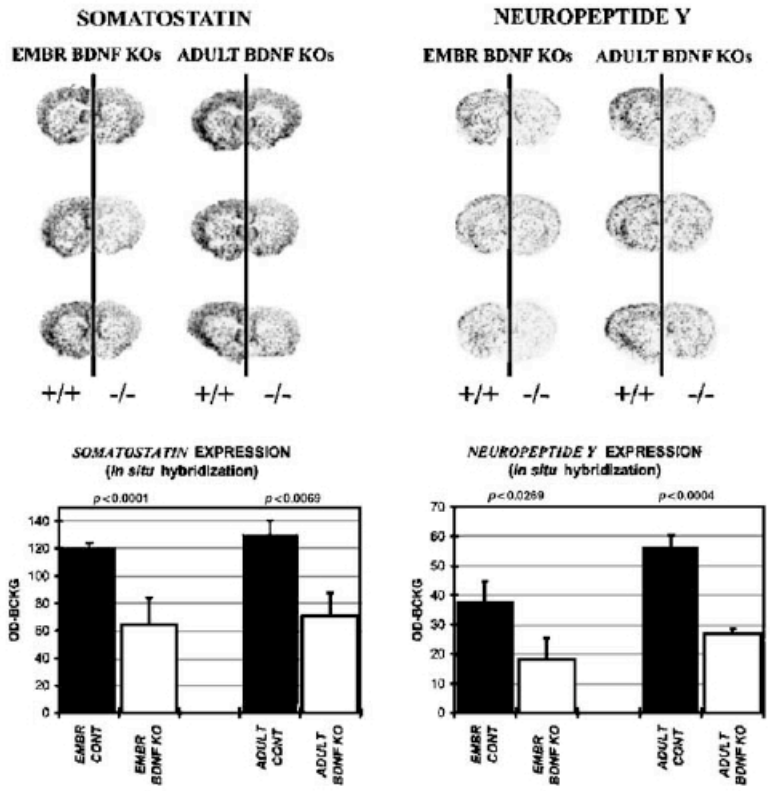

Figure 5 Somatostatin (SST) and neuropeptide Y (NPY) mRNA expression is reduced in mice with embryonic and adulthood brain-derived neurotrophic factor (BDNF)-deletion. *In situ* hybridization was performed on fresh-frozen tissue from a new set of animals using [^{35}S]-labeled long riboprobes against SST and NPY. Upper panels: scanned autoradiographs represent composite pictures from control (left hemibrain) and BDNF knockout (KO) (right hemibrain) mice. Lower panes: quantification of background-corrected neocortical optical density (OD-BCKG) for SST and NPY signal. Error bars represent s.d. Note that both neuropeptides show a highly significant reduction in transcript levels.

Figure 14. Figure 6. BDNF regulation of interneuronal transcripts.

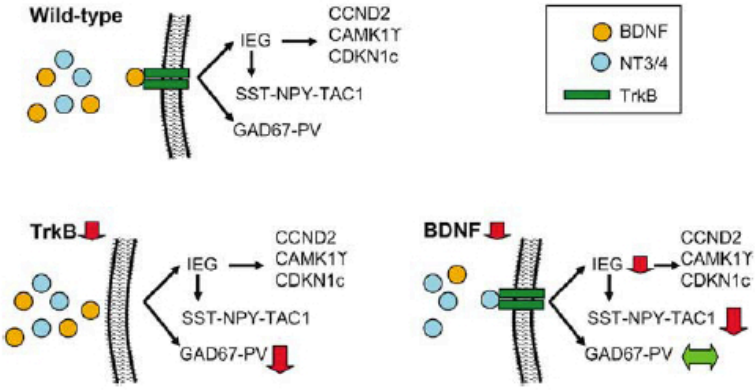

Figure 6 Brain-derived neurotrophic factor (BDNF) regulation of interneuronal transcripts. In wild-type animals BDNF-TrkB signaling is required for maintenance of early immediate genes (IEG), glutamic acid decarboxylase (GAD67), PV, Somatostatin (SST), neuropeptide Y (NPY) and tachykinin 1 (TAC1) expression. Reduction in TrkB, but not BDNF is sufficient to downregulate GAD67 and PV expression. However, BDNF appears to be required for maintenance of the SST-NPY-TAC1 interneuronal neuropeptides.

DISCUSSION

In this study we analyzed neocortical transcriptome changes in response to embryonic and adult conditional ablation of BDNF. This study revealed that: 1) the transcriptomes of the adult and embryonic BDNF-deficient mice show highly correlated similarities, including altered expression of the transcripts encoding neuropeptides (SST, NPY, TAC1), early-immediate genes (ARC, EGR1, EGR2, FOS, DUSP1, DUSP6) and critical cellular signaling systems (CDKN1c, CCND2, CAMK1g, RGS4); 2) the embryonic BDNF KO animals, when compared to the adult BDNF KO mice, reported significant expression changes in several genes related to neuronal differentiation (GAS5, NPTX2, NEUROD6, HOMER1), GTPase activating systems (RAP1GDS1, RAN2BP2, RANGAP1) and multiple other genes; and 3) BDNF appears to be critical for maintaining SST-NPY-TAC1 expression in interneurons in both embryonic and adult KO mice, but without altered expression of GAD1, GAD2, calretinin-CALR or PARV.

Transcriptome similarities between the embryonic and adult BDNF-deficient mice

Deletion of the BDNF gene in embryonic and adult BDNF-deficient mice is primarily characterized by transcript decreases. In the context of the physiological role of BDNF, this apparent “loss of function” is expected; increased BDNF is associated with activity (164, 165), cell survival (166-168), learning and memory (169), synaptic plasticity (170, 171), increased synthesis of mRNA and other processes that can be looked upon as “positive” cellular events. Loss of BDNF would therefore be expected to decrease the expression of genes that mediate these effects. The genes with altered transcription implicate the following processes that are likely to be altered in these mice.

First, a number of the IEGs (ARC, EGR1, EGR2, FOS, DUSP1, DUSP6) showed robust decreases in both adult and embryonic KO animals. In contrast, upregulation of BDNF by exercise (149, 164, 165) or by other in vitro manipulations leads to induction of these genes (172). IEG induction is known to be strongly regulated via the MEK-ERK pathway (173, 174), which is also one of the main effectors of BDNF signaling (175, 176). Hence, we propose that the IEG transcript downregulations we see in the BDNF-deficient animals are due to the lack of release of BDNF and impaired trophic support (177, 178).

Second, the cyclin-dependent kinase inhibitor 1C (CDKN1c) and cyclin D2 (CCND2) also showed expression changes in both groups of KO animals. CDKN1c has been shown to be an inhibitor of the CCND2/CDK complexes (179), and consistent with this functional interaction, CDKN1c is the most upregulated gene product in the BDNF-deficient mice, while CCND2 is one of the genes showing the most robust transcript decreases. In addition, a strong functional relationship exists between cyclins and Ca/CAM kinase activity (180), suggesting that the observed CDKN1c, CCND2 and CAMK2g transcript alterations are causally related. Recent evidence suggests that CCND2 is important in development for neurogenesis, proliferation, and differentiation (181, 182), and may be involved in promotion of GABA-ergic phenotype (183, 184). As CCND2 is under the control of the previously

discussed IEGs, we believe that the CDKN1c, CCND2 and CAMK2g transcript changes are mediated via the BDNF-MEK/ERK-IEG pathway.

Expression differences between the embryonic and adult BDNF deficient mice

Beyond common transcriptome alterations, mice with embryonic and adult deletion of BDNF also showed several significant gene expression differences. Most notably, the embryonic BDNF KO animals, when compared to the adult BDNF KO mice, reported significant expression changes in several genes related to neuronal differentiation (GAS5, NPTX2, NEUROD6, HOMER1) and GTPase activating systems (RAP1GDS1, RAN2BP2, RANGAP1). As alterations in either of these systems may lead to altered behavior (185-187), we propose that some of the observed transcriptome changes, in the frontal cortex or other brain regions, are the underlying cause of the behavioral changes in the mice with conditional ablation of BDNF.

Effect of BDNF on interneuronal gene expression phenotype

As our microarray experiments were performed on bulk cortical tissue, the expression changes we observed in the absence of BDNF reflect a sum of transcriptome changes that may occur in a number of different cell types. In the context of the phenotypic diversity of the neocortex, the transcriptome of projection neurons, glial cells and interneurons could be differentially affected by BDNF ablation. To overcome this limitation of the microarray technology, we decided to focus our primary attention to expression changes related to specific markers of neuronal subpopulations that show a well-defined neocortical distribution.

PV, CCK and SST are expressed in separate classes of cortical interneurons (188-192). In interneurons SST, NPY and TAC1 are co-expressed to a great extent and SST/NPY expression can be induced by a BDNF/TrkB-dependent mechanism (193-195). While we observed a strong downregulation in the SST-NPY-TAC1 transcripts in both adult and embryonic BDNF-ablated mice, we found the expression

of other GABA co-localizing neuropeptides and GABA-production enzymes unchanged. These data are in agreement with our recent findings that PV and GAD1 expression are not directly BDNF-dependent (136). Rather, GAD1 and PV expression depend on the expression of a functional TrkB receptor: TrkB-deficient mice show a remarkable downregulation in GAD1 and PV transcripts, which is not observed in the BDNF-deficient animals. These data, combined with the SST-NPY-TAC1 expression reduction in the BDNF-deleted mice, argue that interneuronal gene expression is regulated in a complex manner (Figure 6). While PV expression may be co-regulated with GAD1, the SST-NPY-TAC1 phenotype appears to be GAD1-independent. This suggests that BDNF may influence different subclasses of interneurons through different molecular mechanisms: the PV-GAD1 regulation is achieved through the TrkB receptor, while the maintenance of SST-NPY-TAC1 interneuronal phenotype may depend on both BDNF and TrkB expression.

BDNF regulation of the transcriptome: relevance to human brain disorders

Multiple lines of evidence imply that the BDNF gene is involved in the pathophysiology of schizophrenia. Although population studies have yielded divergent data about the association of variants in the BDNF gene with increased risk and developmental features of schizophrenia (196-202), human postmortem studies suggest that individuals with schizophrenia have reduced expression of TrkB and BDNF in the cerebral cortex (136, 203-206), as well as decreased BDNF protein levels in the serum (207). In addition, various animal models of schizophrenia consistently show a down-regulation of BDNF transcript or protein (128, 199-202, 208-212). Importantly, just as in our current study of BDNF-ablated animals, SST, NPY and RGS4 transcripts are downregulated in the prefrontal cortex (PFC) of subjects with schizophrenia (153, 213, 214). However, we acknowledge that other, BDNF-independent mechanisms may also account for the altered expression of these genes in schizophrenia (215, 216). The extent to which a BDNF-dependent transcriptome profile is present in schizophrenia remains to be established in hypothesis-driven assessment of gene expression changes in the human PFC.

Our findings are also important in the context of recent research on Alzheimer's disease (AD) related pathology. Existing evidence suggests that BDNF-TrkB controlled SST-NPY levels may play a critical role in the progression of AD. First, SST-NPY containing interneurons have been implicated in learning and memory (217-220) and postmortem brain studies of AD repeatedly observed a severe loss of SST immunoreactive neurons and axons (155, 219, 221-224). In addition, APPswe/PS1dE9 amyloid plaque producing mice show reduced SST levels in the cortex (225), and this is likely mediated through the interference of amyloid-beta (Aβ) with the BDNF-induced activation of the Ras-mitogen-activated protein kinase/extracellular signal-regulated protein kinase (ERK) and phosphatidylinositol 3-kinase (PI3-K)/Akt pathways (226). In contrast, it appears that inducing increased expression of SST may be beneficial for patients suffering from AD: compounds increasing SST expression are in phase II clinical trials as cognition enhancing agents (FK962, Fujisawa Pharmaceutical) (227), and transgenic models of amyloid deposition are reversed by environmental enrichment (228), which is known to induce SST-NPY expression via a BDNF-dependent pathway. Thus, while altered BDNF expression may not represent the primary disturbance in AD, changed expression of, or altered responsiveness to BDNF (and subsequently decreased SST levels) may represent a critical feature of Alzheimer's disease progression.

ACKNOWLEGEMENTS:

We are thankful to Drs. Pat R. Levitt and Etienne Sibille for valuable comments on the manuscript. We also thank for Dr. Dominique Arion, Katherine C. Douglass, Annie Bedison and Melissa Macioce for superb technical assistance with the experiments. This work was supported by R01 MH067234 (KM), 2 P50 MH45156-14 CCNMD Project 2 (KM) and K02 MH070786 (KM).

III. CHAPTER 2- PAPER 2

"Lack of Serotonin$_{1B}$ Receptor Expression Leads to Age-Related Motor Dysfunction, Early Onset of Brain Molecular Aging and Reduced Longevity"

E Sibille[1,4], J Su[1], S Leman[6], AM Le Guisquet[6], Y Ibarguen-Vargas[6], J Joeyen-Waldorf[1], C Glorioso[4], GC Tseng[2], M Pezzone[3], R Hen[5] and C Belzung[6]

Departments of [1]Psychiatry, [2]Biostatistics and [3]Medicine, [4]Center for Neuroscience, University of Pittsburgh, [5]Center for Neurobiology & Behavior, Columbia University, [6]EA3248 Psychobiologie des émotions, Université François Rabelais de Tours, France,

Abbreviated title: Serotonin$_{1B}$ receptor and aging

Correspondence:

- Etienne Sibille, University of Pittsburgh, Department of Psychiatry, 3811 O'Hara Street, BST W1643, Pittsburgh, PA 15213, E-mail: sibilleel@upmc.edu,

- Catherine Belzung, EA3248 Psychobiologie des émotions, Université François Rabelais de Tours, Parc Granmont, Tours 37200, France, E-mail: catherine.belzung@univ-tours.fr.

Keywords: serotonin, aging, longevity, cortex, striatum, transcriptome, Bdnf, Igf1, sirtuin.

Acknowledgments. We thank Irwin Lucki and Anita Bechtholt for help with additional rodent support, Ruomei Liang for technical help, David Lewis and Karoly Mirnics for helpful comments on the manuscript. Support provided by NIMH (ES).

PREFACE

My contribution to this work included performing and analyzing Sirt5 in situ hybridizations on HTR1B KO mice and controls (see Figure 6, see also highlighted image, appendix 3), performing mouse necropsies, and reading and commenting on the manuscript.

ABSTRACT

Normal aging of the brain differs from pathological conditions and is associated with increased risk for psychiatric and neurological disorders. In addition to its role in the etiology and treatment of mood disorders, altered serotonin (5-HT) signaling is considered a contributing factor to aging, however no causative role has been identified in aging. We hypothesized that a deregulation of the 5-HT system would reveal its contribution to age-related processes and investigated behavioral and molecular changes throughout adult life in mice lacking the regulatory presynaptic 5-HT_{1B}-receptor ($5HT_{1B}R$), a candidate gene for 5-HT-mediated age-related functions. We show that the lack of 5-$HT_{1B}R$ (*Htr1b*^{KO}-mice) induced an early age-related motor decline and resulted in decreased longevity. Analysis of life-long transcriptome changes revealed an early and global shift of the gene expression signature of aging in the brain of *Htr1b*^{KO} mice. Moreover, molecular changes reached an apparent maximum effect at 18-months in *Htr1b*^{KO} mice, corresponding to the onset of early death in that group. A comparative analysis with our previous characterization of aging in the human brain revealed a phylogenetic conservation of age-effect from mice to humans, and confirmed the early onset of molecular aging in *Htr1b*^{KO} mice. Potential mechanisms appear independent of known central mechanisms (Bdnf, inflammation), but may include interactions with previously identified age-related systems (IGF-1, sirtuins). In summary, our findings suggest that the onset of age-related events can be influenced by altered 5-HT function, thus identifying 5-HT as a modulator of brain aging, and suggesting age-related consequences to chronic

manipulation of 5-HT.

Introduction.

Aging leads to morphological(34, 229-232) and functional(9, 233-235) changes in the brain and is associated with increased risk for psychiatric and neurological disorders(236-239). However, the mechanisms underlying normal aging of the brain likely differ from those associated with neurodegenerative and pathological conditions and are still poorly understood(38). Several lines of evidence suggest a role for 5-HT during aging, including structural and functional age-related changes in the 5-HT system in rodents(240-242), and in humans, as documented by postmortem receptor binding studies(243-245), RNA level studies(246), in vivo imaging studies(247) and neuroendocrine challenges(236). Depending on the brain region investigated, the 5-HT modulation of cerebral glucose metabolism increases or decreases during normal aging, suggesting a deregulated control of 5-HT(248) (see also (249)). The mechanisms for age-related changes in 5-HT function are not known and may include gene variants, pharmacological manipulation in adult/old population or late-onset functional declines. Based on converging roles in energy metabolism, cellular signaling pathways and synaptic plasticity, interactions between 5-HT, neurotrophic function (Brain-derived neurotrophic factor, BDNF) and insulin-like growth factor (IGF) have been proposed as potential determinants of homeostasis and health during aging(44). Therefore, due to the critical role of 5-HT in mood regulation, age-related changes in 5-HT function are considered a risk factor for developing mood disorders in older subjects(238).

A candidate gene for deregulated 5-HT control in aging is the $5HT_{1B}R$(250).

$5HT_{1B}R$ is the predominant pre-synaptic autoreceptor modulating 5-HT release in the brain(251). Decrease in $5HT_{1B}R$ function, and not in its somatodendritic counterpart ($5HT_{1A}R$), has been reported in aged rodents(250), consistently with the role of this receptor subtype in motor function(252) and with the well-characterized decline in motor function during aging. As aging can be viewed as the accumulation of a variety of events that together create a chronic challenge to the brain, and since 5-HT is a key factor for adaptation to stress(253), we hypothesized that a central deregulation of the 5-HT system *in* $Htr1b^{KO}$ mice would affect the brain response to this challenge and reveal the contribution of 5-HT to age-related processes. Accordingly, inactivation of $5HT_{1B}R$ in $Htr1b^{KO}$ mice(254) results in mostly normal baseline, but altered 5-HT kinetics upon recruitment of the 5-HT system (i.e. increased release and higher synaptic levels), as revealed by pharmacological challenges and microdialysis studies(251, 255, 256). Here we addressed the issue of causality *versus* correlation between 5-HT and aging, by investigating age-related behavioral and molecular changes as a result of the disruption of serotonin signaling through the $5HT_{1B}R$ in $Htr1b^{KO}$ mice. We now show that the lack of $5HT_{1B}R$-mediated signaling induced both an early age-related motor decline and a global early shift of the characteristic gene expression signature of aging in the brain, ultimately resulting in decreased longevity, thus identifying 5-HT as a modulator of brain aging.

Material and Methods:

Animals. All animals were raised under standard conditions: temperature 21±2^{o}C, controlled humidity 20-25%, 12:12 photoperiod with lights on at 8:00 pm in order to test animals during their scotophase. Food and water were available *ad libitum*. Weaning took place at 21±1 days. At this age, animals were ear-punched and genotyped. Littermate wild-type (WT) and *Htr1b*^{KO} mice were used for all behavior and microarray experiments, with the exception of animals used for the 3-month time-point microarray analysis and for the serum level measurements. These latter groups were no more than two generations away from heterozygous breeding. To avoid putative confounding effects of the previously reported increased aggressiveness of *Htr1b*^{KO} mice(254), WT and KO mice were housed under reduced cage density, resulting in normal or low intra-cage aggression in both experimental groups, as revealed by the absence of bite marks or wounds. All experiments were conducted in accordance with the European Communities Council Directive of 24 November 1986 (86/609/EEC) and with the University of Pittsburgh Animal Care and Use Committee.

Behavior. Separate groups of mice were tested at the age of 2, 6, 12 and 18 months, although all animals were generated and born approximately at the same time. This means that all animals were submitted to a battery of tests only once, according to the following schedule: open-field, elevated-plus maze, rotarod and coat hanger tests. At least 1 week separated two different tests.

Open Field. The apparatus consisted of a grey polyvinyl chloride circular open field, 40 cm in diameter and 30 cm high. The floor was divided in 6 peripheral and 1 circular central sectors, all of the same area (180 cm^2) and covered by a white sheet

of paper which was changed after each mouse. A black-white stripped pattern, 30 x 20 cm, was present on the wall and provided a local cue. The device was lit by a red bulb placed 80 cm above the floor of the open field. Each mouse was introduced in the center of the open field and recorded for a period of 5 min. Numbers of peripheral and central sector crossings (total locomotion) and of rearing were recorded.

Elevated Plus maze. The apparatus consists on 2 open and 2 closed 40x10 cm arms, located 40 cm above the floor. Mice were placed in the center and the time and number of entries in the closed and open arms were recorded for 5 minutes.

Rotarod. The apparatus consisted of a rotating horizontal rod located 25 cm above the floor. A fixed and relatively slow rotating speed was chosen (10 revolution per min) in order to increase the sensitivity of this assay at older ages. One block of 10 trials was applied with an inter-trial interval of 10 min. The latency before falling was recorded with a cut-off point of 60 seconds.

Coat hanger. The triangular-shaped apparatus consisted of a horizontal steel wire (diameter: 2 mm, length: 41 cm) flanked at each end by two side-bars (length: 19 cm; inclination: 35 ° from the horizontal axis)(257). The horizontal bar was placed at a 45 cm height from the floor. The mice were placed upside-down in the middle of the horizontal wire and released only after gripping with all four paws. Latency before falling was recorded. A trial ended when the mice fell or reached the top of the apparatus, from which it was retrieved and the maximal score of 1 minute given for latencies before falling. A block of 5 consecutive trials was applied with a 15-minute inter-trial interval and a 1-minute cut-off period per trial.

All behavioural assays were analyzed by ANOVA with age and genotype as fixed factors.

ELISA assays. Blood samples were collected, clotted, and centrifuged at room temperature to obtain serum samples, which were aliquoted into microcentrifuge tubes and stored at -20°C. Serum samples were thawed and diluted in duplicate, and quantitative determination of mouse serum albumin and IgG (Alpha Diagnostic International, San Antonio, TX), IGF-1 (Quantikine, R&D Systems, Inc., Minneapolis, MN), and insulin (Crystal Chem Inc., Downers Grove, IL) were measured using their respective ELISA kits according to specific manufacturer instructions. Within 30 minutes of terminating each reaction assay, optical densities were measured on an ELISA plate reader (SpectraMax Gemini XS, Molecular Devices Corp, Sunnyvale, CA) at a wavelength of 450 nm. Mean absorbance for each duplicate sample was compared with standard curves to obtain concentration values.

Intestinal histology. Small and large intestine were harvested, rinsed gently in saline to remove food and fecal material, and fixed in 4% buffered formaldehyde for 4 hours. After washing twice in PBS for 10 minutes, tissue samples were then cryoprotected in 30% sucrose in PBS overnight at 4°C. After paraffin embedding, tissues were sectioned at 10µm using a sliding microtome, mounted on poly-lysine-coated slides, dried, and stained with hematoxylin and eosin (Sigma, St. Louis, MO).

Immunocytochemistry. Small and large intestine were processed for 5-HT_{1B}R immunocytochemistry. After cryoprotection with sucrose, intestinal samples were frozen in OCT embedding medium (Miles Laboratories, Elkhart, IN), cut in 8µm sections on a cryostat, and thaw mounted on poly-lysine-coated slides. Tissue

sections were re-hydrated in potassium-phosphate buffer solution (KPBS) at room temperature, blocked with 10% normal goat serum, and incubated overnight at 4°C with a rabbit polyclonal IgG antibody to the rat 5-HT_{1B} receptor (Acris Antibodies, Hiddenhausen, Germany), diluted 1:100 in KPBS, 0.05% goat serum and 0.1% Triton X-100. This primary antibody recognizes rat, mouse, and human epitopes corresponding to amino acids 8-26 and 263-278 of the rat 5-HT_{1B}R. The following day, slides were rinsed with KPBS three times and then incubated with a Cy3-conjugated goat anti-rabbit IgG secondary antibody (Jackson ImmunoResearch, West Grove, PA) at room temperature for two hours at a dilution of 1:800 in KPBS, 0.05% goat serum, and 0.1% Triton X-100. Slides were washed three times with KPBS, coverslipped and imaged using an Olympus Fluoview 500 scanning confocal microscope in the Center for Biological Imaging (CBI) at the University of Pittsburgh. Optimal antibody concentrations were determined by serial dilutions. Controls for the specificity of the antisera consisted of incubation of the tissue with normal rabbit serum substituted for the primary antiserum. Using this substitution, no non-specific staining was seen. Positive control consisted of substituting mouse cortex for intestinal tissue.

For the dopamine transporter (DAT), a similar protocol was applied on 20μm post-fixed coronal brain sections incubated with a rat monoclonal anti-DAT antibody (Chemicon International Inc., Temecula, CA) in the presence of avidin and biotin blocking solutions (Vector Laboratories, Burlingame, CA). Slides were developed with the ABC kit (Vector Laboratories, Burlingame, CA). Optimal development time was determined on parallel sections. All experimental samples were processed

simultaneously with pairs of aged-matched WT and KO sections on the same slides. Optical densities were quantified with the ImageJ software (http://rsb.info.nih.gov/ij/).

Microarray samples and processing. Mice were sacrificed by cervical dislocation. Brains were split along the sagittal line, frozen in isopentane and stored at –80°C. To collect samples, frozen brains were cut on a cryostat to the appropriate anatomical level where series of 1 or 2mm diameter micropunches (Sample corer, Fine Science Tools, Foser City, CA) were collected from frontal cortex (CTX) and striatum (STR) and immediately stored in Trizol reagent (Invitrogen, Carlsbad, CA). CTX samples were collected from prelimbic and cingulate cortices corresponding mostly to non-motor areas between Figure18 and 23 (Bregma ~+2 to +1mm) in the Paxinos-Franklin Mouse Brain Atlas(258). Dorsal striatum samples were collected starting at Figure23 in the same atlas (Bregma ~+1 to 0mm). Total RNA was extracted using the Trizol protocol, cleaned with Rneasy microcolumns (QIAGEN, Germany), quantified and verified by chromatography using the Agilent Bioanalyzer system. Microarray samples (n=3-4 per age-, genotype- and brain regions; total, n~60 arrays) were prepared according to the manufacturer's protocol. In brief, 2µg of total RNA were reverse-transcribed and converted into double-stranded cDNA. A biotinylated complementary RNA (cRNA) was then transcribed *in vitro*, using an RNA polymerase T7 promoter site which was introduced during the reverse-transcription of RNA into cDNA. 20µg of fragmented labeled cRNA sample was hybridized onto MOE 430-2.0 Affymetrix oligonucleotide microarrays (Affymetrix, Santa Clara, CA). A high-resolution image of the hybridization pattern on the probe array was obtained by laser

scanning, and fluorescence intensity data were automatically stored in a raw file. To reduce the influence of technical variability, samples were randomly distributed at all experimental steps to avoid any simultaneous processing of related samples. For data extraction, single arrays were analyzed with the Affymetrix Microarray GCOS software. Microarray quality control parameters were as follows: noise (RawQ) less than 5 (CTX: 1.53±0.03; STR: 1.65±0.05), background signal less than 100 (250 targeted intensity for array scaling; CTX: 46.2±0.9; STR: 45.3±0.8), consistent number of genes detected as present across arrays (CTX: 49.7±0.4; STR: 52.6±0.4), consistent scaling factors (CTX: 1.80±0.05; STR: 1.52±0.06), Actin and GAPDH 3'/5' signal ratios less than 3 (CTX: ACT, 2.15±0.19, GAPDH, 1.18±0.09; STR: ACT, 1.43±0.04, GAPDH, 0.90±0.03) and consistent detection of BioB and BioC hybridization spiked controls.

Array statistical analysis. For statistical analysis, probeset signal intensities were extracted with the Robust Multi-array Average (GC-RMA) algorithm(145) (http://www.bioconductor.org). The 45,101 probesets were reduced to ~20,000 probesets after preprocessing and filtering (Present calls ≥ 10%, coefficient of variation superior than 0.1 and averaged expression ≥ 20). The 3-month WT and KO groups were bred at a different experimental time and were not combined in a single large-scale analysis.

Denote by the expression intensities from microarray, where labels indexes for genes, $k = 0, 1$ for genotype (*k*=0: wild-type; *k*=1: knockout), $t = 10, 18, 24$ for age and for biological replicates. Genes with age-related expression changes were selected by the following three analytical procedures.

- *First*, expression intensities of each gene *g* were fitted to a two-way ANOVA model in 10-, 18- and 24-month groups and WT and KO groups:.

In the model, α represents the genotype effect, β the age effect and γ the interaction term.

- *Second*, genotype differences were tested (2-group t-tests) at 3-month of age for all genes identified in (1) and,

- *Third*, one-way ANOVA models within genotype groups (WT and KO) were fitted to genes identified in steps 1 and 2 to characterize the age-related effects in the respective WT or KO experimental groups:.

The goal of the overall analysis was to use the profiles of expression of large groups of genes as an "experimental assay" to identify and measure age-related molecular effects, and to assess the cumulative effects of changes over groups of genes (i.e. correlation, functional analysis…). Therefore thresholds for gene selection were kept at medium stringencies ($p<0.01$, changes greater than 20%). This approach has the advantage of allowing the investigation of such patterns, although the extent and levels of correlations may have been slightly underestimated.

Mouse-Human age-effect correlation. We have previously reported changes in gene expression with age in the human prefrontal CTX using U133Plus-2.0 arrays(60). Human orthologs of genes with age-effect in the mouse were identified between the MOE-430-2.0 and U133Plus-2.0 arrays using the NetAFFX webtools (Affymetrix, Santa Clara, CA). In the case of multiple human probesets for a single mouse probeset, the human probeset with the lowest age-related p-value was

retained. Correlations of age-effects were calculated using log_2Ratio values. In rodents, the ratios were as described in the text and Figures. For humans, the effect of age was calculated as the signal ratio between subjects over 65 years of age *versus* subjects under 30 years(60). Similar results were obtained using different threshold criteria for gene selection in the mouse datasets (In Figure2: $p<0.001$, changes greater than 20%). A similar approach was applied to assess correlations in transcriptome changes in CTX between *Bdnf*^{KO} mice(62) and age-related profiles in *Htr1b*^{KO} mice, as mouse probesets were directly comparable between the two studies.

Age-pattern correlation. To identify patterns of changes in gene expression in relationship to the occurrence of WT/KO behavioral differences (i.e. 10 and 18 months of age), correlation levels were systematically calculated between WT and *Htr1b*^{KO} mice gene expression at the 10 and 18-months time-points and all possible transcript profiles. Profiles were designed based on 2 groups (WT and *Htr1b*^{KO}), 2 time-points (10 and 18-months) and 3 ordinal expression levels (high, medium and low) for a total of $(3^2)^2$= 81 possible patterns. The analysis was limited to the 1097 genes with identified age-effects in either experimental groups. With the exception of a very few probesets (See Table S5), all identified genes were expressed at the same level at the 3-month time point. 99% of the genes had correlation levels greater or equal to 0.7 with at least one pattern. Patterns were then reduced to 3 major profiles: *i)* initial WT/KO differences at 10-months or “early” pattern, *ii)* initial WT/KO differences at 18-months or “late” pattern, and *iii)* overlapping profiles (no WT/KO differences). This approach was more comprehensive than simple group

comparisons (i.e. difference or not at 10 or 18 months), although the vast majority of genes displayed correlation levels only with a very few patterns that corresponded closely to the profiles displayed for averaged values in Figure5.

Functional class scoring analysis. See details at http://www.bioinformatics.ubc.ca/ermineJ/(259, 260). Rather than analyzing genes one at a time, gene functional class scoring gives scores to classes or groups of genes, representing the overall effect of age on these groups of genes. Gene groups were organized according to the Gene Ontology (GO) classification(261) and GO groups with greater than 200 or fewer than 8 genes were screened out. GO groups were scored as described(260), using age-related p-values as gene scores. Briefly, a raw score for each set of genes with a GO family or custom gene group is calculated as the mean of the negative log of the gene scores for all genes in each gene class. When a gene is represented more than once, only the best score is counted. The raw score is transformed into a p-value for age effect on that group by comparing it to an empirically-determined distribution of raw scores. This distribution is obtained by randomly generating gene classes of the same size as the class being tested; this is repeated 100,000 times to generate the distribution of scores expected if high gene scores are not concentrated in the class.

Real-time quantitative PCR was performed as previously described(262). In brief, small PCR products (80-120 base-pairs) were amplified in quadruplets on an Opticon real-time PCR machine (MJ Research, Waltham, MA), using universal PCR conditions (65C to 59C touch-down, followed by 35 cycles [15”at 95C, 10” at 59C and 10” at 72C]). 150 pg of cDNA was amplified in 20µl reactions [0.3X Sybr-green, 3mM

$MgCl_2$, 200μM dNTPs, 200μM primers, 0.5 unit Platinum Taq DNA polymerase (Invitrogen, Carlsbad, CA)]. Primer-dimers were assessed by amplifying primers without cDNA. Primers were retained if they produced no primer-dimers or non-specific signal only after 35 cycles. Results were calculated as relative intensity compared to actin.

***In situ* hybridization** was as previously described(263, 264). Primers were designed using the primer 3 software (http://frodo.wi.mit.edu/cgi-bin/primer3/primer3_www.cgi) to amplify half of the gene coding region and half of the 3' untranslated region of the Sirt5 cDNA (NM 178848; base-pairs 510 through 1144). Primers included SP6 and T7 RNA polymerase promoter tails for sense and antisense *in vitro* transcription from the amplified PCR products. PCR products were amplified from mouse brain cDNA and verified by sequence analysis. Labeled *in vitro* transcription was performed using the Ambion maxiscript kit (Ambion, Inc., Austin, TX) in the presence of ^{35}S-CTP. Probes were purified using the Qiagen Rneasy kit (Qiagen, Inc., Valencia, CA) and the amount of incorporated radioactivity was quantified on a liquid scintillation counter. *In situ* hybridization was performed on 5 coronal sections per mouse. 5 mice were used per genotype and per age group (3, 6, 18, 24 months) according to a standard protocol(264, 265). Briefly, slides were incubated for 10 minutes at room temperature in 4% buffered paraformaldehyde, washed in 0.1M PBS, serially dehydrated in increasing concentrations of ethanol, and then incubated in hybridization buffer overnight at 56°C in the presence of antisense or sense probe (2,000,000 counts per slide). The following day, the slides were washed, RNAse treated, dried and exposed to film. Kodak BioMAx MR film intensities were

determined to be optimal after a 4 day exposure. Images were standardized to C^{14} standards (ARC-146A and ARC-146D; American Radioloabeled Chemicals, Inc, St-Louis, MO) and areas corresponding to cortex and striatum were quantified using the Microcomputer Imaging Device analysis software (MCID I; Imaging Research, London, Ontario, Canada).

Results.

Early onset of age-related motor deficits and reduced longevity in *Htr1b*^{KO} mice.

Htr1b^{KO} mice presented no obvious developmental changes(252, 254), exhibited a normal behavior in young adulthood (Figure1.A-D, 2-month time-points), but displayed an early onset of characteristic age-related motor decline, which became significant at 6 months of age in the rotarod test and at 12 months in the coat hanger test (Figure1.A-B). Total activity in the open field and the elevated plus maze tests were not different from WT controls and declined similarly with age (Figure1.C-D). This early decline in motor behavior in *Htr1b*^{KO} mice was not due to learning deficits(266), as procedural learning curves were essentially parallel between genotypes (Figure1.E). Consistent with previous reports(252) *Htr1b*^{KO} mice displayed normal anxiety-like behavior in young adulthood (FigureS1). Assessing the progression of anxiety-related behaviors over time revealed no age-related genotype difference, although the interpretation of these measurements was limited by the very low activity of older animals in both experimental groups in the challenging

compartments of the behavioral apparatus (center of open field and open arms of the elevated-plus maze; FigureS1).

Figure 15. Figure 1. Early onset of age-related motor decline and reduced longevity in *Htr1b*^{KO} mice.

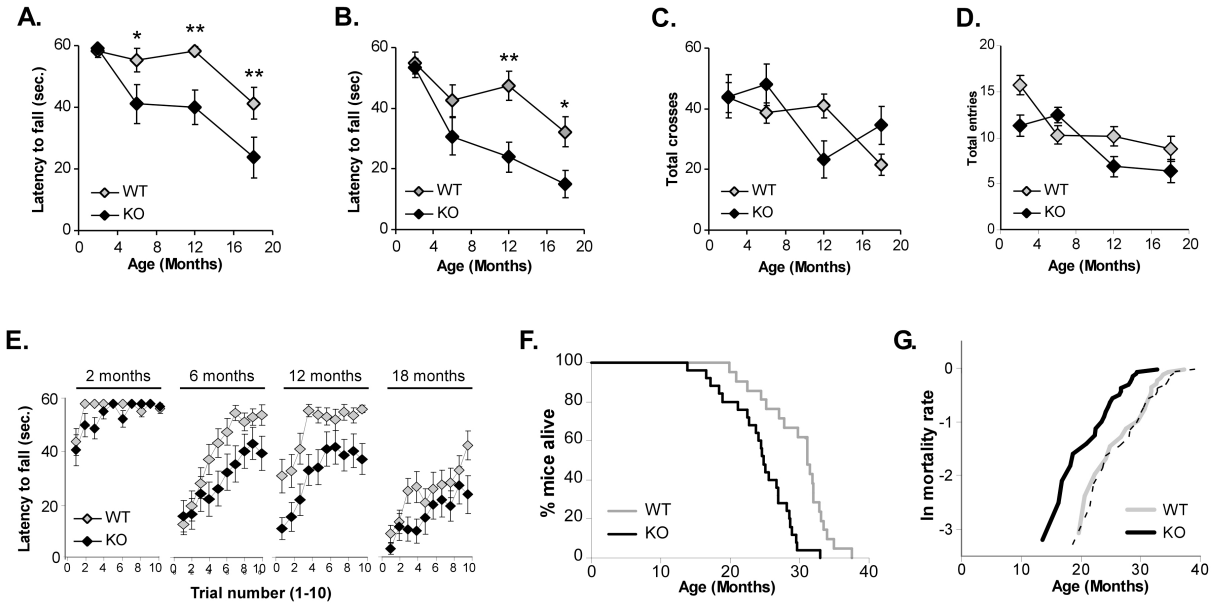

Figure 1. Early onset of age-related motor decline and reduced longevity in *Htr1b*^{KO} mice. A.-B. *Htr1b*^{KO} mice displayed early age-related motor impairment in the rotarod test (**A.**; Latency to fall: $F_{3,117}$=11.37, p<e^{-6}; Genotype effect: F=15.04, p<0.0005; Genotype*Age: F=2.05, p=0.11) and the coat hanger test (**B.**; Latency to fall: $F_{3,117}$=8.67, p<0.0001; Genotype effect: $F_{1,120}$=16.29, p<0.0001; Genotype*Age: $F_{3,117}$=1.98, p=0.12). *Post-hoc* tests: *p<0.05, **p<0.005. **C.-D.** Total activity decreased with age in WT and *Htr1b*^{KO} mice in the open field (OF) (**C.**) and elevated plus maze (EPM) (**D.**) tests (Age effect. OF: F=4.12, p=0.008; EPM: F=20.78, p< e^{-5}), although variability in the 12- and 18-month age-groups suggested a potential age*genotype interaction (Genotype*Age effect. OF: F=3.09, p=0.03; EPM: F=3.4, p=0.02; All other effects, p>0.05). Different cohort of mice were used for each time-

point to avoid memory savings between experiments (A-D: n=13-18 per group and per age). **E.** Procedural learning curves in the rotarod test were essentially similar, but reached lower maximal values in *Htr1b*^{KO} mice (See A.). **F.** Kaplan-Meyer survival curves revealed a significant decreased in longevity in *Htr1b*^{KO} mice ($p<0.0001$). **G.** Mortality curves. *Htr1b*^{KO} mice displayed a 3.75 fold increased hazard ratio ($p<0.0005$). Hatched curve represents *Htr1b*^{KO} mortality curve super-imposed on the WT curve. (F-G, WT, n=21; KO, n=24).

The first death events occurred between 16 and 20 months of age in *Htr1b*^{KO} mice and after 21 months of age in WT mice. *Htr1b*^{KO} mice displayed significantly decreased longevity ($p<0.0001$; Figure1.F), with reductions in maximum (-14%) and average (-19%) lifespans. The largest difference was observed at 30 months of age, where ~60% of WT mice but only ~5% of *Htr1b*^{KO} mice were still alive. Inspection of complementary log-mortality plots (Figure1.G) and of a Cox proportional hazard model revealed that on average *Htr1b*^{KO} mice had a 3.75 fold increase of hazard ratio ($p<0.0005$). Our analysis also revealed that changes in hazard were time-dependent, which means that the increase of hazard could be larger at some points but smaller at other times. However, the averaged slopes of the mortality curves were identical [WT: 0.159 (0.159–0.177), KO: 0.160 (0.160-0.177)] and the time-related differences in estimates were very small, as the *Htr1b*^{KO} mortality curve was virtually super-imposable on the WT curve (Figure1G, hatched curve). Thus, together these results demonstrated a shift of longevity and mortality curves towards earlier ages in *Htr1b*^{KO} mice, and suggested a causative and modulatory role for 5-HT in age-related motor

behavior and longevity.

The "age-related" phenotype of *Htr1b*^{KO} mice appears mediated by brain mechanisms.

The 5-HT$_{1B}$R is the main 5-HT presynaptic auto-receptor in the brain(251) and has limited functions in the periphery. Thus we hypothesized that the age-related phenotype might be mediated by central mechanisms, but first, we investigated selected peripheral systems as potential contributors to the phenotype. WT and *Htr1b*^{KO} mice had indistinguishable morphologic features at all ages, including body weights (Figure2.A). Mild alopecia and kyphosis appeared in both genotypes after 2 years of age (not shown). Necropsy procedures revealed no genotype changes in organs appearance or weight (not shown), including in kidney and lung, two organs with reported roles for 5-HT$_{1B}$R signaling(267, 268). 5-HT modulates gastro-intestinal and immune functions, but the 5-HT$_{1B}$R plays little-to-no role in these systems(269, 270). Correspondingly, 5-HT$_{1B}$R immunoreactivity was undetected in the intestinal tract (not shown) and no changes in colonic morphology were identified (Figure2.B). Elisa immunoassays on serum obtained from young and old mice revealed normal albumin content (Figure2.C), suggesting normal absorptive capacity in *Htr1b*^{KO} mice as compared to controls.

Figure 16. Figure 2. Peripheral markers in *Htr1b*^{KO} and WT mice.

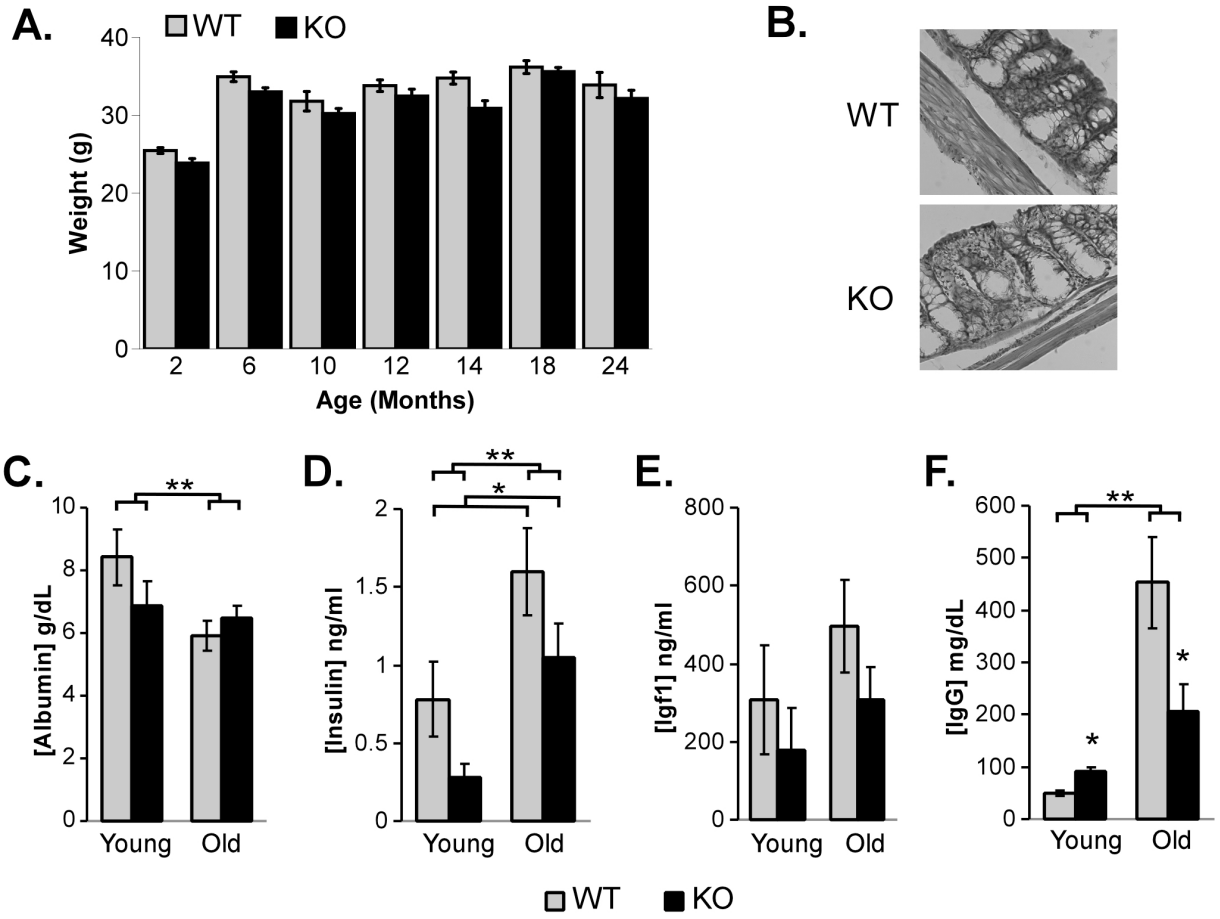

Figure 2. Peripheral markers in *Htr1b*^{KO} and WT mice. **A.** Body weight (n=14-16 per group, p>0.05)**. B.** Colon mucosal and smooth muscle layers and lumen were equivalent in WT and KO mice (hematoxylin/eosin staining; representative sections from old WT and KO groups). **C-E.** Serum levels of albumin (**C.**), insulin (**D.**), insulin-like growth factor 1 (igf1; **E.**) and immunoglobulins (IgG, **F.**). C-E: Young (3 months; WT, n=5; KO, n=5), old (18 months; WT, n=6; KO, n=6). Statistical significance: main-age effects for albumin ($F_{1,22}$= 10.2, p=0.005), insulin ($F_{1,22}$= 11.8, p<0.005) and IgG ($F_{1,22}$= 21.27, p<0.001). Main genotype effect for albumin ($F_{1,22}$= 4.4, p=0.08),

genotype*age interaction ($F_{1,22}$= 9.2, p=0.02). Main-genotype effect for insulin ($F_{1,22}$= 5.02, p<0.05) and age-genotype interaction for IgG ($F_{3,22}$= 6.5, p<0.05). All other effects, p>0.05. *Post-hoc* tests; *, p<0.05. Error bars represent s.e.m.

Due to the endocrine regulation of aging(271) and potential interaction with the 5-HT system(44), we measured circulating levels of insulin and insulin-like growth factor 1 (IGF-1). Both hormones displayed lower levels in young and old KO mice when compared to age-matched control mice (Figure2.C-D), although these differences reached statistical significance only for insulin. Serum levels for insulin increased with age in *Htr1b*^{KO} mice, suggesting that the lower levels in young KO mice were not due to primary deficits in hormone production. The direction of changes also suggests that hormonal levels are not mediating the age-related phenotype of *Htr1b*^{KO} mice for two reasons. First, increased levels above normal, rather than lower insulin levels, are associated with deleterious effects of aging(272). Second, prior studies in model organisms(271), including mice(273), predict a protective effect of decreased IGF-1 levels against aging.

Finally, an immunoassay for circulating immunoglobulin (IgG) revealed a smaller age-related increase in IgG levels in serum of old KO mice (2.3 fold increase) versus age-matched WT controls (9.1 fold increase; Figure2.F), thus suggesting a reduced inflammatory load, or reduced recruitment of the immune system in aging *Htr1b*^{KO} mice. Thus, combined with the limited functions of 5-HT_{1B}R in the periphery, these results suggested that the age-related behavioral phenotype and reduced longevity of *Htr1b*^{KO} mice may have originated from a central deficiency.

Dopaminergic terminal density and area are not affected in old *Htr1b*^{KO} mice.

In the brain, 5-HT_{1B}R modulates the synaptic release of 5-HT in serotonergic projection fields, but also acts as a heterologous autoreceptor indirectly regulating dopamine (DA) functions. Indeed, *Htr1b*^{KO} mice displayed elevated basal DA levels and increased striatal overflow after cocaine challenge(255), suggesting potential interactions between DA and the age-related motor phenotype. Using immunohistochemistry against the DA transporter, we found no differences in DA terminals density in the ventral or dorsal striatum of young and old WT or KO mice ($p>0.5$) (Figure 3.A-B). DA terminal striatal areas were also unchanged between genotype groups (Figure3.C). Representative Figures and measurements are provided at the 18 month time-point, long after the onset of behavioral differences (6-10 months of age) and corresponding to the time of early onset of death events in the KO group. Thus, together these results suggested that the early adulthood onset of the motor phenotype in *Htr1b*^{KO} mice was not due to a structural downregulation of the DA system.

Figure 17. Figure 3. Intact dopaminergic terminal density in old *Htr1b*^{KO} mice.

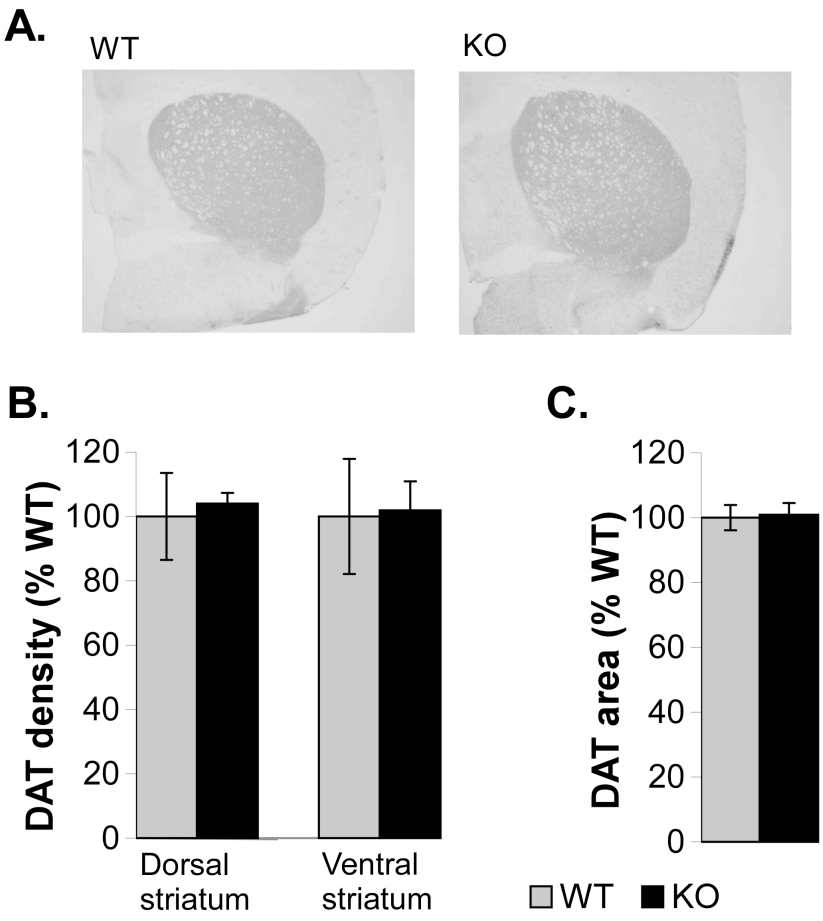

Figure 3. Intact dopaminergic terminal density in old *Htr1b*^{KO} mice.

A. Representative photographs of DA transporter (DAT) immunohistochemistry in 18-month old WT and *Htr1b*^{KO} mice (n=4 per group, p>0.05). **B.** DAT immunoreactivity density. **C.** DAT striatal area. (Similar results were obtained at 3, 6 and 24 months of age).

Altered gene expression in the brain of aging *Htr1b*^{KO} mice corresponds to "normal" aging.

Altered 5-HT signaling in *Htr1b*^{KO} mice could induce brain deficits that are detrimental to long-term brain homeostasis and survival and that are yet unrelated to age-related processes. Thus, as aging is accompanied by characteristic changes in gene expression in the brain(60, 74, 274), we predicted that the "molecular signature of aging" might occur earlier in *Htr1b*^{KO} mice. To this goal we first investigated the nature of life-long gene expression changes in cortex (CTX) and striatum (STR), two brain areas with well-characterized roles for the 5-HT_{1B}R, and then assessed putative differences in the trajectories of age-related changes in *Htr1b*^{KO} mice.

Roughly twice as many genes were affected in correlation with age in CTX of *Htr1b*^{KO} mice, compared to WT mice, with fewer genes affected in STR in both experimental groups (Figure 4.A.; Tables S1-2). Despite a considerable overlap (especially in CTX), some genes were identified only in the WT or in the KO group, reflecting either the presence of different age-related effects, or the limitation of the analytical procedures at detecting milder effects in one or the other group. To address this question, we hypothesized that if selected genes were age-related, then the overall changes in transcript levels should correlate across groups, regardless of whether genes passed statistical thresholds or not. Indeed, genes identified only in *Htr1b*^{KO} mice demonstrated high correlation levels with the effect of aging on the same genes in WT mice (Figure4.B, middle panel), and conversely age-related changes in transcript levels identified only in WT mice correlated highly with changes in KO mice (Figure4.B, left panel), thus revealing that a similar pool of genes was

affected across genotypes. The higher slope values in the correlation graphs of KO-only selected genes [CTX, KO=1.5, WT=1.2; STR (not shown), KO=2.3, WT=1.4] further suggested a larger and more extensive age-effect in *Htr1b*^{KO} mice. Interestingly, correlations were the highest when comparing 18 months-old KO mice to 24 months-old WT mice (Figure4.C), suggesting that *Htr1b*^{KO} mice reached a pronounced age-effect earlier than WT mice. This “maximum” age-effect corresponded to the period where death events started to occur in *Htr1b*^{KO} mice (Figure1.F).

Figure 18. Figure 4. Correlation of age-related gene expression "signatures" in the brains of WT and *Htr1b*^{KO} mice, and phylogenetic conservation of age-effect between mice and humans.

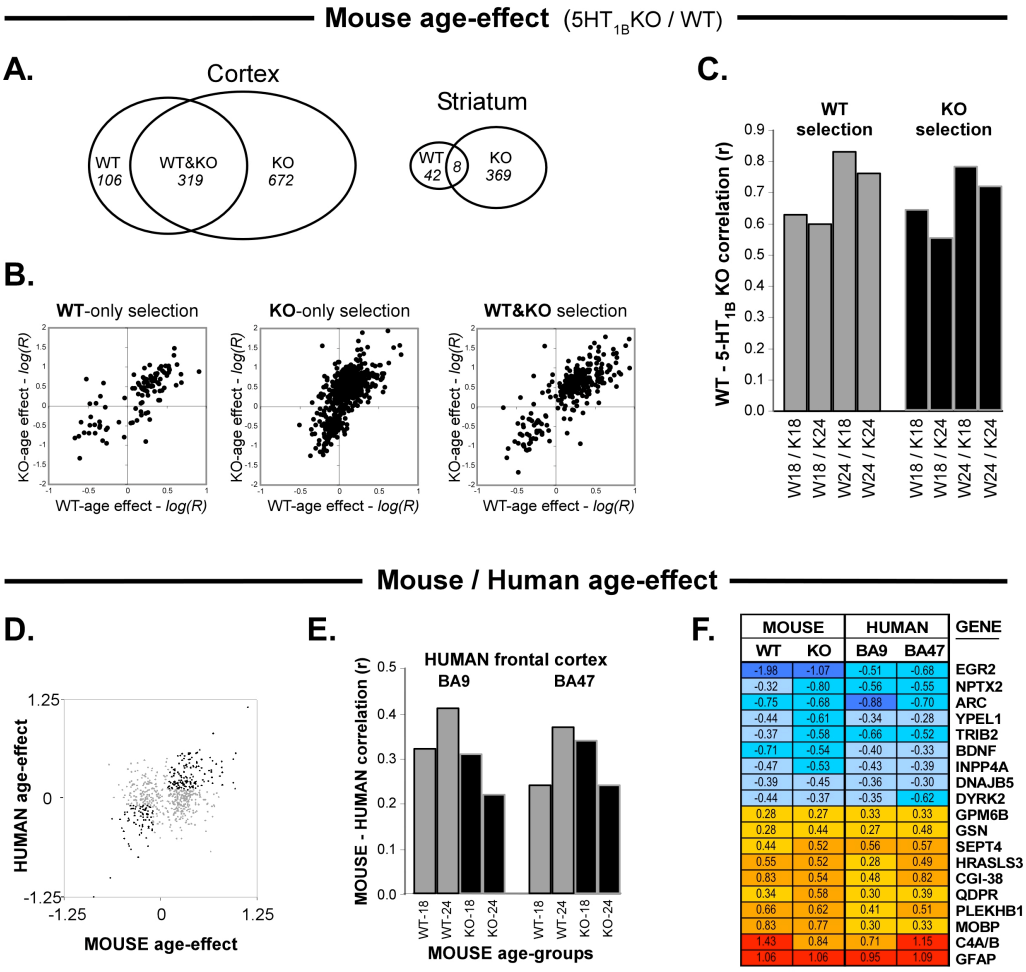

Figure 4. A-C. WT/*Htr1b*^{KO} age-effect comparison. **A.** Venn diagrams of age-related transcript changes in CTX and STR (n=3-4 arrays per age-, genotype- and brain regions; total, n~60 arrays). **B.** Correlation graphs between age-effects (LogR=$\log_2$Old/Young) in CTX between genes identified only in WT (n=106, left), only in KO (n=672, middle) and in both groups (n=319, right).

C. Correlation levels (r) of age-effects between indicated WT and *Htr1b*^{KO} age-groups. All p<0.0001. **D-F.** Mouse/Human age-effect comparison. **D.** Age-effect correlation graph between genes identified in the mouse and for which age-related expression levels of orthologous genes were available in the human CTX(60). Black dots indicate genes with most conserved age-effects that are likely to support a large proportion of the overall correlation (See F. and Table S3.).

E. Correlation levels between age-related transcript changes in WT or *Htr1b*^{KO} mouse CTX and two areas of the human prefrontal CTX. All p<0.005, except WT18 *versus* BA47, p=0.01. Correlations were based on age-effect in rodent (p<0.001) and identifiable human orthologs (WT, n=88 genes; KO, n=271 genes). **F.** Selected genes with conserved age-effects in CTX between mouse and human. Values are in average $\log_2$(Old/Young ratio) (Red: increased; Blue: decreased). See Table S3 for additional genes and details. BA9/47, Brodmann areas 9/47.

Mouse-human phylogenetic conservation of age-effect in brain CTX.

Comparing results to our previous study of the molecular correlates of aging in the human brain(60), we identified highly significant correlations between age-related effects in WT or *Htr1b*^{KO} mice and the two investigated areas of the human prefrontal CTX (Figure4.D-F). Mouse-human correlations of age-effects increased from 18 to 24 months in WT mice, but again were highest for 18 months-old *Htr1b*^{KO} mice (Figure4.E). Selected genes with conserved age effects are displayed in Figure4.F and in the supplemental information (Table S3). Together, these results demonstrated a phylogenetic conservation of age-effect in mammalian CTX and

confirmed the age-related nature and early peak of the brain molecular phenotype of *Htr1b*^{KO} mice.

Early occurrence of the age-related gene expression signature in *Htr1b*^{KO} mice.

With very few exceptions (See last paragraph), all identified genes were expressed at similar levels in WT and KO mice at 3-months of age (Figure5, 3-month time-point), indicating that the molecular correlates of the differential age-related phenotype in *Htr1b*^{KO} mice were initiated later in adulthood, and consistently with the lack of behavioral differences in young adulthood. As predicted, investigating the appearance and progression of age-related changes revealed that over 98% of individual genes affected in CTX displayed early changes in *Htr1b*^{KO} mice when compared to WT controls. 25.6% of changes occurred initially at 10 months (Figure5.A-B, “early” pattern) and 72.6% at 18 months of age (Figure5.C-D, “late” pattern). Likewise, over 97% of age-related genes identified in STR displayed similar anticipated age-related profiles in *Htr1b*^{KO} mice (not shown). This early onset of age-related pattern is illustrated for glial fibrillary acidic protein (Gfap; Figure5.E-F), a marker of age- and brain-related events(275) (i.e. inflammation), which displayed a “late” pattern of changes, with initial WT-KO differences at 18-months of age.

Figure 19. Over 98% of age-related genes displayed early onset of age-related trajectories in *Htr1b*^{KO} mice

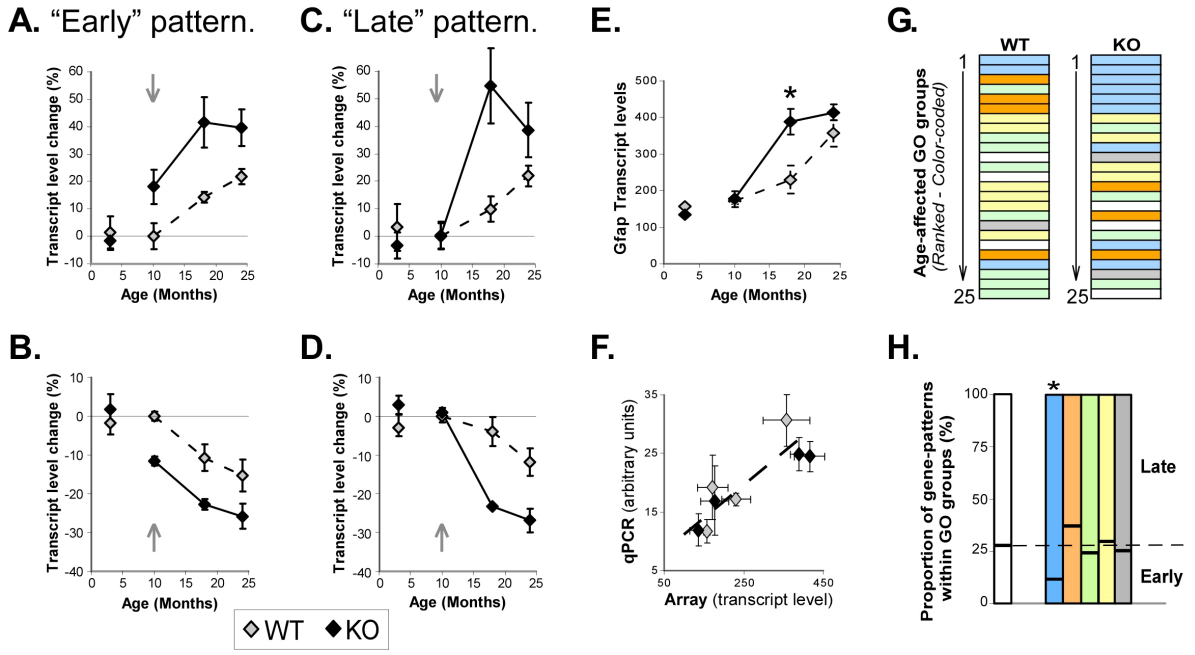

Figure 5. A-D. Averaged transcripts profiles for genes with onset of age-related effects in KO mice occurring initially at 10-months ["Early": 198 increased (**A.**) & 81 decreased (**B.**) genes; 25.6% of age-related genes] or 18 months ["late": 670 increased (**C.**) & 126 decreased (**D.**) genes; 72.6% of age-related genes], compared to the onset of behavioral differences (Vertical gray arrow). <2% of age-affected genes had similar profiles in WT and KO mice (not shown). Values are in percentage of WT levels. The 3-month old groups used for array analysis were bred at a different time and analyzed separately. **E.** Gfap age-related transcript profiles as an example of "late" pattern (Age-effect, $p<0.0005$ in WT and KO; *, WT/KO at 18-month, $p<0.05$). **F.** Confirmation of altered Gfap transcript levels by real-time quantitative PCR (qPCR): Array/qPCR correlation ($r=0.87$, $p=0.005$). Values are mean±sem. **G-H**.

Functional analysis of molecular aging. **G.** The 25 most affected color-coded gene groups in WT and *Htr1b*^{KO} mice are regrouped in 5 main functions: translation (blue), inflammation (red), metabolism (green), cell growth (yellow), cellular respiration (Gray), miscellaneous (White). Details in Table S4. **H.** Proportional representation of genes with "early" (10 months) or "late" (18 months) patterns of initial WT-KO differences in age-related trajectories within the main age-related functions. *p<0.001, difference from expected proportions (White column and hatched bar).

The presence of different age-related patterns of changes in transcript levels raised the question as to whether specific biological functions were associated with these patterns, and could thus have mediated the early onset of behavioral changes in *Htr1b*^{KO} mice. To address this question, we *a)* systematically identified groups of related genes displaying high representation of age-affected genes(259, 260), *b)* compared results between WT and KO mice, and *c)* further investigated whether any of the identified gene groups displayed over- or under-representation of genes with changes occurring in parallel to the onset of behavioral differences (i.e. "early " or "late" patterns). The cumulative effect of aging on gene groups was assessed according to the Gene Ontology classification(261) and is presented in a color-coded fashion for the 25 most affected gene groups in WT or *Htr1b*^{KO} mice (Figure5.G and Table S4). The nature of the identified gene groups revealed that very similar biological functions were affected during aging in WT and *Htr1b*^{KO} mice, albeit with

minor differences: Translation-related gene groups (Blue bars in Figure5.G) were prominent in both groups, but displayed increased "ranked" representation in *Htr1b*^{KO} mice, while the representation of inflammation-related gene groups (Red bars in Figure5.G) was decreased in *Htr1b*^{KO} mice, in reminiscence of previous evidence suggesting reduced inflammation in the periphery (Figure1.E). Results are presented for CTX and were highly similar in STR (not shown). Importantly, the proportion of genes with "early" or "late" onset of WT/KO changes differed only marginally from their expected proportions within the 5 main identified age-related functions (Figure5.H), with the exception of translation-related gene groups that displayed significantly more genes with late-onset differences. Genes with early WT/KO age-related differences were slightly, but non-significantly, over-represented in inflammation-related functions.

Taken together, results from our temporal and functional analyses of age-related changes in gene expression did not identify any specific biological function as the potential source or mediator of the early onset of the age-related phenotype, but rather suggested a global and early shift of the molecular signature of aging in the brain of *Htr1b*^{KO} mice.

A role for Bdnf in age-related transcriptome changes and in the *Htr1b*^{KO} molecular phenotype?

Altered neurotrophic function, including 5-HT/Bdnf interactions, has been suggested to mediate some of the age-related changes occurring in the brain(44). Here, we confirmed the previously reported downregulation of Bdnf transcripts with

age in CTX(60, 264, 276) (WT: -1.63 fold change, p=0.006; KO: -2.24 fold change, p=0.002; Tables S1 and S3) and showed that changes followed an “early” pattern in *Htr1b*^{KO} mice (Table S1), thus suggesting a potential causative role for altered Bdnf function in the *Htr1b*^{KO} age-related phenotype. Therefore, to investigate the potential contribution of Bdnf to the molecular phenotype of *Htr1b*^{KO} mice, we took advantage of a recent report describing CTX gene expression changes occurring downstream from altered Bdnf function in Bdnf knockout mice (embryonic or adult *Bdnf*^{KO,}(62)) and investigated similarities between Bdnf- and age-induced transcriptome changes. In particular, if changes in Bdnf function participated in the age-related *Htr1b*^{KO} molecular phenotype, then the effect of *Bdnf*^{KO} on altered gene transcripts would correlate with the effect of aging, and should mostly follow an early pattern of changes in *Htr1b*^{KO} mice. Here, we identified a moderate, but significant, correlation between changes in *Bdnf*^{KO} mice and age-related changes in *Htr1b*^{KO} or WT mice (r~0.20, p<0.05). Correlations with age-related profiles were slightly higher for adult (r=0.22, p<0.05, n=98 genes) *versus* embryonic *Bdnf*^{KO}-induced changes (r=0.17, p<0.05, n=173 genes). Correlations with *Bdnf*^{KO}-induced changes were also slightly higher when compared to age-related changes in *Htr1b*^{KO} (r=0.23, p<0.05, n=271 genes) *versus* WT mice (r=0.20, p<0.05, n=271 genes). Importantly, genes affected by both Bdnf and aging displayed age-related trajectories that were evenly distributed between “early” and “late” patterns on WT/*Htr1b*^{KO} differences (i.e. 50% “early” patterns genes), suggesting that Bdnf downregulation did not play a major role in the early onset of age-related events in *Htr1b*^{KO} mice.

Together, these comparative studies revealed a potential active role for Bdnf in age-related changes, as altered gene expression induced by decreased Bdnf correlated with aspects of the molecular correlates of aging in the brain ($r \sim 0.20$, $p<0.05$). However, our studies also suggested that the early age-related phenotype in *Htr1b*^{KO} mice was independent of the role of Bdnf in aging.

Increased age-related sirtuin 5 gene expression.

What possible mechanism could induce the early onset of age-related events in *Htr1b*^{KO} mice? Out of ~45,000 transcripts tested, only 8 gene transcripts displayed consistent genotype differences in CTX and STR (Table S5), including at the 3-month time-point that preceded the behavioral differences. Two of these probes corresponded to the sirtuin 5 gene (*Sirt5*), which belongs to a family of protein deacetylases that regulate lifespan in yeast, C.*elegans* and drosophila(277). Increased *Sirt5* transcripts were confirmed by qPCR and *in situ* hybridization and displayed a pattern of increased levels in *Htr1b*^{KO} mice, converging towards WT levels at 24 months (Figure6). The role of sirtuin genes in replicative and chronological aging in lower eukaryotes and mammalian cells is complex(278, 279) and whether the reported increased *Sirt5* transcripts, and potentially Sirtuin 5 function, may mediate the early onset of aging in *Htr1b*^{KO} mice or represent an early adaptive mechanism is currently under investigation.

Figure 20. Figure 5. Upregulated Sirt5 gene expression in CTX of *Htr1b*^{KO} mice.

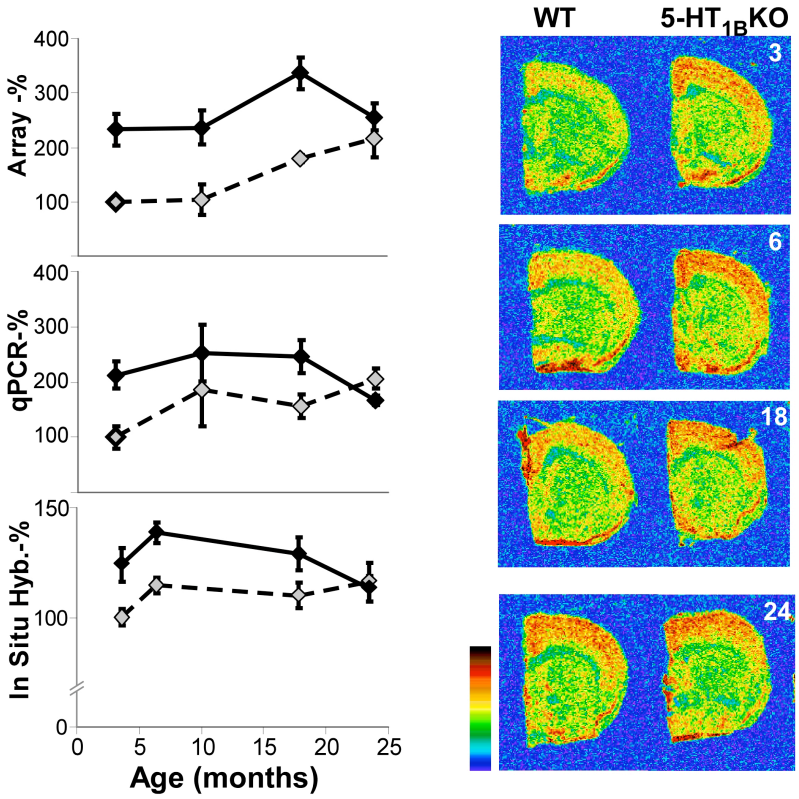

Figure 6. A. Microarray (top), qPCR (middle) and *in situ* hybridization (ISH, bottom) analyses revealed significant increased Sirt5 transcript levels in *Htr1b*^{KO} mice, with normalized differences at 24 months of age. Smaller differences by ISH were mostly due to Sirt5 expression throughout the brain, which precluded background subtraction and likely underestimated specific signal differences. All values are in percentage of young WT controls. Genotype effect: array, $p<0.01$; qPCR, $p<0.05$; ISH, $p<0.01$. Pair-wise correlations (array-qPCR-ISH), all $r>0.65$, $p<0.05$. **B.** Representative color-coded photomicrographs of Sirt5 ^{35}S-ISH at 3, 6, 18 and 24 months of age. Color barcode indicates increased signal intensity.

Discussion.

Together our studies have demonstrated that altering 5-HT signaling through the disruption of the 5-HT_{1B} presynaptic autoreceptor can modulate the onset of selected age-related events in the central nervous system. We have shown that the lack of $5HT_{1B}$R-mediated signaling induced both an early age-related motor decline (Figure1) and an early shift of the characteristic gene expression signature of aging in the brain (Figure5), ultimately resulting in decreased longevity (Figure1). Our results also suggested that the age-related phenotype in *Htr1b*^{KO} mice may have originated in the brain, as peripheral markers revealed no effect (intestinal tract), or changes suggesting protection or adaptive mechanisms (insulin and IGF-1 systems, Figure2) against deleterious aspects of the early onset of age-related events. As aging can be viewed as the accumulation of a variety of events that together create in essence a chronic challenge to the brain, and since the 5-HT system is a key system for homeostatic control and adaptation to stress(80), we have provided here evidence supporting the notion that the interaction of 5-HT with this challenge influences age-dependent behavior and molecular events.

Investigating the nature and progression of age-related changes in brain gene expression throughout the adult life, we have uncovered profound changes in *Htr1b*^{KO} mice, which were characteristic of an early onset of brain molecular aging (Figure4). The age-related nature and early onset of the brain molecular phenotype in *Htr1b*^{KO} mice was further confirmed by cross-species comparisons with the correlates of aging in the human brain(60). Indeed age-related changes occurring in the CTX of WT or *Htr1b*^{KO} mice significantly predicted age-related changes in two areas of the

human CTX, and identified numerous individual genes with similar age-effects across species (Figure4 and Table S3), thus demonstrating a phylogenetic conservation of the molecular correlates of aging from mouse to human. These analyses confirmed numerous prior findings at the level of individual genes (e.g. GFAP, BDNF, MOBP, complement activation, etc.; Table S3), but to our knowledge, this is the first large-scale demonstration of a rodent-human phylogenetic conservation of age-effect in the mammalian CTX, thus validating the use of rodent models to recapitulate aspects of aging of the human brain. Importantly, these cross-species comparisons confirmed the age-related nature and the early onset of the brain molecular phenotype in *Htr1b*^{KO} mice, as *Htr1b*^{KO}-human correlations of age-effect reached similar levels than in WT-human comparisons, albeit at an earlier age (Figure 4.E).

Imaging and molecular studies suggest that age-related changes are continuous and progressive throughout the human adult lifespan(34, 60, 74, 229). Here we provided evidence supporting the notion of a “maximum” age-related molecular effect. Indeed, *Htr1b*^{KO} mice reached an apparent peak in age-related changes in gene transcript levels at 18 month of age (Figure5), which had not yet been attained at the latest time-point investigated in WT mice (24 month of age). Interestingly, the timing of this “maximum” age-effect corresponded to the age where death events started to occur in the KO group, suggesting a failure of the system at maintaining proper homeostasis past this point. Indeed, the decreased correlations of age-related transcriptome profiles that were observed between very old *Htr1b*^{KO} mice and either control mice or human subjects (Figure2) may have reflected the presence of secondary and less-specific events occurring beyond a certain maximum age-related

effect. Nevertheless, despite the potential occurrence of a late breakdown in homeostasis, our results demonstrated mostly a parallel and early age-related phenotype in *Htr1b*^{KO} mice. This trajectory was different from the exponential acceleration in age-related phenotypes and mortality that is commonly observed in mouse models of peripheral/somatic age-related mechanisms(90, 280-282). In particular, the increased in hazard ratio in *Htr1b*^{KO} mice (Figure1.H) appears to be mostly due to a shift of death events towards earlier ages, rather than a progressive increase in frailty leading to an exponential homeostatic failure(90, 280-282). This parallel, rather than exponential, trajectory is consistent with a progressive and cumulative effect over time, rather than an acute and early mechanistic switch leading to a catastrophic failure of the system. Here we suggest that this parallel age-related trajectory in *Htr1b*^{KO} mice is consistent with an altered capacity of the 5-HT system to initially respond to the chronic challenge that is formed over time by various events occurring during brain aging. Indeed, as typical longevity and molecular curves display early “buffer” periods where the cumulative effects of aging are not yet observed (i.e. 3- through 12-month behavioral and gene-expression time-points in WT), *Htr1b*^{KO} mice display a reduced “buffer” period (3-months time-point), resulting in an early onset, rather than altered progression, of age-related phenotypes.

To identify potential mechanisms mediating the early onset of the *Htr1b*^{KO} age-related phenotype, we proceeded with both unbiased surveys of cellular and biological functions and with directed evaluation of markers for candidate biological systems. Systematic analyses of functional relationships and of temporal patterns between age-affected genes (Figure5) did not identify any novel biological functions

being recruited during aging in *Htr1b*^{KO} mice, but rather suggested a global and early onset of the molecular signature of "normal" aging in the brain of *Htr1b*^{KO} mice. Regarding candidate systems, a leading hypothesis for age-related mechanisms centers on the role of oxidative stress and inflammation, as mediators of neuronal damage and subsequent increase in reactive astrocytes(38, 41). Here, our combined observations of decreased ranked representation of inflammation-related functions in the brain, of late appearance of WT/KO differences of a cellular marker of inflammation (Gfap; Figure5.E-F) and of evidence of reduced peripheral inflammation (IgG, Figure2.F) did not support the notion that inflammation-related events mediated the early onset of aging in *Htr1b*^{KO} mice. Nevertheless, we can not rule out the possibility that additional peripheral mechanisms may have contributed to the phenotype, especially in the absence of more direct measurements of reactive oxygen species-mediated damage such as lipid peroxidation and protein carbonylation, which may have contributed to the shortened life expectancy.

Bdnf is a neurotrophic factor supporting neuronal functions during development and in the mature brain. Correlative evidence of decreased Bdnf transcript levels with age in the human frontal CTX(60, 264, 276) has suggested the possibility of a causative role in brain aging. Here, we confirmed the downregulation of Bdnf with aging in the mouse CTX. We also identified a modest but significant correlation between the effects of Bdnf hypofunction in *Bdnf*^{KO} mice(62) and the gene expression correlates of aging in mouse CTX ($r\sim0.20$, $p<0.05$), suggesting that aspects of aging in the brain may occur as a consequence of downregulated Bdnf function. However, although interactions between 5-HT and Bdnf have been documented(283) and

hypothesized to both concur with IGF-1 to influence age-related events(44), our results suggest an age-related phenotype in *Htr1b*^{KO} mice that is independent of Bdnf function.

On the other hand, our studies provided supporting evidence for potential interacting mechanisms between 5-HT and the previously identified age-related IGF-1 and sirtuin systems. A non-significant trend towards downregulated levels of circulating IGF-1 levels in *Htr1b*^{KO} supports the notion of 5-HT/IGF-1 interaction during aging. In this case, lower IGF-1 levels would be protective against aging(273) and thus it is not known whether lower IGF-1 levels represented a direct consequence of altered 5-HT function or rather a reactive/protective process against the detection of an early onset of age-related symptoms, as recently hypothesized for age-related processes in peripheral organs(284). Interestingly, a clear upregulation of sirtuin 5 gene expression was identified in the brain of *Htr1b*^{KO} mice. Sirtuin genes are major cellular components of age-related pathways, however their role in replicative and chronological aging in lower eukaryotes and mammalian cells is complex(278, 279). The role of altered Sirt5 transcripts in the age-related phenotype in *Htr1b*^{KO} mice is currently under investigation, including as a potential mediator of 5-HT control over homeostasis, or as an early mechanism for altering the onset of age-related phenotypes, since Sirt5 transcript changes preceded the appearance of age-related behavioral and molecular changes. Nevertheless, it suggests that the differentiated central nervous system may share common molecular and/or cellular components with age-related mechanisms in peripheral somatic tissues.

Although the observed phenotype originated from a deficiency in 5-HT-mediated

presynaptic inhibition, a limitation in the analysis of potential mechanisms supporting the observed phenotype resides in the fact that the deletion of this receptor altered the kinetics of the 5-HT system(251, 255, 256), and thus could have influenced the behavior, molecular and longevity phenotypes through altered signaling at other 5-HT receptors. Therefore, the observed phenotypes should be considered in the context of altered 5-HT mediated functions in *Htr1b*^{KO} mice. This observation relates to our initial choice of the *Htr1b*^{KO} mice for investigating the role of 5-HT into aging, as we hypothesized that a disrupted 5-HT homeostasis may initially more closely model the evidence of a deregulated control of 5-HT during aging (See Introduction). Moreover, other neurotransmitters systems interacting with $5HT_{1B}R$ and not investigated here may have played a role in the mutant phenotype. In particular, changes in cholinergic functions may have occurred, as suggested by Buhot et al(266), in view of complex changes in memory functions in aging *Htr1b*^{KO} mice(266).

The presence of an early deficit in motor behavior was consistent with the role of $5\text{-}HT_{1B}R$ in motor function(252). The distribution and functional contribution of $5\text{-}HT_{1B}R$ in the spinal cord and cerebellum are low(285, 286), while the nature of the phenotype indicated a deficit in complex motor behavior (rotarod and coat hanger tests), rather than a decrease in locomotor and/or muscle strength (Total activity and rearing in open field and elevated plus maze; early occurrence rather than accelerated frailty). This suggested a deficit in higher coordination, rather than a potential degeneration of spinal motor neurons, although a direct examination of the integrity of these neurons will be necessary to rule out this possibility. In the central nervous system, $5\text{-}HT_{1B}R$ indirectly regulates DA release in STR(255). No evidence

of altered DA terminal density and area was identified in STR of old (and young) WT or KO mice (Figure3), thus also excluding a structural downregulation of the DA system as the cause of the motor deficits in young *Htr1b*^{KO} mice, although a role for altered DA kinetics in aging KO animals can not be ruled out. Moreover, the behavior decline could also be mediated through altered signaling at several other 5-HT receptors, due to altered 5-HT kinetics(251, 255). Thus, currently the exact mechanism leading to the motor phenotype is unknown, and may involve additional brain areas and systems not investigated here. Due to the complex biological nature of motor coordination and for the purpose of this study, we have considered the *Htr1b*^{KO} motor phenotype as an indicator of changes in overall age-related functions, while we have concentrated our molecular studies on FC and STR, as two brain areas with well-described roles for 5-HT$_{1B}$R. Furthermore, investigating the FC allowed for the direct comparison of age-related molecular changes in WT and *Htr1b*^{KO} mice with our prior characterization of aging in the human brain(60). Eventually, studies using regional-, cell type- and time-specific targeted manipulations of 5-HT$_{1B}$R in conditional mutant mice will be necessary to investigate the more specific roles of critical brain regions, time-periods and interacting neurotransmitter systems that may participate in the different aspects of the behavioral and molecular phenotypes, and that underscore the increased vulnerability to age-related events in *Htr1b*^{KO} mice.

In conclusion, our studies suggest a brain-driven age-related phenotype in mice lacking the presynaptic 5-HT$_{1B}$ receptor. The notion of altered longevity and early

onset of age-dependent events due to changes in the brain represents an important novel finding, which is however not unprecedented. For instance, in lower eukaryotes, the well-characterized changes in longevity due to mutations in the IGF-1 pathway is rescued only when signal transduction is restored in neurons and not in other cell types of nematodes(287) and flies(288), therefore providing supporting evidence for a control of age-related processes by the brain. Here, as the “onset” rather than the “nature” of aging was affected in *Htr1b*^{KO} mice, 5-HT can be considered a modulator of “normal” aging of the brain, consistently with its role in adapting to environmental challenges and maintaining homeostasis. As the 5-HT system is the target of chronic pharmacological interventions for psychiatric and other diseases, these results raise the possibility of long-term and/or age-related consequences to 5-HT manipulation that will need to be addressed in future studies. Pursuant is the potential for altered molecular and/or behavioral age-related trajectories in correlation with genetic polymorphisms in the Htr1b gene or other key regulators(83) of the 5-HT system.

IV. CHAPTER 3- PAPER 3 (SUBMITTED)

"Brain Molecular Aging, Promotion of Neurological Disease and Modulation by Sirtuin5 Longevity Gene Polymorphism"

Christin Glorioso,[1] Sunghee Oh,[2] and Etienne Sibille[1]
[1]Department of Psychiatry and Center For Neuroscience, [2]Department of Biostatistics,
University of Pittsburgh, Pittsburgh, PA 15213.

Abbreviated title: Molecular aging and neurological diseases

Correspondence should be addressed to Dr. E.Sibille, University of Pittsburgh, Department of Psychiatry, 3811 O'Hara Street, BST W1643, Pittsburgh, PA 15213, E-mail: sibilleel@upmc.edu

4 Figures and 1 Table; Supplemental material (Detailed Methods and supporting findings)
7-9 pages; Number of words: Abstract (250), Introduction (487), and Discussion (1273)

Keywords: molecular aging, sirtuin, transcriptome, neurological disease, mitochondria

Acknowledgements: Support was provided by National Institutes of Aging (C.G.) National Institutes of Mental Health (E.S.), US, NIH, and by the University of Pittsburgh Institute of Aging (E.S.). The funding agency had no role in the study design, data collection and analysis, decision to publish and preparation of the manuscript. The content is solely the responsibility of the authors and does not necessarily represent the official views of the NIMH or the National Institutes of Health. We thank Drs. Robert Sweet and David Lewis for discussions about the study and Drs. Chris Patil, Joseph Glorioso, Charles Bradberry, and Mark Doyal for

commenting on the manuscript. The authors declare that they have no conflict of interest.

Abstract

Mechanisms determining characteristic age of onset for neurological diseases are largely unknown. Normal brain aging associates with robust and progressive transcriptome changes ("molecular aging"), but the intersection with disease pathways is poorly characterized. Here, using cross-cohort microarray analysis of four human brain areas, we show that neurological disease pathways largely overlap with molecular aging and that subjects carrying a low-expressing polymorphism in a longevity gene (Sirtuin5; $SIRT5_{prom2}$) have older brain molecular ages. Specifically, molecular aging was remarkably conserved across cohorts and brain areas, and included numerous developmental and transcription-regulator genes. Neurological disease-associated genes were highly overrepresented within age-related genes and changed almost unanimously in pro-disease directions, together suggesting an underlying genetic "program" of aging that progressively promotes disease. To test this putative mechanism, we developed and used an age-biosignature to assess five candidate longevity gene polymorphisms' association with molecular aging rates. Most robustly, aging was accelerated in cortex, but not amygdala, of subjects carrying a SIRT5 promoter polymorphism (+9yrs, p=0.004), in concordance with cortex-specific decreased SIRT5 expression. This effect was driven by a set of core transcripts (+24 yrs, p=0.0004), many of which were mitochondrial, including Parkinson's disease genes, PINK1 and DJ1/PARK7, hence promoting $SIRT5_{prom2}$ as a putative risk factor for mitochondrial dysfunction-related diseases, including Parkinson's, through a novel mechanism of accelerated molecular aging. Our results suggest a possible "common mechanism" underlying age of onset across several neurological diseases. Confirming this pathway and its regulation by common genetic variants would provide new strategies for predicting, delaying, and treating neurological diseases.

Introduction

Disease-specific ages of onset are core features of many neurological disorders, ranging from late-onset neurodegenerative diseases such as Alzheimer's and Parkinson's diseases (average onset 60 and 75 years, respectively) (113) to earlier onset psychiatric disorders such as schizophrenia and bipolar disorder (average onset 25 years) (114). The mechanism(s) underlying age thresholds and the factors that contribute to individual variability in ages of onset within diseases are largely unknown. Studies have predominantly focused on contrasting disease brains with age-matched controls, a strategy that may be problematic, as it is becoming increasingly evident that normal aging is an integral aspect and modulator of disease onset and progression. Evidence for this comes from the sheer prevalence of diseases with increasing age, such as Alzheimer's disease, which increases exponentially from age 75 upward reaching nearly 45% by age 95 (113). Additionally, genetic/environmental lifespan extension studies in model organisms have shown that slowing normal aging results in delayed onset of age-related disorders. For example, mice hypermorphic for the longevity gene, Klotho, not only live ~20% longer but also have a corresponding delay in onset of ectopic calcification, osteopenia, arteriosclerosis, emphysema, and insulin resistance (52, 122). This has also been shown in a caloric restriction model of extended longevity in primates, which demonstrated delayed incidence of diabetes, cancer, cardiovascular disease, and brain atrophy (49). It is also becoming clear that age-gated neurological diseases can be delayed by extending normal lifespan, as lifespan extension via reduction of insulin/insulin growth factor signaling resulted in delayed proteotoxicity in both C. elegans and mouse Alzheimer's disease models (123, 124).

What is occurring during the normal aging of the brain that is required for disease onset? Robust morphological and molecular changes progressively occur in the normal aging brain throughout adulthood and into old age (37). Morphological changes include progressive loss of grey matter density (34), disrupted myelination, and increasing reactive gliosis. These changes reflect dendritic shrinkage, synaptic loss, (37, 38) and thickening glial processes (glial dystrophy) (42). Within neurons,

increased DNA damage and reactive oxygen species, calcium dysregulation, mitochondrial dysfunction and inflammatory processes have been reported (Reviewed in (37). Several groups, including our own, have characterized the molecular underpinnings of these changes using human post-mortem brain microarray (60, 74, 75); however, no systematic effort has been undertaken to explore the molecular overlap of normal aging and disease pathways. Moreover, as molecular age accurately predicts chronological age (60), we hypothesized that observed deviations from predicted molecular age trajectory may be under genetic control, whereas longevity gene variants may affect rates of molecular brain aging and risk for neurological diseases, through overlapping age-related and disease pathways.

Materials and Methods

Cohorts and Microarrays. We employed two previously described microarray datasets: Cohort 1 (60) [39 subjects; ages 14-79; prefrontal cortex (PFC) Brodmann area 9 (BA9) and 47 (BA47) samples] and Cohort 2 (289) [36 subjects, ages 23-71; anterior cingulate cortex (ACC) and amygdala samples]. Subject characteristics, dissection protocols, and array controls have been previously described (60, 289) and are summarized in Supplementary Table 1. All subjects were free of age-related neurological diseases at time of death according to medical records and pathologist examination of brain tissue. GC-RMA-extracted data from Affymetrix HU133A (cohort 1) and HU133Plus2.0 (cohort 2) arrays were used. Control variables included technical measures (chip quality controls, RNA integrity, post-mortem interval) and subject characteristics (race, gender, and mode of death). All array data are available at our website (www.sibille.pitt.edu), including a searchable database for age effects on gene transcript levels in the human brain.

Importantly, both cohorts included subjects diagnosed with major depression (Supplementary Table 1). We have previously shown (and confirmed here) that the gene expression correlates of depression were of greatly reduced scope compared to the effects of aging.

Specifically, in Table S1, we show for both cohorts that the effect sizes of aging are between 184 and 986 times greater than the effect sizes of major depression at the same significance cutoff of $p<0.001$ per brain area, depression: 2-6 transcripts per brain area) a nd 40-50 times greater at the $p<0.01$ cutoff, and that major depression effects do not survive Benjamini-Hochberg control for multiple testing. Moreover, as previously described (60), major depression was not associated with deviations in molecular ages (Supplemental Figure S1). So since human brain samples are a limited resource and as the effects of depression are of limited scope and do not associate with altered rates of molecular aging, we have included these subjects in the current analysis in order to increase analytical power (See discussion).

Defining and Validating Age-regulated Genes.

For congruence with the progressive pattern of structural (decreasing grey matter) and functional (cognitive decline) brain aging changes (34, 290), we used best-fit age-regression coefficients to determine significance of age-related gene transcript changes across subjects (Figure 1a, Supplementary Tables 1, 2). For each transcript, equations were generated for linear, log, exponential, and power fits of expression level versus chronological age and the most significant (best-fit) equation was selected (p-values derived from correlation R-values). False discovery rates (FDR) were estimated using Benjamini-Hochberg methodology (291). QPCR validation for 42 array-defined age-regulated genes are described in (60, 289) and in online supplements (Supplementary Figure 2).

Cross-sectional brain area comparisons. Transcripts with age-regression $p<0.001$ were selected for each brain area, and regression equations were solved for percentile expression changes between 20 and 70 years of age. Directed Pearson correlations (292) were performed by correlating these expression changes with transcript levels for the same genes in the other three brain areas.

Age-related Biosignatures. Genes were included in the cross-area biosignature if they displayed age-regression $p<0.01$ with age in 3/4 brain areas and $p<0.05$ in the

fourth, and if directions of age-regulated changes were concordant in all brain areas. Notably, all but one gene that met the first criteria did not pass the second (HTR2A-both probesets increased with age in amygdala but decreased in cortical areas). If more than one probeset per gene met both criteria, the probeset with the lowest p-value across areas was selected to avoid any gene having a greater weighted influence on molecular age. For ACC and amygdala-specific biosignatures, genes were selected if they had age-regression $p<0.01$ in those areas. Cross-area biosignature genes, cross-area equations, regression R-values, p-values, and magnitude of expression changes are available on-line (www.sibille.pitt.edu/data.html).

Transcriptome functional analyses were performed using Ingenuity® version 7.0. and the connectivity map (C-MAP), as described in the respective websites [http://www.ingenuity.com/; http://www.broadinstitute.org /cmap, (293)] and in the supplements.

Molecular ages. Individual predicted molecular ages were calculated for all age-regulated genes using a leave one out approach within ACC or AMY (Supplemental Fig S7), as previously described (60). In short, to describe each sample individually in the general aging trend, we have devised a one-number-summary ("Molecular age") for each sample, describing the "predicted age" of the sample when removed from the analysis. For each sample, the remaining database was analyzed for age-related genes using the same correlation-based methods described above, controlling the FDR at 0.05. For each selected gene, a best-fit regression analysis with age was performed, and the age for the held-out sample was predicted using the resulting function. Extreme outlier molecular ages (+/-10 standard deviations from average chronological age) were removed. The resulting gene-wise predicted values were averaged per sample and used to described the predicted molecular age of each subject.

$SIRt5_{prom2}$ (rs938222) Effects on Molecular Age. $SIRT5_{prom2}$ is located in a mouse/human conserved region predicted by two separate programs to contain a

promoter, TSSG CGG Nucleotide Sequence Analysis (http://genomic.sanger.ac.uk/gf/gf.html) and Promoter 2.0 (http://www.cbs.dtu.dk/services/Promoter/) (Supplementary Figure 6). Cohort 2 subjects were genotyped by sequencing of polymerase chain reaction (PCR) amplified segments of genomic DNA obtained from brain samples. Subjects were 50% C/C and 37% C/T in agreement with Hap-map (www.hapmap.org) published frequencies for CEU subjects (Supplementary Table. 9). Rare T/T subjects were excluded from analysis because of lack of power. Genotypic differences in all gene transcript levels were calculated using two-tailed Students t-tests in middle-aged cross-sectional groups rigorously matched for chronological age, C/C (n=12, average age= 52.1 years, range= 49-63 years) C/T (n=11, average age 52.7 years, range 48-64 years). Similarly significant (although ~10% fewer affected genes) results were obtained using the alternative approach of including all subjects and controlling for age and other parameters by ANOVA.

To assess snp-based group differences, molecular ages were subtracted from chronological ages to assess deviations of molecular from chronological age, thus removing the effect of chronological age. Two-tailed t-tests were performed to obtain p-values associated with difference in total molecular age between genotype-defined groups. A parallel analysis using an ANOVA model yielded similar and significant results, although slightly less robust. This analysis was also performed using only age x snp effect intersection transcripts (Figure4b). We refer to these transcripts here as ‘intersection transcripts’.

Real-time quantitative PCR (qPCR). qPCR was performed as previously described (294). Results were calculated as the geometric mean of relative intensities compared to three internal controls (actin, glyceraldehyde-3-phosphate dehydrogenase and cyclophilin).

Results

Molecular aging is conserved across cohorts and brain areas

At $p<0.001$, 814-1972 transcripts were age-regulated in each brain area with 1-4% estimated FDR (Supplementary Table 1). Array data were previously validated by high correlation with independent quantitative PCR (qPCR) results (n=42 genes, $R=0.72$, $p=10^{-10}$, Supplementary Figure 1) and by known age-regulated genes changing in predicted directions, including up-regulated reactive gliosis markers (GFAP), and down-regulated growth factors (BDNF and IGF-1), synaptic markers (SYN2) and calcium homeostasis genes (CALB-1)(74, 75) (Figure 1a). Expression changes did not reflect age-related changes in cell number, as many neuronal-specific transcripts were unchanged with age [NRSN2 (295); Figure 1a], consistent with stereological studies demonstrating minimal neuronal loss during normal aging (38).

Molecular aging was remarkably conserved across cohorts and brain areas ($p<10^{-10}$, Figure 1b). Gross area-specific differences were only observed in amygdala, with fewer age down-regulated transcripts (Figure 1b, n=87) compared to cortical areas (n=684-1133). We have previously shown that down and up-regulated changes are predominantly of neuronal and glial origin respectively (60, 296) (Supplementary Table 3); thus the fewer observed downregulated neuronally-enriched changes still correlated with changes in other brain areas, but were “noisier” (higher p-values, Supplementary Tables 3-5), consistent with structural MRI studies reporting robust cortical and more variable amygdala age-related grey matter losses (33).

Figure 21. Figure 1. Conserved molecular aging profiles across human brain areas.

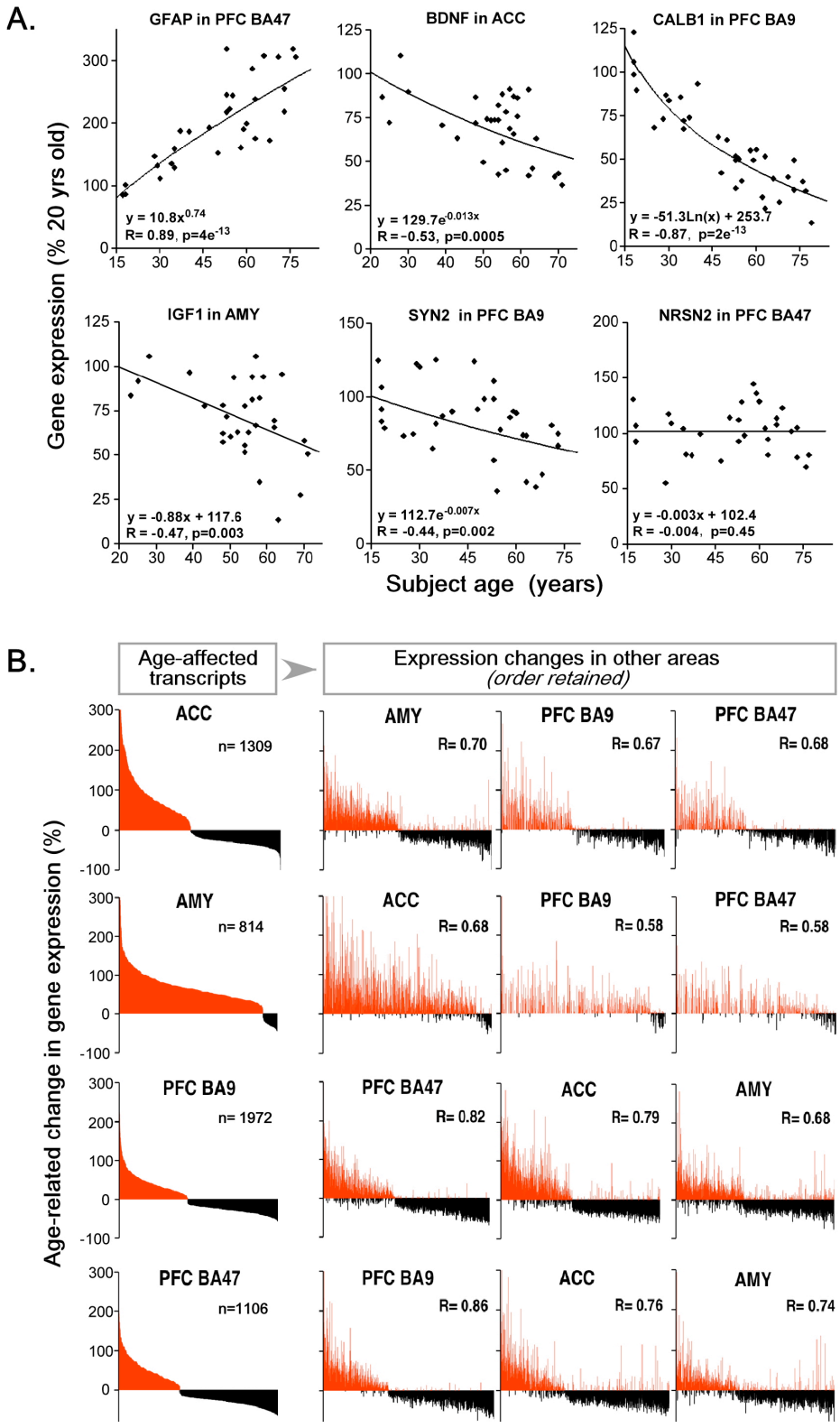

Figure 1. Conserved molecular aging profiles across human brain areas. A) Representative age-regression gene plots and B) cross-area comparisons of age-regulated gene expression changes [70-20 yrs change; ordered from most increased with age (red) to most decreased with age (black)]; n=number of age-regulated genes; R=directed Pearson coefficient.

A novel age-related biosignature predicts chronological age, contains development- and neurological disease-related genes, and is potentially regulated by cell-cycle and neurotransmitter-modulatory drugs

To assess cross-sectional rates of molecular aging, we developed a brain- and age-related biosignature, based on conserved changes across areas (n=356 genes). Transcript levels were converted into "molecular ages" using cross-area age-regression equations, which were averaged to generate a single molecular age per subject per brain area, using a leave-one-out approach to avoid circularity. The biosignature was highly predictive of subject age ($p<10^{-16}$, Figure 2a), confirming its utility as a quantitative assay and the cross-area robustness of age-related transcript changes.

Using large-scale hand-annotated literature information, Ingenuity® biological pathway analysis identified the expected categories of known age-related changes in the biosignature (cell morphology, signaling, immune response, vascular function, cell death, DNA repair and protein modification) (Supplementary Tables 6,7). Additionally, nervous system development was a top category (70 associated genes, Supplementary Table 6), highlighting epigenetic regulators, transcription factors, and histones, as suggested regulators of a putative age-related transcriptional program (Figure 2b). Importantly, neurological disease was a top category (115 associated genes), supporting our hypothesis of disease promotion by normal aging (Supplementary Table 6,7).

We further characterized the age-related biosignature using the microarray drug-matching program, C-MAP (293), by identifying drugs causing transcriptional

changes in cell culture inversely correlating with our biosignature (candidate anti-aging drugs). As an internal validation, C-MAP identified known anti-aging and neuroprotective agents, such as α-estradiol and GW-8510, an inhibitor of neuronal apoptosis (Figure 2c). Interestingly, results pointed to regulatory roles for cell cycle proteins and neurotransmitters as candidate anti-aging drugs, as two of the top six drugs were cyclin-dependent-kinase inhibitors and two were monoaminergic modulators (Figure 2c).

Figure 22. Figure 2. Age-related biosignature: predictability of subject ages and proposed regulatory genes.

a

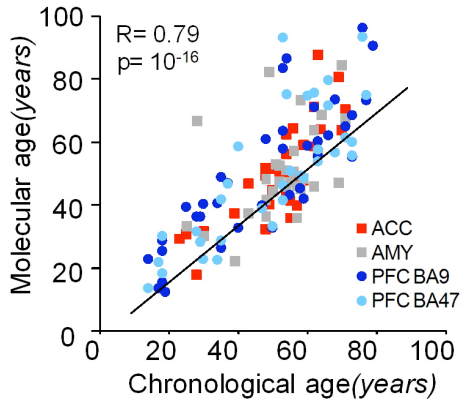

b Epigenetic regulators & Transcription factors

Gene	N	G	B	E(%)	P-val
Histone cluster 1, H2bk			3	-34	1E-16
Down-regulator of Transcription 1			3	-40	5E-11
Methyl CpG Binding Protein 2			3	+24	2E-10
Mitochondrial ribosomal protein S12	3			-39	2E-10
Methyl-CpG Binding Domain 1	3			-18	1E-06
Chromatin Modifying Protein 1B	3			-18	4E-06
Forkhead Box O1		3		+42	2E-06
H3 Histone, family 3A/3B		3		+73	2E-16
Transcription Factor EB		3		+66	6E-09
CREB-regulated Transcription Coactivator		3		+39	3E-10
Jumonji, AT-rich Interactive Domain 1A		3		+42	1E-08
HMG-box Transcription Factor 1		3		+42	1E-11

c C-Map Candidate Brain Aging Drugs

Drug	Mechanism	P-val
Anti-aging		
GW-8510	CDK2 inhibitor; neuroprotective	1E-04
α-estradiol	Estrogen enantiomer; neuroprotective	1E-04
Urapidil	Antihypertensive, α1 adrenergic antagonist, α2 adrenergic agonist, 5HT1A agonist; neroprotective	2E-04
Alsterpaullone	Inhibitor of CDK2, CDK1/Cyclin B, CDK5/p25, GSK-3β, Tau phosphorylation; neuroprotective	5E-04
Skimmianine	Furoquinoline alkaloid (plant extract) used in folk medicine; potentially anti-inflammatory, anti-tumorigenic, MAO inhibitor	6E-04
H-7	PKC inhibitor, decreases calcium current, alters astrocyte morphology	7E-04
Niacin (vitamin B3)	Anti-inflammatory properties; used to treat hypercholesterolemia, arteriosclerosis, and cardiovascular disease	0.005
Biotin (vitamin B7)	Regulates insulin secretion; therapeutic efficacy in diabetes	0.009
Pro-aging		
Wortmannin	Inhibitor of PI3-K cell survival pathway	1E-06
Benzamil	Na/Ca exchange blocker, inhibitor of NGF mediated neurite outgrowth	5E-04

Figure 2. Age-related biosignature. a) predictability of subject ages and b) proposed regulatory genes; red= age-upregulated, blue= age-downregulated. N (neuronally-enriched), G (glial-enriched), B (similarly expressed in neurons and glia), E (expression 70-20 yrs, all brain areas). c) Biosignature-predicted age-modulatory drugs. AD, Alzheimer's disease; PD, Parkinson's disease; HD Huntington's disease; ALS, amyotrophic lateral sclerosis; SCZ, schizophrenia; BPD, bipolar disorder.

Neurological-disease related genes are overrepresented amongst age-regulated genes and change in pro-disease directions

To characterize the extent of overlap between age and disease pathways, we selected a wider gene group (n=3,935) not restricted by significance in all brain areas ($p<0.001$ in one area, or $p<0.01$ in two). Again, neurological disease was a top Ingenuity®-identified functional category, comprising 34% of age-regulated genes (Figure 3a, Supplementary Figure 3). Consistent with our hypothesis, the top indentified diseases, Alzheimer's, Parkinson's, Huntington's, amyotrophic lateral sclerosis, schizophrenia and bipolar disorder were all common neurological diseases with well-defined ages of onset (Supplementary Figure 4). Conversely, disease-associated genes represented only 4% of non-age-regulated genes ($p>0.05$ in all areas), and neurological disease fell to the 44^{th} functional category with no specific diseases represented (Figure 3a, Supplementary Figure 5). Furthermore, investigations into a subset of genes with well-established disease-associations revealed that expression changes were almost unanimously (32/33) in disease-promoting directions (Figure 3b, Table 1, Supplementary Table 8). Examples of age-regulated plots for specific disease-related gene are shown in Figure 3b. Note the discrepancy in rates observed across brain regions for some genes. For instance, clusterin (CLU), an Alzheimer-related gene displayed greatest age-related increase in ACC (red), where neuregulin (NRG-1), a schizophrenia-related gene, showed lowest age-related downregulation in BA9 (Dark blue) (Figure 3b), together providing a potential mechanisms for region-specific onset of pathological symptoms.

Figure 23. Figure 3. Molecular aging of neurological disease genes.

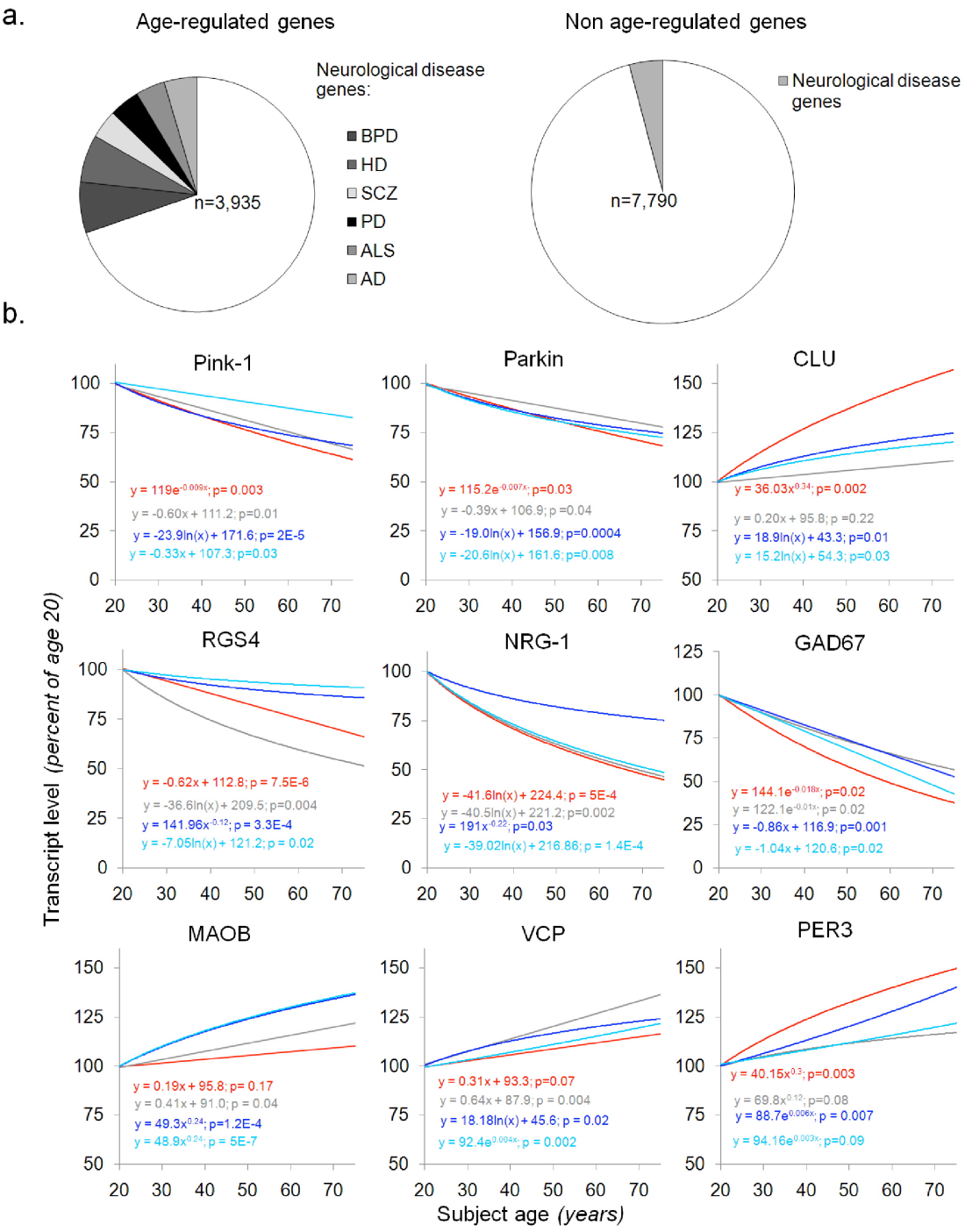

Figure 3. Molecular aging and neurological diseases. a) Percentage of age and non age-regulated genes identified as neurological disease-related by Ingenuity. Left) 34% (n=1,098) of age-regulated genes were neurological disease-related, including AD (n=185), PD (n=170), HD (n=267), ALS (n=164), SCZ (n=161), and BPD associated genes (n=285). Right) 4% (n=321) of non-age regulated genes were neurological disease-related with no specific diseases identified. b) Example plots of age-regulated disease-related genes. Trendlines are best-fit regression lines for ACC (red), Amygdala (grey), PFC BA9 (dark blue), and PFC BA47 (light blue) with color-coded equations and corresponding regression p-values.

Table 4. Table 1. Neurological disease age-regulated gene expression changes are in disease-promoting directions.

	Direction of change in disease						Change with age(%) (p-val)			
Disease-associated gene_symbol	AD	PD	HD	ALS	SCZ	BPD	ACC	AMY	PFC BA9	PFC
Amyloid beta precursor protein binding-1_Fe65	u						-17.4(0.005)	n.s.	-25.9(1.2E-5)	n.s.
Amyloid beta precursor protein binding- 2_APPB2/PAT1	↑						+18.1(0.02)	+10.1(0.04)	+22.1(0.0003)	n.s.
Amyloid precursor-like protein 2_APLP2	↓						-25.4(0.009)	n.s.	-31.1(0.0001)	-30.5(0.008)
Clusterin/Apolipoprotein-J_CLU	↑		↑	↑			+80.5(0.0004)	+29.3(0.02)	+75.8(1.3E-7)	+54.8(5.8E-8)
Monoamine Oxidase B_MAOB	↑	↑	↑	↑			n.s.	+20.5(0.42)	+34.2(0.00006)	+34.9(8.5E-7)
Microtubule-associated protein tau_MAPT	↑	↑					-34.9(0.009)	n.s.	-28.7(2.9E-6)	n.s.
α-synuclein_α-syn	↓	u					-32.6(8.8E-5)	-39.4(0.03)	-19.7(1.7E-6)	-20.3(0.001)
Parkinson Disease-2_Parkin	u	↓					-29.5(0.02)	-19.4(0.04)	-23.9 (0.0003)	-26.0(0.009)
Parkinson Disease-5_UCHL1		↓					-27.2(0.001)	-24.6(0.02)	-14.9(0.002)	n.s.
Parkinson Disease-6_PINK-1		↓					-36.2(0.003)	-29.9(0.009)	-29.8(6.3E-6)	-15.7(0.03)
Parkinson Disease-7_DJ-1		↓					-25.9(0.0006)	-15.3(0.02)	n.s.	n.s.
Parkinson Disease-13_HTRA2		↓					-27.4(0.002)	n.s.	-9.5(0.04)	-25.6(0.0006)
Huntingtin_HD			↓				n.s.	n.s.	-22.9(0.0005)	n.s.
Valosin-containing protein_VCP			↑				n.s.	+32.5(0.003)	+22.9(0.001)	+22.9(0.002)
Mitochondrial Complex 1 Subunit_NDUFB5			↓				-22.0(0.001)	-28.9(0.009)	n.s.	n.s.
Mitochondrial Complex 1 Subunit_NDUSF2			↓				-33.0(0.0003)	n.s.	-16.8(0.002)	n.s.
Mitochondrial Complex 1 Subunit_NDUSF3			↓				-24.4(6.4E-5)	-22.1(0.05)	-15.4(0.01)	-13.9(0.005)
Mitochondrial Complex 1 Subunit_NDUSF3			↓				-17.9(0.0007	n.s.	n.s.	n.s.
Mitochondrial Complex 4 Subunit_COX7B			↓				-22.7(0.0004)	-27.2(0.004)	n.s.	n.s.
Cyclin-dependent Kinase-5_CDK5	↓		↓				-35.3(4E-5)	n.s.	-30.9(1.9E-8)	-25.6(0.0002)
NF-kappa B_NF-kB	↑	↑	↑	↑		↑	+16.2(0.03)	n.s.	+24.0(0.0001)	+15.1(0.01)
Manganese Superoxide dismutase_SOD2	↓			↓	↓		n.s.	n.s.	-50.3(0.0007)	n.s.
Cholecystokinin_CCK	↓	↓			↓		-33.8(0.002)	-29.7(0.03)	-18.1(0.01)	n.s.
Neuropeptide-Y_NPY	↓	u			↓	↓	-33.8(0.02)	-41.7(0.008)	-34.1(0.003)	n.s.
Cannabanoid Receptor-1_CB1	↓	u	↓		↓		n.s.	n.s.	-45.7(2.6E-10)	-39.4(0.002)
Parvalbumin_PVALB	↓	u			↓	↓	-58.6(0.001)	n.s.	n.s.	-34.5(0.02)
Glutamate decarboxylase 1_GAD67		↓			↓	↓	-59.3(0.02)	-39.3(0.02)	-43.2(0.0009)	-51.9(0.02)
GABA transaminase_GABA-T	u				↑		+25.3(0.04)	n.s.	+28.4(0.0003)	n.s.
Brain-derived neurotrophic factor_BDNF	↓	↓	↓		↓	↓	-45.1(0.0005)	n.s.	-39.8(8.9E-6)	-41.8(3.4E-5)
Serotonin 2A Receptor_HTR2A	↓				↓	↓	-40.8(0.0007)	+64.9(0.04)	-39.4(0.0001)	-46.3(0.0008)
Serotonin 5A Receptor_HTR5A					u	u	-39.3(0.0007)	-32.9(0.00005)	-33.2(0.0001)	-34.3(0.05)
Somatostatin_SST	↓	↓	↓		↓		-45.0(0.0001)	-61.4(0.01)	-57.3(5.4E-6)	-39.4(0.001)
Regulator of G-protein signaling-4_RGS4	↓		↓		↓	u	-43.5(0.008)	-75.3(0.006)	-44.7(2.0E-8)	-57.5(2.1E-5)
Reelin_RELN	u	u			↓	↓	-33.0(0.02)	n.s.	n.s.	-38.1(0.0002)
Neuregulin-1_NRG1	u				u	u	-52.3(0.0003)	-50.7(0.001)	-23.7(0.03)	-48.9(0.0002)
Dopamine Receptor D1_DRD1	u		↓		u	u	-50.3(0.008)	n.s.	-33.7(0.001)	-48.7(0.006)
GABA receptor, alpha-5 subunit_GABRA5			↓		u	u	-48.3(0.03)	-59.4(0.02)	-67.0(8.3E-10)	-58.9(0.0003)
Period homolog-3_PER3					u	u	+46.7(0.002)	n.s.	+35.0(0.004)	n.s.
Aryl hydrocarbon receptor nuclear translocator-like_BMAL1					u	u	-37.0(0.005)	n.s.	-44.5(1.4E-5)	-59.3(1.4E-5)

Table 1. Agreement of directions between disease-related and age-regulated (age 70-age 20) gene expression changes. ↓ = decreased mRNA/protein levels reportedly pro-disease; ↑= increased mRNA /protein levels reportedly pro-disease; u= unknown/ unclear reports of directionality in disease (references in supplementary Table 8); n.s.=non-significant (p>0.05) change with age.

$SIRT5_{prom2}$ associates with decreased SIRT5 expression and accelerated molecular aging, particularly of mitochondrial-localized proteins, in a brain area-specific manner

We next hypothesized that longevity genes may regulate brain aging and that polymorphisms in these genes may influence gene sets involved in risk for disease. We assessed 5 polymorphisms in three candidate longevity genes (Supplementary Figure 6, Supplementary Table 9), but focus the remainder of this study on the $SIRT5_{prom2}$ single nucleotide polymorphism (snp), as it was associated with the largest and most statistically robust effects on molecular aging (Supplementary Table 10). We chose SIRT5 due to the increasing role of the sirtuin gene family in neurodegenerative disease (54) and due to our previous observation of altered Sirt5 expression in $htr1b^{KO}$ mouse cortex, a mouse model with anticipated brain aging (63). We also concentrated on cohort 2 subjects, for which genetic material was available.

We show by quantitative polymerase chain reaction (qPCR) that the $SIRT5_{Prom2}$ polymorphism associates with a 45-55% decrease in expression in two SIRT5 transcript variants in ACC (Figure 4a). SIRT5 itself did not display age-regulated expression levels (age-regression p=0.45), thus genotypic differences in expression were present at all ages. No $SIRT5_{Prom2}$ genotype effect on SIRT5 expression was observed in amygdala (Supplementary Figure 8), suggesting a brain-region specific effect of $SIRT5_{Prom2}$. SIRT5 C/C (low-expresser) allele carrier subjects had significantly older ACC molecular ages (+8.6 years, p=0.003, Figure 4b) compared to C/T carriers (Supplementary Figure 7). This resulted from apparent accelerated ACC molecular aging rates in C/C carriers (increased molecular vs. chronological age slope, Figure 4b). Using an amygdala-specific biosignature (Supplementary Figure 7), we show that $SIRT5_{prom2}$ was not associated with altered amygdala molecular aging, consistent with its ACC-specific effect on expression (Supplementary Figure 8).

Figure 24. Figure 4. SIRT5$_{prom2}$ effects on ACC molecular aging

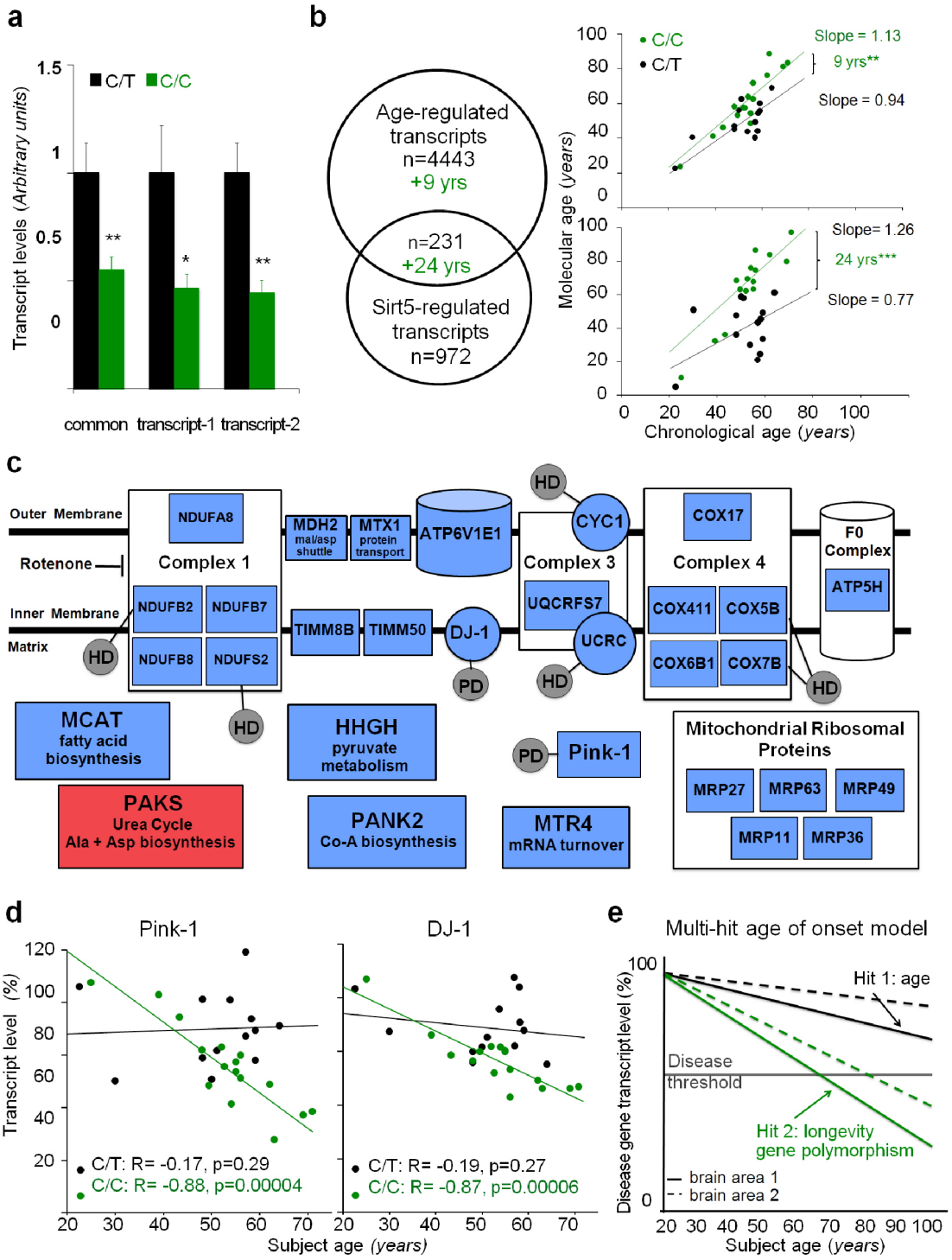

Figure 4. $SIRT5_{prom2}$ effects on ACC molecular aging. a) SIRT5 expression in ACC by prom2 genotype b) Venn diagram (ACC) of age ($p<0.01$) and $SIRT5_{prom2}$ ($p<0.01$) associated transcripts; (number yr)= average number of molecular years greater in C/C subjects than C/T (left); molecular ages of subjects by $SIRT5_{prom2}$ genotype (top-right) based on all age-regulated transcripts and core transcripts (bottom-right) c) Schematic of mitochondrial age-regulated genes with accelerated age-trajectories in SIRT5-low-expresser subjects; blue are age down-regulated transcripts; red are age-upregulated transcripts; grey circles identify HD or PD-associated genes. d) Representative core transcript age-regressions (PD genes) by $SIRT5_{prom2}$ genotype. E) Multi-hit model of age of onset. Rates of age-regulated changes in disease gene expression are accelerated in subjects carrying "risk alleles" of age-modulatory gene polymorphisms (i.e. SIRT5) in a brain area specific manner, resulting in this case in earlier age at which decreased expression reaches a critical theoretical threshold for symptom or disease onset. Conversely, protective factors (genetic and/or environmental) would delaying onset. A similar mechanism would occur for age upregulated disease-related genes.

We investigated whether $SIRT5_{prom2}$'s correlation with older molecular ages was global or potentially driven by a subset of genes. We determined the significance of $SIRT5_{prom2}$ genotype association with transcript changes for all other genes in well age-matched subgroups, as an exploratory approach for potential indirect $SIRT5_{prom2}$-mediated effects (Supplementary Figure S10). $SIRT5_{prom2}$ associated ($p<0.01$) with altered levels for 972 transcripts, including 231 age-regulated transcripts (Figure 3b). These latter transcript changes almost unanimously (98%) associated with older molecular ages in SIRT5-C/C carriers. Indeed, based on these "core" snp-by-age intersection transcripts, subjects carrying the C/C allele were on average 24.1 molecular years older than C/T carriers ($p=0.0004$, Figure 4b). We conjecture that these core transcripts represent proximal effectors in SIRT5's putative modulation of age-related expression changes.

These predominantly (74%) neuronally-enriched transcripts included potential brain-aging regulators, transcription factors (GTF3A , TCF7L2), Histone 3 (H3F3A/3B), Chromatin Modifying Protein 2A (CHMP2A), and CDK5 (Supplementary Table 11). Strikingly, considering SIRT5's mitochondrial localization (54, 297), was that many core transcripts coded for mitochondrial-localized proteins, including numerous components of the electron transport chain (Figure 4c). The top two identified canonical pathways were mitochondrial dysfunction and oxidative phosphorylation, and the top functional categories - genetic and neurological diseases- were predominated by two diseases linked to mitochondrial dysfunction: Parkinson's (9 associated genes) and Huntington's (22 associated genes) (Figure 4c, Supplementary Figures 9-11). Most directly, $SIRT5_{prom2}$ genotype accounted for all age-related declines in expression of the familial Parkinson's genes, PINK1 and DJ1/PARK7 (Figure 4d; qPCR-validated, Supplementary Figure 12). People with loss of expression/function mutations in these genes develop early onset Parkinson's (298). Together, these findings suggest that $SIRT5_{prom2}$ may represent a risk factor for mitochondria-related diseases, potentially including Parkinson's and Huntington's diseases.

Discussion

In this report, we demonstrate that molecular aging of the human brain is highly conserved across cohorts and brain areas, and provide evidence suggesting an underlying transcriptional program that promotes neurological diseases and is under genetic control.

Expanding from our prior report (60), we demonstrate high brain-area and cross-cohort conservation of molecular brain aging, selectively affecting ~5-10% of all detected genes. Consistent with studies in model systems (299-302), the presence of many affected regulators of gene expression (transcription factors, histones, and methylases) suggest an underlying genetic program regulating cascades of downstream gene expression changes and offering potential entry points to molecular dissection of this putative genetic program. Moreover, the characterization

of an age-derived molecular biosignature that is highly predictive of chronological age pointed towards cell-cycle and neurotransmitter-modulating drugs as potential aging-regulators, offering insight into how age-related changes may be regulated by new candidate anti-aging therapies.

A notable feature of this molecular signature of aging is a large over-representation of neurological-related genes almost unanimously affected during age in disease-promoting directions, revealing that pathways to several neurological diseases may actually be intrinsic aspects of normal aging. Furthermore, the top six represented diseases (Alzheimer's, Parkinson's, amyotrophic lateral sclerosis, Huntington's, bipolar disorder and schizophrenia) were not only all neurological, but age-gated. This data suggest a converse interpretation, where age-related diseases may stem from expression changes in the most age-vulnerable genes, hence promoting age-vulnerable genes as novel candidate disease genes. However, the large representation of age-affected schizophrenia and bipolar-related genes is intriguing, as while these diseases are age-gated, their onsets occur at younger ages and they are often considered development-related diseases. Here, as developmental genes were a top represented age-regulated category, our results support the concept that aging and development may share overlapping pathways, or alternatively, that aging may extend from development. This makes conceptual sense, as synaptic pruning for instance is beneficial during development, but related mechanisms may lead to deleterious synaptic losses during aging. Moreover, similar to our observations during adult and late-life aging, changes in the rates of these developmental processes and associated genes can lead to altered brain connectivity or subtle changes in synaptic connections, as observed in bipolar and schizophrenia. This is consistent with the recent study by Colantuoni et al showing robust changes in transcript levels for schizophrenia-related genes during development and early adulthood (303).

An important exception to these age-by-neurological disease observations is the absence of depression-related genes and of related functional groups identified within the age-related transcriptome changes. However, this is in line with our prior (60) and

current (Figure S1) findings describing no correlative effects of depression on the trajectory of molecular aging. Interestingly, depression is not considered to be age-gated, as rates of diseases are consistently high throughout life (304). This is also consistent with our observation that chronic stress does not affect molecular aging in rodent models (C.Glorioso, C.Belzung and E.Sibille, unpublished data). Nevertheless, the presence of subjects with diagnostics of depression is a potential limitation of this study that will need to be addressed in larger studies of control subjects only.

We conjecture that rates of molecular aging of disease-related genes may determine at what age (and therefore if) highly prevalent diseases such as Alzheimer's occur, and at what age less prevalent diseases (Huntington's, Parkinson's) may occur in the context of additional genetic/environmental hits. Supporting this gene expression level "gating" model of age-of-onset, promoter polymorphisms affecting disease-gene expression, such as Parkin for instance, associate with younger disease onset (305). Additionally, the brain-area specificity of neurological disorders can potentially be accounted for by this model, as differences in rates of disease-gene expression changes varied across areas by as much as 2.5 fold. Accordingly, a proposed model suggests that people on an older or accelerated molecular aging trajectory may present earlier onset of age-related functional declines and related diseases (Figure 4e). Conversely, slower molecular age trajectory may have protective effects against the same functional outcomes and neurological disorders.

In support of a genetic modulation/control of this molecular aging-by-disease risk model, we show that the cross-sectional trajectory of a large component of molecular aging was differentially affected in subjects carrying a common polymorphism in the SIRT5 putative longevity gene ($Sirt5_{prom2}$), which we also show correlated with reduced SIRT5 expression. Specifically, the greater age-downregulation of mitochondrial-related subset of genes in association with $Sirt5_{prom2}$ suggests first that molecular aging may be affected in a modular fashion, and second that longevity genes may regulate patterns of transcript changes encompassing different disease pathways. Note here that the present investigation was supported by an a priori

hypothesis for a putative SIRT5 effect, and that the molecular correlates of the $SIRT5_{prom2}$ variant were supported by FDR estimates. However, FDR takes into account a limited amount of information only, namely p-value, rank, number of significant transcripts, and total transcripts tested. It does not take into account other information present in the dataset such as multiple probesets for the same gene with convergent results, relatedness of genes found, and genes with convergent functional information. For example, we show that genes identified $Sirt5_{prom2}$ has an estimated FDR of 19%, which can be interpreted as any single significant $Sirt5_{prom2}$–affected gene is estimated to have an 81% chance of being a true positive. However, the fact that 227 out of the 231 genes (98%) are in pro-aging directions suggests that the actual FDR may be lower. Additionally, many genes converge on a cellular compartment (mitochondria), code for different subunits of the same protein complex (Complex 1 for example; Figure 4D), or are identified by significant effects on multiple probesets coding for the same gene present (Pink-1 and GTF3A for example), together increasing the confidence level in the biological validity of the findings, in addition to statistical criteria. Together, our results suggest that SIRT5-risk allele (C/C) carriers may be at increased risk for mitochondrial-dysfunction related disorders, including Parkinson's and Huntington's diseases.

This proof-of-concept study suggests that genetic modulation of molecular aging may associate with differential regulation of specific age-promoted disease pathways in the human brain. The confirmation of this model would have profound consequences for identifying genetic risk factors and for potential new drug development (i.e. SIRT5 targeting in Parkinson's). To this end, large-scale replication of these findings is needed in other postmortem cohorts and in brain areas directly relevant to respective disorders (i.e. substantia nigra and basal ganglia for Parkinson's). Here, the association with reduced SIRT5 transcript levels suggests that either $SIRT5_{prom2}$ or closely-linked DNA variants may mediate the observed effects, but the extension of these findings to large-scale genetic studies combined with molecular aging assays will need larger test and replication cohorts. Further confirmation of the model will also necessarily come from assessment of live subjects with those neurological disorders and normal control cohorts to assess whether either

disease onset and severity, or age-related functional declines (motor, cognition and emotionality for instance) are differentially associated with this particular SIRT5 snp or with other variants identified using the same methodological approach.

Concluding, our findings suggest a uniting gene-expression level mechanism for age-of-onset across neurological diseases that is congruent with a “common disease - common variant” hypothesis. Confirmation of this model will provide new avenues for predicting disease onset and trajectory and potentially for creation of novel therapeutics through monitoring rates of molecular brain aging (by proxy in peripheral blood for example or by advancing neuroimaging techniques), in concert with assessment of novel age-related genetic risk factors (e.g. $SIRT5_{prom2}$) and associated biological (e.g. mitochondrial dysfunction) or phenotypic (e.g. cognitive decline) mediators.

V. DISCUSSION

Normal human brain aging is an understudied area that has many fundamentally different molecular mechanisms and modulators from the periphery. Understanding these mechanisms is crucial to the creation and safety of new therapies/interventions for neurological functional decline and disease. The research presented here investigates several important pieces of this (highlighted in Figure 25); we demonstrate 1. a causal role of 5-HT and BDNF in modulating molecular brain aging in mice, 2. an associative link between a novel low-expressing Sirt5 polymorphism and human molecular brain aging rates and mitochondrial disease promotion, 3. that human molecular brain aging is so highly robust and conserved that it is suggestive of a “genetically controlled transcriptional program”, and 4. the first evidence for a potential “universal” gene-expression level gating mechanism for neurological disease age-of-onset. Here we discuss these findings in their broader context, including their caveats and future directions.

Figure 25. Investigated aspects of the overarching schema. Neuronal and glial "normal" molecular aging: modulators, mediators, and consequences.

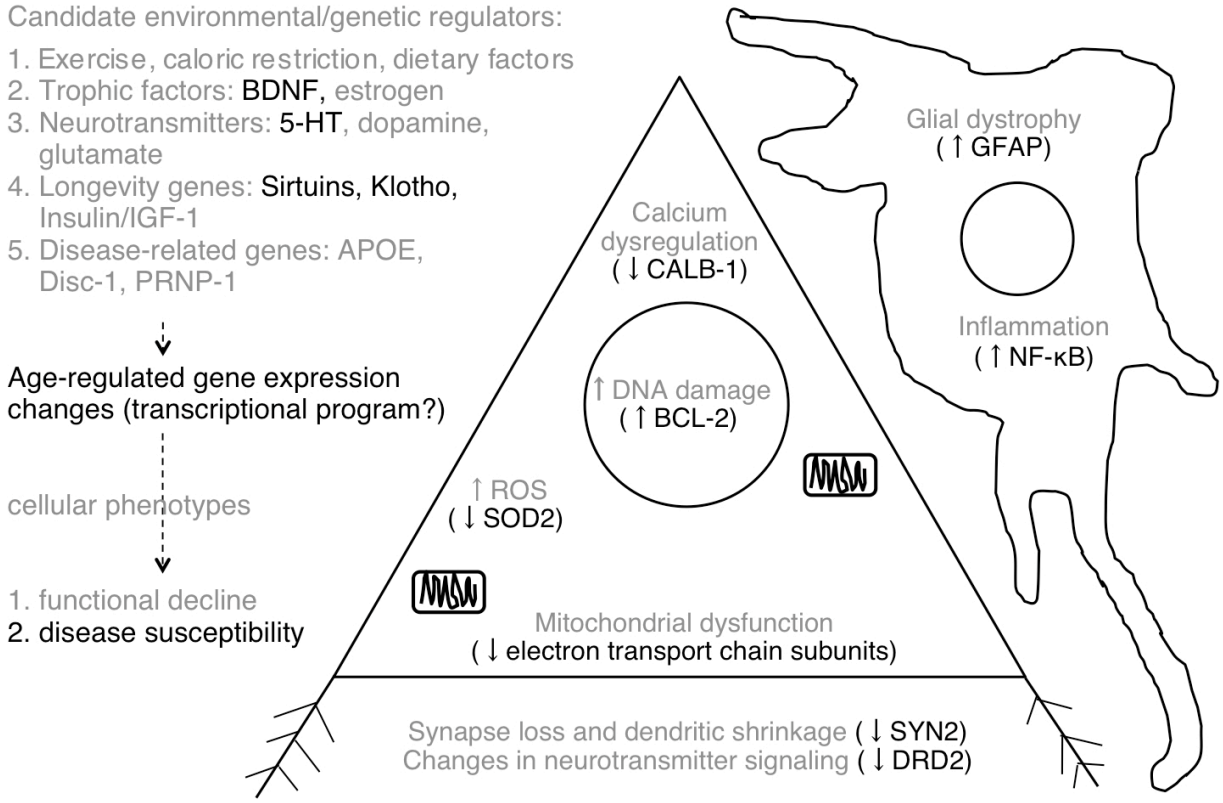

Figure 25. We investigated the causal or associative link between the highlighted candidate genes and age-regulated gene expression changes (molecular brain aging) in mice or humans, respectively. Additionally, we investigated mechanisms of neurological disease promotion by human molecular brain aging. In bold is one example (amongst >1,000) of an age-gated neurological disease (PD) promoting gene expression change (decreased Pink1 expression; loss of function Pink1 mutations cause early onset familial PD) shown to occur during normal aging (see paper 3).

V.A. Microarray signatures of molecular brain aging: advantages and caveats.

All three of the studies presented here employ post-mortem brain microarray to investigate genetic modulation of molecular aging. Given the relative novelty and lingering controversy over this technique, it seems useful to make some opening remarks about it in this context. There are a few distinct advantages to microarray here: 1. it is unbiased, 2. it allows for measurement of overall aging rates as well as investigations into single genes, 3. It is useful as an assay for screening and quantifying modulators of brain aging.

While critics may denote unbiased array approaches as “fishing expeditions”, they are no less legitimate than and are indeed complementary to genome-wide association studies and other genome-wide approaches (CNVs). In fact, results and new leads from these studies are desperately needed in the fields of neurodegenerative and psychiatric disorders. In these highly complex and heterogeneous contexts, purely hypothesis driven research has not been and is unlikely to be successful in uncovering necessary genetic and molecular mechanisms to inform design of much-needed preventative and individualized therapies.

Secondly, microarray has the advantage of assessing molecular brain aging as a whole (at least one “snapshot” of it), as opposed to quantifying a single molecular or functional phenotype (D2 receptor level or age-related working memory for example), as a proxy. It additionally is not limited to this, as individual transcripts or molecular pathways can be investigated, which is especially appealing given that pathway and network analysis software (Ingenuity for example) has rapidly evolved to become highly informative, going far above and beyond what any individual could hand-surmise.

Lastly, drug discovery likely will be hugely influenced in the future by microarray-based pattern matching software, such as c-map (see paper 3, http://www.broadinstitute.org/cmap/, (293, 306)), which can match over one thousand microarray drug signatures from an FDA approved drug library to the microarray signature of any phenomena, to rapidly identify novel candidate drugs, drug classes,

and modulatory mechanisms. We demonstrate the utility of this in paper 3, where by c-map screening of our human molecular brain aging microarray biosignature, we identified known anti-aging and neuroprotective drugs as positive controls as well as new leads for molecular aging mechanisms and therapies. This rapid drug discovery method will have profound consequences for the creation of novel therapies for devastating age-related neurological diseases, for which there are no effective treatment strategies currently. This potential is unique to microarray as no other technique has such a rapid and specific read-out for this purpose.

That being said, there are three potential caveats associated with microarray that should be addressed: 1. observed molecular events are a single “snap-shot” (the RNA level), 2. rates of false discovery must be controlled, and 3. cellular origin of transcript changes are not distinguishable. Firstly, some studies use microarrays to assess gene expression changes as a proxy for protein level or functional changes, in which case expression-protein-function level correlation should be confirmed by western blot and/or functional assays. However, for many purposes (including our own), such as biosignature assessment molecular brain age, use in drug-matching, or studies concerned with gene transcript levels specifically, protein levels/function are not relevant.

Secondly, a criticism often evoked with respect to gene arrays is that they have high rates of false positives. This may stem from lingering impressions from older studies using less reliable pre-human-genome-project array platforms and/or from the relatively poor statistical control observed in many studies to date. However, under the statistical and analytical protocols applied to the papers presented here, we (and our laboratory) routinely obtain high correlation (0.7-0.9) between array results and their independent confirmation by qPCR.

Lastly, the inability to distinguish cellular origin of transcript changes is a drawback in the context of placing expression changes into pathways or establishing molecular cause and effect relationships, but this can be addressed by double-labeling experiments and/or in tissue culture. Additionally, microarray technology is evolving to intrinsically address this caveat. For example, we have created methods to categorize transcripts as predominantly neuronal, glial, or both ((296), paper 3,

appendix 4) and laser capture techniques in combination with more sensitive amplification protocols have enabled arrays experiments on individual cell layers or even individual cells.

In summary, with awareness of it's potential caveats, microarray is an extremely useful unbiased approach to uncovering molecular mechanisms and evaluating/screening for modulators, which can then be confirmed and further investigated on a variety of fronts from molecular studies in tissue culture to functional measures in living human subjects.

V.B. Genetics of "normal" brain aging: what we know now, what we still don't know.

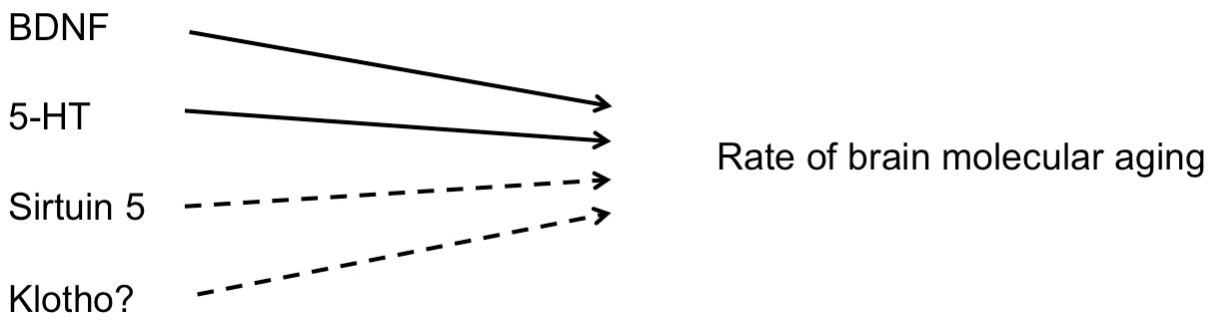

Here we establish the first causal links between brain molecular aging and BDNF and 5-HT in mice (paper 2), as well as associative links with a low-expressing Sirtuin 5 promoter polymorphism and Klotho KL-VS (less robustly) in humans (paper 3). Human association studies and mouse genetic manipulation studies offer convergent information, both required to firmly establish causality. Causality cannot be definitively established in humans because co-segregating genetic/environmental factors may be responsible for (or interacting with) outcome measures. Conversely, biological relevance cannot be definitively established in KO mice because gene KO is not identical to the gene mutations, polymorphisms, and age-regulated declines driving human molecular aging, and because of mouse-human interspecies differences. Indeed, our group has recently shown that while molecular aging of the mouse and human brain correlate modestly, substantial differences exist (292),

highlighting a potential limitation of these studies. This limitation is also revealed in certain neurodegenerative disease mouse models. For example, while PINK-1 mutations in humans cause familial PD, PINK-1 KO mice are not Parkinsonian, displaying only mitochondrial dysfunction without neurodegeneration or shortened lifespan (307, 308). This may reflect differences in brain molecular aging or interacting genetic factors in the two species. Despite these potential caveats, much can still be established in mouse and human genetic studies.

V.B.i. BDNF modulation of brain aging.

BDNF, an exercise and caloric-restriction induced secreted neurotrophic factor that decreases with age (59), has been extensively linked to brain aging. It has been shown to be neuroprotective and required for neurogenesis (59), BDNF infusion can restore age-related LTP impairments in rats (61), the human val66met (secretion deficient) polymorphism is associated with accelerated rates of normal cognitive decline and decreased grey matter volumes (77, 78) and the val66met knock-in mouse displays memory deficits and reduced hippocampal volumes with underlying dendritic shrinkage (309), establishing causality and biological relevance for BDNF in several brain aging measures (see introduction for details). In paper 2, we further this link by demonstrating that the conditional BDNF KO mouse molecular brain signature is correlated with normal mouse molecular brain aging, but also provide evidence that BDNF is not a “global modulator” as the correlation was not high enough to fully account for all age-regulated molecular changes. Many human top age-regulated transcripts (see paper 3), were also top BDNF-regulated transcripts (see paper 1), including RGS4, CCND2, APBAP2, SYN2, SST, NPY, and PENK1, suggesting that a subset of normal age-related molecular changes in both mouse and human are directly modulated by BDNF level.

However, because it was tangential in the context of paper 2 and paper 1 focused primarily on the overlap of BDNF-related changes with GABAergic pathways, and SCHZ and AD-related changes (see paper 1), we have not yet investigated which age-regulated molecular changes/pathways were anticipated in BDNF-ablated

animals. We could explore this by investigating the subset of BDNF-modulated versus BDNF-independent age-related changes using pathway analysis tools, such as Ingenuity(http://www.ingenuity.com/). We could then perform similar analyses in humans with relation to the val66met polymorphism and compare the mouse and human subsets of BDNF-modulated age-regulated changes. Finally, an important question, especially in the context of BDNF being a logical therapeutic candidate for neurodegenerative disease and age-related declines (indeed it is in various stages of drug testing by companies and research groups), is whether BDNF rescue can reverse or delay these age-regulated molecular changes. To this end, we could use the inducible system to ablate and then rescue BDNF expression, and test the reversal of age-regulated expression effects by microarray. Another important point for human therapeutic purposes, given that BDNF is secreted in both a constitutive and activity-dependent manner, is the establishment whether BDNF rescue can be blanket (by infusion or drug induction) or must be up-regulated in a biologically-relevant way. This could also be established in the inducible mouse model with adult BDNF rescue of anticipated molecular aging by intracranial infusion, versus drug targeting, versus exercise, versus inducible expression rescue. In this context, it is also important to establish that BDNF infusion or drug targeting does not cause other unwanted side-effects, such as overgrowth of dendrites, which could cause functional problems in the brain. This could additionally be established using microarray, by testing for molecular consequences that are not related to reversal.

V.B.ii. 5-HT modulation of brain aging.

As was discussed in the introduction, 5-HT has been hypothesized to modulate brain aging because it shares pathways with BDNF and insulin (44), 5-HT selective drugs modulate aging in C. elegans (64-66) and promote neurogenesis in mice (45), and several serotonin signaling polymorphisms have been associated with either age-related cognitive decline and/or grey matter volume loss (81-84). In paper 2, we show the first causal evidence for 5-HT modulation of normal brain aging, demonstrating a global anticipation of age-related molecular changes as well as

longevity and motor correlates in HTR1B KO mice. In paper 3, we translate this to humans, obtaining a negative result between HTR1B G861C polymorphism and human brain aging that should be interpreted in light of it's many caveats.

HTR1B KO mice show a global anticipation of molecular brain aging, ie. 98% of age-regulated genes, which is in contrast to the selective anticipation of age-regulated changes see in BDNF KO mice. Additionally, HTR1B changes correlate only very modestly with BDNF-related molecular changes, suggesting that these two modulators do not share substantial overlapping mechanisms, contrary to what we would have hypothesized based on their shared signaling pathways (44). Together this suggests that 5-HT potentially may be a more robust candidate than BDNF for modulating overall molecular aging, however an obvious next step would be to further establish this by demonstrating that lifespan/healthspan extension in HTR1B over-expressing mice. Interestingly, we did see evidence of cross-talk between Sirtuin and Serotonin pathways as Sirt5 expression was consistently upregulated in KO mice at all ages. This putative link warrants further investigation, perhaps in tissue culture to establish whether HTR1B may directly or indirectly modulate Sirt5 expression.

Importantly, in addition to c. elegans lifespan being modulated by serotonergic drugs (64-66), the HTR1B KO mouse further suggests in mammalian systems that these highly prescribed drugs may be brain age-modulatory. More specifically, the HTR1B/1D agonist migraine medication, Sumatriptan, may delay brain aging or be neuroprotective. Studies of molecular brain aging in mice treated with serotonergic drugs, such as sumatriptan or SSRI's, or epidemiologic studies in humans prescribed these drugs in relation to functional brain aging measurements, are worthwhile next steps in investigating this link.

Another interesting implication of this study is that brain aging may modulate longevity generally, as lifespan was correspondingly shortened in HTR1B KO mice, despite HTR1B being almost exclusively expressed in the brain and peripheral markers being normal. There is precedent for this as neuronal-specific p53 dominant-negative expression or daf-2 KO can extend lifespan in drosophila and nematodes, respectively (58, 310). This broadens the implications of molecular brain aging

studies to include possible implications for longevity generally and peripheral age-related disease.

It is also important to note that while this study establishes 5-HT generally as a brain aging modulator, it doesn't fully address how 5-HT may modulate human brain aging normally. This is for two reasons: 1. Age down-regulation of HTR1B has not been equivocally shown 2. HTR1B KO was not conditional. HTR1B expression does not appear to decrease with age in any of the four human brain areas we assessed (http://www.sibille.pitt.edu/data.html), although we have not yet evaluated many areas of the brain (including those where HTR1B is expressed the highest). Additionally, there is some evidence that HTR1B declines in certain areas of rat brain (311) and also that receptors may decline functionally with age in mice (312). So while overall serotonergic deregulation with age has been hypothesized by us and others (63, 311, 312), the age-related changes in levels and function of serotonergic receptors and signaling is not fully characterized and thus mechanisms behind serotonergic molecular age modulation remain unknown. More thorough characterization of age-related changes in human serotonergic pathways may clarify this, as well as molecular aging studies in other 5-HT receptor KOs or pharmacological models. Lastly, a caveat intrinsic to all non-conditional KO mouse studies is that effects on development of the brain can not be entirely ruled out, and thus further dissection of mechanism using conditional ablation in adulthood versus development may add to mechanistic knowledge.

Lastly, we translated our findings to humans, assessing whether the HTR1B G861C polymorphism, the most consistently associated HTR1B polymorphism with a variety of disorders/phenotypes and thus likely functional (313-317), was associated with rates of human molecular brain aging. These findings were not statistically significant in either the ACC or Amygdala cohort (see appendix 4, paper 3 supplements). However, this negative result should confirmed in other (ideally larger) cohorts, because we were underpowered in this pilot study to see the more subtle effects we might expect with this polymorphism (<4 molecular years), especially given that complete receptor KO only resulted in a 20% anticipation in molecular aging in mice. It is also possible that other HTR1B polymorphisms or other 5-HT

signaling polymorphisms may be more relevant to translation, given that it is unknown how this polymorphism changes HTR1B function.

V.B.iii. Sirt5 modulation of brain aging.

The Sirtuin family of 7 homologues to the yeast longevity gene Sir2, infamous as targets of resveratrol, the putative lifespan extending compound in red wine, have been hypothesized by us and others to be candidate brain aging modulators. This is chiefly because they have been shown to have roles in preventing axonal degeneration (55), neurogenesis (56), and abrogation of protein mis-folding and accumulation (54) (see introduction). However, to date there has been no causal link established between these genes and brain aging specifically, and only one association study has linked a Sirt1 polymorphism to rates of cognitive decline (108). Sirt1 is the most studied of these Nicotinamide-dependent histone/protein deactelylases because it has the greatest homology to Sir2, but even it's biological function and molecular targets are not fully known. We have focused on Sirt5 because it was one of the most upregulated genes in our HTR1B KO mouse model of anticipated brain aging (paper 2) and thus may be an effector in this phenotype. Very little is known about Sirt5 besides that it, as well as Sirt3 and Sirt4, are mitochondrial localized, and it has been shown to deactelyate CPS1, a component of the mitochondrial localized urea cycle (297).

In paper 3, we show that human subjects who are C/T heterozygous for a Sirt5 promoter polymorphism have ~50% less Sirt5 expression and are on average ~9 molecular years older than C/C subjects, both of which were cortex-specific effects. Additionally, and consistent with Sirt5's mitochondrial localization, the most statistically significant age-regulated transcripts were in the mitochondrial dysfunction molecular pathway, including many components of the electron transport chain and 31 genes related to the mitochondrial dysfunction-related diseases, HD and PD. In fact, $Sirt5_{prom2}$ genotype accounted for all age-regulated expression loss of the mitochondrial-located familial Parkinson's disease genes, Pink-1 and DJ-1. Patients with mutations in these genes develop early onset PD and a Pink-1 promoter

polymorphism has been associated with earlier onset of PD, suggesting that the age-regulated loss of expression of Pink-1 and DJ-1 seen in association with $Sirt5_{prom2}$ would promote PD onset.

These findings create many compelling hypotheses and future directions for investigation, but first should be replicated in an additional cohort for confirmation. Interestingly also, these findings are the converse of our observations in the HTR1B KO mouse, where upregulation of Sirt5 was associated with anticipated molecular brain aging, suggesting that perhaps this effect was compensatory to HRT1B's anticipation of brain aging. Future directions include: whether Sirt5 KO mice have accelerated molecular brain aging and/or mitochondrial dysfunction, whether Sirt5 directly or indirectly modulates expression levels of these age-regulated genes in culture and in the Sirt5 KO mouse, and whether $Sirt5_{prom2}$ is associated with age-related cognitive decline or age of onset in PD or HD in living cohorts. Sirtuins are also promising targets for therapeutic intervention, as Sirtuin-specific drugs are already under production in the drug company, Sirtris (http://www.sirtrispharma.com/). If, for example, Sirt5 agonists can directly or indirectly upregulate Pink-1 or DJ-1 expression, which themselves are difficult drug targets, then these drugs may be promising for treatment of Parkinson's disease.

V.B.iv. Klotho and molecular brain aging.

Of the five longevity gene polymorphisms tested for modulation of molecular age in paper 3, we hypothesized that Klotho KL-VS would be most likely to show statistically significant results, because Klotho (and KL-VS) have the strongest evidence for modulating normal brain aging. Specifically, KL KO mice show accelerated neurodegeneration (92), and the KL-VS allele is associated both with human longevity and age-related memory differences (although this may be accounted for by Klotho's baseline effects on IQ) (94,98). What we found was a large (+33 years) statistically significant association with VS heterozygous subjects on a small subset of age-regulated genes (n=18), which, in contrast to $Sirt5_{prom2}$'s effects, was amygdala specific (paper 3, supplementary Figure X). This result was further

supported by correct directionality, ie. the minor VS allele associated with older molecular ages as we would predict from the literature. We did not discuss this result in detail in paper 3 because these findings were much less robust than those in association with $Sirt5_{prom2}$, which we focused on.

However, this does encourage investigation of KL-VS in additional (perhaps larger powered) cohorts. Also, most studies investigating KL-VS have been large enough to evaluate VS homozygotes, which we did not have large enough sample sizes to do. Other logical future directions would be to evaluate the Klotho KO and overexpressing mice for rates of molecular aging, and/or perhaps even create a knock-in mouse of the human KL-VS polymorphism to causally evaluate its molecular effects.

V.C. Brain molecular aging: a genetically modulated transcriptional program?

A few groups, including our own, have investigated human brain molecular aging using microarray and found remarkably consistent results in number (~5-10%) and identity of age-regulated changes (60, 74, 75). Most convincingly, in paper 3 we correlate age-regulated changes from separate cohorts, university brain banks, different microarray chip platforms, and brain areas, demonstrating a remarkable ($p<10^{-6}$) conservation of age-regulated changes (see Figure 1B, paper 3). Furthermore, for the most age-regulated of genes (GFAP and CALB-1, for example) subject age and expression level were so tightly correlated that regression lines assessed using only 36 subjects had p-values of $\sim10^{-13}$ (see Figure 1A, paper 3).

Together, this strongly suggests to us that these selective and extremely consistent changes may be the result of a tightly controlled age-regulated transcriptional program. Moreover, in papers 2 and 3 we provide evidence that this putative program is under genetic control, being anticipated by HTR1B KO and delayed in Sirt5 high-expressing subjects. If this is the case, then what is the mechanism underlying age-regulation of this continuous and progressive program and how is it rate-controlled by genetic modulators?

In paper 3, we begin to investigate these potential mechanisms. We highlight the robust age-regulated changes in expression of transcriptional regulators, such as histones H1 and H3, methylation-related proteins, MECP2 and CHMP2, and transcription factors, DR1, TFEB, and FOXO1, as potential hubs or upstream effectors in this putative transcriptional program. In support of this, FOXO1 is well established (318) and histones and histone targeting drugs (such as HDAC inhibitors) (302, 319, 320) have recently been revealed as longevity modulators in model organisms. Particularly, an example of this mechanism linking longevity genes, such as the Sirtuin family of HDACs, to transcriptional programs which rate-modulate longevity has recently been demonstrated. Specifically, loss of Sirt6 has been shown to cause hyperacetylation of Histone H3 lysine 9 (a top age-regulated gene in our study (paper 3, Figure 2A)), which increases expression of NFκB (another top age-regulated gene in our study) through increasing RELA promoter occupancy, which leads to altered NFκB regulated gene expression and cellular senescence (302). Proving causality in this mechanism of accelerated aging, Sirt6 KO mouse early lethality and degeneration can be rescued by RELA haploinsufficiency(302). Together this leads us to hypothesize the below feasible general mechanism:

Figure 26. Mechanistic schema for genetic modulation of molecular brain aging

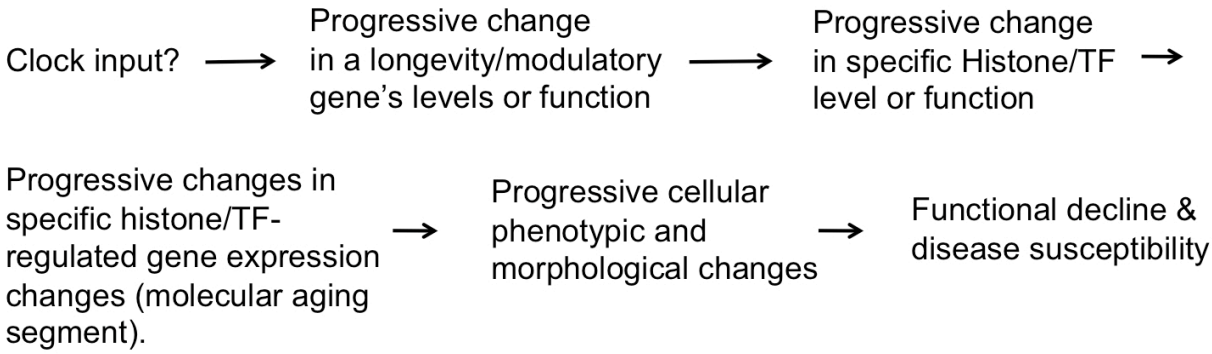

This model suggests that in tissue culture for example, molecular aging could be dissected into segments of age-regulated changes under control of particular

modulators. This fits with our findings surrounding subjects with the low-expressing $Sirt5_{prom2}$ allele, wherein we observed a subset of age-regulated changes were more dramatically accelerated than the rest (paper 3), suggesting that these changes may be most directly effected by lower SIRT5 levels, perhaps through SIRT5's modulation of a transcriptional regulator (such as our observed effects on GTF3A, paper 3) or a more complex multi-step mechanism. To investigate this we could, for example, knock down SIRT5 using RNAi in neuronal culture and see if we could recapitulate the microarray changes observed in low-expressing SIRT5 subjects, establishing causality. We could then systematically knock down candidate "second effector" transcriptional regulators, such as GTF3A, and investigate whether we could still recapitulate the results (using arrays), thereby beginning to place age-regulated changes in a hierarchy. We could then investigate whether SIRT5 directly interacts with or deacetylates these "second effectors". This strategy could be generally applied to a variety of brain molecular aging effectors. We could also directly test if and which cellular morphological and phenotypic outcomes result from a given molecular aging segment of changes downstream of a modulator, thus creating causal links between modulator, molecular aging segment, and phenotype. Molecular aging dissection would not only shed light on aging mechanisms, but also create a plethora of drug targets at different levels of specificity for aging and age-related disease.

Another interesting unknown in this hypothesized mechanistic schema is the upstream "clock input", ie. what counts the days and years of life and translates it into declining function or levels of a molecular aging modulator/longevity gene, such as BDNF or Sirt6? Firstly, counting may be accomplished from mitochondrial output, or accumulating DNA damage and ROS, for example, although this does not account for its translation into steadily declining modulators. This could in some way be related to the fact that Sirtuins are NAD-dependent and thus directly coupled to output from mitochondrial metabolic pathways. Mitochondria also steadily generate ROS from oxidative respiration and the rate of this is slowed by caloric restriction, another known modulator. Additionally, Lu et. al demonstrated that promoter regions of age-regulated genes are more susceptible to DNA damage(74), and while it is

difficult to conceptualize a mechanism whereby promoter damage would directly result in such precise and continuous changes in gene expression, this may play some role in regulating this putative molecular aging program.

It may also be worth speculating about whether redundant mechanisms from other contexts wherein “telling time” is necessary, i.e. for proper rate of cell division in dividing tissues and in development, or for circadian clock regulation, are at play here. To this end, we observed that CDK2 and CDK5 are top age-regulated genes, and the microarray signature drug matching program, C-MAP, pointed to a role for neuroprotective cell-cycle modulating drugs in molecular brain aging (Figure 3C, Paper 3). Could the cell cycle, which plays a large known role in peripheral aging in relation to senescence, have a similar role in non-dividing brain cells but instead “tell time” for age-regulated morphological/phenotypic changes? This remains to be investigated in tissue culture and/or model organisms.

In line with another “clock” theory, that of “developmental drift” put forth by Dr. Stuart Kim and colleagues in relation to c. elegans aging(321), we found that development-related genes were a top Ingenuity indentified age-regulated category, comprising ~1/3 of age-regulated changes(paper 3). The developmental drift theory, in line with our schema, postulates transcriptional programming driving aging, in this case extending from developmental programs, which continue deleteriously through adulthood due to the absence of evolutionary pressure post the reproductive window. This is a particularly logical hypothesis for brain aging, given that aging and development share cellular phenotypic changes. For example, continuation of developmental synaptic pruning programs may result in the deleterious losses of spines and dendritic complexity seen during aging.

In summary, the robustness, consistency, and selectivity of brain molecular aging suggests that it may be a transcriptional program intermediary between longevity/modulatory genes and cellular morphological/phenotypic changes. Thus establishing causality, and determining up-stream modulators and downstream consequences of this program will be crucial to understanding aging mechanisms and creating new therapeutic targets.

V.D Gating of neurological disease by normal brain aging: a universal gene-expression level mechanism?

Why is brain aging required for onset of diseases ranging from psychiatric disorders such SCHZ and BPD to neurodegenerative diseases such as AD, PD, HD and ALS? Why are mutations such as expanded tri-nucleotide repeats in HD or Pink-1 loss-of-function mutations in PD essentially silent in early adulthood, but become progressively more deleterious with age? Here we hypothesize about these largely unanswered questions, but first it is worth framing this discussion in an evolutionary context. Specifically, these age-gated mutations/polymorphisms likely stay in the population because they only become phenotypically expressed and thus impact fitness after the reproductive window.

In paper 3, we hypothesize that a "universal" mechanism potentially drives age-gating of many of these diseases. Namely, that progressive age-regulated loss or gain of neurological-related disease gene expression promotes (as part of the putative transcriptional aging program), and is both additive with and required for disease gene mutations/polymorphisms to cause disease. Also, because age-regulated expression changes are continuous and progressive, this would account for the age-specific gating and progressive nature of these neurological disorders.

The evidence for this is only observational as of yet (see paper 3), but it is compelling. Firstly, the putative highly selective "transcriptional program" of brain aging preferentially regulates neurological disease-related genes. In fact, ~34% of age-regulated genes (>1,000) in the human brain have known association to one or more of six age-gated neurological diseases (AD, PD, HD, ALS, BPD, SCHZ, see paper 3, Figure 3). Conversely, almost no genes with known associations to these diseases have age-independent expression levels (see paper 3, figure 3). This is impressive, given that only 5-10% of the genome is age-regulated. Moreover, the direction of age-regulated expression changes in these disease-associated genes is almost unanimously in directions known to cause or promote disease (see paper 3, table 1).

By way of example, it seems very likely that highly significant 15-35% drops in expression of six different familial PD genes in addition to Complex I (rotenone complex I inhibition causes PD) by age 79 (paper 3, table 1), would modulate or even be “the gating mechanism” for age of PD onset in genetically vulnerable individuals. To put this another way, one could conceive that a loss of function mutation or a low-expressing promoter polymorphism in one copy of Pink-1, for example, would not be sufficient to cause disease in early adulthood, but in conjunction with significant age-regulated loss of expression of the other wild-type Pink-1 allele as well as other familial PD genes by age 70, it may be sufficient to cause disease. From an evolutionary perspective it may thus make sense to look at preferential age-regulation of neurological disease genes in the converse, i.e. the age-gated neurological diseases that are present in the population are the result of insufficient/partial (in the absence of aging) mutations in the most age-vulnerable genes. Thus, all age-regulated genes may be good candidates for disease-related genes.

While this universal transcriptional age-of-onset mechanism is compelling and suggests promising starting points for investigation, many further lines of evidence are required for its confirmation. Remaining questions include 1. are these declines/increases in disease gene expression sufficient to cause disease? 2. are they more rapid/severe or in patients that have earlier disease onset? 3. can delay in declines of age-regulated disease genes prevent or delay disease in animal models?. Evidence for this could begin in human populations looking at disease risk/onset age in association with age-regulated changes in expression levels of disease genes (either by proxy in peripheral blood or if technology advances, by neuroimaging). However, these studies would not establish causation. For this, novel animal models may need to be created where disease gene expression could be progressively up or down regulated to reverse or induce disease in the background of disease causing genetic mutations/polymorphisms. This technology does not currently exist, however, and may be difficult to engineer.

If this mechanism proves to be correct, however, it is very encouraging for the treatment of these devastating age-gated diseases. Firstly, it implies that delaying normal brain aging would likely prevent, delay, or treat these diseases, which there is

already some evidence for in model organisms. Additionally, it provides an assay to determine whether pharmacological or other interventions are successful, i.e. monitoring molecular aging or age-regulated expression changes of specific disease genes (by proxy in peripheral blood/neuroimaging) provides an easy read-out for success of new therapies. It also implies that by monitoring molecular brain aging (perhaps using proxy peripheral blood biosignatures) in conjunction with genetic testing, at-disease-risk individuals could be indentified relatively easily and preventative measures taken before irreversible neurodegeneration ensues.

V.E. Overall conclusion

The molecular genetics of brain aging field is full of promise for pharmacologic, environmental, and genetic manipulation of rates of cognitive decline and age-gated neurological disease. The future is bright for anti-brain-aging measures being effective in treating devastating neurological conditions such as AD, PD, HD, and ALS. Careful investigation of the highly complex and relatively poorly understood mechanisms behind the genetics and molecular pathways of brain aging is required to ensure the efficacy and safety future interventions. Here, using brain microarray in conjunction with genetic studies in mammals, we provide mechanistic leads in biologically relevant contexts to begin to understand these mechanisms. Particularly, molecular dissection of our hypothesized “transcriptional program of molecular brain aging” and it’s potential gating of neurological disease may be very informative. Additionally, we provide support for BDNF, serotonergic drugs, and Sirt5 as candidate therapeutic targets for aging and age-related disease. Molecular aging biosignatures will likely play a key part in testing and monitoring genetic/environmental modulators and interventions in the future. To this end, an interactive database of age-regulated genes in the human brain is freely available at our website (http://www.sibille.pitt.edu/).

APPENDIX A. PAPER 1 SUPPLEMENTS

SUPPLEMENTAL MATERIAL (2 FIGURES +2 TABLES).

For Table layout and further explanation, see Table 1 legend.

Table 5. Supplemental Table 1. Gene expression differences observed in mice with an adult ablation of the BDNF gene.

Supp. Table 2. CHANGED IN EMBRYONIC KO ONLY (p<0.05 and |ALR|>0.263)				Adult KO				Embryonic KO				
Probesets	Name	Symbol	Identifier	EXP AD	CO AD	Ratio AD	P VAL AD	EXP EM	CO EM	Ratio EM	P VAL EM	Combined P
1427683_at	early growth response 2	Egr2	X06746	7.00	7.81	-0.81	0.07995	5.57	6.29	**-0.72**	**0.00360**	**0.002637**
1434403_at	sprouty protein with EVH-1 domain 2	Spred2	AV229054	8.81	9.19	-0.37	0.05799	7.90	8.56	**-0.66**	**0.00903**	**0.004480**
1426980_s_a	RIKEN cDNA E130012A19 gene	---	BC006054	6.54	6.79	-0.25	0.14832	5.63	6.23	**-0.61**	**0.04842**	**0.042632**
1418047_at	neurogenic differentiation 6	Neurod6	NM_009717	7.31	7.46	-0.15	0.63093	6.34	6.94	**-0.60**	**0.00565**	**0.023670**
1418835_at	pleckstrin homology-like domain, A1	Phlda1	NM_009344	7.06	7.14	-0.09	0.66440	5.75	6.33	**-0.58**	**0.00723**	**0.030430**
1423150_at	neuroendocrine protein 1, 7B2 protein	Sgne1	AK019337	10.62	10.88	-0.26	0.49295	9.64	10.21	**-0.57**	**0.00001**	**0.000075**
1423100_at	FBJ osteosarcoma oncogene	Fos	AV026617	9.96	10.30	-0.35	0.12465	8.51	9.06	**-0.56**	**0.04597**	**0.035307**
1423161_s_a	sprouty protein with EVH-1 domain 1	Spred1	AV295157	8.04	8.23	-0.19	0.30073	7.38	7.93	**-0.55**	**0.02840**	**0.049225**
1448117_at	kit ligand	Kitl	BB815530	7.33	7.45	-0.12	0.15542	6.36	6.87	**-0.52**	**0.04354**	**0.040575**
1438009_at	histone 1, H2ae	Hist1h2ae	W91024	5.99	6.37	-0.38	0.25208	5.95	6.44	**-0.49**	**0.00212**	**0.004555**
1448830_at	dual specificity phosphatase 1	Dusp1	NM_013642	9.20	9.52	-0.32	0.05770	8.25	8.73	**-0.48**	**0.04194**	**0.016998**
1425710_a_a	homer homolog 1 (Drosophila)	Homer1	AB019479	7.59	7.71	-0.11	0.69813	6.82	7.28	**-0.46**	**0.02194**	**0.079323**
1416029_at	TGFB inducible early growth response 1	Tieg1	NM_013692	7.27	7.83	-0.55	0.09105	6.70	7.16	**-0.46**	**0.01523**	**0.010515**
1433494_at	downstream of Stk11	Dos	BB180184	9.08	9.32	-0.24	0.16730	8.32	8.76	**-0.44**	**0.01161**	**0.014073**
1455030_at	RIKEN clone:9630021C19	---	AI116234	8.62	8.85	-0.24	0.13102	8.02	8.45	**-0.43**	**0.01251**	**0.012151**
1424443_at	transmembrane 6 superfamily member 1	Tm6sf1	BC023123	5.47	5.27	0.20	0.48044	4.33	4.75	**-0.42**	**0.03891**	**0.093079**
1415855_at	kit ligand	Kitl	NM_013598	7.91	8.14	-0.23	0.14172	6.89	7.31	**-0.42**	**0.02677**	**0.024945**
1455812_x_a	Slit-like 2 (Drosophila)	Slitl2	BB530515	3.92	4.20	-0.29	0.18232	3.33	3.74	**-0.42**	**0.02649**	**0.030585**
1426519_at	proline 4-hydroxylase, alpha 1 polypeptide	P4ha1	BB253720	6.73	6.99	-0.25	0.03974	6.47	6.88	**-0.41**	**0.01551**	**0.005172**
1421571_a_a	lymphocyte antigen 6 complex, locus C	Ly6c	NM_010741	9.24	9.21	0.02	0.80623	8.25	8.66	**-0.41**	**0.00059**	**0.004114**
1436584_at	sprouty homolog 2 (Drosophila)	Spry2	BB529691	8.24	8.64	-0.40	0.05828	7.64	8.04	**-0.40**	**0.01948**	**0.008835**
1425263_a_a	myelin basic protein	Mbp	L07508	7.73	7.77	-0.04	0.83612	7.11	7.51	**-0.40**	**0.03312**	**0.127018**
1455893_at	RIKEN cDNA 2610028F08 gene	---	BG067392	7.40	7.69	-0.29	0.10660	6.78	7.17	**-0.39**	**0.01066**	**0.008840**
1418310_a_a	retinaldehyde binding protein 1	Rlbp1	NM_020599	5.51	5.69	-0.18	0.29744	4.70	5.10	**-0.39**	**0.02715**	**0.046986**
1418710_at	CD59a antigen	Cd59a	NM_007652	7.70	7.80	-0.10	0.41494	7.31	7.70	**-0.39**	**0.00681**	**0.019411**
1417930_at	Ngfi-A binding protein 2	Nab2	NM_008668	8.01	8.33	-0.32	0.05104	7.42	7.79	**-0.37**	**0.03393**	**0.012744**
1416286_at	regulator of G-protein signaling 4	Rgs4	BC003882	10.43	10.78	-0.35	0.06387	9.85	10.20	**-0.35**	**0.00460**	**0.002682**
1418402_at	a disintegrin and metalloproteinase domain 19	Adam19	D50410	7.60	7.83	-0.23	0.12677	7.16	7.51	**-0.35**	**0.04667**	**0.036746**
1452344_at	synaptojanin 2	Synj2	BE944213	7.89	8.14	-0.26	0.05361	7.52	7.87	**-0.35**	**0.01472**	**0.006428**
1426614_at	RIKEN cDNA 3632413B07 gene	3632413B0	BB523906	8.86	8.99	-0.13	0.22781	7.84	8.18	**-0.34**	**0.01506**	**0.022895**
1416515_at	fascin homolog 1	Fscn1	BE952057	8.17	8.29	-0.11	0.70412	7.53	7.86	**-0.33**	**0.00456**	**0.021663**
1448850_a_a	DnaJ (Hsp40) homolog C5	Dnajc5	BC012268	9.84	9.71	0.13	0.28633	9.09	9.42	**-0.33**	**0.01554**	**0.028537**
1422621_at	RAN binding protein 2	Ranbp2	NM_011240	7.14	7.16	-0.02	0.93664	6.28	6.61	**-0.33**	**0.04852**	**0.185919**
1416432_at	6-phosphofructo-2-kinase/fructose-2,6-biphosphatase 3	Pfkfb3	NM_133232	6.07	6.34	-0.27	0.07739	5.06	5.39	**-0.33**	**0.03019**	**0.016493**
1452160_at	TCDD-inducible poly(ADP-ribose) polymerase	Tiparp	BB762264	5.51	5.87	-0.36	0.12212	4.63	4.96	**-0.33**	**0.00977**	**0.009226**
1450740_a_a	microtubule-associated protein, RP/EB family 1	Mapre1	BM228525	8.68	8.74	-0.06	0.84564	7.95	8.28	**-0.32**	**0.02792**	**0.112068**
1421768_a_a	homer homolog 1 (Drosophila)	Homer1	NM_011982	7.21	7.32	-0.12	0.67647	6.38	6.70	**-0.32**	**0.03124**	**0.102642**
1451046_at	zinc finger protein, multitype 1	Zfpm1	AA014267	7.56	7.80	-0.24	0.04611	7.04	7.36	**-0.32**	**0.01008**	**0.004033**
1424768_at	caldesmon 1	Cald1	BC019435	6.32	6.14	0.18	0.45841	5.89	6.20	**-0.31**	**0.04908**	**0.107873**
1427902_at	serine/arginine repetitive matrix 2	Srrm2	BQ176063	8.28	8.37	-0.09	0.70705	7.69	8.00	**-0.31**	**0.04070**	**0.130893**
1435767_at	sodium channel, voltage-gated, type III, beta	Scn3b	BE951842	8.95	9.11	-0.16	0.20375	8.46	8.77	**-0.31**	**0.00246**	**0.004314**
1421962_at	DnaJ (Hsp40) homolog B5	Dnajb5	AI664344	7.92	8.13	-0.21	0.00677	7.42	7.73	**-0.31**	**0.00781**	**0.000574**
1416805_at	RIKEN cDNA 1110032E23 gene	---	NM_133187	5.52	5.61	-0.10	0.46265	4.65	4.96	**-0.31**	**0.03869**	**0.089903**
1452031_at	solute carrier family 1 (glial glutamate transporter)	Slc1a3	BM220359	8.89	8.94	-0.05	0.67492	8.04	8.35	**-0.31**	**0.04650**	**0.140018**
1450326_at	src homology 2 domain-containing transforming C3	Shc3	NM_009167	6.92	7.18	-0.26	0.43698	6.84	7.15	**-0.31**	**0.04600**	**0.098636**
1448943_at	neuropilin	Nrp	AK002673	6.40	6.63	-0.24	0.34780	5.33	5.63	**-0.30**	**0.03929**	**0.072322**
1455143_at	neuroligin 2	Nlgn2	AU042744	9.92	10.00	-0.08	0.75667	9.07	9.37	**-0.30**	**0.03889**	**0.133182**
1460239_at	transmembrane 4 superfamily member 13	Tm4sf13	BB807707	9.96	10.02	-0.06	0.63178	9.52	9.81	**-0.30**	**0.01074**	**0.040675**
1450731_s_a	tumor necrosis factor receptor superfamily, member 21	Tnfrsf21	BG972377	8.35	8.48	-0.13	0.44383	7.55	7.84	**-0.30**	**0.04328**	**0.095130**
1448229_s_a	cyclin D2	Ccnd2	BM118679	6.47	6.62	-0.16	0.32601	5.93	6.22	**-0.29**	**0.00580**	**0.013744**
1418587_at	Tnf receptor-associated factor 3	Traf3	NM_011632	8.55	8.84	-0.28	0.08660	8.00	8.29	**-0.29**	**0.03449**	**0.020351**
1460330_at	annexin A3	Anxa3	AW702161	6.90	7.04	-0.13	0.60326	6.31	6.60	**-0.29**	**0.00780**	**0.029919**
1418084_at	neuropilin	Nrp	NM_008737	6.74	6.97	-0.23	0.14621	6.20	6.48	**-0.28**	**0.00357**	**0.004466**
1425266_a_a	RAP1, GTP-GDP dissociation stimulator 1	Rap1gds1	BC011279	9.89	9.86	0.04	0.80633	9.21	9.49	**-0.28**	**0.04685**	**0.161526**
1417293_at	heparan sulfate 6-O-sulfotransferase 1	Hs6st1	NM_015818	7.40	7.52	-0.12	0.41984	6.49	6.77	**-0.28**	**0.00805**	**0.022617**
1420998_at	ets variant gene 5	Etv5	NM_023794	7.41	7.53	-0.13	0.39673	6.86	7.13	**-0.28**	**0.04347**	**0.087261**
1450082_s_a	ets variant gene 5	Etv5	BG966751	8.14	8.39	-0.25	0.27993	7.72	8.00	**-0.28**	**0.01472**	**0.026745**
1456464_x_a	synaptotagmin 11	Syt11	BB129990	10.42	10.28	0.13	0.49334	9.03	9.31	**-0.27**	**0.02610**	**0.068920**
1420008_s_a	cDNA sequence BC037006	BC037006	AU017197	9.07	9.30	-0.22	0.06838	8.55	8.82	**-0.27**	**0.01750**	**0.009250**
1450227_at	ankyrin repeat domain 6	Ankrd6	BM199504	7.09	7.01	0.08	0.34436	6.59	6.85	**-0.26**	**0.04695**	**0.082851**
1417111_at	mannosidase 1, alpha	Man1a	BB070019	8.22	8.17	0.05	0.41337	7.53	7.80	**-0.26**	**0.04823**	**0.097985**
1451264_at	RIKEN cDNA 4930488L10 gene	4930488L1	BC019939	8.11	8.48	-0.38	0.06498	7.60	7.86	**-0.26**	**0.03320**	**0.015403**
1449030_at	synapsin II	Syn2	BM936504	9.76	9.43	0.33	0.16956	9.68	9.42	**0.27**	**0.00896**	**0.011375**
1426068_at	solute carrier family 7, member 4	Slc7a4	BC016100	10.16	9.93	0.23	0.05625	9.86	9.59	**0.27**	**0.00694**	**0.003454**
1448110_at	semaphorin 4A	Sema4a	NM_013658	8.95	8.82	0.13	0.29366	8.32	8.05	**0.27**	**0.01042**	**0.020779**
1427044_a_a	amphiphysin	Amph	BQ177140	10.20	10.06	0.14	0.28991	9.61	9.33	**0.28**	**0.03969**	**0.062875**
1451092_a_a	RAN GTPase activating protein 1	Rangap1	AV258722	10.02	10.03	0.00	0.93052	9.41	9.13	**0.28**	**0.03613**	**0.147683**
1449410_a_a	growth arrest specific 5	Gas5	NM_013525	10.29	10.56	-0.27	0.18080	9.80	9.52	**0.28**	**0.03913**	**0.042100**
1428262_at	tubulin-specific chaperone e	Tbce	AK011899	7.86	7.84	0.01	0.89171	7.54	7.26	**0.28**	**0.00170**	**0.011334**
1416996_at	TBC1 domain family, member 8	Tbc1d8	BC005421	8.12	7.88	0.24	0.02742	7.24	6.95	**0.29**	**0.02031**	**0.004728**
1422580_at	myosin, light polypeptide 4	Myl4	NM_010858	8.52	8.05	0.47	0.05170	7.47	7.17	**0.29**	**0.01517**	**0.006391**
1427011_a_a	LanC-like 1	Lancl1	AW107959	10.61	10.72	-0.11	0.45075	9.97	9.68	**0.30**	**0.04989**	**0.107825**
1417988_at	regulated endocrine-specific protein 18	Resp18	NM_009049	9.29	9.09	0.20	0.16830	8.45	8.15	**0.30**	**0.02328**	**0.025633**
1420388_at	protease, serine, 12 neurotrypsin (motopsin)	Prss12	NM_008939	9.22	8.96	0.26	0.04414	8.89	8.58	**0.30**	**0.01920**	**0.006840**
1417619_at	Gadd45 gamma interacting protein 1	Gadd45gip	NM_026320	7.24	7.03	0.21	0.25530	6.38	6.07	**0.31**	**0.03902**	**0.055879**
1448979_at	muted	Muted	NM_139063	7.97	7.81	0.16	0.20583	7.57	7.26	**0.32**	**0.00024**	**0.000538**
1421339_at	exostoses (multiple)-like 3	Extl3	NM_018788	6.27	6.19	0.08	0.78789	6.65	6.33	**0.32**	**0.03813**	**0.135352**
1424048_a_a	RIKEN cDNA 1500005G05 gene	1500005G0	BC024618	7.80	7.54	0.26	0.14963	7.20	6.88	**0.32**	**0.00421**	**0.005269**
1417288_at	pleckstrin homology domain-containing A2	Plekha2	BC010215	8.51	8.34	0.18	0.06584	7.96	7.64	**0.32**	**0.03960**	**0.018120**
1421093_at	solute carrier family 7, member 10	Slc7a10	NM_017394	8.42	8.30	0.11	0.12429	8.16	7.83	**0.32**	**0.02330**	**0.019820**
1419398_a_a	deleted in polyposis 1	Dp1	NM_007874	10.28	9.97	0.31	0.08339	9.76	9.43	**0.33**	**0.00457**	**0.003383**
1419687_at	RIKEN cDNA D930010J01 gene	D930010J0	NM_134147	7.71	7.43	0.28	0.07793	6.98	6.65	**0.33**	**0.01220**	**0.007564**
1448201_at	secreted frizzled-related sequence protein 2	Sfrp2	NM_009144	6.03	5.63	0.40	0.06491	5.38	5.05	**0.33**	**0.01146**	**0.006104**
1428966_at	RIKEN cDNA 2610204K14 gene	2610204K1	AK018614	9.31	9.40	-0.09	0.27899	8.88	8.54	**0.34**	**0.00323**	**0.007211**
1427038_at	preproenkephalin 1	Penk1	M13227	9.22	8.86	0.37	0.08052	8.63	8.47	**0.35**	**0.01677**	**0.010273**
1448028_at	RIKEN cDNA C530046L02 gene	C530046L0	BF536757	8.90	8.78	0.12	0.41878	8.00	7.62	**0.37**	**0.04896**	**0.100209**
1418149_at	chromogranin A	Chga	NM_007693	9.51	9.25	0.26	0.14020	8.93	8.54	**0.39**	**0.01487**	**0.014950**
1417219_s_a	thymosin, beta 10	Tmsb10	NM_025284	8.85	8.62	0.23	0.09688	7.79	7.39	**0.40**	**0.00224**	**0.002048**
1449960_at	neuronal pentraxin 2	Nptx2	NM_016789	6.52	6.44	0.07	0.64422	6.40	5.99	**0.41**	**0.03622**	**0.111021**
1419040_at	cytochrome P450, family 2, subfamily d, polypeptide 22	Cyp2d22	BF683039	7.95	8.00	-0.05	0.79526	7.26	6.80	**0.45**	**0.01025**	**0.047375**
1422552_at	RIKEN cDNA 2410012A13 gene	2410012A1	NM_023396	8.37	7.76	0.61	0.09098	7.15	6.69	**0.47**	**0.04446**	**0.026332**
1436902_x_a	thymosin, beta 10	Tmsb10	BB096368	10.82	10.59	0.23	0.06035	10.28	9.81	**0.47**	**0.02427**	**0.011021**
1420720_at	neuronal pentraxin 2	Nptx2	BC026054	7.36	7.23	0.13	0.65458	7.39	6.90	**0.49**	**0.04813**	**0.140427**
1432332_a_a	DNA segment, Chr 7, Roswell Park 2 complex	D7Rp2e	AK008430	8.55	8.77	-0.22	0.43202	8.17	7.65	**0.52**	**0.03422**	**0.077082**
1434292_at	RIKEN cDNA E130013N09 gene	E130013N0	BI731047	10.60	10.47	0.13	0.63777	9.74	9.21	**0.53**	**0.04471**	**0.129943**
1434216_a_a	DNA segment, Chr 7, Roswell Park 2 complex	D7Rp2e	BG070689	9.12	9.53	-0.41	0.39441	8.79	8.05	**0.74**	**0.02101**	**0.048005**

Table 6. Supplemental Table 2. Gene expression differences observed in mice with an embryonic ablation of the BDNF gene.

For Table layout and further explanation, see Table 1 legend.

I

Supp. Table 1. CHANGED IN ADULT KO ONLY (p<0.05 and |ALR|>0.263)				Adult KO				Embryonic KO				
Probesets	Name	Symbol	Identifier	EXP AD	CO AD	Ratio AD	P VAL AD	EXP EM	CO EM	Ratio EM	P VAL EM	Combined P
1448756_at	S100 calcium binding protein A9 (calgranulin B)	S100a9	NM_009114	5.77	7.00	**-1.23**	**0.04804**	6.31	7.22	-0.91	0.43884	**0.102452**
1428301_at	RIKEN cDNA 2610042L04 gene	---	BM195235	7.81	8.97	**-1.16**	**0.04744**	6.27	6.84	-0.57	0.12880	**0.037258**
1416783_at	tachykinin 1	Tac1	NM_009311	5.58	6.45	**-0.86**	**0.03929**	4.79	5.10	-0.31	0.05258	**0.014836**
1424903_at	jumonji, AT rich interactive domain 1D (Rbp2 like)	Jarid1d	AF127244	4.39	5.24	**-0.85**	**0.01186**	4.83	4.90	-0.07	0.27653	**0.022037**
1422169_a_at	brain derived neurotrophic factor	Bdnf	AY057913	7.08	7.74	**-0.66**	**0.01110**	6.55	6.83	-0.28	0.07254	**0.006539**
1418937_at	deiodinase, iodothyronine, type II	Dio2	NM_010050	8.44	8.95	**-0.51**	**0.02570**	8.06	8.27	-0.21	0.10691	**0.018952**
1427526_at	FGFR1 oncogene partner 2	Fgfr1op2	AB041650	4.45	4.95	**-0.49**	**0.02686**	3.79	3.82	-0.03	0.71455	**0.095066**
1449188_at	midnolin	Midn	NM_021565	6.58	7.01	**-0.43**	**0.00426**	5.84	6.09	-0.25	0.09632	**0.003608**
1423978_at	SH3-binding kinase	Sbk	BC025837	7.48	7.90	**-0.43**	**0.04402**	6.68	7.08	-0.41	0.11136	**0.030971**
1431506_s_at	peptidyl prolyl isomerase H	Ppih	AK008394	6.74	7.14	**-0.40**	**0.02558**	5.88	5.81	0.07	0.51574	**0.070285**
1455439_a_at	lectin, galactose binding, soluble 1	Lgals1	AI642438	7.18	7.57	**-0.39**	**0.00969**	6.60	6.86	-0.26	0.01907	**0.001774**
1420502_at	spermidine/spermine N1-acetyl transferase 1	Sat1	NM_009121	7.63	8.02	**-0.39**	**0.01818**	7.50	7.36	0.14	0.09497	**0.012712**
1438370_x_at	---	---	BB357126	10.47	10.85	**-0.39**	**0.00394**	9.87	10.15	-0.29	0.07322	**0.002637**
1419573_a_at	lectin, galactose binding, soluble 1	Lgals1	NM_008495	7.29	7.66	**-0.37**	**0.00974**	6.90	7.14	-0.24	0.01056	**0.001047**
1425320_at	RIKEN cDNA A830023I12 gene	---	BC007165	5.52	5.89	**-0.36**	**0.01776**	5.32	5.35	-0.03	0.84443	**0.077977**
1450626_at	mannosidase, beta A, lysosomal	Manba	NM_027288	5.64	6.00	**-0.36**	**0.01813**	5.31	5.15	0.16	0.10632	**0.013976**
1424704_at	runt related transcription factor 2	Runx2	D14636	6.09	6.44	**-0.35**	**0.03434**	5.48	5.49	-0.02	0.74813	**0.119765**
1419308_at	inversin	Invs	NM_010569	7.01	7.36	**-0.35**	**0.00870**	6.36	6.38	-0.02	0.53798	**0.029788**
1417406_at	SERTA domain containing 1	Sertad1	AF366401	7.68	8.03	**-0.34**	**0.01664**	7.07	7.16	-0.09	0.10769	**0.013122**
1451037_at	protein tyrosine phosphatase, non-receptor type 9	Ptpn9	BB224063	7.71	8.05	**-0.34**	**0.02627**	7.25	7.46	-0.21	0.02510	**0.005489**
1416514_a_at	fascin homolog 1, actin bundling protein	Fscn1	NM_007984	9.42	9.75	**-0.32**	**0.02729**	8.69	8.99	-0.30	0.12205	**0.022328**
1423427_at	adenylate cyclase activating polypeptide 1	Adcyap1	AI323434	7.99	8.31	**-0.32**	**0.00169**	7.35	7.56	-0.20	0.00926	**0.000189**
1449038_at	hydroxysteroid 11-beta dehydrogenase 1	Hsd11b1	NM_008288	8.07	8.38	**-0.31**	**0.01381**	7.85	7.80	0.05	0.74067	**0.057096**
1435415_x_at	MARCKS-like protein	Mlp	BB491008	6.25	6.55	**-0.31**	**0.00225**	5.85	6.10	-0.26	0.11124	**0.002323**
1437521_s_at	RIKEN cDNA E230022H04 gene	---	BB312224	7.41	7.71	**-0.31**	**0.03076**	7.12	7.01	0.10	0.58634	**0.090453**
1416326_at	cysteine-rich protein 1 (intestinal)	Crip1	NM_007763	7.36	7.67	**-0.30**	**0.02053**	6.77	6.79	-0.02	0.50645	**0.057882**
1449773_s_at	growth arrest and DNA-damage-inducible 45 beta	Gadd45b	AI323528	7.31	7.61	**-0.30**	**0.03240**	6.70	6.64	0.06	0.54541	**0.088984**
1431394_a_at	RIKEN cDNA 4921513O20 gene	---	AK014938	7.67	7.97	**-0.30**	**0.00446**	7.43	7.49	-0.06	0.64195	**0.019618**
1452161_at	TCDD-inducible poly(ADP-ribose) polymerase	Tiparp	BB707122	7.07	7.37	**-0.30**	**0.03540**	6.61	6.79	-0.18	0.24169	**0.049286**
1451601_a_at	cDNA sequence BC011467	BC011467	BC025823	8.53	8.82	**-0.30**	**0.04017**	8.19	8.39	-0.20	0.06091	**0.017157**
1438177_x_at	lysosomal apyrase-like 1	Lysal1	AV255351	8.90	9.19	**-0.29**	**0.03179**	8.41	8.42	-0.01	0.95903	**0.136891**
1450011_at	hydroxysteroid (17-beta) dehydrogenase 12	Hsd17b12	AK012103	8.85	9.14	**-0.29**	**0.01448**	8.25	8.40	-0.15	0.00025	**0.000050**
1448799_s_at	mitochondrial ribosomal protein S12	Mrps12	NM_011885	9.31	9.59	**-0.29**	**0.02437**	8.82	8.80	0.02	0.82107	**0.098289**
1433913_at	expressed sequence C80913	---	AV094811	7.62	7.90	**-0.28**	**0.03651**	6.63	6.50	0.13	0.15905	**0.035703**
1417218_at	RIKEN cDNA 2810048G17 gene	---	NM_133746	6.49	6.76	**-0.27**	**0.00195**	5.83	6.01	-0.17	0.07996	**0.001525**
1426366_at	eukaryotic translation initiation factor 2C, 2	Eif2c2	AW553784	6.13	6.40	**-0.27**	**0.02782**	7.54	7.59	-0.05	0.80123	**0.107086**
1448812_at	RIKEN cDNA 2410018L13 gene	---	NM_016677	9.62	9.35	**0.27**	**0.00807**	9.07	8.98	0.09	0.31595	**0.017775**
1436849_x_at	glucosidase, alpha, acid	Gaa	BB357227	9.18	8.91	**0.27**	**0.02505**	8.42	8.16	0.26	0.08104	**0.014617**
1421321_a_at	neuroepithelial cell transforming gene 1	Net1	NM_019671	6.75	6.48	**0.28**	**0.01681**	5.96	5.80	0.16	0.07392	**0.009555**
1425329_a_at	diaphorase 1 (NADH)	Dia1	AF332060	7.41	7.13	**0.28**	**0.04311**	7.06	6.96	0.10	0.39737	**0.086797**
1419741_at	suppressor of Ty 16 homolog	Supt16h	BC012433	9.35	9.07	**0.28**	**0.01969**	8.80	8.67	0.12	0.67510	**0.070737**
1437591_a_at	WD repeat domain 1	Wdr1	AW542545	8.46	8.17	**0.29**	**0.04649**	7.65	7.64	0.01	0.85012	**0.167214**
1418922_at	immunoglobulin superfamily, member 4B	Igsf4b	NM_053199	9.14	8.85	**0.29**	**0.03372**	8.50	8.36	0.14	0.09595	**0.021789**
1460352_s_at	PIP 3 kinase, regulatory, polypeptide 4, p150	Pik3r4	BC017537	7.25	6.95	**0.30**	**0.04661**	6.37	6.43	-0.06	0.78532	**0.157681**
1427123_s_at	coatomer protein complex, subunit gamma 2	Copg2as2	BE653037	10.22	9.92	**0.30**	**0.01551**	9.74	9.70	0.04	0.73472	**0.062383**
1425662_at	cytidine and dCMP deaminase domain 1	Cdadc1	AV348063	5.65	5.34	**0.31**	**0.02739**	5.02	4.75	0.27	0.10087	**0.019042**
1448715_x_at	intracisternal A particles	Iap	NM_010490	11.65	11.33	**0.32**	**0.04278**	10.83	10.69	0.14	0.50102	**0.103795**
1426339_at	adenylate kinase 5	Ak5	AB060081	9.56	9.24	**0.32**	**0.04304**	8.97	8.83	0.14	0.07770	**0.022410**
1451310_a_at	cathepsin L	Ctsl	J02583	9.67	9.33	**0.33**	**0.01345**	8.99	9.03	-0.04	0.52444	**0.041994**
1449027_at	ras homolog gene family, member U	Rhou	NM_133955	8.56	8.22	**0.34**	**0.01408**	7.53	7.39	0.14	0.32818	**0.029464**
1449151_at	PCTAIRE-motif protein kinase 3	Pctk3	NM_008795	8.61	8.26	**0.35**	**0.01661**	8.10	7.98	0.11	0.12188	**0.014577**
1419601_at	potassium inwardly-rectifying channel, J10	Kcnj10	AF322631	9.06	8.71	**0.35**	**0.02395**	8.49	8.51	-0.03	0.84518	**0.099186**
1422185_a_at	diaphorase 1 (NADH)	Dia1	NM_029787	8.72	8.38	**0.35**	**0.03289**	8.23	8.08	0.15	0.08203	**0.018658**
1423630_at	cytoglobin	Cygb	BM899392	8.27	7.91	**0.36**	**0.00421**	7.87	7.64	0.23	0.02091	**0.000911**
1420841_at	protein tyrosine phosphatase, receptor type, F	Ptprf	NM_011213	8.53	8.17	**0.36**	**0.00257**	7.96	7.96	0.00	0.99261	**0.017797**
1425563_s_at	protocadherin 10	Pcdh10	AF334801	8.73	8.37	**0.37**	**0.04935**	8.01	7.76	0.25	0.24701	**0.065916**
1450889_at	actin dependent regulator of chromatin a3	Smarca3	BB206482	7.29	6.91	**0.38**	**0.03547**	6.59	6.52	0.07	0.34970	**0.066858**
1450486_a_at	opioid receptor-like	Oprl	X91813	8.66	8.28	**0.38**	**0.01172**	8.06	7.99	0.07	0.52257	**0.037333**
1428089_at	RIKEN cDNA 3200001I04 gene	---	AK014285	10.45	10.06	**0.38**	**0.00717**	9.88	9.74	0.13	0.20268	**0.010943**
1454015_a_at	cadherin 13	Cdh13	AK016527	5.25	4.84	**0.41**	**0.03716**	3.48	3.39	0.09	0.23507	**0.050144**
1431645_a_at	GDP dissociation inhibitor 3	Gdi3	AK013104	9.02	8.61	**0.41**	**0.04741**	8.21	8.11	0.10	0.38086	**0.090546**
1419637_s_at	RIKEN cDNA 4833420G17 gene	---	BG067119	9.18	8.77	**0.41**	**0.03988**	8.98	8.89	0.08	0.52871	**0.102449**
1423744_x_at	eukaryotic translation initiation factor 2, subunit 3	Eif2s3x	BC006682	9.91	9.49	**0.42**	**0.04712**	9.07	9.08	-0.01	0.81147	**0.163036**
1455447_at	RIKEN cDNA D430019H16 gene	D430019H	BM116882	9.98	9.56	**0.42**	**0.00405**	9.38	9.24	0.14	0.09672	**0.003462**
1455136_at	ATPase, Na+/K+ transporting, alpha 2 polypeptide	Atp1a2	BG175915	9.38	8.96	**0.42**	**0.01490**	8.58	8.60	-0.01	0.95987	**0.075062**
1431293_a_at	RIKEN cDNA 1110019C08 gene	---	AK012260	7.82	7.40	**0.42**	**0.03984**	7.64	7.66	-0.02	0.90405	**0.155720**
1427672_a_at	tetratricopeptide repeat gene, X chromosome	Utx	AJ002730	7.96	7.53	**0.43**	**0.00285**	7.39	7.25	0.14	0.22988	**0.005466**
1450243_a_at	Down syndrome critical region gene 1-like 1	Dscr1l1	NM_030598	7.97	7.53	**0.44**	**0.00001**	7.54	7.41	0.13	0.22512	**0.000029**
1426541_a_at	RIKEN cDNA 2310067E08 gene	---	BF168366	5.28	4.84	**0.44**	**0.01524**	5.30	5.07	0.23	0.27834	**0.027411**
1427235_at	tetratricopeptide repeat gene, X chromosome	Utx	AW536493	6.49	6.04	**0.45**	**0.04855**	5.39	5.36	0.03	0.72508	**0.153003**
1419428_a_at	glucosidase, alpha, acid	Gaa	NM_008064	9.65	9.20	**0.46**	**0.01302**	8.73	8.62	0.10	0.56975	**0.043786**
1455316_x_at	---	---	AI987693	11.43	10.96	**0.47**	**0.01843**	10.83	10.89	-0.06	0.82548	**0.078901**
1415935_at	SPARC related modular calcium binding 2	Smoc2	NM_022315	8.33	7.85	**0.47**	**0.00856**	7.84	7.68	0.16	0.22324	**0.013879**
1431569_a_at	RIKEN cDNA 2700050C12 gene	---	AK012406	8.44	7.96	**0.48**	**0.00574**	7.82	7.52	0.30	0.25971	**0.011191**
1460167_at	aldehyde dehydrogenase family 7, member A1	Aldh7a1	BC012407	8.21	7.72	**0.49**	**0.04077**	7.45	7.15	0.30	0.26359	**0.059467**
1422748_at	zinc finger homeobox 1b	Zfhx1b	NM_015753	7.34	6.82	**0.52**	**0.02088**	6.39	6.42	-0.04	0.91408	**0.094648**
1424967_x_at	troponin T2, cardiac	Tnnt2	L47552	5.54	4.99	**0.55**	**0.04675**	5.20	4.98	0.22	0.43535	**0.099625**
1436021_at	RIKEN cDNA A930031D07 gene	---	AI426503	7.94	7.31	**0.63**	**0.03187**	7.13	7.05	0.08	0.72789	**0.110497**
1449123_at	inter-alpha trypsin inhibitor, heavy chain 3	Itih3	NM_008407	8.31	7.67	**0.64**	**0.00437**	7.53	7.16	0.37	0.10354	**0.003933**
1419635_at	RIKEN cDNA 4833420G17 gene	---	NM_026127	5.56	4.91	**0.66**	**0.03306**	6.09	5.75	0.34	0.17292	**0.035241**

all present on >2 chips in adults

Figure 27. Supplemental Figure 1. Assessment of false discovery ratio (FDR)

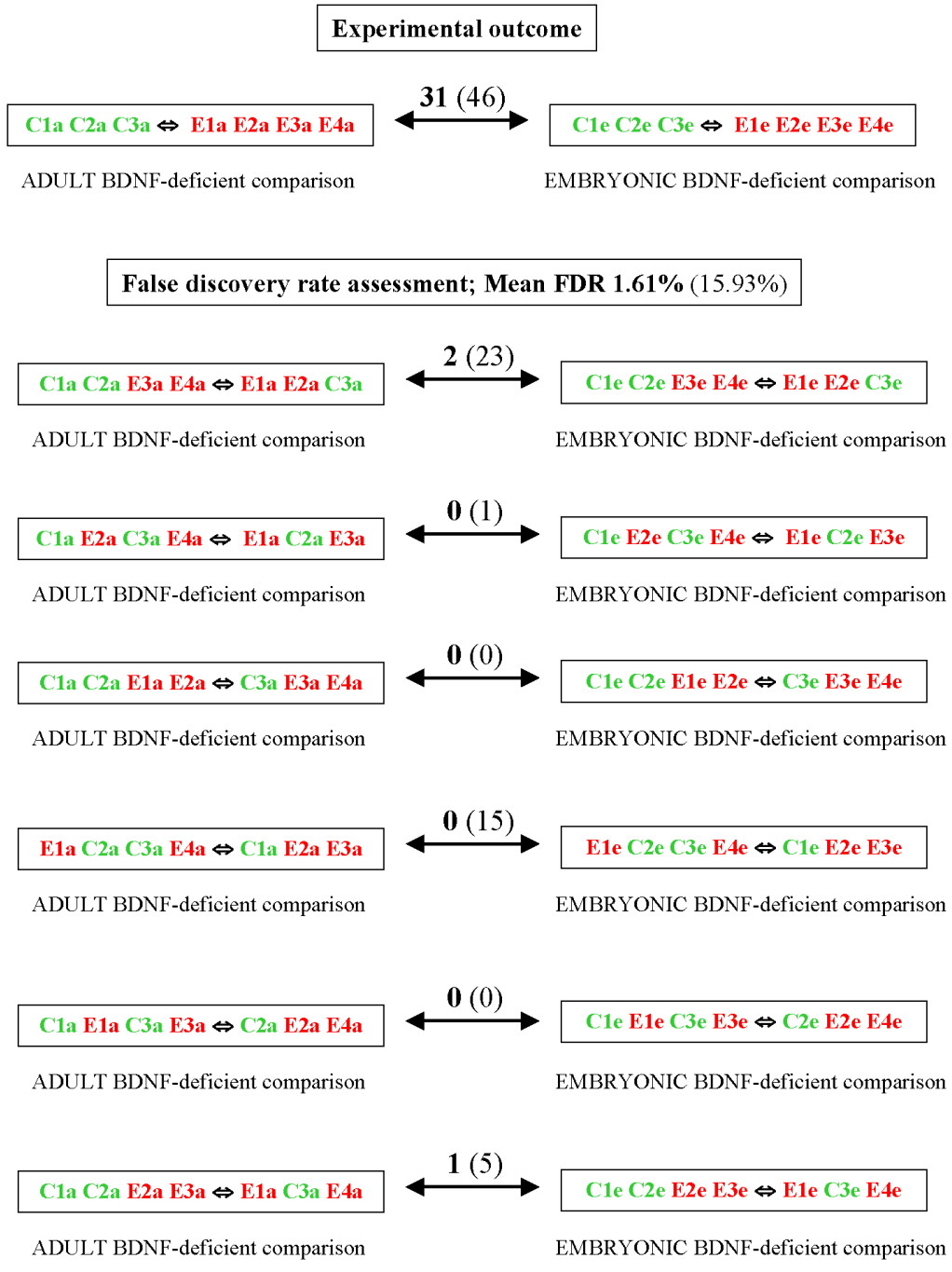

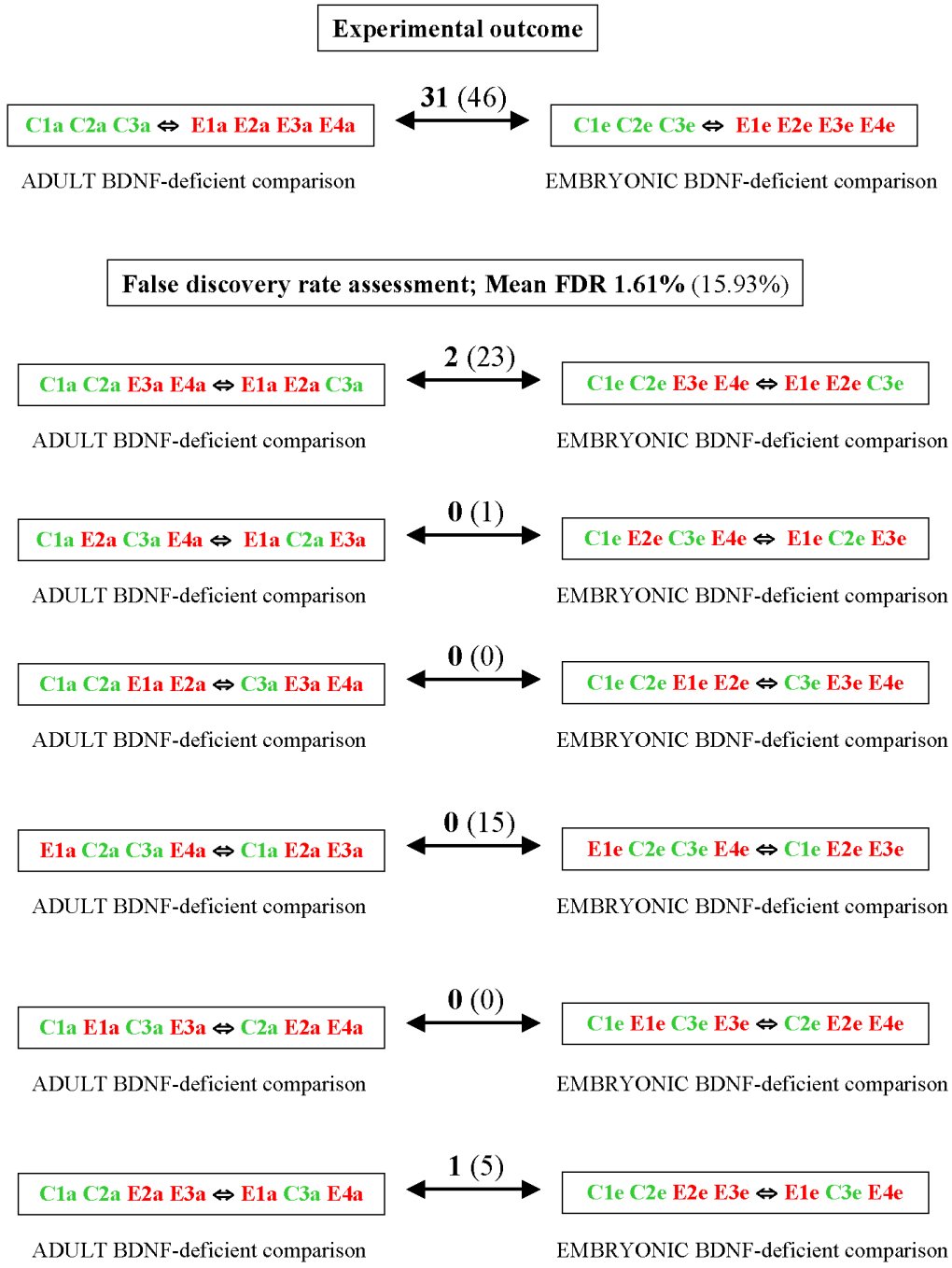
Experimental outcome
C1a C2a C3a ⇔ E1a E2a E3a E4a
31 (46)
C1e C2e C3e ⇔ E1e E2e E3e E4e
ADULT BDNF-deficient comparison
EMBRYONIC BDNF-deficient comparison
False discovery rate assessment; Mean FDR 1.61% (15.93%)
C1a C2a E3a E4a ⇔ E1a E2a C3a
2 (23)
C1e C2e E3e E4e ⇔ E1e E2e C3e
ADULT BDNF-deficient comparison
EMBRYONIC BDNF-deficient comparison
C1a E2a C3a E4a ⇔ E1a C2a E3a
0 (1)
C1e E2e C3e E4e ⇔ E1e C2e E3e
ADULT BDNF-deficient comparison
EMBRYONIC BDNF-deficient comparison
C1a C2a E1a E2a ⇔ C3a E3a E4a
0 (0)
C1e C2e E1e E2e ⇔ C3e E3e E4e
ADULT BDNF-deficient comparison
EMBRYONIC BDNF-deficient comparison
E1a C2a C3a E4a ⇔ C1a E2a E3a
0 (15)
E1e C2e C3e E4e ⇔ C1e E2e E3e
ADULT BDNF-deficient comparison
EMBRYONIC BDNF-deficient comparison
C1a E1a C3a E3a ⇔ C2a E2a E4a
0 (0)
C1e E1e C3e E3e ⇔ C2e E2e E4e
ADULT BDNF-deficient comparison
EMBRYONIC BDNF-deficient comparison
C1a C2a E2a E3a ⇔ E1a C3a E4a
1 (5)
C1e C2e E2e E3e ⇔ E1e C3e E4e
ADULT BDNF-deficient comparison
EMBRYONIC BDNF-deficient comparison

Top panel represents experimental outcome with 31 definitively and 46 putatively changed genes. FDR was assessed in a permutation test, where experimental and control microarrays were randomly assigned to two groups within their own condition. These groups were assessed for gene expression differences with the same analysis as in the experimental – control comparison. C1-3 denote control samples, E1-4 denote experimental samples (a=adult, e=experimental). For each analysis number on arrow denote the number of genes with changed expression in a permutation. Number of putatively changed genes is denoted in parenthesis. Note that in this test, the FDR was <2% (<16% for the putatively changed genes).

Figure 28. Supplemental Figure 2. Two-way clustering of the normalized expression levels for 46 putatively changed genes across the adult and embryonic BDNF-ablated mice.

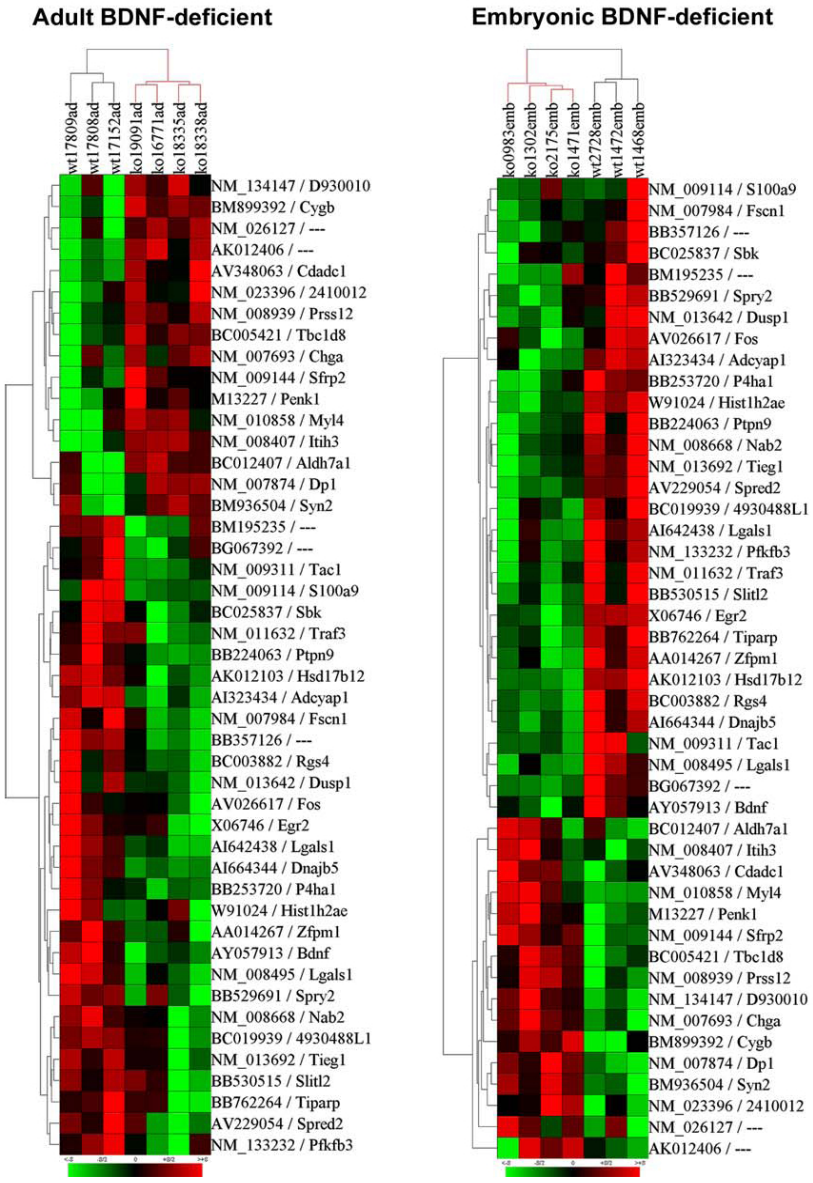

Clustering is performed and represented similar to that seen in Figure 1. For source data and abbreviations see Table 2. Note that the wild-type and BDNF-ablated mice separate according to genotype (vertical dendrogram) in both groups of BDNF-deficient mice. Together with a low FDR, this suggests that the majority of the presented data represents true biological discovery.

APPENDIX B- PAPER 2 HIGHLIGHTED IMAGE

Molecular Psychiatry (2007) 12, 975

www.nature.com/mp

IMAGE

Upregulated sirtuin 5 gene expression in frontal cortex of serotonin 1b receptor knock out mice

E Sibille[1,2], J Su[1], S Leman[3], AM Le Guisquet[3], Y Ibarguen-Vargas[3], J Joeyen-Waldorf[1], C Glorioso[2], GC Tseng[4], M Pezzone[5], R Hen[6] and C Belzung[3]

[1]*Department of Psychiatry, University of Pittsburgh, Pittsburgh, PA, USA;* [2]*Center for Neuroscience, University of Pittsburgh, Pittsburgh, PA, USA;* [3]*EA3248 Psychobiologie des émotions, Faculté des Sciences et Techniques, Université François Rabelais, Tours, France;* [4]*Department of Biostatistics, University of Pittsburgh, Pittsburgh, PA, USA;* [5]*Department of Medicine, University of Pittsburgh, Pittsburgh, PA, USA and* [6]*Center for Neurobiology and Behavior, Columbia University, New York, NY, USA*

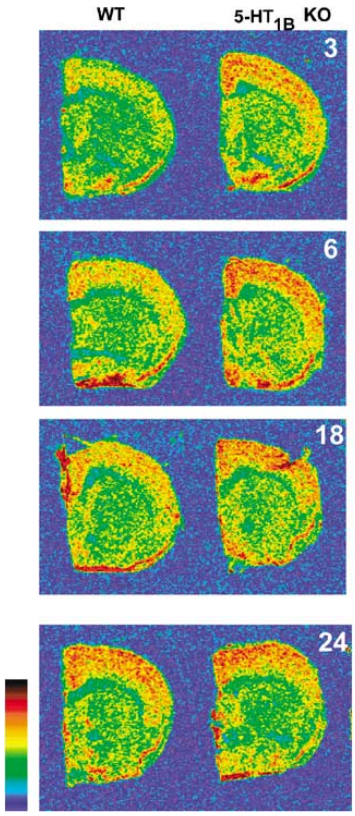

Molecular Psychiatry (2007) **12,** 975; doi:10.1038/sj.mp.4002115

Our studies have demonstrated that altering serotonin (5-HT) signaling through the disruption of the 5-HT1B presynaptic autoreceptor can modulate the onset of selected age-related events in the central nervous system. A clear upregulation of sirtuin 5 (Sirt5) gene expression was identified in the brain of serotonin 1b receptor knock out (Htr1bKO) mice. Sirtuin genes are major cellular components of age-related pathways. The role of altered Sirt5 transcripts in the age-related phenotype in Htr1bKO mice is currently under investigation, including an early mechanism for altering the onset of age-related phenotypes, since Sirt5 transcript changes preceded the appearance of age-related behavioral and molecular changes. Representative color-coded photomicrographs of sirtuin 5 gene (Sirt5) $_{35}$S *in situ* hybridization histochemistry at 3, 6, 18 and 24 months of age. Color barcode indicates increased signal intensity. For more information on this topic see the paper by Sibille *et al.* on pages 1042–1056.

APPENDIX C- PAPER 3 SUPPLEMENTS

SUPPLEMENTAL INFORMATION.

Lack of Serotonin$_{1B}$ Receptor Expression Leads to Age-Related Motor Dysfunction, Early Onset of Brain Molecular Aging and Reduced Longevity.

Etienne Sibille[1,4], Jing Su[1], Samuel Leman[6], Anne-Marie Le Guisquet[6], Y. Ibarguen-Vargas[6], Jennifer Joeyen-Waldorf[1], Christin A. Glorioso[4], George C. Tseng[2], Michael Pezzone[3], René Hen[5] and Catherine Belzung[6].

Departments of [1]Psychiatry, [2]Biostatistics and [3]Medicine, [4]Center for Neuroscience, University of Pittsburgh, [5]Center for Neurobiology & Behavior, Columbia University, [6]EA3248 Psychobiologie des émotions, Université François Rabelais de Tours, France,

---

1. Array MIAME format.

2. Figure S1. Anxiety-like behaviors in aging WT and *Htr1b^{KO}* mice in the open field (OF) and the elevated plus maze (EPM) tests.

3. Table S1. WT and *Htr1b^{KO}* age-affected genes in CTX
(Sample provided; separate downloadable Excel file).

4. Table S2. WT and *Htr1b^{KO}* age-affected genes in STR
(Sample provided; separate downloadable Excel file).

5. Table S3. Selected mouse-human orthologous gene with conserved age-effects on gene transcript levels.

6. Table S4. Functional analysis of age-related gene expression in WT and *Htr1b^{KO}*

mice.

7. Table S5. Consistent WT- *Htr1b*^{KO} gene expression differences.

8. References.

---

1. MINIMUM INFORMATION ABOUT A MICROARRAYS EXPERIMENT (MIAME)

1.1. Array design description

2.1.1. Array used: Affymetrix mouse genome MOE430v2.0 (information regarding the details of this array can be found at www.affymetrix.com).

2.1.2. Normalization: All arrays were scaled to 250 to correct for differences in overall signal before analysis in Microarray Suite 5.0 (MAS5.0, Affymetrix, Inc., Santa Clara, Ca). MAS5.0 extracted data were used to assess quality control parameters. All other analyses were performed with data extracted with the Robust Multi-array Average algorithm (GC-RMA)(145)

Authors and contact information:

Etienne Sibille[1,4], Jing Su[1], Samuel Leman[6], Anne-Marie Le Guisquet[6], Y. Ibarguen-Vargas[6], Jennifer Joeyen-Waldorf[1], Christin A. Glorioso[4], George C. Tseng[2], Michael Pezzone[3], René Hen[5] and Catherine Belzung[6].

Departments of [1]Psychiatry, [2]Biostatistics and [3]Medicine, [4]Center for Neuroscience, University of Pittsburgh, [5]Center for Neurobiology & Behavior, Columbia University, [6]EA3248 Psychobiologie des émotions, Université François Rabelais de Tours, France,

Correspondence should be addressed to :

- Dr. Etienne Sibille, University of Pittsburgh, Department of Psychiatry, 3811 O'Hara Street, BST W1656, Pittsburgh, PA 15213, E-mail: sibilleel@upmc.edu, or

- Dr. Catherine Belzung, EA3248 Psychobiologie des émotions, Université François Rabelais de Tours, Parc Granmont, Tours 37200, France, E-mail: catherine.belzung@univ-tours.fr.

1.2. Experimental design:

1.2.1. Type of experiment: Determination of the relationship between gene expression levels and aging throughout the lifespan. In particular, we investigated the nature of life-long gene expression changes in the cortex (CTX) and striatum (STR), two brain areas with well-characterized roles for the 5-HT$_{1B}$ receptor, and assessed putative differences in the trajectories of age-related changes in 5-HT$_{1B}$KO and WT control mice.

1.2.2. Experimental factors: Levels of expression.

1.2.3. Number of hybridizations in the study: ~ 50.

1.2.4. A common reference RNA was not used.

1.2.5. Quality control measures. Arrays were only used if: the noise (Raw Q) was less than 5, the background signal was less than 100 (250 targeted intensity for array scaling), the 3'/5' signal ratios of Actin and GAPDH were less than 3, the overall number of genes detected as present across arrays was consistent across arrays and in excess of 50%, the scaling factor was consistent for arrays compared, and the detection of spiked controls BioB and BioC hybridization was in the appropriate amounts. Labeled RNA was used for the array analysis if the 260/280 ratio was between 1.8 and 2.1. Arrays were done in monoplicate. Real-time PCR reactions were performed to validate array results using RNA from the same samples.

1.3 Samples used, extract preparation and labeling:

1.3.1. Bio-source properties: Animals were raised under standard conditions (21^{o}C, 25% humidity, 12hr photoperiod, *ad libitum* food and water). WT and KO 129/Sv littermates were used for all behavior and array experiments, except for the 3-month time-point microarray analysis and for serum level measurements. These latter groups were no more than two generations away from heterozygous breeding. To avoid putative confounding effects of the previously reported increased aggressiveness of 5-HT_{1B}KO mice, mice were housed under reduced cage density, resulting in low intra-cage aggression in both groups, as revealed by the absence of bite marks or wounds. All experiments were conducted in accordance with the European Communities Council Directive of 24 November 1986 (86/609/EEC) and with the University of Pittsburgh Animal Care and Use Committee.

1.3.1. Biomaterial manipulations: Mice were sacrificed by cervical dislocation. Brains were split along the sagittal line, frozen in isopentane and stored at –80°C. To collect samples, frozen brains were cut on a cryostat to the appropriate anatomical level where series of 1 or 2mm diameter micropunches (Sample corer, Fine Science Tools, Foser City, CA), were collected from frontal cortex (CTX) and striatum (STR) and immediately stored in Trizol reagent (Invitrogen, Carlsbad, CA). CTX samples were collected from prelimbic and cingulate cortices corresponding mostly to non-motor areas between Figure18 and 23 (Bregma ~+2 to +1mm) in the Paxinos-Franklin Mouse Brain Atlas(258). Dorsal striatum samples were collected starting at Figure23 in the same atlas (Bregma ~+1 to 0mm).

1.3.3. Extract preparation: Total RNA was extracted using the Trizol protocol, cleaned with Rneasy microcolumns (QIAGEN, Germany), quantified and verified by chromatography using the Agilent Bioanalyzer system.

1.3.4. Microarray samples were prepared according to the manufacturer's protocol (www.affymetrix.com/ support). In brief, 2µg of total RNA were reverse-transcribed and converted into double-stranded cDNA. A biotinylated complementary RNA (cRNA) was then transcribed *in vivo*, using an RNA polymerase T7 promoter site which was introduced during the reverse-transcription of RNA into cDNA. 20µg of fragmented labeled cRNA sample was hybridized onto MOE 430-2.0 Affymetrix oligonucleotide microarrays (Affymetrix, Santa Clara, CA). A high-resolution image of the hybridization pattern on the probe array was obtained by laser scanning, and fluorescence intensity data were automatically stored in a raw file. To reduce the influence of technical variability, samples were randomly distributed at all experimental steps to avoid any simultaneous processing of related samples. For data extraction, single arrays were analyzed with the Affymetrix Microarray GCOS software. Microarray quality control parameters were as follows: noise (RawQ) less than 5 (CTX: 1.53±0.03; STR: 1.65±0.05), background signal less than 100 (250 targeted intensity for array scaling; CTX: 46.2±0.9; STR: 45.3±0.8), consistent number of genes detected as present across arrays (CTX: 49.7±0.4; STR: 52.6±0.4), consistent scaling factors (CTX: 1.80±0.05; STR: 1.52±0.06), Actin and GAPDH 3'/5' signal ratios less than 3 (CTX: ACT, 2.15±0.19, GAPDH, 1.18±0.09; STR: ACT, 1.43±0.04, GAPDH, 0.90±0.03) and consistent detection of BioB and BioC hybridization spiked controls.

1.4. Measurement data and specifications:

See Methods in manuscript.

Figure 29. Figure S1. Anxiety-like behaviors in aging WT and *Htr1b*^{KO} mice in the open field (OF) and the elevated plus maze (EPM) tests.

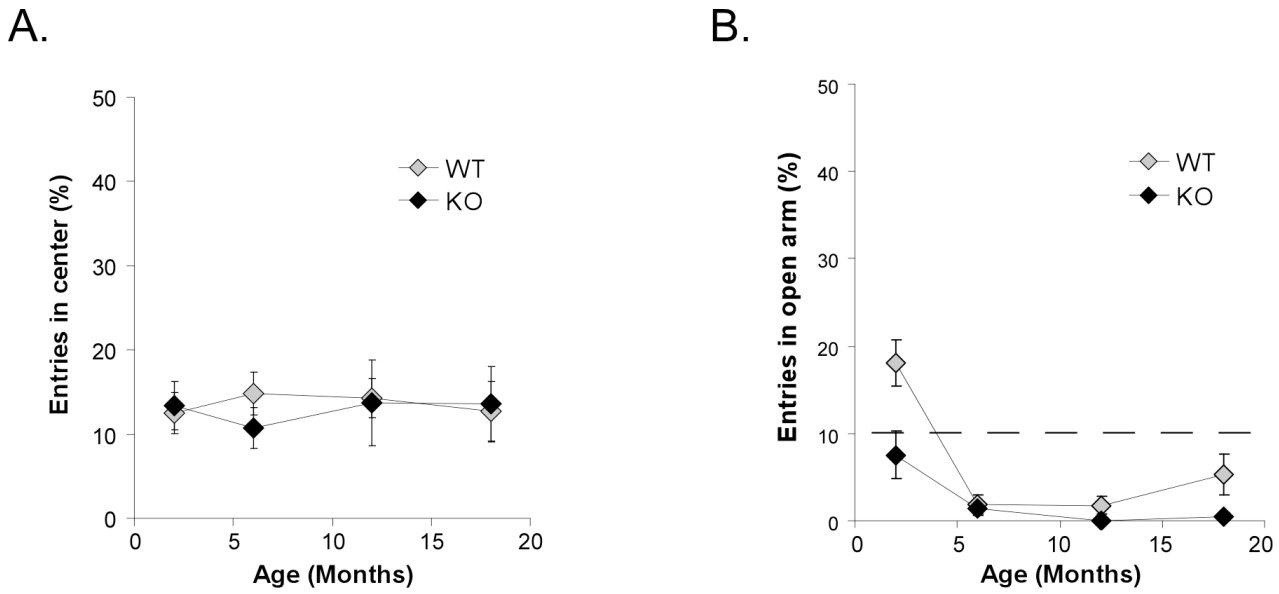

The number of entries into the aversive center of the OF or the open arms of the EPM are indicators of anxiety-like behavior or fearfulness.

In the OF (**A.**), WT and *Htr1b*^{KO} mice displayed the same proportion of entries into the aversive center at all ages (Age effect: F=1.23, p=0.23; Genotype effect: F=0.08, p=0.77; Genotype*Age: F=1.47, p=0.23).

In the EPM (**B.**), WT and *Htr1b*^{KO} mice displayed a very low level of activity in the aversive open arms of the apparatus. Although most parameters reached statistical significance (Age effect: F=20.8, p<0.01; Genotype effect: F=12.7, p<0.001; Genotype*Age: F=3.4, p<0.05), 7 out of 8 averaged data points were below 10% of the total activity (hatched bar), indicating a very low level of confidence for these measurements of anxiety-like behaviors. A-B: n=15 animals per group.

Together, and in agreement with the initial behavioral characterization(252) results from these two independent behavioral tests did not suggest any effect of $5HT_{1B}R$ disruption on the baseline and on the age-related progression of anxiety-like behaviors in *Htr1b*^{KO} mice.

Table 7. Table S1. WT and *Htr1b*^{KO} age-affected genes in CTX

Sample of Table S1

Full Table is available and includes 1097 genes (Separate downloadable Excel file).

Table S1. WT and *Htr1b*^{KO} age-affected genes in CTX									
Probe Set ID	Representative Public ID	Gene Title	Gene Symbol	Entrez Gene	WT pValue (Anova)	KO pValue (Anova)	WT Age effect (alr)	KO Age effect (alr)	Age-pattern (E=early; L=late; n=no change)
1415772_at	BF118393	nucleolin	Ncl	17975	0.0149612	0.0006681	0.38	0.89	E
1416030_a_at	NM_008568	minichromosome maintenance deficient 7 (S. cerevisiae)	Mcm7	17220	0.0018001	0.0072354	0.80	1.24	E
1416044_at	NM_022009	flightless I homolog (Drosophila)	Fliih	14248	0.0000265	0.0734507	0.43	0.57	E
1416134_at	NM_007467	amyloid beta (A4) precursor-like protein 1	Aplp1	11803	0.0071146	0.0104835	0.30	0.38	E
1416173_at	BC004844	pescadillo homolog 1, containing BRCT domain (zebrafish)	Pes1	64934	0.1023053	0.000705	0.01	-0.62	E
1416473_a_at	NM_020043	---	---	---	0.2832501	0.0036003	-0.08	-0.68	E
1416577_a_at	NM_019712	ring-box 1	Rbx1	56438	0.0964434	1.599E-05	-0.29	-1.22	E
1416591_at	AF327929	RAB34, member of RAS oncogene family	Rab34	19376	0.002573	0.0113814	0.48	0.88	E
1416764_at	NM_025562	tetratricopeptide repeat domain 11	Ttc11	66437	0.0009502	0.0119824	0.35	0.69	E
1416772_at	NM_009949	carnitine palmitoyltransferase 2	Cpt2	12896	0.0005253	0.2788918	0.44	0.67	E
1416922_a_at	AK018668	BCL2/adenovirus E1B 19kDa-interacting protein 3-like	Bnip3l	12177	0.0062431	0.0146311	0.28	0.25	E
1416960_at	NM_024256	beta-1,3-glucuronyltransferase 3 (glucuronosyltransferase I)	B3gat3	72727	0.0037089	0.0111122	0.40	0.64	E
1417022_at	NM_007515	solute carrier family 7 (cationic amino acid transporter, y+ system), me	Slc7a3	11989	0.0085308	0.0036918	0.11	0.23	E
1417140_a_at	NM_008977	protein tyrosine phosphatase, non-receptor type 2	Ptpn2	19255	0.0016382	0.0985287	0.23	0.60	E
1417149_at	NM_011031	procollagen-proline, 2-oxoglutarate 4-dioxygenase (proline 4-hydroxyla	P4ha2	18452	0.3449515	0.0016923	0.06	-0.31	E
1417270_at	NM_021312	WD repeat domain 12	Wdr12	57750	0.4279264	1.517E-05	-0.11	0.23	E
1417342_at	NM_025800	---	---	---	0.000393	0.004272	0.37	-0.03	E
1417360_at	NM_026810	mutL homolog 1 (E. coli)	Mlh1	17350	0.0408748	0.0071944	0.37	0.01	E
1417406_at	AF366401	SERTA domain containing 1	Sertad1	55942	0.0002687	0.014782	-0.53	-0.46	E
1417427_at	NM_026616	RIKEN cDNA 1500026D16 gene	1500026D16Rik	68209	0.2526463	0.0004189	0.03	0.88	E
1417463_a_at	NM_025605	RIKEN cDNA 2400001E08 gene /// similar to RIKEN cDNA 2400001E	1E08Rik /// LOC	433216 /// 66508	0.0674273	6.665E-05	-0.25	-0.90	E
1417501_at	NM_015797	F-box only protein 6b	Fbxo6b	50762	0.0024756	0.0242692	0.59	0.72	E
1417607_at	NM_009943	cytochrome c oxidase, subunit VI a, polypeptide 2	Cox6a2	12862	0.0006435	0.0033857	0.30	0.70	E
1417698_at	AV325174	general transcription factor IIF, polypeptide 1	Gtf2f1	98053	0.0001518	0.0016469	0.34	0.79	E
1417708_at	D45858	synaptotagmin 3	Syt3	20981	0.0103733	0.0019688	0.62	0.67	E

Table 8. Table S2. WT and *Htr1b*^{KO} age-affected genes in STR

Sample of Table S2

Full Table is available and includes 419 genes (Separate downloadable Excel file).

Table S2. WT and *Htr1b*^{KO} age-affected genes in STR									
Probe Set ID	Representative Public ID	Gene Title	Gene Symbol	Entrez Gene	WT pValue (Anova)	KO pValue (Anova)	WT Age effect (alr)	KO Age effect (alr)	Age-pattern (E=early; L=late; n=no change)
1415685_at	NM_133767	mitochondrial translational initiation factor 2	Mtif2	76784	0.2586547	0.0081698	0.22	0.79	E
1415699_a_at	BC003350	G protein pathway suppressor 1	Gps1	209318	0.0692371	0.0005853	0.31	0.86	E
1415751_at	BC020024	heterochromatin protein 1, binding protein 3	Hp1bp3	15441	0.3431784	0.0033801	0.24	0.94	E
1415754_at	BC024419	RIKEN cDNA 1810060D16 gene	1810060D16Rik	69833	0.0651459	0.0069346	0.25	0.55	E
1415756_a_at	BB667523	SNAP-associated protein	Snapap	20615	0.1163544	0.0015702	0.40	0.48	E
1415980_at	NM_026468	ATP synthase, H+ transporting, mitochondrial F0 complex, subunit c (	Atp5g2	67942	0.1198264	0.003291	0.44	1.08	E
1416005_at	NM_008947	protease (prosome, macropain) 26S subunit, ATPase 1	Psmc1	19179	0.2294616	0.0030208	0.33	0.88	E
1416093_a_at	NM_025570	mitochondrial ribosomal protein L20	Mrpl20	66448	0.242453	0.0016652	0.30	0.66	E
1416096_at	NM_134044	expressed sequence AI413782	AI413782	104799	0.1976613	3.185E-05	0.27	0.98	E
1416209_at	NM_008133	glutamate dehydrogenase 1	Glud1	14661	0.3361043	0.0021869	0.30	0.99	E
1416448_at	NM_025922	inosine triphosphatase (nucleoside triphosphate pyrophosphatase)	Itpa	16434	0.1690921	0.0016085	0.32	0.95	E
1416482_at	BB833716	tetratricopeptide repeat domain 3	Ttc3	22129	0.0711391	0.0073192	0.66	1.39	E
1416800_at	AV320241	transient receptor potential cation channel, subfamily M, member 7	Trpm7	58800	0.0974659	0.0039039	0.28	0.68	E
1417044_at	NM_025304	leucine carboxyl methyltransferase 1	Lcmt1	30949	0.201501	0.0060636	0.24	0.78	E
1417138_s_at	NM_025554	polymerase (RNA) II (DNA directed) polypeptide E	Polr2e	66420	0.0112703	0.0007155	0.40	0.79	E
1417211_a_at	NM_023483	RIKEN cDNA 1110032A03 gene	1110032A03Rik	68721	0.2109555	0.0056434	0.24	0.71	E
1417219_s_at	NM_025284	thymosin, beta 10	Tmsb10	19240	0.4144897	0.0059138	0.28	0.82	E
1417259_a_at	NM_009798	capping protein (actin filament) muscle Z-line, beta	Capzb	12345	0.3001028	0.0087546	0.32	1.13	E
1417313_at	NM_025349	LSM7 homolog, U6 small nuclear RNA associated (S. cerevisiae)	Lsm7	66094	0.0085711	0.0112115	0.35	0.76	E
1417340_at	NM_023140	thioredoxin-like 2	Txnl2	30926	0.205615	0.0036877	0.25	0.60	E
1417501_at	NM_015797	F-box only protein 6b	Fbxo6b	50762	0.3297972	0.002918	0.39	1.02	E
1417516_at	NM_007837	DNA-damage inducible transcript 3	Ddit3	13198	0.0714007	0.0092445	0.41	0.84	E
1417670_at	NM_011592	translocator of inner mitochondrial membrane 44	Timm44	21856	0.174136	0.0007696	0.25	0.70	E
1417699_at	AV325174	general transcription factor IIF, polypeptide 1	Gtf2f1	98053	0.2103756	0.0070991	0.53	1.13	E
1417914_at	BB645629	RAP2B, member of RAS oncogene family	Rap2b	74012	0.2536993	0.0084971	0.37	0.65	E

Table 9. Table S3. Selected mouse (left) -human (right) orthologous gene with conserved age-effects on gene transcript levels.

Probe Set (MOE 430plus)	Name	WT_p-ANOVA	KO_p-ANOVA	WT_24/10_alr	KO_24/10_alr	Ortholog Probe Set (U133A)	Name	BA9_p-Pearson	BA47_p-Pearson	BA9 65/30_alr	BA47 65/30_alr
1427682_A_AT	early growth response 2	0.0013328	0.0195222	-1.98	-1.066	205249_AT	"early growth response 2 (Krox-20 homolog, Drosophila	0.0516435	0.0195773	-0.51	-0.68
1418687_AT	activity regulated cytoskeletal-associated protein	0.0045531	0.0095457	-0.752	-0.681	210090_AT	activity-regulated cytoskeleton-associated protein	0.0122961	0.0442099	-0.88	-0.7
1420720_AT	neuronal pentraxin 2	0.0092875	0.0127091	-0.32	-0.8	213479_AT	neuronal pentraxin II	0.0003607	0.0423215	-0.56	-0.55
1431182_AT	heat shock protein 8	0.34338	0.0039684	-0.258	-1.027	210338_S_AT	heat shock 70kD protein 8	0.0000601	0.0071898	-0.45	-0.43
1426640_S_AT	tribbles homolog 2 (Drosophila)	0.0162826	0.0002661	-0.366	-0.58	202479_S_AT	GS3955 protein	4.14E-06	0.0023797	-0.66	-0.52
1433575_AT	SRY-box containing gene 4	0.0051392	0.0412361	-0.266	-0.221	201417_AT		0.0007209	0.0000445	-0.75	-0.88
1443851_AT		0.0046244	0.0042152	-0.443	0.017	220673_S_AT	HEAT-like repeat-containing protein	8.12E-07	0.0034501	-0.95	-0.62
1422169_A_AT	brain derived neurotrophic factor	0.0078755	0.0018665	-0.707	-0.538	206382_S_AT	brain-derived neurotrophic factor	0.0016739	0.0414814	-0.4	-0.33
1421360_AT	inositol polyphosphate-4-phosphatase, type I	0.0066009	0.0002961	-0.466	-0.528	208363_S_AT	"inositol polyphosphate-4-phosphatase, type I, 107kD"	0.0001777	0.0567653	-0.43	-0.39
1428637_AT	RIKEN cDNA 1810038L18 gene	0.000779	0.0132375	-0.437	-0.369	202969_AT	dual-specificity tyrosine-(Y)-phosphorylation regulated	0.0005383	0.0016092	-0.35	-0.62
1436329_AT	early growth response 3	0.0100278	5.73E-05	-0.228	-0.599	206115_AT	early growth response 3	0.0048858	0.0107399	-0.36	-0.58
1458897_AT	---	0.1668409	0.000507	-0.116	-0.452	205139_S_AT	uronyl 2-sulfotransferase	0.0004657	0.0000927	-0.42	-0.76
1421048_A_AT	yippee-like 1 (Drosophila)	0.0001706	0.0047193	-0.435	-0.607	213996_AT	hypothetical protein	0.0000105	0.0175583	-0.34	-0.28
1437690_X_AT	casein kinase 1, delta	0.0040205	0.0034826	-0.364	-0.6	207945_S_AT	"casein kinase 1, delta"	0.0099899	0.0720921	-0.33	-0.33
1416029_AT	TGFB inducible early growth response 1	0.0095015	0.0548452	-0.499	-0.084	202393_S_AT	TGFB inducible early growth response	0.0469049	0.0529649	-0.37	-0.64
1427247_AT	DNA segment, Chr 3, Brigham & Women's Genetics 05	0.0080076	0.0687587	-0.271	-0.193	213496_AT	KIAA0455 gene product	0.0000023	0.000024	-0.52	-0.6
1449243_a_at	chemokine (C-X3-C) receptor 1	0.970821	0.0003451	0.03	-0.36	205898_at	chemokine (C-X3-C) receptor 1	0.0082222	0.0076477	-0.62	-0.62
1416292_at	calcium/calmodulin-dependent protein kinase IV	0.0026631	0.7783929	-0.57	0	210349_at	calcium/calmodulin-dependent protein kinase IV	1.29E-07	5.12E-07	-0.47	-0.46
1450436_S_AT	DnaJ (Hsp40) homolog, subfamily B, member 5	0.0006407	0.0026737	-0.392	-0.454	212817_AT	"DnaJ (Hsp40) homolog, subfamily B, member 5"	0.000112	0.0135398	-0.36	-0.3
1417206_at	nucleolar protein 4	0.001351	0.0079077	-0.36	-0.45	206045_s_at	nucleolar protein 4	0.0184934	0.3391558	-0.31	-0.35
1417192_at	synaptojanin 1	0.0055938	0.0029978	-0.09	-0.36	207594_s_at	synaptojanin 1	0.0019484	0.0660988	-0.51	-0.45
1435194_AT	---	0.0059329	0.0006746	-0.295	-0.253	211016_X_AT	heat shock 70kD protein 4	0.0009669	0.1078793	-0.39	-0.47
1427703_AT	platelet-activating factor acetylhydrolase, isoform 1b, b	0.0012187	0.4226489	-0.38	-0.136	211547_S_AT	"platelet-activating factor acetylhydrolase, isoform 1b, a	0.0017336	0.0691322	-0.46	-0.41
1428074_AT	RIKEN cDNA 2310037P21 gene	0.2977136	0.0015621	-0.094	-0.495	213338_AT	Ras-induced senescence 1	0.0035361	0.1646017	-0.42	-0.28
1460153_AT		0.0009399	0.0240609	-0.377	-0.095	207268_X_AT	abl-interactor 12 (SH3-containing protein)	4.84E-06	0.0073678	-0.46	-0.34
1450061_AT	ectodermal-neural cortex 1	0.0175545	0.004138	-0.074	-0.37	201340_S_AT	ectodermal-neural cortex (with BTB-like domain)	0.0049957	0.2336682	-0.48	-0.31
1437468_X_AT	F-box and WD-40 domain protein 11	0.2552625	0.0007842	-0.097	-0.401	209456_S_AT	f-box and WD-40 domain protein 1B	0.001933	0.0649664	-0.29	-0.45
1435382_AT	necdin	0.2417987	5.08E-05	-0.066	-0.426	209550_AT	necdin homolog (mouse)	0.0005254	0.0439387	-0.33	-0.41
1423154_AT	cDNA sequence BC005537	0.5458642	0.0001693	0.084	-0.397	213872_AT	hypothetical protein FLJ12619	0.0001686	0.0207822	-0.51	-0.38
1417004_at	dynamin 1-like	0.0011735	0.0047851	-0.34	-0.28	203105_s_at	dynamin 1-like	0.0044663	0.1543467	-0.27	-0.27
1443119_AT		0.0200215	0.0090703	-0.117	-0.295	217008_S_AT	"glutamate receptor, metabotropic 7"	0.0010944	0.0012481	-0.28	-0.45
1429201_AT	cylindromatosis (turban tumor syndrome)	0.5527123	0.0032935	-0.056	-0.323	221903_S_AT	cylindromatosis (turban tumor syndrome)	0.0062671	0.0728261	-0.27	-0.38
1440029_AT	---	0.4669375	0.0004628	-0.086	-0.296	208065_AT	"sialyltransferase 8C (alpha2,3Galbeta1,4GlcNAcalpha	0.002497	0.0151207	-0.36	-0.28
1418492_AT	gremlin 2 homolog, cysteine knot superfamily (Xenopus	0.9994964	0.0038965	0.003	-0.365	220794_AT	hypothetical protein FLJ21195 similar to protein related	0.0164607	0.3186448	-0.26	-0.32
1443581_AT		0.0022068	0.9713292	-0.276	-0.013	201998_AT	"sialyltransferase 1 (beta-galactoside alpha-2,6-sialytra	0.0000991	0.0018422	-0.29	-0.3
1435204_AT	protein arginine N-methyltransferase 4	0.1053744	0.0071755	0.078	-0.275	207772_S_AT	HMT1 hnRNP methyltransferase-like 3 (S. cerevisiae)	0.0002937	0.0214037	-0.32	-0.34
1425942_A_AT	glycoprotein m6b	0.0127751	0.0035588	0.283	0.275	209167_AT	glycoprotein M6B	0.0051502	0.0516999	0.327	0.335
1434369_A_AT	crystallin, alpha B	0.1111725	0.0084827	0.285	0.048	209283_AT	"crystallin, alpha B"	0.0078834	0.0106725	0.359	0.558
1424613_AT	G protein-coupled receptor, family C, group 5, member	0.0021535	0.086935	0.284	0.154	203632_S_AT	"G protein-coupled receptor, family C, group 5, member	0.0589844	0.2558768	0.417	0.41
1415702_a_at	microtubule-associated protein 4	0.0022656	0.1222461	0.35	0.28	243_g_at	microtubule-associated protein 4	0.0000013	0.0041515	0.28	0.37
1452141_A_AT	selenoprotein P, plasma, 1	7.23E-05	0.0561718	0.306	0.06	201427_S_AT	"selenoprotein P, plasma, 1"	0.0156092	0.2247726	0.557	0.369
1419574_AT	zinc finger protein 292	0.4953035	0.003014	0.135	0.315	212368_AT	KIAA0530 protein	0.0000454	0.001439	0.46	0.385
1437041_AT	RIKEN cDNA 5730406M06 gene	0.0026204	0.1703747	0.289	0.18	212177_AT		0.0068773	0.0679474	0.547	0.282
1434768_AT	ceroid-lipofuscinosis, neuronal 2	0.0805289	0.0014011	0.151	0.339	200743_S_AT	"ceroid-lipofuscinosis, neuronal 2, late infantile (Jansky-	0.0031158	0.0031409	0.386	0.453
1456599_AT	nuclear transport factor 2-like export factor 2	0.0012009	0.1188901	0.333	0.147	209628_AT	hypothetical protein P15-2	0.0013243	0.0501442	0.563	0.292
1422643_AT	monooxygenase, DBH-like 1	0.1812211	0.0074221	0.394	0.093	209708_AT	DKFZP564G202 protein	0.0005377	0.0007117	0.479	0.374
1416718_AT	brevican	0.1080981	0.0002459	0.326	0.474	221623_AT	chondroitin sulfate proteoglycan BEHAB/brevican	0.0105726	0.0071874	0.28	0.294
1424863_A_AT	homeodomain interacting protein kinase 2	0.5405814	0.0042386	0.172	0.293	219028_AT	homeodomain interacting protein kinase 2	0.0001044	0.0063474	0.488	0.423
1426913_AT	lanosterol synthase	0.0121357	0.0016408	0.082	0.524	202245_AT	"lanosterol synthase (2,3-oxidosqualene-lanosterol cycl	0.0024999	0.0026663	0.366	0.407
1451628_A_AT	ankyrin 3, epithelial	0.2539431	0.0011714	0.189	0.429	215314_AT		0.0257008	0.0083065	0.29	0.493
1460178_AT	RIKEN cDNA 1300002A08 gene	0.0177834	0.0063818	0.283	0.349	221834_AT		0.0145455	0.0001602	0.417	0.353
1433937_AT	transformation related protein 53 binding protein 2	0.057443	0.0002378	0.324	0.362	203120_AT	"tumor protein p53 binding protein, 2"	0.0183084	0.0547678	0.354	0.394
1425292_AT	dystrobrevin alpha	0.9273448	0.0010999	0.031	0.483	205741_S_AT	"dystrobrevin, alpha"	0.0077086	0.0154941	0.353	0.565
1426100_A_AT	thymidine kinase 2, mitochondrial	0.0017953	0.0299289	0.331	0.224	208246_X_AT	hypothetical protein FLJ20006	0.0253447	0.0126437	0.329	0.568
1428792_AT	breast carcinoma amplified sequence 1	0.051817	0.00023	0.439	0.116	204378_AT	breast carcinoma amplified sequence 1	0.0000217	0.0083438	0.433	0.428
1415812_AT	gelsolin	0.0203665	0.0004658	0.284	0.445	200696_S_AT	"gelsolin (amyloidosis, Finnish type)"	0.3678919	0.0921259	0.274	0.484
1439506_AT		0.0009673	0.0004785	0.53	-0.021	204073_S_AT	chromosome 11open reading frame 9	0.0376351	0.2420263	0.442	0.54
1448139_AT	megalencephalic leukoencephalopathy with subcortical	0.0377584	0.0086297	0.292	0.471	213395_AT	KIAA0027 protein	0.0356807	0.0157808	0.305	0.423
1430979_A_AT	peroxiredoxin 2	0.0057256	0.0074036	0.474	0.261	215067_X_AT		0.0305583	0.0112094	0.265	0.493
1426983_AT	formin binding protein 1	0.0020284	0.0540552	0.235	0.305	212288_AT	formin-binding protein 17	0.0004488	0.0065427	0.51	0.464
1423392_AT	chloride intracellular channel 4 (mitochondrial)	0.2218292	1.31E-05	0.295	0.381	201560_AT	chloride intracellular channel 4	0.0295409	0.189024	0.493	0.422
1423664_AT	quininoid dihydropteridine reductase	0.0043225	0.0008	0.34	0.577	209123_AT	quinoid dihydropteridine reductase	0.0113559	0.0005076	0.3	0.388
1438169_A_AT	FERM domain containing 4B	0.6322576	1.02E-05	0.153	0.447	213056_AT	KIAA1013 protein	0.002784	0.7764223	0.692	0.328
1430077_AT	RIKEN cDNA 2610019N13 gene	0.0078503	0.3226144	0.295	0.123	213742_AT		0.0000127	0.0005221	0.698	0.524
1425241_A_AT	WD repeat and SOCS box-containing 1	0.0001679	0.0344981	0.468	0.142	201296_S_AT	DKFZP564A122 protein	0.0047039	0.0108068	0.551	0.495
1421863_AT	vesicle-associated membrane protein 1	0.0027545	0.0274791	0.363	0.24	213326_AT	vesicle-associated membrane protein 1 (synaptobrevin	0.0003793	0.0059673	0.779	0.317
1423136_AT	fibroblast growth factor 1	0.005536	0.0811996	0.341	0.24	205117_AT	fibroblast growth factor 1 (acidic)	1.79E-06	0.0001358	0.579	0.597
1429055_AT	RIKEN cDNA 4930506M07 gene	0.0795008	0.002516	0.383	0.619	221802_S_AT	KIAA1598 protein	0.0003052	0.0134474	0.485	0.321
1416265_at	cysteine and glycine-rich protein 1	0.0057117	0.3647913	0.84	0.25	200621_at	cysteine and glycine-rich protein 1	0.0086367	0.0039843	0.28	0.44
1417275_AT	myelin and lymphocyte protein, T-cell differentiation pro	0.0340422	1.821E-05	0.574	0.364	204777_S_AT	"mal, T-cell differentiation protein"	0.0284007	0.2220586	0.445	0.456
1451611_AT	HRAS like suppressor 3	0.0096161	1.286E-06	0.551	0.521	209581_AT	similar to rat HREV107	0.0285975	0.0123918	0.281	0.491
1420847_A_AT	fibroblast growth factor receptor 2	0.0069401	0.0033976	0.832	0.328	203638_S_AT	"fibroblast growth factor receptor 2 (bacteria-expressed	0.0462936	0.2122701	0.391	0.315
1416200_AT	RIKEN cDNA 9230117N10 gene	0.0031627	1.994E-06	0.552	0.585	209821_AT	DVS27-related protein	0.0636023	0.0449541	0.446	0.306
1417143_AT	endothelial differentiation, lysophosphatidic acid G-prot	0.1431929	2.542E-05	0.34	0.399	204036_AT	"endothelial differentiation, lysophosphatidic acid G-pro	8.88E-06	0.0082517	0.59	0.567
1438030_AT	RAS, guanyl releasing protein 3	0.0338677	0.0011402	0.407	0.647	205801_S_AT	KIAA0846 protein	0.0068883	0.067449	0.548	0.385
1448507_AT	EF hand domain containing 1	0.0099086	2.735E-05	0.63	0.436	209343_AT	hypothetical protein FLJ13612	0.0143545	0.0549715	0.506	0.481
1448729_A_AT	septin 4	0.0009017	0.0011722	0.438	0.519	210657_S_AT	peanut-like 2 (Drosophila)	0.000001	0.0001201	0.562	0.572
1417962_s_at	ecotropic viral integration site 2a	0.0048469	6.591E-06	0.55	0.7	204774_at	ecotropic viral integration site 2A	0.02612	0.6942543	0.52	0.35
1444089_AT		0.0650302	0.0004292	0.464	0.46	215918_S_AT		1.94E-07	0.0001832	0.658	0.565
1416371_AT	apolipoprotein D	3.82E-06	0.0002867	0.84	0.603	201525_AT	apolipoprotein D	0.0042165	0.062215	0.281	0.429
1451537_AT	chitinase 3-like 1	0.1291879	0.0037829	0.197	0.359	209396_S_AT	chitinase 3-like 1 (cartilage glycoprotein-39)	0.000021	0.0005071	0.776	0.829
1428011_A_AT	Erbb2 interacting protein	0.0514487	0.0003892	0.363	0.377	217941_S_AT	erbb2 interacting protein	3.07E-06	0.0047523	0.886	0.553
1416178_A_AT	pleckstrin homology domain containing, family B (evect	0.0028986	0.0001122	0.662	0.618	209504_S_AT	PH domain containing protein in retina 1	0.0000116	0.000174	0.409	0.512
1417133_AT	peripheral myelin protein	0.0005518	9.568E-06	0.559	0.79	210139_S_AT	peripheral myelin protein 22	0.0494921	0.3203462	0.404	0.467
1421010_AT	myelin-associated oligodendrocytic basic protein	0.0037618	0.0008846	0.827	0.768	207659_S_AT	myelin-associated oligodendrocyte basic protein	0.0022105	0.035891	0.305	0.327
1455123_AT	suppression of tumorigenicity 18	0.1763238	2.144E-05	0.649	0.375	206135_AT	KIAA0535 gene product	0.0041	0.0585507	0.76	0.608
1416343_A_AT	lysosomal membrane glycoprotein 2	0.0015131	0.0040765	0.593	0.85	203042_AT	lysosomal-associated membrane protein 2	0.0333556	0.2901985	0.653	0.411
1427183_AT	epidermal growth factor-containing fibulin-like extracellu	0.6504041	0.0039652	0.041	0.58	201842_S_AT	EGF-containing fibulin-like extracellular matrix protein 1	0.0152327	0.0180719	0.938	0.966
1416713_AT	RIKEN cDNA 2700055K07 gene	5.68E-06	0.0066579	0.826	0.538	218876_AT	brain specific protein	0.0030713	0.0004404	0.482	0.815
1418472_AT	aspartoacylase (aminoacylase) 2	0.0107989	7.394E-05	0.728	1.161	206030_AT	"aspartoacylase (aminoacylase 2, Canavan disease)"	0.0994242	0.774631	0.446	0.493
1449254_AT	secreted phosphoprotein 1	0.0001368	0.0044651	1.103	0.849	209875_S_AT	"secreted phosphoprotein 1 (osteopontin, bone sialopro	0.0539174	0.4944016	0.644	0.565
1418021_AT	complement component 4 (within H-2S)	0.0007357	0.0051543	1.433	0.837	208451_S_AT	complement component 4B	0.0023164	0.0000851	0.708	1.152
1447825_x_at	glial fibrillary acidic protein	0.0102907	0.0005349	1.06	1.06	203540_at	glial fibrillary acidic protein	5.08E-09	1.51E-08	0.95	1.09

Alr, average log-ratio. See Methods for details. Blue, increased; Red, decreased.

Table 10. Table S4. Functional analysis of age-related gene expression in WT and *Htr1b*^{KO} mice.

CTX-WT

ID	Name		Probes	Genes	Rank	CorrectedPvalue
GO:0005830	cytosolic ribosome (sensu Eukaryota)	Translation	63	38	1	<1E-08
GO:0005840	ribosome	Translation	108	79	2	0.00000346
GO:0006954	inflammatory response	Inflammation	85	69	3	0.00000517
GO:0030005	di-, tri-valent inorganic cation homeostasis	Metabolism	51	36	4	0.00004019
GO:0009611	response to wounding	Inflammation	123	99	5	0.0000944
GO:0006935	chemotaxis	Inflammation	59	40	6	0.00010729
GO:0006092	main pathways of carbohydrate metabolism	Metabolism	116	86	7	0.00010967
GO:0045892	negative regulation of transcription, DNA-dependent	Transcription	136	93	8	0.00011498
GO:0019752	carboxylic acid metabolism	Metabolism	106	85	9	0.00011581
GO:0009986	cell surface	Misc	70	46	10	0.00011747
GO:0009058	biosynthesis	Metabolism	61	41	11	0.00011879
GO:0007417	central nervous system development	Cell Growth	147	100	12	0.00013275
GO:0007409	axonogenesis	Cell Growth	115	72	13	0.0001444
GO:0006916	anti-apoptosis	Cell Growth	96	64	14	0.00015296
GO:0040007	growth	Cell Growth	60	41	15	0.00015502
GO:0006519	amino acid and derivative metabolism	Metabolism	57	46	16	0.00019032
GO:0043066	negative regulation of apoptosis	Cell Growth	108	71	17	0.00019742
GO:0042623	ATPase activity, coupled	Cellular respiration	108	84	18	0.000203
GO:0008083	growth factor activity	Cell Growth	114	81	19	0.00023467
GO:0007200	G-protein signaling, coupled to IP3 second messenger (phospholip	Signalling	67	47	20	0.00029125
GO:0007046	ribosome biogenesis	Translation	76	53	21	0.00029893
GO:0042221	response to chemical substance	Inflammation	107	78	22	0.00029969
GO:0044255	cellular lipid metabolism	Metabolism	91	72	23	0.00030308
GO:0016853	isomerase activity	Metabolism	59	46	24	0.00055084
GO:0005764	lysosome	Metabolism	98	75	25	0.00057615

CTX-KO

ID	Name		Probes	Genes	Rank	CorrectedPvalue
GO:0005830	cytosolic ribosome (sensu Eukaryota)	Translation	63	38	1	<1E-08
GO:0005840	ribosome	Translation	108	79	2	<1E-08
GO:0005842	cytosolic large ribosomal subunit (sensu Eukaryota)	Translation	30	18	3	<1E-08
GO:0015934	large ribosomal subunit	Translation	34	21	4	<1E-08
GO:0007046	ribosome biogenesis	Translation	76	53	5	0.00000105
GO:0042254	ribosome biogenesis and assembly	Translation	61	41	6	0.0000099
GO:0040008	regulation of growth	Cell Growth	85	52	7	0.00008448
GO:0016788	hydrolase activity, acting on ester bonds	Cell Growth	54	38	8	0.00024338
GO:0001558	regulation of cell growth	Cell Growth	103	62	9	0.00055466
GO:0016070	RNA metabolism	Translation	158	93	10	0.00079316
GO:0016049	cell growth	Cell Growth	100	60	11	0.00125948
GO:0048232	male gamete generation	Cell Growth	122	100	12	0.00136211
GO:0006092	main pathways of carbohydrate metabolism	Metabolism	116	86	13	0.00142609
GO:0006954	inflammatory response	Inflammation	85	69	14	0.00145012
GO:0015078	hydrogen ion transporter activity	Cellular respiration	72	49	15	0.00146913
GO:0050953	sensory perception of light	Misc	95	63	16	0.00209872
GO:0042802	protein self binding	Misc	64	48	17	0.00220462
GO:0009611	response to wounding	Inflammation	123	99	18	0.0022083
GO:0008610	lipid biosynthesis	Metabolism	73	54	19	0.0029772
GO:0000398	nuclear mRNA splicing, via spliceosome	Translation	155	94	20	0.00301446
GO:0005125	cytokine activity	Inflammation	76	62	21	0.00404566
GO:0016282	eukaryotic 43S preinitiation complex	Translation	26	17	22	0.00498591
GO:0016853	isomerase activity	Metabolism	59	46	23	0.0058096
GO:0042598	vesicular fraction	Signalling	90	63	24	0.00600246
GO:0042623	ATPase activity, coupled	Cellular respiration	108	84	25	0.00603844

Top 25 ranked GO families most affected during aging in CTX of WT and *Htr1b*^{KO} mice. Color codes are as in Figure5. “Probes” indicate the number of MOE-430-2.0 probesets represented in the respective GO groups. “Genes” indicate the number of genes taken in consideration for analysis (i.e., detected signal, reduced probeset redundancy).

Table 11. Table S5. Consistent WT- *Htr1b*^{KO} gene expression differences

						CORTEX		STRIATUM	
Probe Set ID	Public ID	UniGene ID	Gene Title	Gene Symbol	Entrez Gene	p value	KO/WT age Fold change	p value	KO/WT age Fold change
1439195_at	BB471698	---	---	---	---	0.0075	-2.82	0.0142	-9.16
1429951_at	AK005150	Mm.343095	single-stranded DNA binding protein 2	Ssbp2	66970	0.0035	-4.37	0.0078	-7.75
1431354_a_a	AK020164	Mm.70690	phenylalanine-tRNA synthetase 2 (mitochondrial)	Fars2	69955	0.0149	1.40	0.0063	1.33
1436401_at	AV024863	Mm.298576	RIKEN cDNA 9330128J19 gene	9330128J19Ri	271144	0.0038	1.33	0.0025	1.36
1428916_s_a	AK002609	Mm.35325	sirtuin 5 (silent mating type information regulation 2 homolog)	Sirt5	68346	0.0021	1.66	0.0142	1.39
1415966_a_a	NM_133666	---	NADH dehydrogenase flavoprotein 1	Ndufv1	---	0.0209	1.58	0.0017	1.95
1428915_at	AK002609	Mm.35325	sirtuin 5 (silent mating type information regulation 2 homolog)	Sirt5	68346	0.0034	1.96	0.0234	1.81
1427229_at	BB123978	Mm.316652	3-hydroxy-3-methylglutaryl-Coenzyme A reductase	Hmgcr	15357	0.0197	1.50	0.0037	2.09
1417432_a_a	NM_008142	Mm.2344	guanine nucleotide binding protein, beta 1	Gnb1	14688	0.0187	1.87	0.0171	3.01

8 probesets (out of 45,101 tested) displayed consistent genotype differences in CTX and STR.

APPENDIX D: PAPER 3 SUPPLEMENTS

Molecular Brain Aging, Promotion of Neurological Disease and Sirtuin5 Longevity Gene Polymorphism

Christin Glorioso,[1] Sunghee Oh,[2] Etienne Sibille[1*]

[1]Department of Psychiatry and Center For Neuroscience, [2]Department of Biostatistics, University of Pittsburgh, Pittsburgh, PA 15213. *Correspondence should be addressed. E-mail: sibilleel@upmc.edu

Table of Contents

D. Table S5. Percentage of transcripts in same or opposite direction as other brain areas broken down by increased or decreased with age Cross area brain aging biosignature

A. Methods for Ingenuity® analysis

B. Table S6. Summary of Ingenuity® biosignature findings

C. Table S7. Top Ingenuity® biosignature networks

D. Methods and references for C-MAP drug matching of the biosignature

III. Neurological disease-associated genes

A. Figure S3. Ingenuity® functional analysis of all age-regulated genes

B. Figure S4. Age-regulated genes associated with the top six neurological diseases

C. Figure S5. Ingenuity® functional analysis of non-age-regulated genes

D. Table S8. References for direction of disease gene changes in disease (support for Table 1)

IV. Candidate longevity gene polymorphisms

A. Rationale for candidate longevity gene snps chosen

B. Chromosomal context of Sirt5 prom polymorphisms and their proximity to conserved predicted promoter regions, including Figure S6.

C. Table S9. Frequencies of snps and methods for snp genotyping

D. Rationale for focusing on Sirt5 prom2 and not prom1 or 3

E. Figure S7. Leave one out molecular ages of subjects calculated using ACC or AMY specific age-regulated genes (support for Figure 3C)

F. Table S10. Significance of genotypic effects on molecular age in ACC and AMY

G. Figure S8. Quantitative PCR of SIRT5 expression by $SIRT_{prom2}$ genotype in AMY

H. Figure S9. Ingenuity® Canonical Pathways significantly affected by $SIRT5_{prom2\ i}$ntersection transcripts in ACC

I. Figure S10. Ingenuity® Functional Categories significantly affected by $SIRT5_{prom2}$ intersection transcripts in ACC

J. Figure S11. Huntington's and Parkinson's associated genes affected

I. Cohorts

Table 12. A. Table S1. Summary of Cohorts

	Cohort 1		Cohort 2	
Number of Subjects	37		39	
Age Range	23- 71		14- 79	
Exclusion Criteria	Neurodegenerative disease, schizophrenia, bipolar disorder, prolonged post-mortem interval /agonal time, illicit drugs.		Neurodegenerative disease, schizophrenia, bipolar disorder, prolonged post-mortem interval /agonal time, illicit drugs.	
Included Diagnoses	Major Depression (50% of Subjects)		Major Depression (50% of Subjects)	
Microarray Platform	Affymetrix U133 Plus		Affymetrix U133A	
Number of Probesets/Genes in Data Sets				
Genes (Expressed Genes)	21,115 (15,522)		13,795 (13,520)	
Probesets (Expressed Probesets)	54,715 (35,122)		22,177 (21,961)	
Brain Areas	ACC (BA25)	AMY	PFC (BA9)	PFC (BA47)
Aging Significant Probesets (% of total)				
α				
0.001	1309 (3.9%)	814 (2.3%)	1972 (9.0%)	1106 (4.6%)
0.01	4443 (13.3%)	2820 (8%)	4240 (19.3%)	2801 (12.8%)
Aging Estimated False Discovery Rate (FDR)				
α				
0.001	2.8%	4.3%	1.2%	2.0%
0.01	8.0%	12.4%	5.2%	7.8%
Major Depression Significant Probesets (fold change < aging at same α)				
α				
0.001	4 (330X)	4 (200X)	2 (986X)	6 (184X)
0.01	93 (48X)	69 (40X)	87 (49X)	68 (41X)

Major Depression FDR				
α				
0.001	>100%	>100%	>100%	>100%
0.01	>100%	>100%	>100%	>100%

B. Effects of depression do not associate with altered rates of molecular aging: Subjects with a lifetime diagnosis of depression do not age at different molecular rates than subjects without a lifetime diagnosis of major depression in these cohorts and in the brain areas investigated. This was discussed in Erraji et al(60) and is also shown in Figure S1.

Figure 30. Figure S1. Molecular Ages by Depression Status.

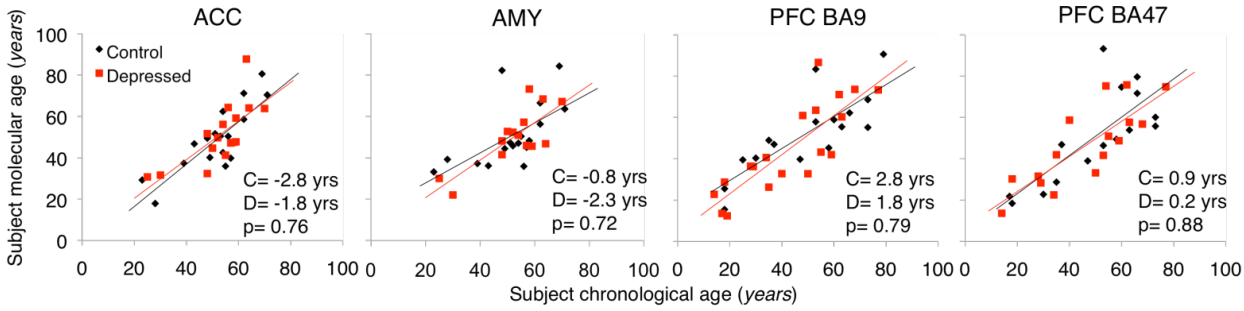

Molecular ages were calculated using the cross-area age biosignature (See section IV in supplements). C and D refer to Control and Depressed group averages for (molecular age-chronological age) and p-values were generated from performing two group t-tests on these values.

C. Cohort 1 (PFC BA9&47) Description adapted from Erraji-Benchekroun et al. 2005[1]

Subjects

Samples from 39 subjects, ranging from 14 to 79 years of age (44 +/-20 years, Mean +/-SD) were obtained from the brain collection of the Human Neurobiology Core of the Conte Center for the Neuroscience of Mental Disorders, the New York

State Psychiatric Institute. All cases were clinically free of neurologic disease, as determined by psychological autopsy(322) and neuropathologic examination, including thioflavine S or immunohistochemical stains on fixed tissue for senile plaques and neurofibrillary tangles. Varying degrees of atherosclerosis were present in subjects aged 45 or older, and several specimens included foci of encephalomalacia, as expected during normal aging. Several subjects contained senile plaques or neurofibrillary tangles, but never in sufficient numbers to suggest a diagnosis of Alzheimer's disease. No other significant abnormalities were observed. All subjects died rapidly, 20 of which committed suicide (psychological autopsies indicated that 17 of them had a lifetime diagnosis of major depression) and 19 died of causes other than suicide. An independent study assessed the effect of suicide and depression on gene expression and within current analytical limits, found no evidence for molecular differences that correlated with depression and suicide(323). Using body fluids and brain tissue, a toxicologic screen was carried out for the presence of psychotropic or illegal drugs. All samples were psychotropic medication–free with minimal other drug exposures. Caucasians represented 71%, African Americans 8%, Hispanics 18%, and Asians 2% of the sample. Average postmortem interval and brain pH were 17 ± 1 and 6.53 ± 0.21, respectively. As a group, male subjects (n = 30) did not differ significantly from female subjects (n = 9) on age, race, postmortem delay, or brain pH. No interaction among experimental, demographic, and clinical parameters and age were found(262, 323). Hence, we combined all samples for this aging study. Details of dissections have been described in our previous publications[1,22]. RNA extraction, microarray samples preparation, and quality control were performed according to the manufacturer protocol (http://www.affymetrix.com) and in our previous publication(262). Samples were hybridized to Affymetrix U133A microarrays.

D. Cohort 2 (AMY and ACC). Adapted from Sibille et al. 2009 [3]

Subjects

39 all male subject (ages 23-71) brain samples were obtained during autopsies conducted at the Allegheny County Medical Examiner's Office. Subjects

with advanced disease stages (i.e., cancer, neurodegenerative disorders) and prolonged postmortem interval PMI (>28hrs) were excluded. All subjects were white Caucasian and were selected for rapid modes of death and short agonal phases, to limit the influence of agonal factors on RNA quality and pH. Toxicological screens on peripheral fluids identified the presence of at least one antidepressant in 5 subjects, including four different tricyclics, one selective serotonin reuptake inhibitor and one weak dopamine reuptake inhibitor.

Dissections

Details of Amygdala and ACC dissections are described in our previous publication[3] and was adapted from Hamidi et al.(324). Samples were hybridized onto Human Genome U133 Plus 2.0 arrays (Affymetrix, Santa Clara, CA). Array parameters described in Sibille et al. 2009 [3].

E. Data Extraction, normalization, and creation of best-fit age-trajectory equations

Log_2-transformed probeset signal intensities were extracted and normalized with the Robust Multi-array Average (GC-RMA) algorithm for each brain area for both datasets. Probesets were considered present if they had expression levels greater than 25 in at least 2 datasets in order to preserve area/cohort specificities if present. Expression values were then converted for comparability by simple division to be a fraction of their mean value of all expression values for their probeset in each brain area separately. Then, for each probeset, a separate equation was generated for linear, log, exponential, and power fits of expression versus subject age and the best-fit line (highest regression coefficient) was chosen for each probeset, creating a unique age-regression equation per probeset. Lastly, expression values were converted a second time by simple division to be a percentage of their expression at age 20 yrs (calculated by solving their equation for this value), which was set to 100% expression. Equations were re-calculated using this value. This created equations and expression values directly comparable across datasets that are a percentage of expression at age 20 yrs, which was set to 100% expression, without transforming or altering original expression. P-values for age-trajectory equations were calculated by converting regression coefficients of equations taking into account the number of

subjects in each brain area. Full datasets of all genes in all brain areas with age-regression equations, pvalues , expression differences, and cellular origins (Supplemental Dataset 1) are available as downloadable files from our website (www.sibille.pitt.edu).

II. Quantitative PCR (QPCR) validation of age-regulated expression changes.

QPCR validation (methods described in previous publications) of a set of 42 age-regulated ($p<0.01$) genes in total was performed and published for in cohorts 1 and 2 for validation of prior studies (60, 289)[,21]. Results were re-analyzed here for age effects (see below) and converted to percent change over 50 years of (Age 70-Age 20) for comparability of results to current array data results.

Figure 31. Figure S2. Correlation of Quantitative PCR and Microarray Quantification of Gene Expression Levels.

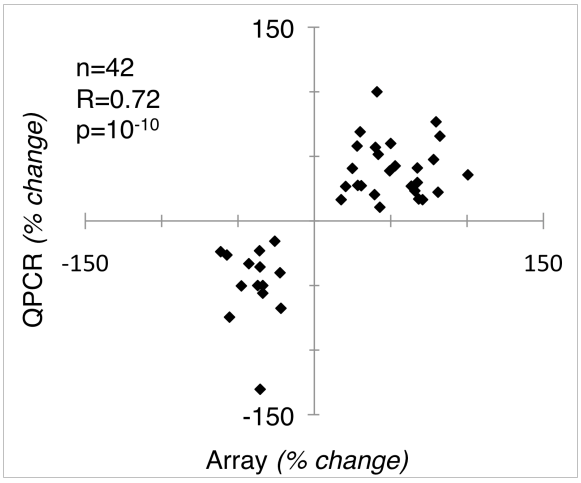

III. Comparing age-related changes across brain areas.

Table 13. A. Table S2. Percentage of each best-fit equation type by brain area.

	Linear (%)	Exponential (%)	Power (%)	Log (%)
ACC	36	21	30	13
AMY	12	23	60	5
BA9	34	27	16	22
BA47	29	22	20	29

Table 14. B. Table S3. Percentage of transcripts age up or down-regulated and cellular origin

	Increased with Age (p<0.001)					Decreased with Age (p<0.001)				
	n (% of total)	m(%)	N(%)	G(%)	B(%)	n(% of total)	m (%)	N(%)	G(%)	B(%)
ACC	582 (44.5)	+95.1	3.0	73.7	23.4	726 (55.5)	-31.8	57.9	3.6	38.7
AMY	726 (88.6)	+74.8	6.1	47.0	47.0	87 (10.7)	-33.1	32.2	5.8	63.2
BA9	838 (42.5)	+47.7	3.4	66.8	17.1	1133 (57.5)	-29.5	59.0	8.5	32.5
BA47	420 (37.9)	+59.7	12.4	49.1	38.8	684 (61.8)	-31.9	69.9	6.6	23.7

Average magnitude (age 70-age 20) and cellular origin of age-regulated expression changes by up and down-regulated (Supporting Figure 1B). (n) number, (m) average magnitude, (N) neuronal, (G) Glial, (B) expressed in both neurons and glia.

Table 15. C. Table S4. Percentage of transcripts changing in the same/opposite direction with age across brain areas

	ACC		AMY		BA9		BA47	
	Same (%)	Opposite(%)	Same(%)	Opposite(%)	Same(%)	Opposite(%)	Same(%)	Opposite(%)
ACC	-	-	89.1	10.9	90	11	88.6	12.4
AMY	89.9	11.1	-	-	90.5	10.5	84.1	15.9
BA9	87.4	14.6	79.4	20.6	-	-	88.3	14.7
BA47	88.0	12.0	84.1	15.9	94.1	5.9	-	-

Age-related expression changes (Supporting Figure 1B) compared across brain areas. “Same”, expression changed in the same direction; “Opposite”, expression changed in the opposite direction.

Table 16. D. Table S5. Percentage of transcripts changing in the same/opposite direction with age across brain areas by significance

	ACC (%)				AMY (%)				BA9 (%)				BA47 (%)			
	S -S	S-NS	O-S	O-NS	S -S	S-NS	O-S	O-NS	S -S	S-NS	O-S	O-NS	S -S	S-NS	O-S	O-NS
ACC	-	-	-	-	43.0	46.1	0.7	8.7	75.1	14.9	1.0	9.0	57.4	31.2	1.0	10.4
AMY	60.2	29.7	0.9	9.8	-	-	-	-	67.3	23.2	3.0	6.5	47.0	37.1	2.7	13.8
BA9	58.0	29.5	2.1	10.4	31.8	47.6	2.6	18.0	-	-	-	-	65.4	22.9	3.0	8.7
BA47	54.1	33.9	1.2	10.8	34.8	50.5	1.4	13.3	77.9	16.2	0.5	5.4	-	-	-	-

Age-related expression changes compared across areas (Supporting Figure1B). Analyzed by percentage of transcripts in same (S) or opposite (O) directions across two brain areas and (-) whether they were significant $p<0.05$ (S) or non-significant (NS).

IV. Cross-area Brain Aging Biosignature.

A. Methods Ingenuity gene network and functional analysis

Analyses were performed using Ingenuity systems version 7.0. (http://www.ingenuity.com/). Methods are briefly described below.

Network Generation

Selected gene identifiers and corresponding expression changes were uploaded and overlaid onto a global molecular network in the Ingenuity knowledge base. Networks of these genes were then algorithmically generated based on their connectivity with scores used to rank networks according to their degree of relevance to the Network Eligible molecules in your dataset. The score takes into account the number of Network Eligible molecules in the network and its size, as well as the total number of Network Eligible molecules analyzed and the total number of molecules in Ingenuity's knowledge base that could potentially be included in networks. The network Score is based on the hypergeometric distribution and is calculated with the right-tailed Fisher's Exact Test. The score is the negative log of this p-value.

Functional Analysis

The Functional Analysis identified the biological functions and/or diseases that were most significant to the data set. Genes from the dataset that were associated with biological functions and/or diseases in the Ingenuity knowledge base were considered for the analysis. Fischer's exact test was used to calculate a p-value determining the probability that each biological function and/or disease assigned to that data set is due to chance alone.

Functional Analysis of a Network

The Functional Analysis of a network identified the biological functions and/or diseases that were most significant to the genes in the network. Fischer's exact test was used to calculate a p-value determining the probability that each biological function and/or disease assigned to that network is due to chance alone.

Canonical Pathways

Canonical Pathways are a type of functional analysis (see above). Canonical Pathways are well-characterized metabolic and cell signaling pathways that have been curated and hand-drawn by Ph.D. level scientists. The information contained in Canonical Pathways comes from specific journal articles, review articles, text books,

and KEGG Ligand. They are distinct from networks because they are generated prior to data input based on the literature and have directionality. P-values are based the overrepresentation of genes in the queried dataset in a particular canonical pathway compared to all genes in that pathway present in the Ingenuity database (ratios).

Ingenuity Analysis of the biosignature

356 age-biomarkers were used for gene network and associated functional analysis. A summary of functional and network analysis is shown below. The top 5 identified gene networks ($p<e^{-35}$) encompassed most known age-related biological functions (Signaling, immune response, vascular function, cell death, DNA repair and protein modification; Networks 1-5) and confirmed the substantial overlap between age and disease-related genes (Genetic, neurological and psychiatric disorders; Networks 3-4; Table S7).

Table 17. B. Table S6 Summary of Ingenuity analysis of the biosignature

Top Networks

ID	Associated Network Functions	Score
1	Cell-To-Cell Signaling and Interaction, Cell-mediated Immune Response, Hematological System Development and Function	39
2	Nervous System Development and Function, Tissue Development, DNA Replication, Recombination, and Repair	37
3	Genetic Disorder, Neurological Disease, Cell Death	35
4	Genetic Disorder, Neurological Disease, Psychological Disorders	35
5	Post-Translational Modification, Protein Folding, Nervous System Development and Function	35

Top Bio Functions

Diseases and Disorders

Name	p-value	# Molecules
Genetic Disorder	1.21E-18 - 2.70E-02	152
Neurological Disease	1.21E-18 - 2.70E-02	115
Psychological Disorders	2.49E-09 - 2.30E-02	34
Cancer	8.36E-07 - 2.70E-02	127
Dermatological Diseases and Conditions	1.40E-05 - 2.70E-02	20

Molecular and Cellular Functions

Name	p-value	# Molecules
Cell Morphology	5.20E-07 - 2.70E-02	57
Cell Death	1.40E-05 - 2.70E-02	84
Cellular Assembly and Organization	5.37E-05 - 2.70E-02	60
Cell Signaling	3.50E-04 - 2.70E-02	40
Cellular Development	3.60E-04 - 2.70E-02	84

Physiological System Development and Function

Name	p-value	# Molecules
Nervous System Development and Function	5.20E-07 - 2.70E-02	70
Behavior	2.75E-05 - 2.70E-02	28
Tissue Development	7.63E-05 - 2.70E-02	36
Embryonic Development	4.24E-04 - 2.70E-02	24
Hepatic System Development and Function	7.25E-04 - 2.70E-02	3

Top Canonical Pathways

Name	p-value	Ratio
14-3-3-mediated Signaling	1.4E-03	9/112 (0.08)
Integrin Signaling	3.38E-03	12/198 (0.061)
CXCR4 Signaling	4.63E-03	10/164 (0.061)
Neuregulin Signaling	6.58E-03	7/98 (0.071)
VEGF Signaling	7.02E-03	7/95 (0.074)

Table 18. C. Table S7. Top age-biomarker gene networks and associated functions

Network	Molecules in Network	Score	Focus Molecule	Top Functions
1	↑**ADAM17**, ADCY, Calcineurin protein(s), ↓**CALM3**, Calmodulin, CaMKII, ↑**CD44**, Ck2, Clathrin protein, ↓**CRYM**, ↓**CX3CL1**, ↑**DLG1**, ↓**DLG3**, ↓**DUSP14**, ↑**GAB2**, ↑**KCNJ2**, ↓**KCNQ3**, ↑**KIF13B**, ↓**MAPK1**, Metalloprotease, ↑**MYO6**, NMDA Receptor, ↓**NRGN**, ↑**PICALM**, ↑**PIP4K2A**, Pp2b, ↓**PPEF1**, ↓**PPP3CB**, Ptk, ↓**RIT2**, ↑**SEMA4C**, ↑**TJAP1**, ↑**VCAN**, ↑**ZHX2**, ↑**ZHX3**	39	25	Cell-To-Cell Signaling and Interaction, Cell-mediated Immune Response, Hematological System Development an Function
2	↑**ADAMTS1**, Ap1, Caspase, ↑**CD59**, ↑**CDKN1C**, ↑**CLDND1**, ↑**CLIC4**, ↑**CLU**, ↓**CRH**, ↓**CRIP2**, Cyclin A, Cyclin E, Cytochrome c, ↓**FAM162A**, ↑**H3F3A (includes EG:3020)**, hCG, Histone h3, Insulin, ↑**LDB3**, ↑**LPIN1**, ↑**MAL**, ↓**MBD1**, ↑**MECP2**, Mek, ↑**MLL**, ↑**MT1G**, ↑**MT2A**, P38 MAPK, ↑**PIGA**, ↓**PRKCB**, ↑**RPS6KA5**, Rsk, ↑**SAFB2**, ↑**UNG**, ↑**VAMP3**	37	24	Nervous System Development and Function, Tissue Development, DNA Replication, Recombination, and Repai
3	↓**ADRA2A**, Alcohol group acceptor phosphotransferase, ↓**CALB1**, CD3, ↑**CFLAR**, ENaC, ↑**HBP1**, HDL, ↑**HIPK2**, IKK, ↑**ITPKB**, ↑**LITAF**, ↓**MAP2K4**, ↑**MAP4K4**, ↓**NEK2**, Nfat, NFkB, ↑**RARRES3**, ↓**RASGRF1**, ↑**RHOG**, ↑**SDC4**, ↑**SEMA3B**, ↑**SEPT4**, ↓**SERPINF1**, ↑**SGK1**, ↑**SLC11A2**, ↑**ST18**, TCR, ↓**TOLLIP**, ↓**UBE2N**, Ubiquitin, VitaminD3-VDR-RXR, ↑**WNK1**, ↑**WSB1**, ↓**WTAP**	35	25	Genetic Disorder, Neurological Disease, Cell Death
4	↓**ACTN2**, ↑**AHCYL1**, ALP, Alpha Actinin, Calpain, ↑**CAPN3**, ↑**CSRP1**, ↑**DDR1**, ↓**DOK5**, ERK, Fgf, ↑**FGF1**, ↓**FGF13**, G alphai, ↓**HOMER1**, ↑**LPAR1**, ↑**LTBP1**, Mmp, ↓**NELL1**, ↓**NPPA**, ↑**PALLD**, ↑**PKD2 (includes EG:5311)**, Pkg, PLC, PLC gamma, ↓**PLCB1**, ↓**PNOC**, ↓**PTPRR**, ↑**RASGRP3**, ↓**RGS4**, Tgf beta, ↑**TGFB3**, ↑**TNS1**, ↑**TOB1**, Tubulin	35	23	Genetic Disorder, Neurological Disease, Psychological Disorders
5	14-3-3, ↑**AKAP1**, ↓**ATXN10**, ↑**BTG1**, ↑**C19ORF2**, ↑**C22ORF9**, ↓**DNAJA1**, ↓**DR1**, Dynamin, ↑**EZH1**, G alpha, G protein beta gamma, ↑**GFAP**, Gpcr, Hsp70, Hsp90, ↓**HSPA8***, IFN BetaΔ, Jnk, ↑**KIF5B**, ↑**NDRG1**, ↓**NRG1**, ↑**NUMA1**, Proteasome, ↓**RAP1GDS1**, RNA polymerase II, ↓**SNCA**, STAT, ↑**TCEB3**, ↑**TNPO1**, ↑**TOB2**, ↑**TSR1**, ↓**VDAC1**, ↓**YWHAZ**, ↑**ZNF451**	35	23	Post-Translational Modification, Protein Folding, Nervous System Development and Function

Genes in bold (Red, increased; Green, decreased) identify age biomarkers included in the networks. Other genes and molecular functions represent added indirect nodes in networks. Scores are negative log (p-value). The top functions indicate the biological functions and/or diseases that were most significant to the genes in the network.

D. Methods CMAP

The connectivity map is a resource freely available from the Broad Institute at MIT (http://www.broadinstitute.org/cmap/) first described by Lamb et al in 2006 (293). C-Map is a large reference database of genome-wide expression profiles from cultured human cell lines treated under standard conditions with FDA approved small molecules, shRNAs, and organic compounds (collectively referred to as perturbagens) and a pattern-matching software to enable data mining. C-MAP (Build 02) contains data from 1309 perturbagens in a total of 7056 gene expression profiles (6100 individual instances defined as one treatment and vehicle pair), across four human cell lines (breast cancer MCF7, acute myeloid leukemia HL-60, prostate cancer PC3 and melanoma SKMEL5) on the Affymetrix HGU133A arrays. The C-Map pattern-matching algorithm is based on the non-parametric rank statistic, the Kolmogorov-Smirnov statistic. Permuted p-values are an estimate of the likelihood that the enrichment of a set of instances in the list of all instances in a given result would be observed by chance. This value is determined empirically by computing the enrichment of one hundred thousand sets of instances selected at random from the set of all instances in the result. The C-MAP website also provides links for each compound to ChemBank (a database for structures and synonyms, http://chembank.broad.mit.edu), and displays the Anatomical Therapeutic Chemical classification assigned by the World Health Organization to drug substances. A full listing of C-MAP-biosignature results and associated statistics is available for download upon publication (supplementary dataset 3).

Descriptions of drug mechanisms for Figure 2C were obtained from ChemBank (http://chembank.broad.mit.edu) in addition to the references below.

C-MAP Candidate Brain Aging Drugs

Drug	Mechanism	P-val
Anti-aging		
GW-8510	CDK2/CDK5 inhibitor; neuroprotective(325)	1E-4
α-estradiol	Estrogen enantiomer; neuroprotective(326)	1E-4
Urapidil	Antihypertensive, α1 adrenergic antagonist, α2 adrenergic agonist, 5HT1A agonist, neroprotective(327)	2E-4
Alsterpaullone	Inhibitor of CDK2, CDK1/Cyclin B, CDK5/p25, GSK-3β, Tau phosphorylation; neuroprotective (328)	5E-4
Skimmianine	Furoquinoline alkaloid (plant extract) used in folk medicine; potentially anti-inflammatory, antitumorigenic, and an MAO inhibitor (329, 330)	6E-4
H-7	PKC inhibitor, decreases calcium current, alters astrocyte morphology(331)	7E-4
Niacin (Vitamin B3)	Anti-inflammatory properties; used to treat hypercholesterolemia, arteriosclerosis, and cardiovascular disease (332)	0.005
Biotin (Vitamin B7)	Regulates insulin secretion; therapeutic efficacy in diabetes (333, 334)	0.009
Pro-Aging		
Wortmannin	inhibitor of PI3-K cell survival pathway, mTOR, DNA-PK, MAPK, and PI4-K(335)	1E-6
Benzamil	Na/Ca exchange blocker, inhibitor of NGF mediated neurite outgrowth(336)	5E-4

V. Neurological disease-associated gene analysis.

Figure 32. A. Figure S3. Top 20 Ingenuity® Functional Categories associated with age-regulated genes (Figure adapted from Ingenuity®).

Criteria for selection for age regulated genes were age-regression p<0.001 in at least one area or p<0.01 in two brain areas (n=3,935). The top four functions were largely driven by the six neurologic diseases focused on in the paper (AD, PD, ALS, HD, SCHZ and BPD). The top diseases in the top "genetic disease" category were all age-related and included autoimmune disease (529 genes), coronary artery disease (291 genes), bipolar disorder (285 genes), insulin-dependent diabetes mellitus (270 genes), Huntington's disease (267 genes), Alzheimer's disease (187 genes), Parkinson's disease (170 genes), amyotrophic lateral sclerosis (170 genes), schizophrenia (161 genes), prostate cancer (113 genes), colon cancer (103 genes), and autism (27 genes). Top Neurologic diseases were the six aforementioned and also included several types of brain cancer, autism, and epilepsy. The third ranked category, Skeletal and muscular disorders, were largely driven by PD and HD, which ingenuity considers to be in this category. The 421 genes associated with psychological disorders were almost entirely driven by Schizophrenia and Bipolar disorder.

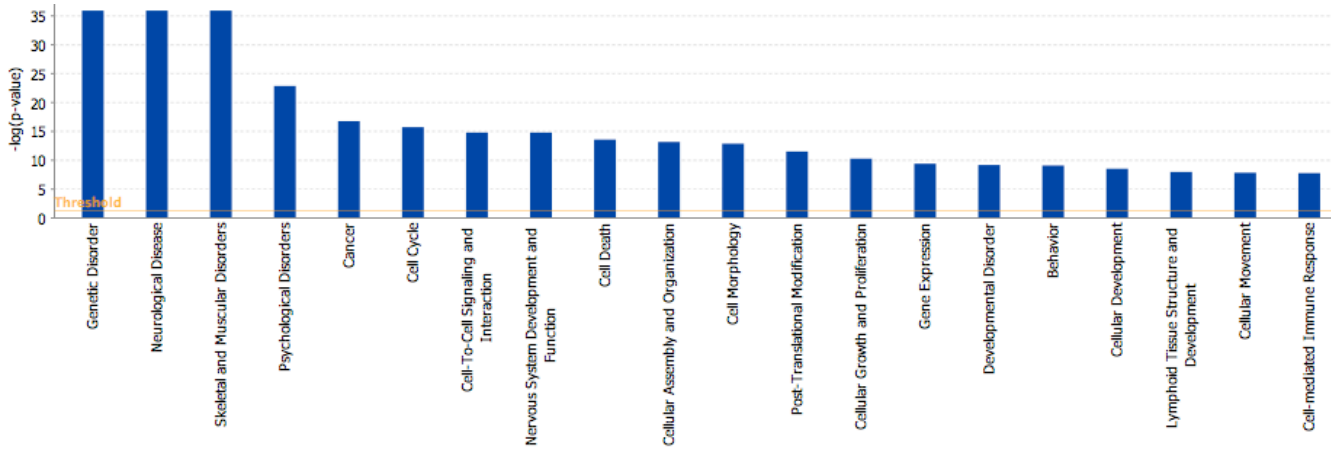

Figure 33. B. Figure S4. Age-regulated genes associated with the top six neurological diseases.

Top (most associated genes) neurologic diseases represented (Figure adapted from Ingenuity®). Disease associations are based on Ingenuity's database of hand-curated literature searches performed by PhD level scientists. Depicted direction of age-regulated changes are from the ACC dataset and are not necessarily congruent with the direction of change in the other three brain areas. A complete listing of age-regulated directions for all genes in all brain areas will be available for download upon publication (Supplementary dataset 1). Genes with asterisks have more than one probeset per gene represented in the selection. Directions of change for these genes are that of the probeset with the most significant p-value.

Bipolar Disorder (285 Genes)

↓A2BP1, ↑ABAT*, ↑ABCA1*, ↓ADORA1, ↓ADRA1D, ↓ADRA2A, ↑ALDH5A1, ↓ANK2, ↓ANK3, ↑ANXA3, ↓ARNT2, ↓ARNTL*, ↑ATP10D, ↓ATP2B2*, ↓ATP2C1, ↓ATP5C1, ↓ATP6V0D1, ↓ATP6V1D, ↓BAI3, ↑BAZ1A*, ↓BDNF, ↓BNC2, ↑BRD1*, ↓BRE*, ↑BTN3A1, ↓BTRC*, ↓C11ORF41, ↑C14ORF159, ↑C18ORF1, ↓CA4*, ↓CA10, ↓CACNB2*, ↑CAPN3*, ↓CARKD, CD36, ↑CDC42BPA, ↓CDH12, ↓CDH13, ↓CDH18, ↓CEPT1, ↓CERK, ↓CHN2, ↑CLMN, ↓CNTNAP2*, ↓COL5A2*, ↓COX5A, ↓COX6C, ↓COX7A2, ↓COX7B, ↑CREB5, ↑CRIM1, ↓CRMP1, ↓CTNNA2, ↓CUX2, ↓DCTN5*, ↑DIP2C, ↓DLG3*, ↓DLG4, ↓DOCK3, ↑DOCK10, ↓DRD1, ↓DRD5, ↑DTNA*, ↓DUSP6*, ↓ECOP, ↓ERG, ↑FAM114A1, ↓FAM115A*, ↑FAM13A, ↑FAM171A1, ↓FARP1, ↓FARS2, ↓FBXO9*, ↓FGF12, ↓FHL2, ↓FHOD3 (includes EG:80206), ↑FLJ11151, ↑FOXO1*, ↑FRY*, ↑G3BP2, ↓G6PD, ↑GAB2, ↓GABBR2*, ↓GABRA4, ↓GABRA5*, ↑GABRB1, ↑GABRB2, ↓GABRB3, ↓GABRD, ↓GABRG2, ↓GABRG3, ↓GAD1, ↓GALNT1*, ↓GLRX3*, ↑GNA14, ↓GNAS*, ↓GNAZ, ↓GRIK1, ↓GRIN2A, ↑GRIN2C, ↑GRM3, ↓GRM7*, ↑HIP1R*, ↓HS6ST1, ↑HSD17B4, ↓HTR2A*, ↓HTR5A, ↓HTRA2, ↓INPP4A*, ↓ITPR1, ↑JAM3, ↓KALRN*, ↑KANK1, ↑KCND2, KCNH1, ↓KCNJ6, ↑KCNMA1, ↑KCNN3, ↓KCNQ2, ↑KCNS1, ↑KIF16B, ↓KIFAP3, ↓KITLG*, KPNA6, ↓LDB2, ↓LGI2, ↓LOC26010, ↑LRRC2, ↑LTBP1, ↓MAN1A1*, ↑MAP4K4*, ↑MARCKS (includes EG:4082)*, ↑MBNL2, ↑MED13L*, ↑METAP2 (includes EG:10988), ↑MLC1, ↑MOBP*, ↑MPST, ↓MRLC2, ↓MRPL3, ↓MRPS12, ↑MSRB2*, ↑MTMR3, ↑MTR, ↓MYO16, ↓MYT1L, ↓NAPG, ↑NAV2 (includes EG:89797), ↑NCAM1*, ↓NDUFAB1, ↑NEK4, ↑NIPBL*, ↓NMT1*, ↑NR3C1*, ↑NR3C2, ↑NRF1, ↓NRG1, ↓NRXN1*, ↓NRXN3*, ↓OBFC1, ↓ODZ3, ↓OLFML2B, ↓OPTN, ↓OXCT1, ↓PALB2, ↑PALLD*, ↑PARD3, ↓PARK2, ↑PARVB, ↓PBRM1, ↓PCMT1*, ↓PDHX, ↓PDYN, ↑PER3, ↑PFTK1, ↑PGCP, ↑PHF17, ↑PHLDB1, ↓PI4KA*, ↑PIP4K2A*, ↓PIP5K1B, ↑PLSCR4, ↓PLXND1, ↓PPP2R5C*, ↓PPP3CA*, ↓PRDM2*, ↓PRKACB, ↓PRKAR1A, ↑PRKCA, ↓PRKCB*, ↑PRKDC, ↓PROM1, ↑PRPF40A, ↓PSMA5, ↓PSMB2, ↓PSMC6, ↑PTCH1, ↑PTK2, ↓PTPRF, ↑PTPRG, ↓PTPRN2*, ↓PTPRR*, ↑QKI*, ↑RABGAP1L*, ↓RALB, ↓RAP1GAP (includes EG:5909), ↓RARB, ↑RBM16, ↑RBM26, ↓RELN, ↓RERE, ↓RFC3*, ↓RGS4*, ↓RGS6*, ↓RGS17, ↑RHOC, ↓RIT2, ↑RNF144A, ↓RPA3, ↑RPRD2, ↑RPS6KC1, ↑SCN1A, ↓SCN2A, ↓SCN2B, ↓SCN3B*, ↓SCN8A, ↓SERINC2, ↓SETBP1, ↓SEZ6L*, ↑SFI1, ↑SFPQ*, ↑SGMS1, ↓SH3BP5, ↓SLC1A1*, ↑SLC1A4, ↓SLC1A7, ↓SLC25A4, ↑SLC25A16, ↑SLCO3A1, ↓SLIT3*, ↓SNCA*, ↓SNX16, ↑SNX27, ↓SORBS2, ↓SPOCK1, ↓SPRED2, ↑SQRDL (includes EG:58472), ↑SQSTM1, ↓SRGAP3, ↓SST, ↑ST18, ↓STAB1, ↓SUCLG1, ↑SUCLG2*, ↓SULF1, ↓SYN2, ↓SYNGR1, ↓SYNJ1, ↓TACC2*, ↑TCF4, ↓TGOLN2 (includes EG:10618)*, ↓THRB (includes EG:7068), ↓TIAM1, ↑TJP2, ↓TLE4, ↑TLL2, ↑TOX (includes EG:9760)*, ↓TRPM2, ↑TTBK2, ↓TTLL7, ↓UQCC, ↓UQCRC2, ↓VAMP7, ↓VAPB*, ↓VDAC1, ↓VDAC2, ↑VPS54, ↑WFS1, ↑WWOX, ↓XPO7, ↓YWHAH, ↑ZCCHC24*, ↑ZEB2, ↓ZNF3, ↓ZNF410

Huntington's Disease (267 Genes)

↓A2BP1, ↑ACADM, ↓ACP1*, ↓ACTB*, ↓ACTN2*, ↓ADCY2*, ↓ADCY7, ↑AEBP1, ↑AHCYL1*, ↓AK1, ↑ALDH6A1*, ↓AP1S1*, ↑APLNR, ↑AQP1*, ↓ARMCX2, ↓ARPP-19*, ↓ARPP-21, ↑ASCL1*, ↓ATP2A2*, ↓ATP2B2*, ↓ATP5C1, ↓ATP6AP2, ↓B3GNT2, ↓B4GALT5, ↓BASP1, ↑BBOX1, ↑BCL2, ↑BCL6, ↑BCL2L1, ↓BDNF, ↑BTN3A1, ↓C3, ↑C4A*, ↓C5ORF13*, ↓CA11, ↓CAB39, ↓CACNB3*, ↓CALB1*, ↑CAMK4, ↓CAMK2A, CAMK2B, ↓CAMKK2*, ↑CASP7, ↓CCKBR, ↑CD44*, ↓CDK5, ↓CDK5R1, ↑CDKN1C*, ↑CFLAR*, ↓CHAF1B, ↓CHGB, ↑CHI3L1*, ↓CHN1 (includes EG:1123), ↑CLU*, ↓CNR1*, COL4A3, ↓COX7A2, ↓COX7B, CRB1, ↑CREB1, ↑CRIM1, ↑CRYAB, ↓CRYM, ↑CSRP2*, ↓CX3CL1*, ↓CYC1, ↓CYCS (includes EG:54205), ↓CYP26B1, ↑CYTH1, ↑DAAM2, ↓DDX1, ↓DGKB, ↓DIO2, ↓DIRAS2, ↑DKK3, ↓DNAJA1*, ↓DNAJB12, ↓DRD1, ↓DRD5, ↑DTNA*, ↓DYNC1I1, ↓EGR2, ↓EGR4*, ↓EIF3E, ↓ELMO1, ↓EML1 (includes EG:2009), ↑EMX2, ↓EPHA4, ↓ETV5, ↑FAM107A*, ↓FAM173A, ↑FGF2, ↓FGF12, ↓FGF13, ↓FOXG1, ↓GABRA4, ↓GABRA5*, ↑GABRB2, ↓GABRD, ↓GABRG2, ↓GAPDH (includes EG:2597)*, ↑GFAP, ↓GHITM, ↓GLRB*, ↓GNAL*, ↓GNB1*, ↓GNB5*, ↓GNG3, ↑GNG7, ↓GTF3A, ↓GUCY1B3, ↑HBP1, ↓HINT1*, ↑HMGB2, ↓HMGCR, ↓HNRNPU, ↓HOMER1, ↓HPCA, ↓HSBP1*, ↓HSPA8*, ↓HTT, ↑ID4, ↓IGF1*, ↑IMPA1, ↑INPP1, ↓ITFG1, ↑ITGB4*, ↑ITPKB, ↓ITPR1, ↓IVNS1ABP, ↓KCNAB1*, ↓KCNAB2, ↓KCNIP1, KCNK2, ↑KCNN3, ↓KCNQ2, ↑KCTD13, ↓LAMB1, ↑LAPTM4B, ↓LDHA, ↑LPL*, ↑MAFF, ↓MAN1A1*, ↑MAOB, ↓MAP2, ↓MAP2K4*, ↓MAST3, ↑MBNL2, ↓METTL9, ↓MFN2, ↓MLF1, ↑MPDZ, ↑MT1E, ↑MT1G, ↑MT1H, ↑MT1M*, ↑MT1X*, ↑MT2A, ↓MYEF2, ↓MYO1B*, ↓MYO5A, ↓MYT1L, ↓NBEA (includes EG:26960), ↑NDRG1, ↓NDRG3*, ↓NDUFB5, ↓NDUFS2, ↓NDUFS3, ↓NDUFS5, ↓NME1, ↑NPM1 (includes EG:4869), ↓NPY, ↓NR4A1, ↓NRGN, ↑NTRK2, ↓OPTN, ↓PCDH7, ↓PCMT1*, ↑PDCL, ↑PDE4DIP*, ↓PENK, ↑PGAM2, ↓PGK1*, ↓PGRMC1, ↓PKIA, ↓PLCB1*, ↑PLK2, ↑PLOD2, ↑PLSCR4, ↑PMP22, ↓PPARGC1A, ↓PPM1B, ↑PPM2C, ↓PPP1R1A, ↓PPP3CA*, ↑PRDX2, ↓PREPL, ↓PRKCB*, ↓PRKCG, ↑PSMB9, ↑PTK2B, ↓PTPN3, ↓RAB11A, ↓RAB6A*, ↓RAP1GAP (includes EG:5909), ↓RARB, ↑RARRES3, ↑RASL12, ↓RBP4, ↓RERE, ↓RGS4*, ↓RGS14*, ↑RHOBTB3*, ↑RHOG, ↓ROCK2, ↑ROM1, ↓RPH3A, ↓RTN2*, ↑RYR3, ↑RYR1 (includes EG:6261), ↑SAP18, ↑SCD, ↓SCG2, ↑SCN1A, ↓SCN2A, ↓SCN2B, ↓SCN3B*, ↓SCN8A, ↑SDC4, ↑SEC24A, ↑SEPHS1, ↓SEPT5, ↑SERPINA3, ↓SERPINI1, ↑SETDB1, ↑SGK1, ↑SH3BP4, ↑SLC14A1, ↓SLC17A7*, ↓SLC1A1*, ↑SLC1A4, ↓SLC1A7, ↓SNAP25, ↑SOX9, ↓SRD5A1*, ↑SRPX, ↓SST, ↓SSX2IP*, ↑STOM, ↑STRN4, ↓SUB1*, ↓SYNJ1, ↓TAC1, ↑TGM2, ↓TMEFF1, ↓TPI1*, ↓TPM3, ↓TSN, ↓UCHL1, ↓UCRC, ↑VAMP1, ↑VCAN*, ↑WNK1*, ↑WWTR1, ↓YWHAZ*, ↑ZBTB16, ↑ZMYND8*

Alzheimer's Disease (185 Genes)

↓A2BP1, ↑ABAT*, ↓ACLY, ↑ACSL4, ↓ADCY2*, ↓ADRA1D, ↓ADRA2A, ↑AFF1, ↓AJAP1 (includes EG:55966), ↑ALDH5A1, ↓ANK3, ↓ANO3 (includes EG:63982), ↑ARAP2*, ↓ATP5A1, ↓ATP6V1C1*, ↓ATP8A2, ↓ATRNL1*, ↑BAT2, ↓BCHE, ↓BDNF, ↑BIN1*, ↓BLMH, ↓BNC2, ↓BRE*, ↓C14ORF132, ↓CA10, ↓CACNA2D1, ↓CANX, ↓CAPRIN1, ↑CBS (includes EG:875), ↓CDC42EP3, ↓CDH8, ↓CDH13, ↓CDK5, ↓CDK5R1, ↑CHL1, ↑CLU*, ↓CNKSR2, ↓CNR1*, ↓CNTNAP2*, ↓COL5A2*, ↓CRYM, ↑CSRP2*, ↓CTBP2, ↓CTSB*, ↑DARS, ↑DBT, ↓DIAPH2, ↑DICER1*, ↑DLC1, ↓DOK5, ↓DRD1, ↓DRD5, ↑ELF1, ↓EML1 (includes EG:2009), ↑EPB41L2, ↑FAM53B, ↓FAM5C, ↓FGF12, ↓FHOD3 (includes EG:80206), ↑FOLH1*, ↓FOXO3, ↑GAB2, ↓GARNL4, ↑GFAP, ↓GFOD1, ↓GLT8D2, ↓GNB1*, ↑GNG4, ↓GOLM1, ↑GREB1, ↓GRIA1, ↓GRIA4, ↓GRIN2A, ↑GRIN2C, ↓GRM2, ↑GRM3, ↓GRM5*, ↓GRM7*, ↓HAPLN1*, ↑HIPK2*, ↓HIVEP2*, ↓HMGCR, ↓HNRNPU, ↓HSPA6, ↓HSPD1, ↓HTR2A*, ↓HTT, ↓IGF1*, ↓IGFBP2, ↑IL1RAPL1, ↑INPP1, ↑INSR, ↓KCNC4, ↑KCNMA1, ↑KIAA0427, ↑KIF16B, ↓LARGE, ↑LARP4, ↓LONP2, ↑MAOB, ↓MAPK9*, ↓MAPT*, ↑ME1, ↑MECP2*, ↑MED13L*, ↓MICAL2, ↑MOBP*, ↑MYLK, ↑MYST4, ↓MYT1L, ↓NBL1*, ↓NDUFAB1, ↓NELL1, ↓NPDC1, ↑NR3C1*, ↓NRXN3*, ↑NTRK2, ↓NTRK3*, ↓OPCML*, ↓PARK2, ↑PAXIP1, ↑PCDH9, ↓PDHX, ↑PDK3*, ↓PKIA, ↑PLA2G4A, ↓PLCB1*, ↑POU2F1, ↓PPM1B, ↓PREP, ↑PRKCA, ↓PRKCB*, ↑PRKDC, ↓PRNP, ↓PSAP, ↓PSMD1, ↓PTGS2, ↑PTPRD, ↓RAB3B, ↓RAB6A*, ↓RABL5, ↑RELA (includes EG:5970), ↓RELN, ↓RICH2, ↓RIMS1, ↓RTN1, ↑RYR3, ↓SCG5, ↑SERPINA3, ↓SIGLEC7, ↑SLC22A5, ↓SLC3A1, ↓SLIT3*, ↓SNCA*, ↓SOD2, ↓SORBS2, ↓SPOCK1, ↑SPON1*, ↑STARD13, ↓STK24*, ↓STX2, ↓STYK1*, ↓SV2B, ↓SYNGR1, ↓TACC2*, ↑TCF12, ↑TF*, ↑TGFBR3, ↑TGM2, ↑TIMP1, ↑TLL2, TNPO3, ↓TPST2, ↓TRIO*, ↓TTC3*, ↓TUBA1C*, ↓TUBB3*, ↓TUBB2C, ↓TUBG1, ↓TUBG2, ↑UBE4A, ↓UCHL1, ↑WWOX, ↑YES1*, ↓YWHAZ*, ↓ZFP64*

Parkinson's Disease (170 Genes)

↑ACTR3, ↓ADRA1D, ↓ADRA2A, ↑AKAP13*, ↑ANXA2*, ↑ARL6IP5, ↓ATRNL1*, ↑BBOX1, ↑BCAS1, ↓BCHE, ↑BCL2, ↓BCR, ↓BDNF, ↓BTRC*, ↓C14ORF132, ↑C18ORF1, ↓CA4*, ↑CAPN3*, ↑CAST*, ↑CD9, ↑CDC42BPA, ↓CDH12, ↓CDH13, ↓CHN1 (includes EG:1123), ↓CNR1*, ↓CPEB1, ↓CSE1L, CTNS, ↓CXORF40A, ↑DDX18*, ↓DIAPH2, ↑DMD, ↓DRD1, ↓DRD5, ↓ECOP, ↑ENAH, ↓EPHA4, ↓ERG, ↓FAM5C, ↑FAM70A, ↓FARP1, ↓FGF12, ↓FHOD3 (includes EG:80206), ↑FTH1, ↑FTL, ↑GAB2, ↓GABBR2*, ↓GABRA4, ↓GABRA5*, ↑GABRB1, ↑GABRB2, ↓GABRB3, ↓GABRD, ↓GABRG2, ↓GABRG3, ↓GARNL4, ↑GFAP, ↑GLT25D2, ↓GNAS*, ↑GNG7, ↑GPC4, ↑GRB10*, ↓GRIA1, ↓GRIA4, ↓GRIN2A, ↑GRIN2C, ↓GRM7*, ↑HIGD1A, ↓HMOX2, ↓HMP19, ↓HOMER1, ↓HTR2A*, ↓HTRA2, ↓IGF1*, ↑IL1RAPL1, ↑ITSN2*, ↑JMJD2C, ↑KAT2B, ↓KCNAB1*, ↓KCNC4, ↓KCNJ6, ↓KCNQ3, ↑KIAA0427, ↓LDHA, ↓LONP2, ↑LPP (includes EG:4026), ↑MACF1*, ↑MAOB, ↑MAP4*, ↓MAPRE2*, ↓MAPT*, ↑MBP*, ↓MDH1, ↑MOG*, ↑NARG1L, ↓NAV3, ↑NDRG2, ↓NELL1, ↓NR4A2, ↓NRXN1*, ↓NTRK3*, ↓OGT (includes EG:8473)*, ↓ORC4L*, ↑PADI2, ↓PAK1, ↑PAQR6, ↓PARK2, ↓PARK7, ↓PBX1, ↓PCGF3, ↓PDXK, ↓PGK1*, ↑PIGG, ↓PINK1*, ↓PLCB4*, ↓PLXDC1, ↑POLA1, ↓PRDM2*, ↑PRDX2, ↑PRKCA, ↓PSMC1, ↑PTCD3, ↓PTGS2, ↓PTPRR*, ↑RBMS1, ↑RELA (includes EG:5970), ↓RMND5B, ↑RNF114*, ↓RNF5 (includes EG:6048), ↓RPL15, ↑RPS4X*, ↑SERPINA3, ↑SERPINB1, ↑SGMS1, ↑SLC14A1, ↓SLC25A6, ↑SLC9A8, ↑SLC9A3R1, ↓SNCA*, ↓SNCAIP, ↑SNX10, ↑SPP1, ↑STARD13, ↓SUMO3*, ↓SYT17, ↓TAC1, ↓TACC2*, ↑TGM2, ↓THRB (includes EG:7068), ↓THY1*, ↑TLE2, TNPO3, ↓TOR1A, ↑TOX (includes EG:9760)*, ↓TRHDE, ↑TRPS1, ↓TUBA1B, ↓TUBA1C*, ↓TUBB2B, ↑TULP3, ↑TYMS, ↓UCHL1, ↓UCHL5, ↓ULK2*, ↓USP10, ↓UST, ↑VIM, ↑VWA5A, ↑WWOX, ↑ZHX2

Amyotrophic Lateral Sclerosis (164 Genes)

↓A2BP1, ↑ABAT*, ↓ACTB*, ↓ADCY2*, ↓ADORA1, ↓AKAP7, ↓AKAP12, ↓AKR1C2, ↑ALDH5A1, ↑ANXA5, ↓APOO, ↓ARNT2, ↓ATP2B2*, ↓BAD*, ↑BCL2, ↑BCL2L1, ↓BNC2, ↓BRE*, ↑C18ORF1, ↑C2CD2 (includes EG:25966), ↑CAPZA1, ↑CAST*, CD36, ↑CDC2L5, ↓CDH12, ↓CDH13, ↓CHP*, ↑CLU*, ↑COLEC12, ↑CREB5, ↑CREB3L2, ↑CSRP1, ↓CTNND2, ↓DCLK1*, ↑DDX3X, ↓DGKB, ↓DHRS3, ↓DIAPH2, ↑DMD, ↑DTNA*, ↑ENDOD1, ↑ENOSF1*, ↓ERG, ↓FAM149A, ↓FAM49A*, ↓FARS2, ↑FGF1*, ↓FGF12, ↓FHOD3 (includes EG:80206), ↑FNBP1*, ↑FNDC3A, ↓GABBR2*, ↓GARNL4, ↓GLT8D2, ↑GNA14, ↑GNG7, ↑GPC4, ↓GRIN2A, ↑GRIN2C, ↑GRM3, ↓GRM7*, ↓HMGCR, ↓HTR2A*, ↓IGF1*, ↑IL1RAPL1, ↓INA, ↑INSR, ↓IQCE, ↑IQGAP1, ↑JARID2, ↑JARID1A (includes EG:5927)*, ↑JMJD2B, ↑KCNMA1, ↑KCNN3, ↑KIAA0427, ↑KIF13B, ↑LAMP2*, ↓LARGE, ↓LASP1, ↑LPL*, ↑MAOB, ↓MAPK1*, ↓MGLL, ↑MPZL1, ↑MYO10, ↑NAMPT, ↓NAV3, ↑NAV2 (includes EG:89797), ↓NELL1, ↓NKRF, ↓NLGN4X, ↓NPTXR, ↓NRXN1*, ↓NRXN3*, ↑NSMAF, ↓NTRK3*, ↓OGT (includes EG:8473)*, ↓OPCML*, ↓PARK2, ↑PARVB, ↓PBX1, ↑PCSK6, ↓PFN2, ↓PLCB1*, ↓PPP1R12B, ↓PPP1R16B, ↑PRKCA, ↓PTGS2, ↑PTPRD, ↓PTPRN2*, ↑RBKS*, ↓RGS6*, ↓RIMBP2, ↓RNF14, ↓RXRA, ↑SCN1A, ↓SCN2A, ↓SCN2B, ↓SCN3B*, ↓SCN8A, ↑SEPT9*, ↓SEZ6L*, ↑SGMS1, ↓SHROOM2, ↓SLC1A1*, ↑SLC1A4, ↓SLC1A7, ↓SLC35C1, ↑SLC9A8, ↓SLIT3*, ↓SOD2, ↓SORBS2, ↑SPAG16, ↑SREBF1, ↓SRGAP3, ↑STAG2*, ↑SYNJ2*, ↑T, ↓TACC2*, ↑TBL1X*, ↑TGIF1, ↓TGOLN2 (includes EG:10618)*, ↑TLE2, ↑TMCC2, ↑TNIK, TNPO3, ↓TRIM27*, ↓TTC3*, ↓TULP4, ↑UNC13A, ↑VAMP1, ↓VAPB*, ↑VCAN*, ↓VLDLR, ↓WDFY3, ↑WWOX, ↑ZBTB20, ↓ZFP64*, ↑ZFP36L1*, ↓ZFPM2, ↑ZHX2, ↑ZNF189, ↑ZNF423, ↑ZNF652

Schizophrenia (161 Genes)

↑ABCB1, ↓ACOT7*, ↓ADRA1D, ↓ADRA2A, ↓APC*, ↑APOL2, ↓ATP1A1, ↓ATP2B2*, ↓ATP8A2, ↓BAALC, ↓BDNF, ↑BRD1*, ↓C5ORF13*, ↑CALR, ↓CALY, ↓CAP2*, ↑CCND2*, ↑CDKN1B, ↓CHGB, ↑CHI3L1*, ↑CHL1, ↓CHN2, ↓CLINT1, ↑CNP, ↓CNR1*, ↓CNTNAP2*, ↓CRYM, ↑CSRP1, ↑DDR1*, ↓DLG3*, ↓DLG4, ↓DRD1, ↓DRD5, ↓EGR3, ↑ERBB3, ↑FGF1 ↑FGFR1, ↑FOLH1*, ↓FXYD6, ↓FZD3, ↓GABRA4, ↓GABRA5*, ↑GABRB1, ↑GABRB2, ↓GABRB3, ↓GABRD, ↓GABRG2, ↓GABRG3, ↓GAD1, ↑GALNT7, ↓GLRB*, ↓GNAS*, ↓GOT1, ↑GPR37*, ↓GRIA1, ↓GRIA4, ↓GRIK1, ↓GRIN2A, ↑GRIN2C, ↑GRM3, ↓GRM5*, ↓GRM7*, ↑GSN, ↓HOMER1, ↓HPCAL1*, ↑HSPA2, ↓HSPH1, ↓HTR2A*, ↓HTR5A, ↓IPO5, ↑JARID2, ↓KCNK1, ↑KCNMA1, ↑KCNN3, ↓KIF2A*, ↑KLC1*, ↓LRRC8B, ↑MAG, ↑MAL, ↑MARCKS (includes EG:4082)*, ↓MDH1, ↑MED12*, ↑MLC1, ↓MMD, ↑MOG*, ↑MPZL1, ↑MTR, ↑MYO9B, ↑NCAM1*, ↑NDE1, ↓NDN, ↓NELL1, ↓NELL2, ↓NPY, ↑NR3C1*, ↓NRG1, ↓NRXN1*, ↓NSF, ↑NTRK2, ↓OLFM1*, ↓OXCT1, ↑PAX6, ↑PER3, ↓PFN2, ↓PI4KA*, ↑PIP4K2A*, ↑PLA2G4A, ↑PLP1, ↓PNOC, ↓PPP1R16B, ↑PPP3CB*, ↓PRKCB*, ↑PRODH, ↓PSAP, ↓PTGS2, ↑QKI*, ↑RCBTB1, ↓RELN, ↓RGS4*, ↓RGS7, ↓RIMS3, ↓RIT2, ↓RTF1, ↓RTN1, ↓RXRA, ↓RXRB, ↑S100B, ↓SCG2, ↓SCG5, ↑SCN1A, ↑SEPP1, ↑SEPT11, ↓SERPINI1, ↑SLC14A1, ↓SLC17A7*, ↓SLC1A1*, ↑SLC31A2, ↓SLIT3*, ↓SMARCA2*, ↓SNAP25, ↓SNAP29, ↓SNTG ↓SOD2, ↑SOX10, ↓SST, ↓STMN2*, ↓STX1A, ↓SYN2, ↓SYNGR1, ↓TAC1, ↑TAX1BP3*, ↑TF*, ↑TNXB, ↓TUBA1C*, ↓TUBB3*, ↓TUBB2C, ↓TUBG1, ↓TUBG2, ↑TXNIP*, ↓VDAC1, ↓YWHAH

Figure 34. C. Figure S5. Top 20 Ingenuity® functional categories analysis of genes that were not age-regulated.

Criteria for non-age-regulated genes were p>0.05 in all four brain areas (n=7790). The top category of non- age regulated genes was cellular growth and proliferation, which is logical for the non-dividing tissue of the brain. Notably, neurologic disease was not in the top 20 categories, ranking 44th.

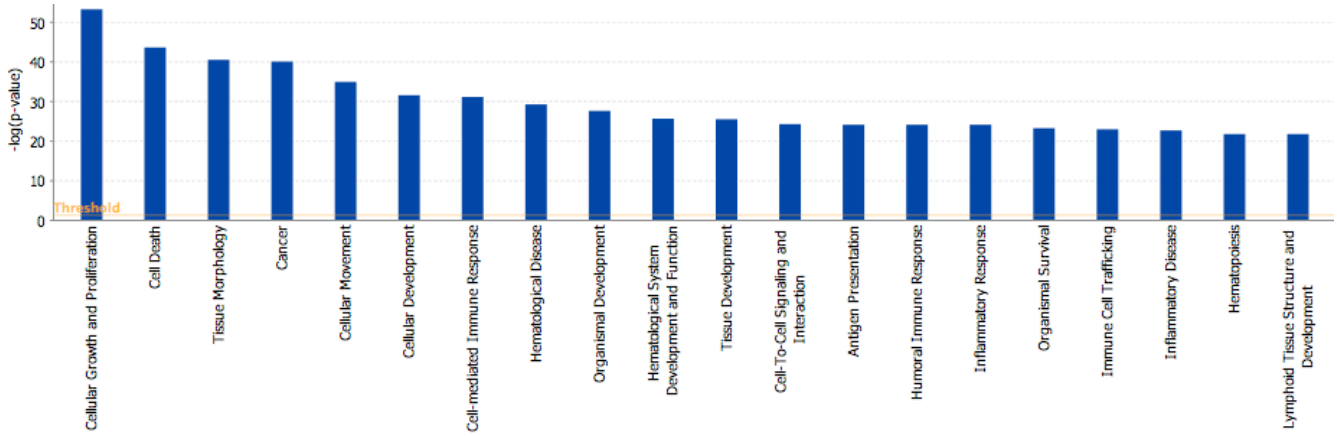

Table 19. Table S8. References for Direction of Neurologic Disease Expression Changes in Disease (Supporting Table 1).

Disease-associated gene_symbol	Direction of Change in Disease AD	PD	HD	ALS	SCZ	BPD	References for Pro-disease Directions
Amyloid beta precursor protein binding-1_Fe65	u						FE65 mRNA levels in AD human brain are decreased in cortex, however this appears to be cell type and brain region dependent; additionally it is unclear whether loss of FE65 would be pro or anti-disease (337-340)
Amyloid beta precursor protein binding- 2_APPB2/PAT1	↑						Involved in APP transport/processing; overexpression results in Aβ accumulation (341, 342)
Amyloid precursor-like protein 2_APLP2	↓						Decreased mRNA levels in AD brain (343, 344)
Clusterin/Apolipoprotein-J_CLU	↑		↑	↑			Increased mRNA levels in AD brains, HD striatum, and ALS spinal cord (345-348)
Monoamine Oxidase B_MAOB	↑	↑	↑	↑			Increased mRNA levels in AD Cortex, HD Caudate and ALS spinal cord, also increased activity in PD brain. MAO-B inhibitors are a common treatment for PD (349-352)
Microtubule-associated protein tau_MAPT	↑	↑					AD and PD associated with higher mRNA levels, polymorphic haplotypes and toxic gain of function mutations (353, 354)
α-synuclein_α-syn	↓	u					Decreased mRNA levels in AD PFC; increased/decreased in PD brain (355, 356)
Parkinson Disease-2_Parkin	↓	↓					Associated with low expressing promoter polymorphisms in PD, and decreased mRNA levels in AD brain; also Parkin levels prevents Aβ accumulation in primary cortical neurons (305, 357-359)
Parkinson Disease-5_UCHL1	↓	↓					Decreased mRNA levels in PD and AD brains (357)
Parkinson Disease-6_Pink1		↓					Loss of function mutations cause familial PD; knock-down of Pink-1 in cell lines causes PD-like mitochondrial dysfunction (360)
Parkinson Disease-7_DJ-1		↓					Loss of function mutations in familial PD, decreased mRNA levels in PD Substantia Nigra(361)
Parkinson Disease-13_HTRA2		↓					Loss of function mutations in PD, loss of function mutations cause mitochondrial dysfunction and neurodegeneration in mice (362, 363)
Huntingtin_HD			↓				Loss of WT Huntington is pro-disease as Huntingtin KO mice have a neurodegenerative phenotype, loss of wt huntingtin causes more severe/rapid degeneration and death in HD YAC128 mouse model, and the addition of wt huntingtin to mutant HD cell lines reduces cellular toxicity. (364-366)
Valosin-containing protein_VCP			↑				Mutant VCP is associated with Paget's disease. While the levels of increased or decreased wt VCP is unknown in disease, a drosophila overepression model suggests that increased VCP would increase aggregate formation and be pro-disease (367)
Mitochondrial Complex 1 Subunit_NDUFB5			↓				Decreased mRNA levels in HD caudate (350)
Mitochondrial Complex 1 Subunit_NDUSF2			↓				Decreased mRNA levels in HD caudate (350)
Mitochondrial Complex 1 Subunit_NDUSF3			↓				Decreased mRNA levels in HD caudate (350)
Mitochondrial Complex 1 Subunit_NDUSF3			↓				Decreased mRNA levels in HD caudate (350)
Mitochondrial Complex 4 Subunit_COX7B			↓				Decreased mRNA levels in HD caudate (350)
Cyclin-dependent Kinase-5_CDK5	↓		↓				HD is Associated with decreased CDK5 protein in striatum and AD hippocampus (368, 369)

NF-kappa B_NF-kB	↑	↑	↑	↑		↑	Increased mRNA levels in ALS Spinal Cord, AD hippocampus, PD brainstem and midbrain, BPD cortex, cultured HD neurons, HD mouse model (370-374)
Manganese Superoxide dismutase_SOD2	↓			↓			Associated polymorphisms with AD; knock-down accelerates disease progression in AD and ALS mouse models (375, 376)
Cholecystokinin_CCK	↓	↓			↓		Decreased mRNA levels in SCZ, AD and PD PFC (377, 378)
Neuropeptide-Y_NPY	↓	u			↓	↓	Decreased mRNA levels in SCZ, BPD, and AD cortex (377, 379-381)
Cannabanoid Receptor-1_CB1	↓	u	↓		↓		Decreased mRNA and protein levels in SCZ PFC, decreased mRNA in HD Globus Pallidus and AD caudate, increased/decreased in PD brain (382-385)
Parvalbumin_PVALB	↓	u			↓	↓	Decreased mRNA levels in SCZ PFC, AD parahippocampal gyrus, and BPD cortex. In PD there is reports of decreased levels in globus pallidus and substantia nigra and PV is decreased in a Parkinsonian mouse model. However, there is one report of increased PV mRNA levels in PD Substantia Nigra (264, 386-391)
Glutamate decarboxylase 1_GAD67		↓			↓	↓	Decreased mRNA levels in PD globus pallidus and SCZ PFC (377, 392)
GABA transaminase_GABA-T	u				↑		Increased mRNA levels in SCZ cortex and increased/decreased AD brain (377, 393-395)
Brain-derived neurotrophic factor_BDNF	↓	↓	↓		↓	↓	Decreased mRNA levels in SCZ PFC, BPD hippocampus and decreased in mRNA & protein in multiple brain areas in AD, PD, and HD (136, 396-398)
Serotonin 2A Receptor_HTR2A	↓				↓	↓	Decreased mRNA levels in SCZ, BPD, and AD Cortex (399-402)
Serotonin 5A Receptor_HTR5A					u	u	Associated polymorphisms in SCZ and BPD-direction of mRNA levels changes have not been investigated (403, 404)
Somatostatin_SST	↓	↓	↓		↓		Decreased mRNA levels in SCZ, AD and PD Cortex and HD striatum (377, 379, 396, 405, 406)
Regulator of G-protein signaling-4_RGS4	↓		↓		↓	u	Decreased mRNA levels in SCZ and AD PFC , multiple PD brain areas, and HD Striatum (153, 407-409)
Reelin_RELN	u	u			↓	↓	Decreased mRNA levels in SCZ, BPD, PD and AD cortex (410-412)
Neuregulin-1_NRG1	u				u	u	Reports are mixed as to whether NRG1 mRNA levels are increased or decreased in SCZ and are isoform specific; NRG1 polymorphisms are associated with BPD and psychosis in AD but direction of mRNA level changes have not been investigated (413-417)
Dopamine Receptor D1_DRD1	u		↓		u	u	Decreased mRNA levels in SCZ hippocampus; linkage to DRD1 haplotypes in BPD with direction of levels changes not investigated (418, 419)
GABA receptor, alpha-5 subunit_GABRA5			↓		u	u	Decreased mRNA levels in HD caudate; associated polymorphisms with BPD and age of onset in SCZ-direction of associated levels changes have not been investigated (350, 420, 421)
Period homolog-3_PER3					u	u	Associated polymorphisms with BPD and SCZ-direction of mRNA level changes have not been investigated (422, 423)
Aryl hydrocarbon receptor nuclear translocator-like_BMAL1					u	u	Associated polymorphisms in SCZ and BPD-direction of mRNA level changes have not been investigated (422, 424)

VI. Candidate Longevity Gene SNPs

A. Rationale for candidate longevity gene snps chosen.

We chose five candidate snps in three genes for this study that are 1. likely to affect brain aging specifically, as rates of aging are known to be tissue specific, and 2. known to affect expression or function of their gene product. We have previously shown that the Serotonin Receptor 1B (htr1b) knock-out (KO) mouse is a model of anticipated molecular brain aging and reduced longevity so we sought to translate these findings using the $HTR1B_{G(861)C}$ human polymorphism which is associated with decreased gene expression in human cortex(63, 317). We chose Sirt5, a homologue of the Sirtuin family of longevity genes with increasing evidence for a role in neurodegenerative disease(54), because it displayed altered expression in $htr1b^{KO}$ mouse cortex, potentially mediating the anticipated brain age phenotype(63). No functional polymorphisms in the Sirt5 gene have been described to date. Thus, we chose the Sirt5 prom1, 2, and 3 polymorphisms for their potential to affect gene expression due to their location in a mouse-human conserved promoter region (see below for details). Lastly, we chose $Klotho_{KL\text{-}VS}$ because it alters two amino acids in this longevity gene and is associated both with human lifespan and rates of age-related memory decline(93, 98).

Figure 35. B. Figure S6. Chromosomal context of Sirt5 prom polymorphisms and there proximity to conserved and predicted promoter regions

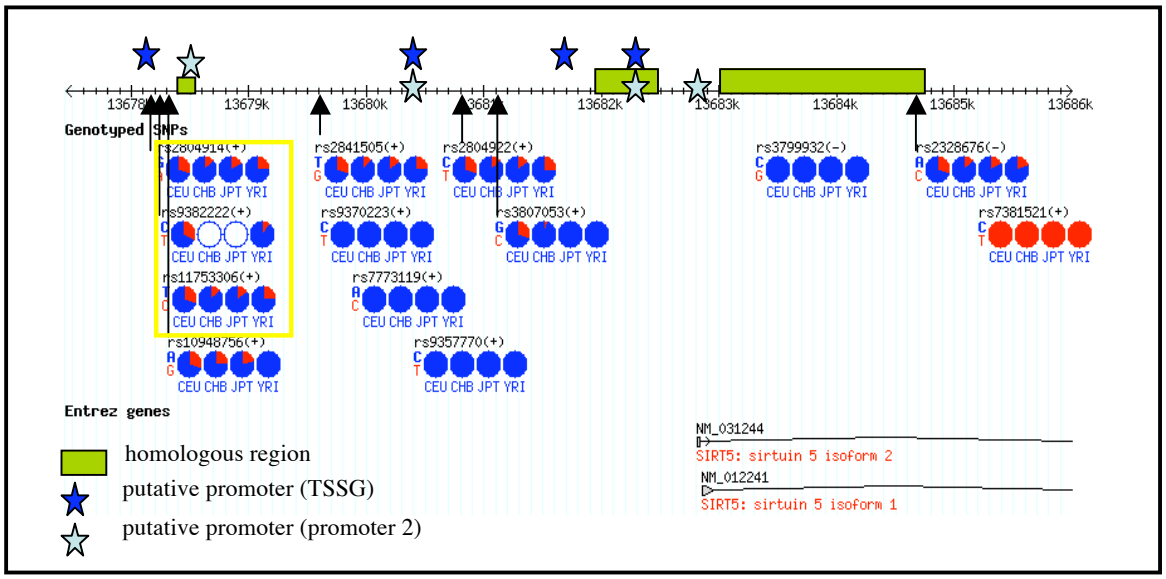

Chromosomal context of human Sirt5 including up to 5kb upstream of the start of transcription and areas of homology between mouse and human DNA (green boxes) and putative promoter regions (stars) are shown in this diagram adapted from Hapmap (www.hapmap.org). The Sirt5 prom 1, 2, and 3 snps (leftmost to rightmost) are in the yellow highlighted box. Homologous regions were determined by NCBI-blast analysis of full-length mouse and human gene sequences. For promoter prediction, the programs TSSG (recognition of human polII promoter region and start of transcription) at CGG Nucleotide Sequence Analysis (http://genomic.sanger.ac.uk/gf/gf.html) and Promoter 2.0 (http://www.cbs.dtu.dk/services/Promoter/) were used. Snp circles reflect the frequency of genotypes in four different ethnic populations for each snp. We only considered snps with at least a 25% frequency of the minor (red pie slice) allele in people of European (CEU) descent in order to retain power in our array cohort, which is predominantly of European background. We chose these three snps because of their proximity to both a putative promoter and an evolutionarily conserved region, hypothesizing that they may effect expression.

C. Snp genotyping.

HTR1B and SIRT5 genotypes were determined by direct sequencing of PCR amplified genomic DNA samples extracted from subject brain samples. The $Klotho_{KL-VS}$ minor allele creates a unique MaeIII restriction site and thus Klotho was genotyped by PCR amplification followed by restriction digest and diagnostic gel(95).

Table 20. Table S9. Candidate Longevity SNP Subject Genotypes and Comparison with Reported Frequencies.

Gene	refsnp (common name)	Allele	Allele frequencies	Hapmap(CEU)*or Ensembl** Published frequencies
HTR-1B	rs6296 (G861C)	G/G, G/C, C/C	0.44, 0.47, 0.0	0.40 , 0.52, 0.08*
SIRT5	rs2804914 (prom1)	G/G, G/A, A/A	0.44, 0.55, 0.0	0.46, 0.46, 0.09*
	rs938222 (prom2)	C/C, C/T, T/T	0.50, 0.37, 0.13	0.43, 0.46, 0.10*
	rs11753306 (prom3)	T/T, T/C, C/C	0.42, 0.58, 0.0	0.47, 0.45, 0.08*
Klotho	rs9536314 (KL-VS)	T/T, T/G, G/G	0.76, 0.24, 0.0	0.79, 0.21, 0.0 **

*Hapmap (CEU) frequencies (http://www.hapmap.org) are from a single study of 30 father-mother-son trios from a sample of Utah residents of European descent. **Ensembl database (http://ensembl.org) is another database that compiles snp frequencies which we used when Hapmap frequencies were not available for a snp.

D. Rationale for focusing on Sirt5 prom2 and not prom1 or 3.

The three Sirtuin 5 snps were in close proximity to each other and prom 1 and 3 were in almost complete linkage disequilibrium. Prom2 was in partial linkage disequilibrium with prom1 and 3. All three Sirtuin 5 snps had overlapping affected transcripts due to linkage disequilibrium between the snps. We focused exclusively on Prom2 because it had the largest number of significant transcripts associated with it and the most significant effects on molecular age. A further study with larger subject numbers would be needed to determine if prom1 or 3 interact or modify prom2 effects on molecular age.

Figure 36. E. Figure S7. Leave one out molecular ages of subjects calculated using ACC (n=4443) or AMY (n=2820) specific age-regulated genes (p<0.01)

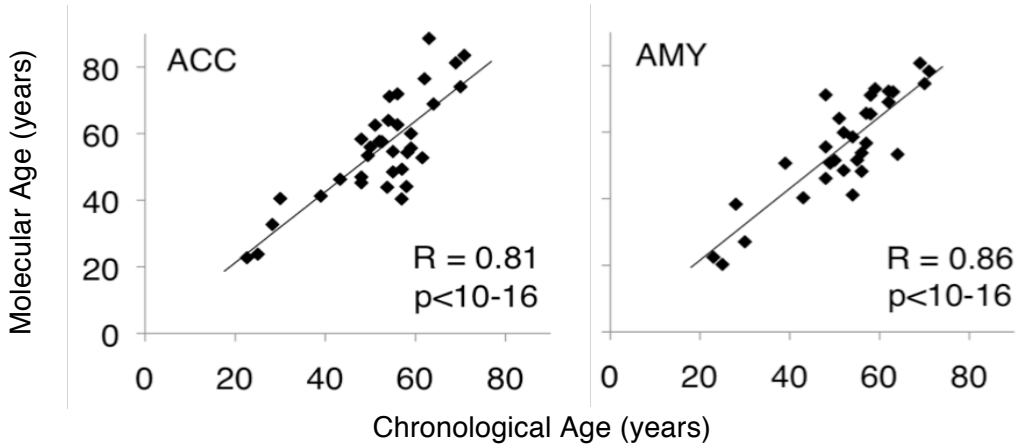

Table 21. F. Table S10. Significance of genotypic effects on molecular age in ACC and AMY

	Intersection transcripts : n in pro-aging direction/ total	Molecular Years Different (p-val)	Intersection FDR	Difference in total molecular age using all age transcripts (p-val)
ACC				
Sirt 5 prom2	227/231	CC +24 (0.0001)	19%	CC +9.1 yrs (0.004)
Klotho KL-VS	7/9	VS +11.1 (0.12)	100%	VS +0.46 (0.9)
HTR1B	18/23	GG +9.8 (0.12)	100%	GG +7.9 (0.09)
AMY				
Sirt 5 prom2	30/48	CT +2.0 (0.55)	100%	CT +2.2 (0.69)
Klotho KL-VS	38/39	VS +23.6 (0.001)	100%	VS +4.7 (0.18)
HTR1B	14/24	GG +5.3 (0.25)	100%	GG -0.6 (0.86)

Figure 35. G. Figure S8. Quantitative PCR of Sirt5 expression by $Sirt_{prom2}$ genotype in AMY. Methods for QPCR are described above in Section II. Expression differences were non- significant.

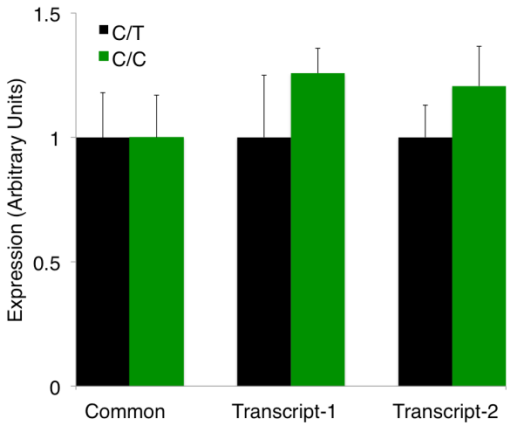

Figure 36. H. Figure S9. Ingenuity® Canonical Pathways significantly affected by $Sirt5_{prom2}$ intersection transcripts in ACC (n=231).

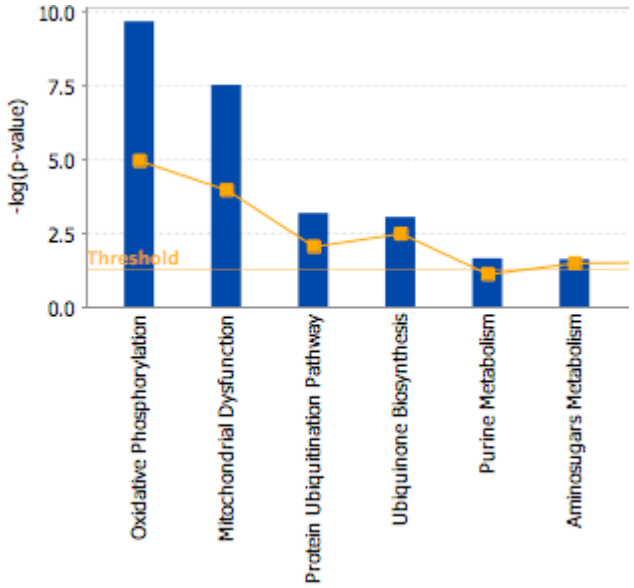

A full list of $Sirt5_{prom2}$ intersection transcripts and expression changes can be found in Supplementary dataset 4. The top 2 pathways were oxidative phosphorylation (n=15 genes) and mitochondrial dysfunction (n=13 genes).

Figure 37. I. Figure S10. Ingenuity® Functional Categories significantly affected by $Sirt5_{prom2}$ genotype.

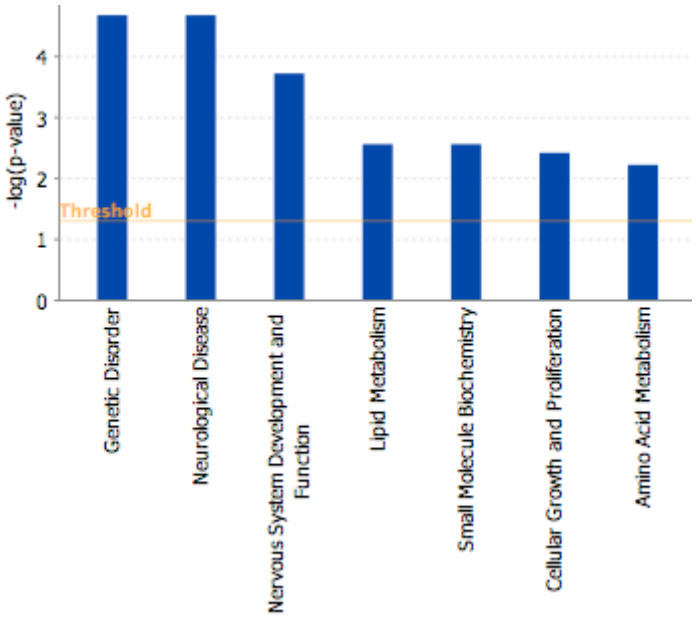

The top two neurologic disorders were related to mitochondrial dysfunction, Huntington's (n=22 genes) and Parkinson's disease (n=9 genes).

Figure 38. J. Figure S11. Huntington's and Parkinson's associated genes affected by $Sirt5_{prom2}$ genotype in ACC. Starred genes have more than one probeset represented.

Huntington's Disease (22 genes)

Parkinson's Disease (9 genes)

Table 22. K. Table S11. Table for Schematic Figure 3D- Mitochondrial Age-regulated Transcripts Effected By Sirt5 Genotype in ACC.

CC-CT (%) are the differences in average expression in age-matched groups (see Section VI-E). CC-CT (years) were calculated by averaging molecular-chronological year deviations for a gene in age-matched groups (see Section VI-E). Age expression differences and p-values were determined from age regression lines (see Section I-E). N (neuronally-enriched expression), G (Glial-enriched expression), B (expressed to similar levels in both neurons and glia) (see Section III-C for methods of determining cellular origin of transcript changes. A complete list of $Sirt5_{prom2}$ affected genes in the below format will be available for download upon publication (Supplementary dataset 4).

Probeset ID	Gene Name	Gene Symbol	CC-CT (%)	CC-CT (years)	Snp P-val	Age, 70-20(%)	Age P-val	N	G	B
210149_s_at	ATP synthase, H+ transporting, mitochondrial F0 complex, subunit d	ATP5H	-17.2	31.6	6.2E-04	-27.2	8.1E-03	1	0	0
208678_at	ATPase, H+ transporting, lysosomal 31kDa, V1 subunit E1	ATP6V1E1	-13.3	25.6	9.4E-03	-25.9	5.6E-03	0	0	1
203880_at	COX17 cytochrome c oxidase assembly homolog	COX17	-14.9	28.7	6.7E-03	-25.9	7.5E-03	0	0	1

	(S. cerevisiae)									
202698_x_at	cytochrome c oxidase subunit IV isoform 1	COX4I1	-11.9	23.4	2.3E-03	-25.4	2.0E-03	0	0	1
213735_s_at	cytochrome c oxidase subunit Vb	COX5B	-11.8	32.5	3.3E-03	-18.1	8.4E-03	0	0	1
201441_at	cytochrome c oxidase subunit Vib polypeptide 1 (ubiquitous)	COX6B1	-13.7	31.0	1.5E-03	-22.1	5.1E-03	0	0	1
202110_at	cytochrome c oxidase subunit VIIb	COX7B	-11.3	25.0	9.1E-04	-22.7	3.8E-04	1	0	0
201066_at	cytochrome c-1	CYC1	-11.3	31.3	1.4E-03	-18.1	2.2E-03	0	0	1
205012_s_at	hydroxyacylglutathione hydrolase	HAGH	-16.6	30.6	1.1E-03	-27.2	3.1E-03	1	0	0
213132_s_at	malonyl CoA:ACP acyltransferase (mitochondrial)	MCAT	-23.5	32.4	4.2E-03	-36.2	7.1E-03	1	0	0
213333_at	malate dehydrogenase 2, NAD (mitochondrial)	MDH2	-14.2	24.0	4.5E-03	-29.5	1.5E-03	1	0	0
204386_s_at	mitochondrial ribosomal protein 63	MRP63	-10.6	32.3	3.5E-03	-16.4	6.3E-03	0	0	1
224330_s_at	mitochondrial ribosomal protein L27	MRPL27	-10.8	29.8	7.6E-03	-18.1	7.1E-03	0	0	1
224331_s_at	mitochondrial ribosomal protein L36	MRPL36	-15.9	27.0	2.7E-05	-29.5	6.1E-04	0	0	1
203152_at	mitochondrial ribosomal protein L40	MRPL40	-11.4	35.1	1.4E-03	-16.2	6.4E-03	0	0	1
223480_s_at	mitochondrial ribosomal protein L47	MRPL47	-13.6	23.9	4.3E-04	-28.4	1.6E-04	0	0	1
201717_at	mitochondrial ribosomal protein L49	MRPL49	-7.2	23.4	7.6E-03	-15.4	3.9E-03	0	0	1
211595_s_at	mitochondrial ribosomal protein S11	MRPS11	-15.2	25.7	9.5E-03	-29.5	6.8E-03	0	0	1
224948_at	mitochondrial ribosomal protein S24	MRPS24	-16.6	28.2	5.7E-03	-29.5	8.6E-03	1	0	0
220688_s_at	mRNA turnover 4 homolog	MRTO4	-12.2	20.7	3.1E-03	-29.5	8.1E-04	1	0	0
218160_at	NADH dehydrogenase (ubiquinone) 1 alpha subcomplex, 8, 19kDa	NDUFA8	-13.3	25.6	7.4E-03	-25.9	1.7E-03	1	0	0
218200_s_at	NADH dehydrogenase (ubiquinone) 1 beta subcomplex, 2, 8kDa	NDUFB2	-12.5	21.1	8.8E-03	-29.5	1.2E-03	0	0	1
202839_s_at	NADH dehydrogenase (ubiquinone) 1 beta subcomplex, 7, 18kDa	NDUFB7	-13.5	27.0	3.6E-03	-25.0	3.3E-03	0	0	1
201226_at	NADH dehydrogenase (ubiquinone) 1 beta subcomplex, 8, 19kDa /// SEC31 homolog B	NDUFB8 /// SEC31B	-9.2	28.0	1.2E-03	-16.4	1.4E-03	1	0	0
201966_at	NADH dehydrogenase (ubiquinone) Fe-S protein 2, 49kDa (NADH-coenzyme Q reductase)	NDUFS2	-15.0	22.8	6.4E-03	-33.0	3.1E-03	0	0	1
218809_at	pantothenate kinase 2 (Hallervorden-Spatz syndrome)	PANK2	-16.6	25.1	7.5E-03	-33.0	1.6E-03	1	0	0
200006_at	Parkinson disease (autosomal recessive, early	DJ-1	-12.9	24.9	3.0E-03	-25.9	5.5E-04	0	0	1

	onset) 7									
209019_s_at	PTEN induced putative kinase 1	PINK-1	-18.6	31.4	1.6E-03	-29.5	7.2E-03	1	0	0
209018_s_at	PTEN induced putative kinase 1	PINK-1	-17.5	24.2	6.9E-03	-36.2	2.9E-03	1	0	0
224913_s_at	translocase of inner mitochondrial membrane 50 homolog	TIMM50	-21.0	27.8	7.2E-03	-37.7	5.2E-03	1	0	0
218357_s_at	translocase of inner mitochondrial membrane 8 homolog B	TIMM8B	-9.6	23.6	2.6E-03	-20.4	3.2E-03	0	0	1
218190_s_at	ubiquinol-cytochrome c reductase complex (7.2 kD)	UCRC	-9.4	21.2	8.4E-03	-22.1	1.2E-04	1	0	0
208909_at	ubiquinol-cytochrome c reductase, Rieske iron-sulfur polypeptide 1	UQCRFS1	-14.0	24.5	9.1E-03	-28.6	1.4E-03	1	0	0

Figure 39. L. Figure S12. QPCR validation Pink1 and DJ-1 expression differences by $Sirt5_{prom2}$ genotype.

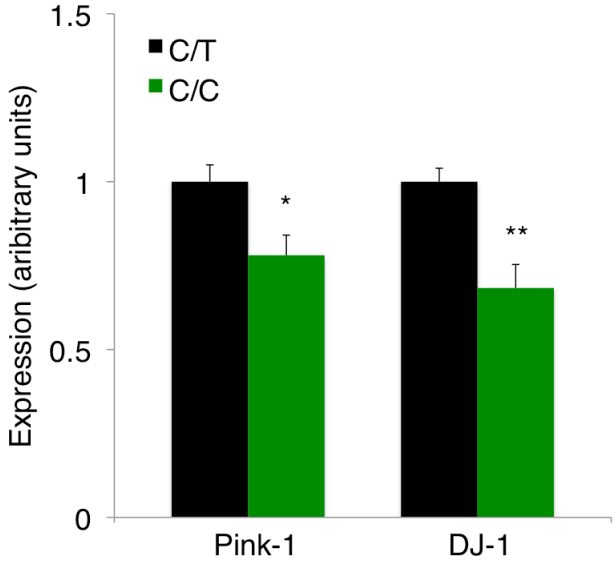

Quantitative PCR was performed as described above (Section II). Differences in expression were calculated for age-matched cohorts used to determine snp-affected transcripts (Section V-E). * denotes genotypic expression difference $p<0.05$ and ** denotes genotypic expression difference $p<0.01$

REFERENCES

1. Salthouse TA. *Adult Cognition*. Springer-Verlag: New York, 1982.

2. Salthouse TA. *Mechanisms of age-cognition relations in adulthood*. Lawrence Earlbaum Associates: Hillsdale, NJ, 1996.

3. Schaie KW. *Intellectual development in adulthood.* Cambridge University Press: Cambridge, 1996.

4. Christensen H. What cognitive changes can be expected with normal ageing? *Aust N Z J Psychiatry* 2001 Dec; **35**(6)**:** 768-775.

5. Ruffman T, Henry JD, Livingstone V, Phillips LH. A meta-analytic review of emotion recognition and aging: implications for neuropsychological models of aging. *Neurosci Biobehav Rev* 2008; **32**(4)**:** 863-881.

6. Park DC, Reuter-Lorenz P. The adaptive brain: aging and neurocognitive scaffolding. *Annu Rev Psychol* 2009; **60:** 173-196.

7. Wechsler D. *Manual for the Weschler Adult Intelligence Scale- Revised*. The Psychological Corporation: New York, 1981.

8. Kaufman AS. *Assessing adolescent and adult intelligence.* Allyn & Bacon: Boston, 1990.

9. Park DC, Lautenschlager G, Hedden T, Davidson NS, Smith AD, Smith PK. Models of visuospatial and verbal memory across the adult life span. *Psychol Aging* 2002 Jun; **17**(2)**:** 299-320.

10. Fozard JL, Vercryssen M, Reynolds SL, Hancock PA, Quilter RE. Age differences and changes in reaction time: the Baltimore Longitudinal Study of Aging. *J Gerontol* 1994 Jul; **49**(4)**:** P179-189.

11. Era P, Jokela J, Heikkinen E. Reaction and movement times in men of different ages: a population study. *Percept Mot Skills* 1986 Aug; **63**(1)**:** 111-130.

12. Kauranen K, Vanharanta H. Influences of aging, gender, and handedness on motor performance of upper and lower extremities. *Percept Mot Skills* 1996 Apr; **82**(2)**:** 515-525.

13. Volkow ND, Logan J, Fowler JS, Wang GJ, Gur RC, Wong C *et al.* Association between age-related decline in brain dopamine activity and impairment in frontal and cingulate metabolism. *Am J Psychiatry* 2000 Jan; **157**(1)**:** 75-80.

14. Volkow ND, Gur RC, Wang GJ, Fowler JS, Moberg PJ, Ding YS *et al.* Association between decline in brain dopamine activity with age and cognitive and motor impairment in healthy individuals. *Am J Psychiatry* 1998 Mar; **155**(3)**:** 344-349.

15. Mather M, Carstensen LL. Aging and motivated cognition: the positivity effect in attention and memory. *Trends Cogn Sci* 2005 Oct; **9**(10)**:** 496-502.

16. Hasin DS, Goodwin RD, Stinson FS, Grant BF. Epidemiology of major depressive disorder: results from the National Epidemiologic Survey on Alcoholism and Related Conditions. *Arch Gen Psychiatry* 2005 Oct; **62**(10)**:** 1097-1106.

17. Hawton K, van Heeringen K. Suicide. *Lancet* 2009 Apr 18; **373**(9672)**:** 1372-1381.

18. De Leo D, Padoani W, Scocco P, Lie D, Bille-Brahe U, Arensman E *et al.* Attempted and completed suicide in older subjects: results from the WHO/EURO Multicentre Study of Suicidal Behaviour. *Int J Geriatr Psychiatry* 2001 Mar; **16**(3)**:** 300-310.

19. Fiske A, Wetherell JL, Gatz M. Depression in older adults. *Annu Rev Clin Psychol* 2009; **5:** 363-389.

20. Wilson RS, Beckett LA, Barnes LL, Schneider JA, Bach J, Evans DA *et al.* Individual differences in rates of change in cognitive abilities of older persons. *Psychol Aging* 2002 Jun; **17**(2)**:** 179-193.

21. Deary IJ, Gow AJ, Taylor MD, Corley J, Brett C, Wilson V *et al.* The Lothian Birth Cohort 1936: a study to examine influences on cognitive ageing from age 11 to age 70 and beyond. *BMC Geriatr* 2007; **7:** 28.

22. Mattay VS, Goldberg TE, Sambataro F, Weinberger DR. Neurobiology of cognitive aging: insights from imaging genetics. *Biol Psychol* 2008 Sep; **79**(1)**:** 9-22.

23. Deary IJ, Whiteman MC, Pattie A, Starr JM, Hayward C, Wright AF *et al.* Cognitive change and the APOE epsilon 4 allele. *Nature* 2002 Aug 29; **418**(6901)**:** 932.

24. Anstey K, Christensen H. Education, activity, health, blood pressure and apolipoprotein E as predictors of cognitive change in old age: a review. *Gerontology* 2000 May-Jun; **46**(3)**:** 163-177.

25. Deary IJ, Wright AF, Harris SE, Whalley LJ, Starr JM. Searching for genetic influences on normal cognitive ageing. *Trends Cogn Sci* 2004 Apr; **8**(4)**:** 178-184.

26. Fillit HM, Butler RN, O'Connell AW, Albert MS, Birren JE, Cotman CW *et al.* Achieving and maintaining cognitive vitality with aging. *Mayo Clin Proc* 2002 Jul; **77**(7)**:** 681-696.

27. Joseph J, Cole G, Head E, Ingram D. Nutrition, brain aging, and neurodegeneration. *J Neurosci* 2009 Oct 14; **29**(41)**:** 12795-12801.

28. Muscari A, Giannoni C, Pierpaoli L, Berzigotti A, Maietta P, Foschi E *et al.* Chronic endurance exercise training prevents aging-related cognitive decline in healthy older adults: a randomized controlled trial. *Int J Geriatr Psychiatry* 2009 Dec 23.

29. Panza F, Solfrizzi V, Colacicco AM, D'Introno A, Capurso C, Torres F *et al.* Mediterranean diet and cognitive decline. *Public Health Nutr* 2004 Oct; **7**(7)**:** 959-963.

30. Tisserand DJ, van Boxtel MP, Pruessner JC, Hofman P, Evans AC, Jolles J. A voxel-based morphometric study to determine individual differences in gray matter density associated with age and cognitive change over time. *Cereb Cortex* 2004 Sep; **14**(9)**:** 966-973.

31. Tisserand DJ, Pruessner JC, Sanz Arigita EJ, van Boxtel MP, Evans AC, Jolles J *et al.* Regional frontal cortical volumes decrease differentially in aging: an MRI study to compare volumetric approaches and voxel-based morphometry. *Neuroimage* 2002 Oct; **17**(2)**:** 657-669.

32. Smith CD, Chebrolu H, Wekstein DR, Schmitt FA, Markesbery WR. Age and gender effects on human brain anatomy: a voxel-based morphometric study in healthy elderly. *Neurobiol Aging* 2007 Jul; **28**(7)**:** 1075-1087.

33. Good CD, Johnsrude IS, Ashburner J, Henson RN, Friston KJ, Frackowiak RS. A voxel-based morphometric study of ageing in 465 normal adult human brains. *Neuroimage* 2001 Jul; **14**(1 Pt 1)**:** 21-36.

34. Resnick SM, Pham DL, Kraut MA, Zonderman AB, Davatzikos C. Longitudinal magnetic resonance imaging studies of older adults: a shrinking brain. *J Neurosci* 2003 Apr 15; **23**(8)**:** 3295-3301.

35. Gianaros PJ, Greer PJ, Ryan CM, Jennings JR. Higher blood pressure predicts lower regional grey matter volume: Consequences on short-term information processing. *Neuroimage* 2006 Jun; **31**(2)**:** 754-765.

36. Seshadri S, Wolf PA, Beiser A, Elias MF, Au R, Kase CS *et al.* Stroke risk profile, brain volume, and cognitive function: the Framingham Offspring Study. *Neurology* 2004 Nov 9; **63**(9)**:** 1591-1599.

37. Yankner BA, Lu T, Loerch P. The aging brain. *Annu Rev Pathol* 2008; **3:** 41-66.

38. Morrison JH, Hof PR. Life and death of neurons in the aging brain. *Science* 1997 Oct 17; **278**(5337)**:** 412-419.

39. Dickstein DL, Kabaso D, Rocher AB, Luebke JI, Wearne SL, Hof PR. Changes in the structural complexity of the aged brain. *Aging Cell* 2007 Jun; **6**(3)**:** 275-284.

40. Duan H, Wearne SL, Rocher AB, Macedo A, Morrison JH, Hof PR. Age-related dendritic and spine changes in corticocortically projecting neurons in macaque monkeys. *Cereb Cortex* 2003 Sep; **13**(9)**:** 950-961.

41. Finch CE. Neurons, glia, and plasticity in normal brain aging. *Neurobiol Aging* 2003 May-Jun; **24 Suppl 1:** S123-127; discussion S131.

42. Conde JR, Streit WJ. Microglia in the aging brain. *J Neuropathol Exp Neurol* 2006 Mar; **65**(3)**:** 199-203.

43. Unger JW. Glial reaction in aging and Alzheimer's disease. *Microsc Res Tech* 1998 Oct 1; **43**(1)**:** 24-28.

44. Mattson MP, Maudsley S, Martin B. A neural signaling triumvirate that influences ageing and age-related disease: insulin/IGF-1, BDNF and serotonin. *Ageing Res Rev* 2004 Nov; **3**(4)**:** 445-464.

45. Mattson MP, Maudsley S, Martin B. BDNF and 5-HT: a dynamic duo in age-related neuronal plasticity and neurodegenerative disorders. *Trends Neurosci* 2004 Oct; **27**(10)**:** 589-594.

46. Mattson MP. Glutamate and neurotrophic factors in neuronal plasticity and disease. *Ann N Y Acad Sci* 2008 Nov; **1144:** 97-112.

47. Backman L, Nyberg L, Lindenberger U, Li SC, Farde L. The correlative triad among aging, dopamine, and cognition: current status and future prospects. *Neurosci Biobehav Rev* 2006; **30**(6)**:** 791-807.

48. Narasimhan SD, Yen K, Tissenbaum HA. Converging pathways in lifespan regulation. *Curr Biol* 2009 Aug 11; **19**(15)**:** R657-666.

49. Colman RJ, Anderson RM, Johnson SC, Kastman EK, Kosmatka KJ, Beasley TM *et al.* Caloric restriction delays disease onset and mortality in rhesus monkeys. *Science* 2009 Jul 10; **325**(5937)**:** 201-204.

50. Witte AV, Fobker M, Gellner R, Knecht S, Floel A. Caloric restriction improves memory in elderly humans. *Proc Natl Acad Sci U S A* 2009 Jan 27; **106**(4)**:** 1255-1260.

51. Papaconstantinou J. Insulin/IGF-1 and ROS signaling pathway cross-talk in aging and longevity determination. *Mol Cell Endocrinol* 2009 Feb 5; **299**(1)**:** 89-100.

52. Kurosu H, Yamamoto M, Clark JD, Pastor JV, Nandi A, Gurnani P *et al.* Suppression of aging in mice by the hormone Klotho. *Science* 2005 Sep 16; **309**(5742)**:** 1829-1833.

53. Bartke A. Long-lived Klotho mice: new insights into the roles of IGF-1 and insulin in aging. *Trends Endocrinol Metab* 2006 Mar; **17**(2)**:** 33-35.

54. Gan L, Mucke L. Paths of convergence: sirtuins in aging and neurodegeneration. *Neuron* 2008 Apr 10; **58**(1)**:** 10-14.

55. Araki T, Sasaki Y, Milbrandt J. Increased nuclear NAD biosynthesis and SIRT1 activation prevent axonal degeneration. *Science* 2004 Aug 13; **305**(5686)**:** 1010-1013.

56. Libert S, Cohen D, Guarente L. Neurogenesis directed by Sirt1. *Nat Cell Biol* 2008 Apr; **10**(4)**:** 373-374.

57. Droge W, Schipper HM. Oxidative stress and aberrant signaling in aging and cognitive decline. *Aging Cell* 2007 Jun; **6**(3)**:** 361-370.

58. Bauer JH, Poon PC, Glatt-Deeley H, Abrams JM, Helfand SL. Neuronal expression of p53 dominant-negative proteins in adult Drosophila melanogaster extends life span. *Curr Biol* 2005 Nov 22; **15**(22)**:** 2063-2068.

59. Tapia-Arancibia L, Aliaga E, Silhol M, Arancibia S. New insights into brain BDNF function in normal aging and Alzheimer disease. *Brain Res Rev* 2008 Nov; **59**(1)**:** 201-220.

60. Erraji-Benchekroun L, Underwood MD, Arango V, Galfalvy H, Pavlidis P, Smyrniotopoulos P *et al.* Molecular aging in human prefrontal cortex is selective and continuous throughout adult life. *Biol Psychiatry* 2005 Mar 1; **57**(5)**:** 549-558.

61. Rex CS, Lauterborn JC, Lin CY, Kramar EA, Rogers GA, Gall CM *et al.* Restoration of long-term potentiation in middle-aged hippocampus after induction of brain-derived neurotrophic factor. *J Neurophysiol* 2006 Aug; **96**(2)**:** 677-685.

62. Glorioso C, Sabatini M, Unger T, Hashimoto T, Monteggia LM, Lewis DA *et al.* Specificity and timing of neocortical transcriptome changes in response to BDNF gene ablation during embryogenesis or adulthood. *Mol Psychiatry* 2006 Jul; **11**(7)**:** 633-648.

63. Sibille E, Su J, Leman S, Le Guisquet AM, Ibarguen-Vargas Y, Joeyen-Waldorf J *et al.* Lack of serotonin1B receptor expression leads to age-related motor dysfunction,

early onset of brain molecular aging and reduced longevity. *Mol Psychiatry* 2007 Nov; **12**(11)**:** 1042-1056, 1975.

64. Petrascheck M, Ye X, Buck LB. An antidepressant that extends lifespan in adult Caenorhabditis elegans. *Nature* 2007 Nov 22; **450**(7169)**:** 553-556.

65. Petrascheck M, Ye X, Buck LB. A high-throughput screen for chemicals that increase the lifespan of Caenorhabditis elegans. *Ann N Y Acad Sci* 2009 Jul; **1170:** 698-701.

66. Murakami H, Bessinger K, Hellmann J, Murakami S. Manipulation of serotonin signal suppresses early phase of behavioral aging in Caenorhabditis elegans. *Neurobiol Aging* 2008 Jul; **29**(7)**:** 1093-1100.

67. Sze JY, Victor M, Loer C, Shi Y, Ruvkun G. Food and metabolic signalling defects in a Caenorhabditis elegans serotonin-synthesis mutant. *Nature* 2000 Feb 3; **403**(6769)**:** 560-564.

68. Cotzias GC, Miller ST, Tang LC, Papavasiliou PS. Levodopa, fertility, and longevity. *Science* 1977 Apr 29; **196**(4289)**:** 549-551.

69. Cotzias GC, Miller ST, Nicholson AR, Jr., Maston WH, Tang LC. Prolongation of the life-span in mice adapted to large amounts of L-dopa. *Proc Natl Acad Sci U S A* 1974 Jun; **71**(6)**:** 2466-2469.

70. Diaz-Torga G, Feierstein C, Libertun C, Gelman D, Kelly MA, Low MJ *et al.* Disruption of the D2 dopamine receptor alters GH and IGF-I secretion and causes dwarfism in male mice. *Endocrinology* 2002 Apr; **143**(4)**:** 1270-1279.

71. Backman L, Ginovart N, Dixon RA, Wahlin TB, Wahlin A, Halldin C *et al.* Age-related cognitive deficits mediated by changes in the striatal dopamine system. *Am J Psychiatry* 2000 Apr; **157**(4)**:** 635-637.

72. Luo Y, Roth GS. The roles of dopamine oxidative stress and dopamine receptor signaling in aging and age-related neurodegeneration. *Antioxid Redox Signal* 2000 Fall; **2**(3)**:** 449-460.

73. Rollo CD. Dopamine and aging: intersecting facets. *Neurochem Res* 2009 Apr; **34**(4)**:** 601-629.

74. Lu T, Pan Y, Kao SY, Li C, Kohane I, Chan J *et al.* Gene regulation and DNA damage in the ageing human brain. *Nature* 2004 Jun 24; **429**(6994)**:** 883-891.

75. Berchtold NC, Cribbs DH, Coleman PD, Rogers J, Head E, Kim R *et al.* Gene expression changes in the course of normal brain aging are sexually dimorphic. *Proc Natl Acad Sci U S A* 2008 Oct 7; **105**(40)**:** 15605-15610.

76. Egan MF, Kojima M, Callicott JH, Goldberg TE, Kolachana BS, Bertolino A *et al.* The BDNF val66met polymorphism affects activity-dependent secretion of BDNF and human memory and hippocampal function. *Cell* 2003 Jan 24; **112**(2)**:** 257-269.

77. Nemoto K, Ohnishi T, Mori T, Moriguchi Y, Hashimoto R, Asada T *et al.* The Val66Met polymorphism of the brain-derived neurotrophic factor gene affects age-related brain morphology. *Neurosci Lett* 2006 Apr 10-17; **397**(1-2)**:** 25-29.

78. Harris SE, Fox H, Wright AF, Hayward C, Starr JM, Whalley LJ *et al.* The brain-derived neurotrophic factor Val66Met polymorphism is associated with age-related change in reasoning skills. *Mol Psychiatry* 2006 May; **11**(5)**:** 505-513.

79. Sublette ME, Baca-Garcia E, Parsey RV, Oquendo MA, Rodrigues SM, Galfalvy H *et al.* Effect of BDNF val66met polymorphism on age-related amygdala volume changes in healthy subjects. *Prog Neuropsychopharmacol Biol Psychiatry* 2008 Oct 1; **32**(7)**:** 1652-1655.

80. Caspi A, Sugden K, Moffitt TE, Taylor A, Craig IW, Harrington H *et al.* Influence of life stress on depression: moderation by a polymorphism in the 5-HTT gene. *Science* 2003 Jul 18; **301**(5631)**:** 386-389.

81. O'Hara R, Schroder CM, Mahadevan R, Schatzberg AF, Lindley S, Fox S *et al.* Serotonin transporter polymorphism, memory and hippocampal volume in the elderly: association and interaction with cortisol. *Mol Psychiatry* 2007 Jun; **12**(6)**:** 544-555.

82. Gondo Y, Hirose N, Arai Y, Yamamura K, Shimizu K, Takayama M *et al.* Contribution of an affect-associated gene to human longevity: prevalence of the long-allele genotype of the serotonin transporter-linked gene in Japanese centenarians. *Mech Ageing Dev* 2005 Nov; **126**(11)**:** 1178-1184.

83. Payton A, Gibbons L, Davidson Y, Ollier W, Rabbitt P, Worthington J *et al.* Influence of serotonin transporter gene polymorphisms on cognitive decline and cognitive abilities in a nondemented elderly population. *Mol Psychiatry* 2005 Dec; **10**(12)**:** 1133-1139.

84. Reynolds CA, Jansson M, Gatz M, Pedersen NL. Longitudinal change in memory performance associated with HTR2A polymorphism. *Neurobiol Aging* 2006 Jan; **27**(1)**:** 150-154.

85. Houlihan LM, Harris SE, Luciano M, Gow AJ, Starr JM, Visscher PM *et al.* Replication study of candidate genes for cognitive abilities: the Lothian Birth Cohort 1936. *Genes Brain Behav* 2009 Mar; **8**(2)**:** 238-247.

86. Starr JM, Fox H, Harris SE, Deary IJ, Whalley LJ. COMT genotype and cognitive ability: a longitudinal aging study. *Neurosci Lett* 2007 Jun 21; **421**(1)**:** 57-61.

87. de Frias CM, Annerbrink K, Westberg L, Eriksson E, Adolfsson R, Nilsson LG. COMT gene polymorphism is associated with declarative memory in adulthood and old age. *Behav Genet* 2004 Sep; **34**(5)**:** 533-539.

88. Rowe JB, Hughes L, Williams-Gray CH, Bishop S, Fallon S, Barker RA *et al.* The val(158)met COMT polymorphism's effect on atrophy in healthy aging and Parkinson's disease. *Neurobiol Aging* 2008 Aug 26.

89. De Luca M, Rose G, Bonafe M, Garasto S, Greco V, Weir BS *et al.* Sex-specific longevity associations defined by Tyrosine Hydroxylase-Insulin-Insulin Growth Factor 2 haplotypes on the 11p15.5 chromosomal region. *Exp Gerontol* 2001 Nov; **36**(10)**:** 1663-1671.

90. Kuro-o M, Matsumura Y, Aizawa H, Kawaguchi H, Suga T, Utsugi T *et al.* Mutation of the mouse klotho gene leads to a syndrome resembling ageing. *Nature* 1997 Nov 6; **390**(6655)**:** 45-51.

91. Uchida A, Komiya Y, Tashiro T, Yorifuji H, Kishimoto T, Nabeshima Y *et al.* Neurofilaments of Klotho, the mutant mouse prematurely displaying symptoms resembling human aging. *J Neurosci Res* 2001 May 15; **64**(4)**:** 364-370.

92. Thomson PA, Harris SE, Starr JM, Whalley LJ, Porteous DJ, Deary IJ. Association between genotype at an exonic SNP in DISC1 and normal cognitive aging. *Neurosci Lett* 2005 Nov 25; **389**(1)**:** 41-45.

93. Arking DE, Krebsova A, Macek M, Sr., Macek M, Jr., Arking A, Mian IS *et al.* Association of human aging with a functional variant of klotho. *Proc Natl Acad Sci U S A* 2002 Jan 22; **99**(2)**:** 856-861.

94. Arking DE, Atzmon G, Arking A, Barzilai N, Dietz HC. Association between a functional variant of the KLOTHO gene and high-density lipoprotein cholesterol, blood pressure, stroke, and longevity. *Circ Res* 2005 Mar 4; **96**(4)**:** 412-418.

95. Arking DE, Becker DM, Yanek LR, Fallin D, Judge DP, Moy TF *et al.* KLOTHO allele status and the risk of early-onset occult coronary artery disease. *Am J Hum Genet* 2003 May; **72**(5)**:** 1154-1161.

96. Imamura A, Okumura K, Ogawa Y, Murakami R, Torigoe M, Numaguchi Y *et al.* Klotho gene polymorphism may be a genetic risk factor for atherosclerotic coronary artery disease but not for vasospastic angina in Japanese. *Clin Chim Acta* 2006 Mar 6.

97. Ogata N, Matsumura Y, Shiraki M, Kawano K, Koshizuka Y, Hosoi T *et al.* Association of klotho gene polymorphism with bone density and spondylosis of the lumbar spine in postmenopausal women. *Bone* 2002 Jul; **31**(1)**:** 37-42.

98. Deary IJ, Harris SE, Fox HC, Hayward C, Wright AF, Starr JM *et al.* KLOTHO genotype and cognitive ability in childhood and old age in the same individuals. *Neurosci Lett* 2005 Apr 11; **378**(1)**:** 22-27.

99. Bonafe M, Barbieri M, Marchegiani F, Olivieri F, Ragno E, Giampieri C *et al.* Polymorphic variants of insulin-like growth factor I (IGF-I) receptor and phosphoinositide 3-kinase genes affect IGF-I plasma levels and human longevity: cues for an evolutionarily conserved mechanism of life span control. *J Clin Endocrinol Metab* 2003 Jul; **88**(7)**:** 3299-3304.

100. Kenyon C. The plasticity of aging: insights from long-lived mutants. *Cell* 2005 Feb 25; **120**(4)**:** 449-460.

101. Flachsbart F, Caliebe A, Kleindorp R, Blanche H, von Eller-Eberstein H, Nikolaus S *et al.* Association of FOXO3A variation with human longevity confirmed in German centenarians. *Proc Natl Acad Sci U S A* 2009 Feb 24; **106**(8)**:** 2700-2705.

102. Pawlikowska L, Hu D, Huntsman S, Sung A, Chu C, Chen J *et al.* Association of common genetic variation in the insulin/IGF1 signaling pathway with human longevity. *Aging Cell* 2009 Aug; **8**(4)**:** 460-472.

103. Bonafe M, Olivieri F. Genetic polymorphism in long-lived people: cues for the presence of an insulin/IGF-pathway-dependent network affecting human longevity. *Mol Cell Endocrinol* 2009 Feb 5; **299**(1)**:** 118-123.

104. Bishop NA, Guarente L. Genetic links between diet and lifespan: shared mechanisms from yeast to humans. *Nat Rev Genet* 2007 Nov; **8**(11)**:** 835-844.

105. Finkel T, Deng CX, Mostoslavsky R. Recent progress in the biology and physiology of sirtuins. *Nature* 2009 Jul 30; **460**(7255)**:** 587-591.

106. Rose G, Dato S, Altomare K, Bellizzi D, Garasto S, Greco V *et al.* Variability of the SIRT3 gene, human silent information regulator Sir2 homologue, and survivorship in the elderly. *Exp Gerontol* 2003 Oct; **38**(10)**:** 1065-1070.

107. Bellizzi D, Rose G, Cavalcante P, Covello G, Dato S, De Rango F *et al.* A novel VNTR enhancer within the SIRT3 gene, a human homologue of SIR2, is associated with survival at oldest ages. *Genomics* 2005 Feb; **85**(2)**:** 258-263.

108. Kuningas M, Putters M, Westendorp RG, Slagboom PE, van Heemst D. SIRT1 gene, age-related diseases, and mortality: the Leiden 85-plus study. *J Gerontol A Biol Sci Med Sci* 2007 Sep; **62**(9)**:** 960-965.

109. Smith JD. Apolipoproteins and aging: emerging mechanisms. *Ageing Res Rev* 2002 Jun; **1**(3)**:** 345-365.

110. Kachiwala SJ, Harris SE, Wright AF, Hayward C, Starr JM, Whalley LJ *et al.* Genetic influences on oxidative stress and their association with normal cognitive ageing. *Neurosci Lett* 2005 Sep 30; **386**(2)**:** 116-120.

111. Berr C, Richard F, Dufouil C, Amant C, Alperovitch A, Amouyel P. Polymorphism of the prion protein is associated with cognitive impairment in the elderly: the EVA study. *Neurology* 1998 Sep; **51**(3)**:** 734-737.

112. Rujescu D, Hartmann AM, Gonnermann C, Moller HJ, Giegling I. M129V variation in the prion protein may influence cognitive performance. *Mol Psychiatry* 2003 Nov; **8**(11)**:** 937-941.

113. Nussbaum RL, Ellis CE. Alzheimer's disease and Parkinson's disease. *N Engl J Med* 2003 Apr 3; **348**(14)**:** 1356-1364.

114. Tsuang MT, Tohen M. *Textbook in Psychiatric Epidemiology*. 2 edn. Wiley: Weinheim, Germany, 2002.

115. Feher A, Juhasz A, Rimanoczy A, Kalman J, Janka Z. Association between BDNF Val66Met polymorphism and Alzheimer disease, dementia with Lewy bodies, and Pick disease. *Alzheimer Dis Assoc Disord* 2009 Jul-Sep; **23**(3)**:** 224-228.

116. Bialecka M, Kurzawski M, Klodowska-Duda G, Opala G, Tan EK, Drozdzik M. The association of functional catechol-O-methyltransferase haplotypes with risk of Parkinson's disease, levodopa treatment response, and complications. *Pharmacogenet Genomics* 2008 Sep; **18**(9)**:** 815-821.

117. Numata S, Ueno S, Iga J, Yamauchi K, Hongwei S, Ohta K *et al.* Brain-derived neurotrophic factor (BDNF) Val66Met polymorphism in schizophrenia is associated with age at onset and symptoms. *Neurosci Lett* 2006 Jun 19; **401**(1-2)**:** 1-5.

118. Qin W, Chachich M, Lane M, Roth G, Bryant M, de Cabo R *et al.* Calorie restriction attenuates Alzheimer's disease type brain amyloidosis in Squirrel monkeys (Saimiri sciureus). *J Alzheimers Dis* 2006 Dec; **10**(4)**:** 417-422.

119. Maswood N, Young J, Tilmont E, Zhang Z, Gash DM, Gerhardt GA *et al.* Caloric restriction increases neurotrophic factor levels and attenuates neurochemical and behavioral deficits in a primate model of Parkinson's disease. *Proc Natl Acad Sci U S A* 2004 Dec 28; **101**(52)**:** 18171-18176.

120. Nagahara AH, Merrill DA, Coppola G, Tsukada S, Schroeder BE, Shaked GM *et al.* Neuroprotective effects of brain-derived neurotrophic factor in rodent and primate models of Alzheimer's disease. *Nat Med* 2009 Mar; **15**(3)**:** 331-337.

121. Kim D, Nguyen MD, Dobbin MM, Fischer A, Sananbenesi F, Rodgers JT *et al.* SIRT1 deacetylase protects against neurodegeneration in models for Alzheimer's disease and amyotrophic lateral sclerosis. *EMBO J* 2007 Jul 11; **26**(13)**:** 3169-3179.

122. Masuda H, Chikuda H, Suga T, Kawaguchi H, Kuro-o M. Regulation of multiple ageing-like phenotypes by inducible klotho gene expression in klotho mutant mice. *Mech Ageing Dev* 2005 Dec; **126**(12)**:** 1274-1283.

123. Cohen E, Bieschke J, Perciavalle RM, Kelly JW, Dillin A. Opposing activities protect against age-onset proteotoxicity. *Science* 2006 Sep 15; **313**(5793)**:** 1604-1610.

124. Cohen E, Paulsson JF, Blinder P, Burstyn-Cohen T, Du D, Estepa G *et al.* Reduced IGF-1 signaling delays age-associated proteotoxicity in mice. *Cell* 2009 Dec 11; **139**(6)**:** 1157-1169.

125. Angelucci F, Brene S, Mathe AA. BDNF in schizophrenia, depression and corresponding animal models. *Mol Psychiatry* 2005 Jan 18.

126. Mody I. The GAD-given Right of Dentate Gyrus Granule Cells to Become GABAergic. *Epilepsy Curr* 2002 Sep; **2**(5)**:** 143-145.

127. Marty S, Berninger B, Carroll P, Thoenen H. GABAergic stimulation regulates the phenotype of hippocampal interneurons through the regulation of brain-derived neurotrophic factor. *Neuron* 1996 Mar; **16**(3)**:** 565-570.

128. de Lima AD, Opitz T, Voigt T. Irreversible loss of a subpopulation of cortical interneurons in the absence of glutamatergic network activity. *Eur J Neurosci* 2004 Jun; **19**(11)**:** 2931-2943.

129. Chattopadhyaya B, Di Cristo G, Higashiyama H, Knott GW, Kuhlman SJ, Welker E *et al.* Experience and activity-dependent maturation of perisomatic GABAergic innervation in primary visual cortex during a postnatal critical period. *J Neurosci* 2004 Oct 27; **24**(43)**:** 9598-9611.

130. Huang ZJ, Kirkwood A, Pizzorusso T, Porciatti V, Morales B, Bear MF *et al.* BDNF regulates the maturation of inhibition and the critical period of plasticity in mouse visual cortex. *Cell* 1999 Sep 17; **98**(6)**:** 739-755.

131. Bramham CR, Messaoudi E. BDNF function in adult synaptic plasticity: The synaptic consolidation hypothesis. *Prog Neurobiol* 2005 Aug 10.

132. Baldelli P, Novara M, Carabelli V, Hernandez-Guijo JM, Carbone E. BDNF up-regulates evoked GABAergic transmission in developing hippocampus by potentiating presynaptic N- and P/Q-type Ca2+ channels signalling. *Eur J Neurosci* 2002 Dec; **16**(12)**:** 2297-2310.

133. Markram H, Toledo-Rodriguez M, Wang Y, Gupta A, Silberberg G, Wu C. Interneurons of the neocortical inhibitory system. *Nat Rev Neurosci* 2004 Oct; **5**(10)**:** 793-807.

134. McBain CJ, Fisahn A. Interneurons unbound. *Nat Rev Neurosci* 2001 Jan; **2**(1)**:** 11-23.

135. Monteggia LM, Barrot M, Powell CM, Berton O, Galanis V, Gemelli T *et al.* Essential role of brain-derived neurotrophic factor in adult hippocampal function. *Proc Natl Acad Sci U S A* 2004 Jul 20; **101**(29)**:** 10827-10832.

136. Hashimoto T, Bergen SE, Nguyen QL, Xu B, Monteggia LM, Pierri JN *et al.* Relationship of brain-derived neurotrophic factor and its receptor TrkB to altered inhibitory prefrontal circuitry in schizophrenia. *J Neurosci* 2005 Jan 12; **25**(2)**:** 372-383.

137. Niblock MM, Brunso-Bechtold JK, Riddle DR. Laminar variation in neuronal viability and trophic dependence in neocortical slices. *J Neurosci Res* 2001 Sep 1; **65**(5)**:** 455-462.

138. Itami C, Mizuno K, Kohno T, Nakamura S. Brain-derived neurotrophic factor requirement for activity-dependent maturation of glutamatergic synapse in developing mouse somatosensory cortex. *Brain Res* 2000 Feb 28; **857**(1-2)**:** 141-150.

139. Lotto RB, Asavaritikrai P, Vali L, Price DJ. Target-derived neurotrophic factors regulate the death of developing forebrain neurons after a change in their trophic requirements. *J Neurosci* 2001 Jun 1; **21**(11)**:** 3904-3910.

140. Chen J, Kelz MB, Zeng G, Sakai N, Steffen C, Shockett PE *et al.* Transgenic animals with inducible, targeted gene expression in brain. *Mol Pharmacol* 1998 Sep; **54**(3)**:** 495-503.

141. Radomska HS, Gonzalez DA, Okuno Y, Iwasaki H, Nagy A, Akashi K *et al.* Transgenic targeting with regulatory elements of the human CD34 gene. *Blood* 2002 Dec 15; **100**(13)**:** 4410-4419.

142. Perl AK, Wert SE, Nagy A, Lobe CG, Whitsett JA. Early restriction of peripheral and proximal cell lineages during formation of the lung. *Proc Natl Acad Sci U S A* 2002 Aug 6; **99**(16)**:** 10482-10487.

143. Rios M, Fan G, Fekete C, Kelly J, Bates B, Kuehn R *et al.* Conditional deletion of brain-derived neurotrophic factor in the postnatal brain leads to obesity and hyperactivity. *Mol Endocrinol* 2001 Oct; **15**(10)**:** 1748-1757.

144. Irizarry RA, Hobbs B, Collin F, Beazer-Barclay YD, Antonellis KJ, Scherf U *et al.* Exploration, normalization, and summaries of high density oligonucleotide array probe level data. *Biostatistics* 2003 Apr; **4**(2)**:** 249-264.

145. Irizarry RA, Bolstad BM, Collin F, Cope LM, Hobbs B, Speed TP. Summaries of Affymetrix GeneChip probe level data. *Nucleic Acids Res* 2003 Feb 15; **31**(4)**:** e15.

146. Mirnics K, Pevsner J. Progress in the use of microarray technology to study the neurobiology of disease. *Nat Neurosci* 2004 May; **7**(5)**:** 434-439.

147. Unger T, Korade Z, Lazarov O, Terrano D, Sisodia SS, Mirnics K. True and false discovery in DNA microarray experiments: transcriptome changes in the hippocampus of Presenilin-1 mutant mice. *Methods* 2005; (in press.).

148. Mirnics K, Korade Z, Arion D, Lazarov O, Unger T, Macioce M *et al.* Presenilin-1-dependent transcriptome changes. *J Neurosci* 2005 Feb 9; **25**(6)**:** 1571-1578.

149. Lazarov O, Robinson J, Tang I, Korade Mirnics Z, Hairston V, Lee M-Y *et al.* Environmental enrichment reduces A-beta levels and amyloid deposition in transgenic mice. *Cell* 2005**:** in press.

150. Lepre J, Rice JJ, Tu Y, Stolovitzky G. Genes@Work: an efficient algorithm for pattern discovery and multivariate feature selection in gene expression data. *Bioinformatics* 2004 May 1; **20**(7)**:** 1033-1044.

151. Mimmack ML, Brooking J, Bahn S. Quantitative polymerase chain reaction: validation of microarray results from postmortem brain studies. *Biol Psychiatry* 2004 Feb 15; **55**(4)**:** 337-345.

152. Mirnics K, Middleton FA, Marquez A, Lewis DA, Levitt P. Molecular characterization of schizophrenia viewed by microarray analysis of gene expression in prefrontal cortex. *Neuron* 2000 Oct; **28**(1)**:** 53-67.

153. Mirnics K, Middleton FA, Stanwood GD, Lewis DA, Levitt P. Disease-specific changes in regulator of G-protein signaling 4 (RGS4) expression in schizophrenia. *Mol Psychiatry* 2001 May; **6**(3)**:** 293-301.

154. Hendry SH, Jones EG, Emson PC. Morphology, distribution, and synaptic relations of somatostatin- and neuropeptide Y-immunoreactive neurons in rat and monkey neocortex. *J Neurosci* 1984 Oct; **4**(10)**:** 2497-2517.

155. Chan-Palay V. Somatostatin immunoreactive neurons in the human hippocampus and cortex shown by immunogold/silver intensification on vibratome sections: coexistence with neuropeptide Y neurons, and effects in Alzheimer-type dementia. *J Comp Neurol* 1987 Jun 8; **260**(2)**:** 201-223.

156. Eriksdotter-Nilsson M, Meister B, Hokfelt T, Elde R, Fahrenkrug J, Frey P *et al.* Glutamic acid decarboxylase- and peptide-immunoreactive neurons in cortex cerebri following development in isolation: evidence of homotypic and disturbed patterns in intraocular grafts. *Synapse* 1987; **1**(6)**:** 539-551.

157. Gascon E, Vutskits L, Zhang H, Barral-Moran MJ, Kiss PJ, Mas C *et al.* Sequential activation of p75 and TrkB is involved in dendritic development of subventricular zone-derived neuronal progenitors in vitro. *Eur J Neurosci* 2005 Jan; **21**(1)**:** 69-80.

158. Marty S, Berzaghi Mda P, Berninger B. Neurotrophins and activity-dependent plasticity of cortical interneurons. *Trends Neurosci* 1997 May; **20**(5)**:** 198-202.

159. Marty S. Differences in the regulation of neuropeptide Y, somatostatin and parvalbumin levels in hippocampal interneurons by neuronal activity and BDNF. *Prog Brain Res* 2000; **128:** 193-202.

160. Morris BJ. Neuronal localisation of neuropeptide Y gene expression in rat brain. *J Comp Neurol* 1989 Dec 15; **290**(3)**:** 358-368.

161. McDonald AJ. Coexistence of somatostatin with neuropeptide Y, but not with cholecystokinin or vasoactive intestinal peptide, in neurons of the rat amygdala. *Brain Res* 1989 Oct 23; **500**(1-2)**:** 37-45.

162. Papadopoulos GC, Parnavelas JG, Cavanagh ME. Extensive co-existence of neuropeptides in the rat visual cortex. *Brain Res* 1987 Sep 8; **420**(1)**:** 95-99.

163. Chronwall BM, Chase TN, O'Donohue TL. Coexistence of neuropeptide Y and somatostatin in rat and human cortical and rat hypothalamic neurons. *Neurosci Lett* 1984 Dec 21; **52**(3)**:** 213-217.

164. Cotman CW, Engesser-Cesar C. Exercise enhances and protects brain function. *Exerc Sport Sci Rev* 2002 Apr; **30**(2)**:** 75-79.

165. Tong L, Shen H, Perreau VM, Balazs R, Cotman CW. Effects of exercise on gene-expression profile in the rat hippocampus. *Neurobiol Dis* 2001 Dec; **8**(6)**:** 1046-1056.

166. Walton M, Connor B, Lawlor P, Young D, Sirimanne E, Gluckman P *et al.* Neuronal death and survival in two models of hypoxic-ischemic brain damage. *Brain Res Brain Res Rev* 1999 Apr; **29**(2-3)**:** 137-168.

167. Mattson MP, Scheff SW. Endogenous neuroprotection factors and traumatic brain injury: mechanisms of action and implications for therapy. *J Neurotrauma* 1994 Feb; **11**(1)**:** 3-33.

168. Nakazawa T, Tamai M, Mori N. Brain-derived neurotrophic factor prevents axotomized retinal ganglion cell death through MAPK and PI3K signaling pathways. *Invest Ophthalmol Vis Sci* 2002 Oct; **43**(10)**:** 3319-3326.

169. Yamada K, Mizuno M, Nabeshima T. Role for brain-derived neurotrophic factor in learning and memory. *Life Sci* 2002 Jan 4; **70**(7)**:** 735-744.

170. Shieh PB, Ghosh A. Molecular mechanisms underlying activity-dependent regulation of BDNF expression. *J Neurobiol* 1999 Oct; **41**(1)**:** 127-134.

171. Black IB. Trophic regulation of synaptic plasticity. *J Neurobiol* 1999 Oct; **41**(1)**:** 108-118.

172. Zhang J, Zhang D, McQuade JS, Behbehani M, Tsien JZ, Xu M. c-fos regulates neuronal excitability and survival. *Nat Genet* 2002 Apr; **30**(4)**:** 416-420.

173. Ryser S, Massiha A, Piuz I, Schlegel W. Stimulated initiation of mitogen-activated protein kinase phosphatase-1 (MKP-1) gene transcription involves the synergistic action of multiple cis-acting elements in the proximal promoter. *Biochem J* 2004 Mar 1; **378**(Pt 2)**:** 473-484.

174. Murphy LO, MacKeigan JP, Blenis J. A network of immediate early gene products propagates subtle differences in mitogen-activated protein kinase signal amplitude and duration. *Mol Cell Biol* 2004 Jan; **24**(1)**:** 144-153.

175. Barnea A, Roberts J, Croll SD. Continuous exposure to brain-derived neurotrophic factor is required for persistent activation of TrkB receptor, the ERK signaling pathway, and the induction of neuropeptide Y production in cortical cultures. *Brain Res* 2004 Sep 10; **1020**(1-2)**:** 106-117.

176. Rakhit S, Clark CJ, O'Shaughnessy C T, Morris BJ. NMDA and BDNF induce distinct profiles of Extracellular regulated kinase (ERK), Mitogen and stress activated kinase (MSK) and Ribosomal S6 kinase (RSK) phosphorylation in cortical neurones. *Mol Pharmacol* 2004 Dec 29.

177. Spalding KL, Rush RA, Harvey AR. Target-derived and locally derived neurotrophins support retinal ganglion cell survival in the neonatal rat retina. *J Neurobiol* 2004 Sep 5; **60**(3)**:** 319-327.

178. Wetmore C, Olson L, Bean AJ. Regulation of brain-derived neurotrophic factor (BDNF) expression and release from hippocampal neurons is mediated by non-NMDA type glutamate receptors. *J Neurosci* 1994 Mar; **14**(3 Pt 2)**:** 1688-1700.

179. Bryja V, Pachernik J, Faldikova L, Krejci P, Pogue R, Nevriva I *et al.* The role of p27(Kip1) in maintaining the levels of D-type cyclins in vivo. *Biochim Biophys Acta* 2004 May 3; **1691**(2-3)**:** 105-116.

180. Morris TA, DeLorenzo RJ, Tombes RM. CaMK-II inhibition reduces cyclin D1 levels and enhances the association of p27kip1 with Cdk2 to cause G1 arrest in NIH 3T3 cells. *Exp Cell Res* 1998 May 1; **240**(2)**:** 218-227.

181. Ross ME, Risken M. MN20, a D2 cyclin found in brain, is implicated in neural differentiation. *J Neurosci* 1994 Nov; **14**(11 Pt 1)**:** 6384-6391.

182. Tamaru T, Okada M, Nakagawa H. Differential expression of D type cyclins during neuronal maturation. *Neurosci Lett* 1994 Feb 28; **168**(1-2)**:** 229-232.

183. Kabos P, Kabosova A, Neuman T. Blocking HES1 expression initiates GABAergic differentiation and induces the expression of p21(CIP1/WAF1) in human neural stem cells. *J Biol Chem* 2002 Mar 15; **277**(11)**:** 8763-8766.

184. Xie F, Raetzman LT, Siegel RE. Neuregulin induces GABAA receptor beta2 subunit expression in cultured rat cerebellar granule neurons by activating multiple signaling pathways. *J Neurochem* 2004 Sep; **90**(6)**:** 1521-1529.

185. Klugmann M, Wymond Symes C, Leichtlein CB, Klaussner BK, Dunning J, Fong D *et al.* AAV-mediated hippocampal expression of short and long Homer 1 proteins differentially affect cognition and seizure activity in adult rats. *Mol Cell Neurosci* 2005 Feb; **28**(2)**:** 347-360.

186. Feldker DE, Datson NA, Veenema AH, Proutski V, Lathouwers D, De Kloet ER *et al.* GeneChip analysis of hippocampal gene expression profiles of short- and long-attack-latency mice: technical and biological implications. *J Neurosci Res* 2003 Dec 1; **74**(5)**:** 701-716.

187. D'Adamo P, Wolfer DP, Kopp C, Tobler I, Toniolo D, Lipp HP. Mice deficient for the synaptic vesicle protein Rab3a show impaired spatial reversal learning and increased explorative activity but none of the behavioral changes shown by mice deficient for the Rab3a regulator Gdi1. *Eur J Neurosci* 2004 Apr; **19**(7)**:** 1895-1905.

188. Gonchar Y, Burkhalter A. Three distinct families of GABAergic neurons in rat visual cortex. *Cereb Cortex* 1997 Jun; **7**(4)**:** 347-358.

189. Kawaguchi Y, Kondo S. Parvalbumin, somatostatin and cholecystokinin as chemical markers for specific GABAergic interneuron types in the rat frontal cortex. *J Neurocytol* 2002 Mar-Jun; **31**(3-5)**:** 277-287.

190. Demeulemeester H, Vandesande F, Orban GA, Brandon C, Vanderhaeghen JJ. Heterogeneity of GABAergic cells in cat visual cortex. *J Neurosci* 1988 Mar; **8**(3)**:** 988-1000.

191. Alho H, Ferrarese C, Vicini S, Vaccarino F. Subsets of GABAergic neurons in dissociated cell cultures of neonatal rat cerebral cortex show co-localization with specific modulator peptides. *Brain Res* 1988 Apr 1; **467**(2)**:** 193-204.

192. Kubota Y, Kawaguchi Y. Two distinct subgroups of cholecystokinin-immunoreactive cortical interneurons. *Brain Res* 1997 Mar 28; **752**(1-2)**:** 175-183.

193. Nawa H, Bessho Y, Carnahan J, Nakanishi S, Mizuno K. Regulation of neuropeptide expression in cultured cerebral cortical neurons by brain-derived neurotrophic factor. *J Neurochem* 1993 Feb; **60**(2)**:** 772-775.

194. Mizuno K, Carnahan J, Nawa H. Brain-derived neurotrophic factor promotes differentiation of striatal GABAergic neurons. *Dev Biol* 1994 Sep; **165**(1)**:** 243-256.

195. Reibel S, Vivien-Roels B, Le BT, Larmet Y, Carnahan J, Marescaux C *et al.* Overexpression of neuropeptide Y induced by brain-derived neurotrophic factor in the rat hippocampus is long lasting. *Eur J Neurosci* 2000 Feb; **12**(2)**:** 595-605.

196. Egan MF, Weinberger DR, Lu B. Schizophrenia, III: brain-derived neurotropic factor and genetic risk. *Am J Psychiatry* 2003 Jul; **160**(7)**:** 1242.

197. Szekeres G, Juhasz A, Rimanoczy A, Keri S, Janka Z. The C270T polymorphism of the brain-derived neurotrophic factor gene is associated with schizophrenia. *Schizophr Res* 2003 Dec 1; **65**(1)**:** 15-18.

198. Krebs MO, Guillin O, Bourdell MC, Schwartz JC, Olie JP, Poirier MF *et al.* Brain derived neurotrophic factor (BDNF) gene variants association with age at onset and therapeutic response in schizophrenia. *Mol Psychiatry* 2000 Sep; **5**(5)**:** 558-562.

199. de Krom M, Bakker SC, Hendriks J, van Elburg A, Hoogendoorn M, Verduijn W *et al.* Polymorphisms in the brain-derived neurotrophic factor gene are not associated with either anorexia nervosa or schizophrenia in Dutch patients. *Psychiatr Genet* 2005 Jun; **15**(2)**:** 81.

200. Anttila S, Illi A, Kampman O, Mattila KM, Lehtimaki T, Leinonen E. Lack of association between two polymorphisms of brain-derived neurotrophic factor and response to typical neuroleptics. *J Neural Transm* 2005 Jun; **112**(7)**:** 885-890.

201. Galderisi S, Maj M, Kirkpatrick B, Piccardi P, Mucci A, Invernizzi G *et al.* COMT Val(158)Met and BDNF C(270)T polymorphisms in schizophrenia: a case-control study. *Schizophr Res* 2005 Feb 1; **73**(1)**:** 27-30.

202. Neves-Pereira M, Cheung JK, Pasdar A, Zhang F, Breen G, Yates P *et al.* BDNF gene is a risk factor for schizophrenia in a Scottish population. *Mol Psychiatry* 2005 Feb; **10**(2)**:** 208-212.

203. Takahashi M, Shirakawa O, Toyooka K, Kitamura N, Hashimoto T, Maeda K *et al.* Abnormal expression of brain-derived neurotrophic factor and its receptor in the corticolimbic system of schizophrenic patients. *Mol Psychiatry* 2000 May; **5**(3)**:** 293-300.

204. Iritani S, Niizato K, Nawa H, Ikeda K, Emson PC. Immunohistochemical study of brain-derived neurotrophic factor and its receptor, TrkB, in the hippocampal formation of schizophrenic brains. *Prog Neuropsychopharmacol Biol Psychiatry* 2003 Aug; **27**(5)**:** 801-807.

205. Weickert CS, Hyde TM, Lipska BK, Herman MM, Weinberger DR, Kleinman JE. Reduced brain-derived neurotrophic factor in prefrontal cortex of patients with schizophrenia. *Mol Psychiatry* 2003 Jun; **8**(6)**:** 592-610.

206. Weickert CS, Ligons DL, Romanczyk T, Ungaro G, Hyde TM, Herman MM *et al.* Reductions in neurotrophin receptor mRNAs in the prefrontal cortex of patients with schizophrenia. *Mol Psychiatry* 2005 Jul; **10**(7)**:** 637-650.

207. Toyooka K, Asama K, Watanabe Y, Muratake T, Takahashi M, Someya T *et al.* Decreased levels of brain-derived neurotrophic factor in serum of chronic schizophrenic patients. *Psychiatry Res* 2002 Jul 31; **110**(3)**:** 249-257.

208. Lipska BK, Khaing ZZ, Weickert CS, Weinberger DR. BDNF mRNA expression in rat hippocampus and prefrontal cortex: effects of neonatal ventral hippocampal damage and antipsychotic drugs. *Eur J Neurosci* 2001 Jul; **14**(1)**:** 135-144.

209. Ashe PC, Chlan-Fourney J, Juorio AV, Li XM. Brain-derived neurotrophic factor (BDNF) mRNA in rats with neonatal ibotenic acid lesions of the ventral hippocampus. *Brain Res* 2002 Nov 22; **956**(1)**:** 126-135.

210. Fiore M, Korf J, Antonelli A, Talamini L, Aloe L. Long-lasting effects of prenatal MAM treatment on water maze performance in rats: associations with altered brain development and neurotrophin levels. *Neurotoxicol Teratol* 2002 Mar-Apr; **24**(2)**:** 179-191.

211. Fumagalli F, Molteni R, Roceri M, Bedogni F, Santero R, Fossati C *et al.* Effect of antipsychotic drugs on brain-derived neurotrophic factor expression under reduced N-methyl-D-aspartate receptor activity. *J Neurosci Res* 2003 Jun 1; **72**(5)**:** 622-628.

212. Fumagalli F, Bedogni F, Perez J, Racagni G, Riva MA. Corticostriatal brain-derived neurotrophic factor dysregulation in adult rats following prenatal stress. *Eur J Neurosci* 2004 Sep; **20**(5)**:** 1348-1354.

213. Erdely HA, Lahti RA, Roberts RC, Vogel MW, Tamminga CA. Reduced levels of RGS4 mRNA and protein in schziophrenia. *Society for Neuroscience Online Abstract Viewer/Itinerary Planner* 2003; **2003**(Washington, DC)**:** Program No. 317.318.

214. Hashimoto T, Arion D, Unger T, Mirnics K, Lewis DA. Analysis of the GABA-related transcriptome in the prefrontal cortex of subjects with schizophrenia. *2005 Abstract Viewer/Itinerary Planner Washington, DC: Society for Neuroscience,* 2005; **2005, Online:** Program No. 675.674.

215. Chowdari KV, Mirnics K, Semwal P, Wood J, Lawrence E, Bhatia T *et al.* Association and linkage analyses of RGS4 polymorphisms in schizophrenia. *Hum Mol Genet* 2002 Jun 1; **11**(12)**:** 1373-1380.

216. Mirnics K, Middleton FA, Lewis DA, Levitt P. Analysis of complex brain disorders with gene expression microarrays: schizophrenia as a disease of the synapse. *Trends Neurosci* 2001 Aug; **24**(8)**:** 479-486.

217. Bennett GW, Ballard TM, Watson CD, Fone KC. Effect of neuropeptides on cognitive function. *Exp Gerontol* 1997 Jul-Oct; **32**(4-5)**:** 451-469.

218. Matsuoka N, Maeda N, Yamaguchi I, Satoh M. Possible involvement of brain somatostatin in the memory formation of rats and the cognitive enhancing action of FR121196 in passive avoidance task. *Brain Res* 1994 Apr 11; **642**(1-2)**:** 11-19.

219. Schettini G. Brain somatostatin: receptor-coupled transducing mechanisms and role in cognitive functions. *Pharmacol Res* 1991 Apr; **23**(3)**:** 203-215.

220. Craft S, Asthana S, Newcomer JW, Wilkinson CW, Matos IT, Baker LD *et al.* Enhancement of memory in Alzheimer disease with insulin and somatostatin, but not glucose. *Arch Gen Psychiatry* 1999 Dec; **56**(12)**:** 1135-1140.

221. Morrison JH, Rogers J, Scherr S, Benoit R, Bloom FE. Somatostatin immunoreactivity in neuritic plaques of Alzheimer's patients. *Nature* 1985 Mar 7-13; **314**(6006)**:** 90-92.

222. Davies P, Katzman R, Terry RD. Reduced somatostatin-like immunoreactivity in cerebral cortex from cases of Alzheimer disease and Alzheimer senile dementa. *Nature* 1980 Nov 20; **288**(5788)**:** 279-280.

223. Arai H, Moroji T, Kosaka K. Somatostatin and vasoactive intestinal polypeptide in postmortem brains from patients with Alzheimer-type dementia. *Neurosci Lett* 1984 Nov 23; **52**(1-2)**:** 73-78.

224. Davies P, Terry RD. Cortical somatostatin-like immunoreactivity in cases of Alzheimer's disease and senile dementia of the Alzheimer type. *Neurobiol Aging* 1981 Spring; **2**(1)**:** 9-14.

225. Savonenko A, Xu GM, Melnikova T, Morton JL, Gonzales V, Wong MP *et al.* Episodic-like memory deficits in the APPswe/PS1dE9 mouse model of Alzheimer's disease: relationships to beta-amyloid deposition and neurotransmitter abnormalities. *Neurobiol Dis* 2005 Apr; **18**(3)**:** 602-617.

226. Tong L, Balazs R, Thornton PL, Cotman CW. Beta-amyloid peptide at sublethal concentrations downregulates brain-derived neurotrophic factor functions in cultured cortical neurons. *J Neurosci* 2004 Jul 28; **24**(30)**:** 6799-6809.

227. ADEAR. FK962 - Evaluation in Mild to Moderate AD. *http://wwwalzheimersorg/clintrials/fullrecasp?PrimaryKey=197* 2005.

228. Lazarov O, Robinson J, Tang YP, Hairston IS, Korade-Mirnics Z, Lee VM *et al.* Environmental enrichment reduces Abeta levels and amyloid deposition in transgenic mice. *Cell* 2005 Mar 11; **120**(5)**:** 701-713.

229. Sowell ER, Peterson BS, Thompson PM, Welcome SE, Henkenius AL, Toga AW. Mapping cortical change across the human life span. *NatNeurosci* 2003; **6**(3)**:** 309-315.

230. Terry RD, DeTeresa R, Hansen LA. Neocortical cell counts in normal human adult aging. *AnnNeurol* 1987; **21**(6)**:** 530-539.

231. Bertoni-Freddari C, Fattoretti P, Paoloni R, Caselli U, Galeazzi L, Meier-Ruge W. Synaptic structural dynamics and aging. *Gerontology* 1996; **42**(3)**:** 170-180.

232. Pakkenberg B, Gundersen HJ. Neocortical neuron number in humans: effect of sex and age. *JComp Neurol* 1997; **384**(2)**:** 312-320.

233. Thibault O, Hadley R, Landfield PW. Elevated postsynaptic [Ca2+]i and L-type calcium channel activity in aged hippocampal neurons: relationship to impaired synaptic plasticity. *JNeurosci* 2001; **21**(24)**:** 9744-9756.

234. Davare MA, Hell JW. Increased phosphorylation of the neuronal L-type Ca2+ channel Cav1.2 during aging. *ProcNatlAcadSciUSA* 2003; **100**(26)**:** 16018-16023.

235. Verkhratsky A, Toescu EC. Calcium and neuronal ageing. *Trends Neurosci* 1998; **21**(1)**:** 2-7.

236. Lerer B, Gillon D, Lichtenberg P, Gorfine M, Gelfin Y, Shapira B. Interrelationship of age, depression, and central serotonergic function: evidence from fenfluramine challenge studies. *IntPsychogeriatr* 1996; **8**(1)**:** 83-102.

237. Mattson MP, Magnus T. Ageing and neuronal vulnerability. *Nat Rev Neurosci* 2006; **7**(4)**:** 278-294.

238. Meltzer CC, Smith G, DeKosky ST, Pollock BG, Mathis CA, Moore RY *et al.* Serotonin in aging, late-life depression, and Alzheimer's disease: the emerging role of functional imaging. *Neuropsychopharmacology* 1998; **18**(6)**:** 407-430.

239. Reynolds CF, III, Kupfer DJ. Depression and aging: a look to the future. *PsychiatrServ* 1999; **50**(9)**:** 1167-1172.

240. Carlsson A. Neurotransmitter changes in the aging brain. *DanMedBull* 1985; **32 Suppl 1:** 40-43.

241. Davidoff MS, Lolova IS. Age-related changes in serotonin-immunoreactivity in the telencephalon and diencephalon of rats. *J Hirnforsch* 1991; **32**(6)**:** 745-753.

242. Nishimura A, Ueda S, Takeuchi Y, Matsushita H, Sawada T, Kawata M. Vulnerability to aging in the rat serotonergic system. *Acta Neuropathol(Berl)* 1998; **96**(6)**:** 581-595.

243. Arango V, Ernsberger P, Marzuk PM, Chen JS, Tierney H, Stanley M *et al.* Autoradiographic demonstration of increased serotonin 5-HT2 and beta-adrenergic receptor binding sites in the brain of suicide victims. *ArchGenPsychiatry* 1990; **47**(11)**:** 1038-1047.

244. Marcusson J, Oreland L, Winblad B. Effect of age on human brain serotonin (S-1) binding sites. *JNeurochem* 1984; **43**(6)**:** 1699-1705.

245. Marcusson JO, Morgan DG, Winblad B, Finch CE. Serotonin-2 binding sites in human frontal cortex and hippocampus. Selective loss of S-2A sites with age. *Brain Res* 1984; **311**(1)**:** 51-56.

246. Bach-Mizrachi H, Underwood MD, Kassir SA, Bakalian MJ, Sibille E, Tamir H *et al.* Neuronal tryptophan hydroxylase mRNA expression in the human dorsal and median raphe nuclei: major depression and suicide. *Neuropsychopharmacology* 2006 Apr; **31**(4)**:** 814-824.

247. Meltzer CC, Smith G, Price JC, Reynolds CF, III, Mathis CA, Greer P *et al.* Reduced binding of [18F]altanserin to serotonin type 2A receptors in aging: persistence of effect after partial volume correction. *Brain Res* 1998; **813**(1)**:** 167-171.

248. Goldberg S, Smith GS, Barnes A, Ma Y, Kramer E, Robeson K *et al.* Serotonin modulation of cerebral glucose metabolism in normal aging. *Neurobiol Aging* 2004; **25**(2)**:** 167-174.

249. van Luijtelaar MG, Tonnaer JA, Steinbusch HW. Aging of the serotonergic system in the rat forebrain: an immunocytochemical and neurochemical study. *Neurobiol Aging* 1992; **13**(2)**:** 201-215.

250. David DJ, Bourin M, Hascoet M, Colombel MC, Baker GB, Jolliet P. Comparison of antidepressant activity in 4- and 40-week-old male mice in the forced swimming test: involvement of 5-HT1A and 5-HT1B receptors in old mice. *Psychopharmacology (Berl)* 2001; **153**(4)**:** 443-449.

251. Trillat AC, Malagie I, Scearce K, Pons D, Anmella MC, Jacquot C *et al.* Regulation of serotonin release in the frontal cortex and ventral hippocampus of homozygous mice lacking 5-HT1B receptors: in vivo microdialysis studies. *JNeurochem* 1997; **69**(5)**:** 2019-2025.

252. Ramboz S, Saudou F, Amara DA, Belzung C, Dierich A, LeMeur M *et al.* Behavioral characterization of mice lacking the 5-HT1B receptor. *NIDA Res Monogr* 1996; **161:** 39-57.

253. Caspi A, Moffitt TE. Gene-environment interactions in psychiatry: joining forces with neuroscience. *Nat Rev Neurosci* 2006; **7**(7)**:** 583-590.

254. Saudou F, Amara DA, Dierich A, LeMeur M, Ramboz S, Segu L *et al.* Enhanced aggressive behavior in mice lacking 5-HT1B receptor. *Science* 1994; **265**(5180)**:** 1875-1878.

255. Shippenberg TS, Hen R, He M. Region-specific enhancement of basal extracellular and cocaine-evoked dopamine levels following constitutive deletion of the Serotonin(1B) receptor. *JNeurochem* 2000; **75**(1)**:** 258-265.

256. Ase AR, Reader TA, Hen R, Riad M, Descarries L. Altered serotonin and dopamine metabolism in the CNS of serotonin 5-HT(1A) or 5-HT(1B) receptor knockout mice. *J Neurochem* 2000; **75**(6)**:** 2415-2426.

257. Joyal CC, Beaudin S, Lalonde R. Longitudinal age-related changes in motor activities and spatial orientation in CD-1 mice. *Arch Physiol Biochem* 2000; **108**(3)**:** 248-256.

258. Paxinos G, Franklin KBJ. *The mouse brain in stereotoxic coordinates*, vol. 2nd Edition. Academic Press: San Diego, CA, 2001.

259. Pavlidis P, Qin J, Arango V, Mann JJ, Sibille E. Using the gene ontology for microarray data mining: a comparison of methods and application to age effects in human prefrontal cortex. *Neurochem Res* 2004 Jun; **29**(6)**:** 1213-1222.

260. Pavlidis P, Lewis DP, Noble WS. Exploring gene expression data with class scores. *PacSympBiocomput* 2002**:** 474-485.

261. Ashburner M, Ball CA, Blake JA, Botstein D, Butler H, Cherry JM *et al.* Gene ontology: tool for the unification of biology. The Gene Ontology Consortium. *NatGenet* 2000; **25**(1)**:** 25-29.

262. Galfalvy HC, Erraji-Benchekroun L, Smyrniotopoulos P, Pavlidis P, Ellis SP, Mann JJ *et al.* Sex genes for genomic analysis in human brain: internal controls for comparison of probe level data extraction. *BMC Bioinformatics* 2003 Sep 8; **4:** 37.

263. Sibille E, Hen R. Serotonin(1A) receptors in mood disorders: a combined genetic and genomic approach. *BehavPharmacol* 2001; **12**(6-7)**:** 429-438.

264. Hashimoto T, Volk DW, Eggan SM, Mirnics K, Pierri JN, Sun Z *et al.* Gene expression deficits in a subclass of GABA neurons in the prefrontal cortex of subjects with schizophrenia. *J Neurosci* 2003 Jul 16; **23**(15)**:** 6315-6326.

265. Sibille E, Hen R. Serotonin(1A) receptors in mood disorders: a combined genetic and genomic approach. *Behav Pharmacol* 2001 Nov; **12**(6-7)**:** 429-438.

266. Buhot MC, Wolff M, Benhassine N, Costet P, Hen R, Segu L. Spatial learning in the 5-HT1B receptor knockout mouse: selective facilitation/impairment depending on the cognitive demand. *LearnMem* 2003; **10**(6)**:** 466-477.

267. Keegan A, Morecroft I, Smillie D, Hicks MN, MacLean MR. Contribution of the 5-HT(1B) receptor to hypoxia-induced pulmonary hypertension: converging evidence using 5-HT(1B)-receptor knockout mice and the 5-HT(1B/1D)-receptor antagonist GR127935. *CircRes* 2001; **89**(12)**:** 1231-1239.

268. Ciaranello RD, Tan GL, Dean R. G-protein-linked serotonin receptors in mouse kidney exhibit identical properties to 5-HT1b receptors in brain. *J Pharmacol Exp Ther* 1990; **252**(3)**:** 1347-1354.

269. Gershon MD. Review article: serotonin receptors and transporters -- roles in normal and abnormal gastrointestinal motility. *AlimentPharmacolTher* 2004; **20 Suppl 7:** 3-14.

270. Mossner R, Lesch KP. Role of serotonin in the immune system and in neuroimmune interactions. *Brain BehavImmun* 1998; **12**(4)**:** 249-271.

271. Tatar M, Bartke A, Antebi A. The endocrine regulation of aging by insulin-like signals. *Science* 2003; **299**(5611)**:** 1346-1351.

272. Suji G, Sivakami S. Glucose, glycation and aging. *Biogerontology* 2004; **5**(6)**:** 365-373.

273. Holzenberger M, Dupont J, Ducos B, Leneuve P, Geloen A, Even PC *et al.* IGF-1 receptor regulates lifespan and resistance to oxidative stress in mice. *Nature* 2003; **421**(6919)**:** 182-187.

274. Lee CK, Klopp RG, Weindruch R, Prolla TA. Gene expression profile of aging and its retardation by caloric restriction. *Science* 1999; **285**(5432)**:** 1390-1393.

275. DeVellis JS. *Neuroglia in the Aging Brain*. Humana Press: Totowa, NJ, 2002.

276. Webster MJ, Weickert CS, Herman MM, Kleinman JE. BDNF mRNA expression during postnatal development, maturation and aging of the human prefrontal cortex. *Brain ResDevBrain Res* 2002; **139**(2)**:** 139-150.

277. Hekimi S, Guarente L. Genetics and the specificity of the aging process. *Science* 2003; **299**(5611)**:** 1351-1354.

278. Fabrizio P, Gattazzo C, Battistella L, Wei M, Cheng C, McGrew K *et al.* Sir2 blocks extreme life-span extension. *Cell* 2005; **123**(4)**:** 655-667.

279. Parker JA, Arango M, Abderrahmane S, Lambert E, Tourette C, Catoire H *et al.* Resveratrol rescues mutant polyglutamine cytotoxicity in nematode and mammalian neurons. *Nat Genet* 2005; **37**(4)**:** 349-350.

280. Kujoth GC, Hiona A, Pugh TD, Someya S, Panzer K, Wohlgemuth SE *et al.* Mitochondrial DNA mutations, oxidative stress, and apoptosis in mammalian aging. *Science* 2005; **309**(5733)**:** 481-484.

281. Mounkes LC, Kozlov S, Hernandez L, Sullivan T, Stewart CL. A progeroid syndrome in mice is caused by defects in A-type lamins. *Nature* 2003; **423**(6937)**:** 298-301.

282. Trifunovic A, Wredenberg A, Falkenberg M, Spelbrink JN, Rovio AT, Bruder CE *et al.* Premature ageing in mice expressing defective mitochondrial DNA polymerase. *Nature* 2004; **429**(6990)**:** 417-423.

283. Malberg JE, Eisch AJ, Nestler EJ, Duman RS. Chronic antidepressant treatment increases neurogenesis in adult rat hippocampus. *JNeurosci* 2000; **20**(24)**:** 9104-9110.

284. Niedernhofer LJ, Garinis GA, Raams A, Lalai AS, Robinson AR, Appeldoorn E *et al.* A new progeroid syndrome reveals that genotoxic stress suppresses the somatotroph axis. *Nature* 2006; **444**(7122)**:** 1038-1043.

285. Alvarez FJ, Pearson JC, Harrington D, Dewey D, Torbeck L, Fyffe RE. Distribution of 5-hydroxytryptamine-immunoreactive boutons on alpha-motoneurons in the lumbar spinal cord of adult cats. *J Comp Neurol* 1998; **393**(1)**:** 69-83.

286. Wallis DI. 5-HT receptors involved in initiation or modulation of motor patterns: opportunities for drug development. *Trends Pharmacol Sci* 1994; **15**(8)**:** 288-292.

287. Wolkow CA, Kimura KD, Lee MS, Ruvkun G. Regulation of C. elegans life-span by insulinlike signaling in the nervous system. *Science* 2000; **290**(5489)**:** 147-150.

288. Hwangbo DS, Gershman B, Tu MP, Palmer M, Tatar M. Drosophila dFOXO controls lifespan and regulates insulin signalling in brain and fat body. *Nature* 2004; **429**(6991)**:** 562-566.

289. Sibille E, Wang Y, Joeyen-Waldorf J, Gaiteri C, Surget A, Oh S *et al.* A Molecular Signature of Depression in the Amygdala. *Am J Psychiatry* 2009 Jul 15.

290. Brickman AM, Zimmerman ME, Paul RH, Grieve SM, Tate DF, Cohen RA *et al.* Regional white matter and neuropsychological functioning across the adult lifespan. *Biol Psychiatry* 2006 Sep 1; **60**(5)**:** 444-453.

291. Benjamini Y, Hochberg, Y. Controlling the false discovery rate: A practical and powerful approach to multiple testing. *J Royal Stat Soc Series B Methodol* 1995; **57:** 289-300.

292. Oh S, Tseng GC, Sibille E. Reciprocal phylogenetic conservation of molecular aging in mouse and human brain. *Neurobiol Aging* 2009 Sep 1.

293. Lamb J, Crawford ED, Peck D, Modell JW, Blat IC, Wrobel MJ *et al.* The Connectivity Map: using gene-expression signatures to connect small molecules, genes, and disease. *Science* 2006 Sep 29; **313**(5795)**:** 1929-1935.

294. Sibille E, Wang Y, Joeyen-Waldorf J, Gaiteri C, Surget A, Oh S *et al.* A molecular signature of depression in the amygdala. *Am J Psychiatry* 2009 Sep; **166**(9)**:** 1011-1024.

295. Nakanishi K, Ida M, Suzuki H, Kitano C, Yamamoto A, Mori N *et al.* Molecular characterization of a transport vesicle protein Neurensin-2, a homologue of Neurensin-1, expressed in neural cells. *Brain Res* 2006 Apr 7; **1081**(1)**:** 1-8.

296. Sibille E, Arango V, Joeyen-Waldorf J, Wang Y, Leman S, Surget A *et al.* Large-scale estimates of cellular origins of mRNAs: enhancing the yield of transcriptome analyses. *J Neurosci Methods* 2008 Jan 30; **167**(2)**:** 198-206.

297. Nakagawa T, Lomb DJ, Haigis MC, Guarente L. SIRT5 Deacetylates carbamoyl phosphate synthetase 1 and regulates the urea cycle. *Cell* 2009 May 1; **137**(3)**:** 560-570.

298. Schapira AH. Mitochondria in the aetiology and pathogenesis of Parkinson's disease. *Lancet Neurol* 2008 Jan; **7**(1)**:** 97-109.

299. Kim S, Benguria A, Lai CY, Jazwinski SM. Modulation of life-span by histone deacetylase genes in Saccharomyces cerevisiae. *Mol Biol Cell* 1999 Oct; **10**(10)**:** 3125-3136.

300. Lin K, Hsin H, Libina N, Kenyon C. Regulation of the Caenorhabditis elegans longevity protein DAF-16 by insulin/IGF-1 and germline signaling. *Nat Genet* 2001 Jun; **28**(2)**:** 139-145.

301. Chen S, Whetstine JR, Ghosh S, Hanover JA, Gali RR, Grosu P *et al.* The conserved NAD(H)-dependent corepressor CTBP-1 regulates Caenorhabditis elegans life span. *Proc Natl Acad Sci U S A* 2009 Feb 3; **106**(5)**:** 1496-1501.

302. Kawahara TL, Michishita E, Adler AS, Damian M, Berber E, Lin M *et al.* SIRT6 links histone H3 lysine 9 deacetylation to NF-kappaB-dependent gene expression and organismal life span. *Cell* 2009 Jan 9; **136**(1)**:** 62-74.

303. Colantuoni C, Hyde TM, Mitkus S, Joseph A, Sartorius L, Aguirre C *et al.* Age-related changes in the expression of schizophrenia susceptibility genes in the human prefrontal cortex. *Brain Struct Funct* 2008 Sep; **213**(1-2)**:** 255-271.

304. Kessler RC, Berglund P, Demler O, Jin R, Koretz D, Merikangas KR *et al.* The epidemiology of major depressive disorder: results from the National Comorbidity Survey Replication (NCS-R). *JAMA* 2003; **289**(23)**:** 3095-3105.

305. Sutherland G, Mellick G, Sue C, Chan DK, Rowe D, Silburn P *et al.* A functional polymorphism in the parkin gene promoter affects the age of onset of Parkinson's disease. *Neurosci Lett* 2007 Mar 6; **414**(2)**:** 170-173.

306. Lamb J. The Connectivity Map: a new tool for biomedical research. *Nat Rev Cancer* 2007 Jan; **7**(1)**:** 54-60.

307. Kitada T, Pisani A, Porter DR, Yamaguchi H, Tscherter A, Martella G *et al.* Impaired dopamine release and synaptic plasticity in the striatum of PINK1-deficient mice. *Proc Natl Acad Sci U S A* 2007 Jul 3; **104**(27)**:** 11441-11446.

308. Gautier CA, Kitada T, Shen J. Loss of PINK1 causes mitochondrial functional defects and increased sensitivity to oxidative stress. *Proc Natl Acad Sci U S A* 2008 Aug 12; **105**(32)**:** 11364-11369.

309. Chen ZY, Jing D, Bath KG, Ieraci A, Khan T, Siao CJ *et al.* Genetic variant BDNF (Val66Met) polymorphism alters anxiety-related behavior. *Science* 2006 Oct 6; **314**(5796)**:** 140-143.

310. Apfeld J, Kenyon C. Cell nonautonomy of C. elegans daf-2 function in the regulation of diapause and life span. *Cell* 1998 Oct 16; **95**(2)**:** 199-210.

311. Mitchell ES, McDevitt RA, Neumaier JF. Adaptations in 5-HT receptor expression and function: implications for treatment of cognitive impairment in aging. *J Neurosci Res* 2009 Sep; **87**(12)**:** 2803-2811.

312. David DJ, Bourin M, Hascoet M, Colombel MC, Baker GB, Jolliet P. Comparison of antidepressant activity in 4- and 40-week-old male mice in the forced swimming test: involvement of 5-HT1A and 5-HT1B receptors in old mice. *Psychopharmacology (Berl)* 2001 Feb; **153**(4)**:** 443-449.

313. Huang YY, Oquendo MA, Friedman JM, Greenhill LL, Brodsky B, Malone KM *et al.* Substance abuse disorder and major depression are associated with the human 5-HT1B receptor gene (HTR1B) G861C polymorphism. *Neuropsychopharmacology* 2003 Jan; **28**(1)**:** 163-169.

314. Lappalainen J, Long JC, Eggert M, Ozaki N, Robin RW, Brown GL *et al.* Linkage of antisocial alcoholism to the serotonin 5-HT1B receptor gene in 2 populations. *Arch Gen Psychiatry* 1998 Nov; **55**(11)**:** 989-994.

315. Levitan RD, Kaplan AS, Masellis M, Basile VS, Walker ML, Lipson N *et al.* Polymorphism of the serotonin 5-HT1B receptor gene (HTR1B) associated with minimum lifetime body mass index in women with bulimia nervosa. *Biol Psychiatry* 2001 Oct 15; **50**(8)**:** 640-643.

316. Smoller JW, Biederman J, Arbeitman L, Doyle AE, Fagerness J, Perlis RH *et al.* Association between the 5HT1B receptor gene (HTR1B) and the inattentive subtype of ADHD. *Biol Psychiatry* 2006 Mar 1; **59**(5)**:** 460-467.

317. Huang YY, Grailhe R, Arango V, Hen R, Mann JJ. Relationship of psychopathology to the human serotonin1B genotype and receptor binding kinetics in postmortem brain tissue. *Neuropsychopharmacology* 1999 Aug; **21**(2)**:** 238-246.

318. Daitoku H, Fukamizu A. FOXO transcription factors in the regulatory networks of longevity. *J Biochem* 2007 Jun; **141**(6)**:** 769-774.

319. Dang W, Steffen KK, Perry R, Dorsey JA, Johnson FB, Shilatifard A *et al.* Histone H4 lysine 16 acetylation regulates cellular lifespan. *Nature* 2009 Jun 11; **459**(7248)**:** 802-807.

320. Zhao Y, Sun H, Lu J, Li X, Chen X, Tao D *et al.* Lifespan extension and elevated hsp gene expression in Drosophila caused by histone deacetylase inhibitors. *J Exp Biol* 2005 Feb; **208**(Pt 4)**:** 697-705.

321. Budovskaya YV, Wu K, Southworth LK, Jiang M, Tedesco P, Johnson TE *et al.* An elt-3/elt-5/elt-6 GATA transcription circuit guides aging in C. elegans. *Cell* 2008 Jul 25; **134**(2)**:** 291-303.

322. Kelly TM, Mann JJ. Validity of DSM-III-R diagnosis by psychological autopsy: a comparison with clinician ante-mortem diagnosis. *Acta Psychiatr Scand* 1996 Nov; **94**(5)**:** 337-343.

323. Sibille E, Arango V, Galfalvy HC, Pavlidis P, Erraji-Benchekroun L, Ellis SP *et al.* Gene expression profiling of depression and suicide in human prefrontal cortex. *Neuropsychopharmacology* 2004 Feb; **29**(2)**:** 351-361.

324. Hamidi M, Drevets WC, Price JL. Glial reduction in amygdala in major depressive disorder is due to oligodendrocytes. *Biol Psychiatry* 2004 Mar 15; **55**(6)**:** 563-569.

325. Johnson K, Liu L, Majdzadeh N, Chavez C, Chin PC, Morrison B *et al.* Inhibition of neuronal apoptosis by the cyclin-dependent kinase inhibitor GW8510: identification of 3' substituted indolones as a scaffold for the development of neuroprotective drugs. *J Neurochem* 2005 May; **93**(3)**:** 538-548.

326. Simpkins JW, Green PS, Gridley KE, Singh M, de Fiebre NC, Rajakumar G. Role of estrogen replacement therapy in memory enhancement and the prevention of neuronal loss associated with Alzheimer's disease. *Am J Med* 1997 Sep 22; **103**(3A)**:** 19S-25S.

327. Prehn JH, Welsch M, Backhauss C, Nuglisch J, Ausmeier F, Karkoutly C *et al.* Effects of serotonergic drugs in experimental brain ischemia: evidence for a protective role of serotonin in cerebral ischemia. *Brain Res* 1993 Dec 10; **630**(1-2)**:** 10-20.

328. Selenica ML, Jensen HS, Larsen AK, Pedersen ML, Helboe L, Leist M *et al.* Efficacy of small-molecule glycogen synthase kinase-3 inhibitors in the postnatal rat model of tau hyperphosphorylation. *Br J Pharmacol* 2007 Nov; **152**(6)**:** 959-979.

329. Jeong SH, Han XH, Hong SS, Hwang JS, Hwang JH, Lee D *et al.* Monoamine oxidase inhibitory coumarins from the aerial parts of Dictamnus albus. *Arch Pharm Res* 2006 Dec; **29**(12)**:** 1119-1124.

330. Varamini P, Javidnia K, Soltani M, Mehdipour AR, Ghaderi A. Cytotoxic Activity and Cell Cycle Analysis of Quinoline Alkaloids Isolated from Haplophyllum canaliculatum Boiss. *Planta Med* 2009 Jun 23.

331. Bedoy CA, Mobley PL. Astrocyte morphology altered by 1-(5-isoquinolinylsulfonyl) 2-methyl piperazine (H-7) and other protein kinase inhibitors. *Brain Res* 1989 Jun 26; **490**(2)**:** 243-254.

332. Kamanna VS, Kashyap ML. Nicotinic acid (niacin) receptor agonists: will they be useful therapeutic agents? *Am J Cardiol* 2007 Dec 3; **100**(11 A)**:** S53-61.

333. Romero-Navarro G, Cabrera-Valladares G, German MS, Matschinsky FM, Velazquez A, Wang J *et al.* Biotin regulation of pancreatic glucokinase and insulin in primary cultured rat islets and in biotin-deficient rats. *Endocrinology* 1999 Oct; **140**(10)**:** 4595-4600.

334. Singer GM, Geohas J. The effect of chromium picolinate and biotin supplementation on glycemic control in poorly controlled patients with type 2 diabetes mellitus: a placebo-controlled, double-blinded, randomized trial. *Diabetes Technol Ther* 2006 Dec; **8**(6)**:** 636-643.

335. Vanhaesebroeck B, Leevers SJ, Ahmadi K, Timms J, Katso R, Driscoll PC *et al.* Synthesis and function of 3-phosphorylated inositol lipids. *Annu Rev Biochem* 2001; **70:** 535-602.

336. Drummond HA, Furtado MM, Myers S, Grifoni S, Parker KA, Hoover A *et al.* ENaC proteins are required for NGF-induced neurite growth. *Am J Physiol Cell Physiol* 2006 Feb; **290**(2)**:** C404-410.

337. Xie Z, Dong Y, Maeda U, Xia W, Tanzi RE. RNA interference silencing of the adaptor molecules ShcC and Fe65 differentially affect amyloid precursor protein processing and Abeta generation. *J Biol Chem* 2007 Feb 16; **282**(7)**:** 4318-4325.

338. McLoughlin DM, Miller CC. The FE65 proteins and Alzheimer's disease. *J Neurosci Res* 2008 Mar; **86**(4)**:** 744-754.

339. Sabo SL, Lanier LM, Ikin AF, Khorkova O, Sahasrabudhe S, Greengard P *et al.* Regulation of beta-amyloid secretion by FE65, an amyloid protein precursor-binding protein. *J Biol Chem* 1999 Mar 19; **274**(12)**:** 7952-7957.

340. Hu Q, Jin LW, Starbuck MY, Martin GM. Broadly altered expression of the mRNA isoforms of FE65, a facilitator of beta amyloidogenesis, in Alzheimer cerebellum and other brain regions. *J Neurosci Res* 2000 Apr 1; **60**(1)**:** 73-86.

341. Kuan YH, Gruebl T, Soba P, Eggert S, Nesic I, Back S *et al.* PAT1a modulates intracellular transport and processing of amyloid precursor protein (APP), APLP1, and APLP2. *J Biol Chem* 2006 Dec 29; **281**(52)**:** 40114-40123.

342. Zheng P, Eastman J, Vande Pol S, Pimplikar SW. PAT1, a microtubule-interacting protein, recognizes the basolateral sorting signal of amyloid precursor protein. *Proc Natl Acad Sci U S A* 1998 Dec 8; **95**(25)**:** 14745-14750.

343. Alves da Costa C, Sunyach C, Pardossi-Piquard R, Sevalle J, Vincent B, Boyer N *et al.* Presenilin-dependent gamma-secretase-mediated control of p53-associated cell death in Alzheimer's disease. *J Neurosci* 2006 Jun 7; **26**(23)**:** 6377-6385.

344. Johnston JA, Norgren S, Ravid R, Wasco W, Winblad B, Lannfelt L *et al.* Quantification of APP and APLP2 mRNA in APOE genotyped Alzheimer's disease brains. *Brain Res Mol Brain Res* 1996 Dec 31; **43**(1-2)**:** 85-95.

345. Bertrand P, Poirier J, Oda T, Finch CE, Pasinetti GM. Association of apolipoprotein E genotype with brain levels of apolipoprotein E and apolipoprotein J (clusterin) in Alzheimer disease. *Brain Res Mol Brain Res* 1995 Oct; **33**(1)**:** 174-178.

346. May PC, Lampert-Etchells M, Johnson SA, Poirier J, Masters JN, Finch CE. Dynamics of gene expression for a hippocampal glycoprotein elevated in Alzheimer's disease and in response to experimental lesions in rat. *Neuron* 1990 Dec; **5**(6)**:** 831-839.

347. Singhrao SK, Neal JW, Morgan BP, Gasque P. Increased complement biosynthesis by microglia and complement activation on neurons in Huntington's disease. *Exp Neurol* 1999 Oct; **159**(2)**:** 362-376.

348. Grewal RP, Morgan TE, Finch CE. C1qB and clusterin mRNA increase in association with neurodegeneration in sporadic amyotrophic lateral sclerosis. *Neurosci Lett* 1999 Aug 13; **271**(1)**:** 65-67.

349. Emilsson L, Saetre P, Balciuniene J, Castensson A, Cairns N, Jazin EE. Increased monoamine oxidase messenger RNA expression levels in frontal cortex of Alzheimer's disease patients. *Neurosci Lett* 2002 Jun 21; **326**(1)**:** 56-60.

350. Hodges A, Strand AD, Aragaki AK, Kuhn A, Sengstag T, Hughes G *et al.* Regional and cellular gene expression changes in human Huntington's disease brain. *Hum Mol Genet* 2006 Mar 15; **15**(6)**:** 965-977.

351. Mandel S, Grunblatt E, Riederer P, Gerlach M, Levites Y, Youdim MB. Neuroprotective strategies in Parkinson's disease : an update on progress. *CNS Drugs* 2003; **17**(10)**:** 729-762.

352. Ekblom J, Jossan SS, Bergstrom M, Oreland L, Walum E, Aquilonius SM. Monoamine oxidase-B in astrocytes. *Glia* 1993 Jun; **8**(2)**:** 122-132.

353. Pittman AM, Fung HC, de Silva R. Untangling the tau gene association with neurodegenerative disorders. *Hum Mol Genet* 2006 Oct 15; **15 Spec No 2:** R188-195.

354. Wolfe MS. Tau mutations in neurodegenerative diseases. *J Biol Chem* 2009 Mar 6; **284**(10)**:** 6021-6025.

355. Dachsel JC, Lincoln SJ, Gonzalez J, Ross OA, Dickson DW, Farrer MJ. The ups and downs of alpha-synuclein mRNA expression. *Mov Disord* 2007 Jan 15; **22**(2)**:** 293-295.

356. Beyer K, Humbert J, Ferrer A, Lao JI, Carrato C, Lopez D *et al.* Low alpha-synuclein 126 mRNA levels in dementia with Lewy bodies and Alzheimer disease. *Neuroreport* 2006 Aug 21; **17**(12)**:** 1327-1330.

357. West AB, Maraganore D, Crook J, Lesnick T, Lockhart PJ, Wilkes KM *et al.* Functional association of the parkin gene promoter with idiopathic Parkinson's disease. *Hum Mol Genet* 2002 Oct 15; **11**(22)**:** 2787-2792.

358. Li H, Wetten S, Li L, St Jean PL, Upmanyu R, Surh L *et al.* Candidate single-nucleotide polymorphisms from a genomewide association study of Alzheimer disease. *Arch Neurol* 2008 Jan; **65**(1)**:** 45-53.

359. Rosen KM, Moussa CE, Lee HK, Kumar P, Kitada T, Qin G *et al.* Parkin reverses intracellular beta-amyloid accumulation and its negative effects on proteasome function. *J Neurosci Res* 2009 Jul 16.

360. Exner N, Treske B, Paquet D, Holmstrom K, Schiesling C, Gispert S *et al.* Loss-of-function of human PINK1 results in mitochondrial pathology and can be rescued by parkin. *J Neurosci* 2007 Nov 7; **27**(45)**:** 12413-12418.

361. Nural H, He P, Beach T, Sue L, Xia W, Shen Y. Dissembled DJ-1 high molecular weight complex in cortex mitochondria from Parkinson's disease patients. *Mol Neurodegener* 2009; **4:** 23.

362. Jones JM, Datta P, Srinivasula SM, Ji W, Gupta S, Zhang Z *et al.* Loss of Omi mitochondrial protease activity causes the neuromuscular disorder of mnd2 mutant mice. *Nature* 2003 Oct 16; **425**(6959)**:** 721-727.

363. Strauss KM, Martins LM, Plun-Favreau H, Marx FP, Kautzmann S, Berg D *et al.* Loss of function mutations in the gene encoding Omi/HtrA2 in Parkinson's disease. *Hum Mol Genet* 2005 Aug 1; **14**(15)**:** 2099-2111.

364. Ho LW, Brown R, Maxwell M, Wyttenbach A, Rubinsztein DC. Wild type Huntingtin reduces the cellular toxicity of mutant Huntingtin in mammalian cell models of Huntington's disease. *J Med Genet* 2001 Jul; **38**(7)**:** 450-452.

365. Dragatsis I, Levine MS, Zeitlin S. Inactivation of Hdh in the brain and testis results in progressive neurodegeneration and sterility in mice. *Nat Genet* 2000 Nov; **26**(3)**:** 300-306.

366. Van Raamsdonk JM, Pearson J, Rogers DA, Bissada N, Vogl AW, Hayden MR *et al.* Loss of wild-type huntingtin influences motor dysfunction and survival in the YAC128 mouse model of Huntington disease. *Hum Mol Genet* 2005 May 15; **14**(10)**:** 1379-1392.

367. Higashiyama H, Hirose F, Yamaguchi M, Inoue YH, Fujikake N, Matsukage A *et al.* Identification of ter94, Drosophila VCP, as a modulator of polyglutamine-induced neurodegeneration. *Cell Death Differ* 2002 Mar; **9**(3)**:** 264-273.

368. Anne SL, Saudou F, Humbert S. Phosphorylation of huntingtin by cyclin-dependent kinase 5 is induced by DNA damage and regulates wild-type and mutant huntingtin toxicity in neurons. *J Neurosci* 2007 Jul 4; **27**(27)**:** 7318-7328.

369. Miller JA, Oldham MC, Geschwind DH. A systems level analysis of transcriptional changes in Alzheimer's disease and normal aging. *J Neurosci* 2008 Feb 6; **28**(6)**:** 1410-1420.

370. Jiang YM, Yamamoto M, Kobayashi Y, Yoshihara T, Liang Y, Terao S *et al.* Gene expression profile of spinal motor neurons in sporadic amyotrophic lateral sclerosis. *Ann Neurol* 2005 Feb; **57**(2)**:** 236-251.

371. Terai K, Matsuo A, McGeer PL. Enhancement of immunoreactivity for NF-kappa B in the hippocampal formation and cerebral cortex of Alzheimer's disease. *Brain Res* 1996 Sep 30; **735**(1)**:** 159-168.

372. Ghosh A, Roy A, Liu X, Kordower JH, Mufson EJ, Hartley DM *et al.* Selective inhibition of NF-kappaB activation prevents dopaminergic neuronal loss in a mouse model of Parkinson's disease. *Proc Natl Acad Sci U S A* 2007 Nov 20; **104**(47)**:** 18754-18759.

373. Hunot S, Brugg B, Ricard D, Michel PP, Muriel MP, Ruberg M *et al.* Nuclear translocation of NF-kappaB is increased in dopaminergic neurons of patients with parkinson disease. *Proc Natl Acad Sci U S A* 1997 Jul 8; **94**(14)**:** 7531-7536.

374. Spiliotaki M, Salpeas V, Malitas P, Alevizos V, Moutsatsou P. Altered glucocorticoid receptor signaling cascade in lymphocytes of bipolar disorder patients. *Psychoneuroendocrinology* 2006 Jul; **31**(6)**:** 748-760.

375. Esposito L, Raber J, Kekonius L, Yan F, Yu GQ, Bien-Ly N *et al.* Reduction in mitochondrial superoxide dismutase modulates Alzheimer's disease-like pathology and accelerates the onset of behavioral changes in human amyloid precursor protein transgenic mice. *J Neurosci* 2006 May 10; **26**(19)**:** 5167-5179.

376. Muller FL, Liu Y, Jernigan A, Borchelt D, Richardson A, Van Remmen H. MnSOD deficiency has a differential effect on disease progression in two different ALS mutant mouse models. *Muscle Nerve* 2008 Sep; **38**(3)**:** 1173-1183.

377. Hashimoto T, Arion D, Unger T, Maldonado-Aviles JG, Morris HM, Volk DW *et al.* Alterations in GABA-related transcriptome in the dorsolateral prefrontal cortex of subjects with schizophrenia. *Mol Psychiatry* 2008 Feb; **13**(2)**:** 147-161.

378. Mazurek MF, Beal MF. Cholecystokinin and somatostatin in Alzheimer's disease postmortem cerebral cortex. *Neurology* 1991 May; **41**(5)**:** 716-719.

379. Beal MF, Martin JB. Neuropeptides in neurological disease. *Ann Neurol* 1986 Nov; **20**(5)**:** 547-565.

380. Kuromitsu J, Yokoi A, Kawai T, Nagasu T, Aizawa T, Haga S *et al.* Reduced neuropeptide Y mRNA levels in the frontal cortex of people with schizophrenia and bipolar disorder. *Brain Res Gene Expr Patterns* 2001 Aug; **1**(1)**:** 17-21.

381. Caberlotto L, Hurd YL. Reduced neuropeptide Y mRNA expression in the prefrontal cortex of subjects with bipolar disorder. *Neuroreport* 1999 Jun 3; **10**(8)**:** 1747-1750.

382. Eggan SM, Hashimoto T, Lewis DA. Reduced cortical cannabinoid 1 receptor messenger RNA and protein expression in schizophrenia. *Arch Gen Psychiatry* 2008 Jul; **65**(7)**:** 772-784.

383. Glass M, Dragunow M, Faull RL. The pattern of neurodegeneration in Huntington's disease: a comparative study of cannabinoid, dopamine, adenosine and GABA(A) receptor alterations in the human basal ganglia in Huntington's disease. *Neuroscience* 2000; **97**(3)**:** 505-519.

384. Maccarrone M, Battista N, Centonze D. The endocannabinoid pathway in Huntington's disease: a comparison with other neurodegenerative diseases. *Prog Neurobiol* 2007 Apr; **81**(5-6)**:** 349-379.

385. Lastres-Becker I, Cebeira M, de Ceballos ML, Zeng BY, Jenner P, Ramos JA *et al.* Increased cannabinoid CB1 receptor binding and activation of GTP-binding

proteins in the basal ganglia of patients with Parkinson's syndrome and of MPTP-treated marmosets. *Eur J Neurosci* 2001 Dec; **14**(11)**:** 1827-1832.

386. Inaguma Y, Shinohara H, Inagaki T, Kato K. Immunoreactive parvalbumin concentrations in parahippocampal gyrus decrease in patients with Alzheimer's disease. *J Neurol Sci* 1992 Jul; **110**(1-2)**:** 57-61.

387. Pantazopoulos H, Lange N, Baldessarini RJ, Berretta S. Parvalbumin neurons in the entorhinal cortex of subjects diagnosed with bipolar disorder or schizophrenia. *Biol Psychiatry* 2007 Mar 1; **61**(5)**:** 640-652.

388. Hardman CD, Halliday GM. The internal globus pallidus is affected in progressive supranuclear palsy and Parkinson's disease. *Exp Neurol* 1999 Jul; **158**(1)**:** 135-142.

389. Hardman CD, McRitchie DA, Halliday GM, Cartwright HR, Morris JG. Substantia nigra pars reticulata neurons in Parkinson's disease. *Neurodegeneration* 1996 Mar; **5**(1)**:** 49-55.

390. Muramatsu Y, Kurosaki R, Watanabe H, Michimata M, Matsubara M, Imai Y *et al.* Cerebral alterations in a MPTP-mouse model of Parkinson's disease--an immunocytochemical study. *J Neural Transm* 2003 Oct; **110**(10)**:** 1129-1144.

391. Soos J, Engelhardt JI, Siklos L, Havas L, Majtenyi K. The expression of PARP, NF-kappa B and parvalbumin is increased in Parkinson disease. *Neuroreport* 2004 Aug 6; **15**(11)**:** 1715-1718.

392. Nisbet AP, Eve DJ, Kingsbury AE, Daniel SE, Marsden CD, Lees AJ *et al.* Glutamate decarboxylase-67 messenger RNA expression in normal human basal ganglia and in Parkinson's disease. *Neuroscience* 1996 Nov; **75**(2)**:** 389-406.

393. Gluck MR, Thomas RG, Davis KL, Haroutunian V. Implications for altered glutamate and GABA metabolism in the dorsolateral prefrontal cortex of aged schizophrenic patients. *Am J Psychiatry* 2002 Jul; **159**(7)**:** 1165-1173.

394. Aoyagi T, Wada T, Nagai M, Kojima F, Harada S, Takeuchi T *et al.* Increased gamma-aminobutyrate aminotransferase activity in brain of patients with Alzheimer's disease. *Chem Pharm Bull (Tokyo)* 1990 Jun; **38**(6)**:** 1748-1749.

395. Sherif F, Gottfries CG, Alafuzoff I, Oreland L. Brain gamma-aminobutyrate aminotransferase (GABA-T) and monoamine oxidase (MAO) in patients with Alzheimer's disease. *J Neural Transm Park Dis Dement Sect* 1992; **4**(3)**:** 227-240.

396. Zuccato C, Cattaneo E. Brain-derived neurotrophic factor in neurodegenerative diseases. *Nat Rev Neurol* 2009 Jun; **5**(6)**:** 311-322.

397. de Oliveira GS, Cereser KM, Fernandes BS, Kauer-Sant'anna M, Fries GR, Stertz L *et al.* Decreased brain-derived neurotrophic factor in medicated and drug-free bipolar patients. *J Psychiatr Res* 2009 May 26.

398. Dunham JS, Deakin JF, Miyajima F, Payton A, Toro CT. Expression of hippocampal brain-derived neurotrophic factor and its receptors in Stanley consortium brains. *J Psychiatr Res* 2009 Apr 17.

399. Norton N, Owen MJ. HTR2A: association and expression studies in neuropsychiatric genetics. *Ann Med* 2005; **37**(2)**:** 121-129.

400. Lopez-Figueroa AL, Norton CS, Lopez-Figueroa MO, Armellini-Dodel D, Burke S, Akil H *et al.* Serotonin 5-HT1A, 5-HT1B, and 5-HT2A receptor mRNA expression in subjects with major depression, bipolar disorder, and schizophrenia. *Biol Psychiatry* 2004 Feb 1; **55**(3)**:** 225-233.

401. Bowen DM, Procter AW, Mann DM, Snowden JS, Esiri MM, Neary D *et al.* Imbalance of a serotonergic system in frontotemporal dementia: implication for pharmacotherapy. *Psychopharmacology (Berl)* 2008 Mar; **196**(4)**:** 603-610.

402. Lorke DE, Lu G, Cho E, Yew DT. Serotonin 5-HT2A and 5-HT6 receptors in the prefrontal cortex of Alzheimer and normal aging patients. *BMC Neurosci* 2006; **7:** 36.

403. Birkett JT, Arranz MJ, Munro J, Osbourn S, Kerwin RW, Collier DA. Association analysis of the 5-HT5A gene in depression, psychosis and antipsychotic response. *Neuroreport* 2000 Jun 26; **11**(9)**:** 2017-2020.

404. Dubertret C, Hanoun N, Ades J, Hamon M, Gorwood P. Family-based association studies between 5-HT5A receptor gene and schizophrenia. *J Psychiatr Res* 2004 Jul-Aug; **38**(4)**:** 371-376.

405. Epelbaum J, Ruberg M, Moyse E, Javoy-Agid F, Dubois B, Agid Y. Somatostatin and dementia in Parkinson's disease. *Brain Res* 1983 Nov 14; **278**(1-2)**:** 376-379.

406. Norris PJ, Waldvogel HJ, Faull RL, Love DR, Emson PC. Decreased neuronal nitric oxide synthase messenger RNA and somatostatin messenger RNA in the striatum of Huntington's disease. *Neuroscience* 1996 Jun; **72**(4)**:** 1037-1047.

407. Emilsson L, Saetre P, Jazin E. Low mRNA levels of RGS4 splice variants in Alzheimer's disease: association between a rare haplotype and decreased mRNA expression. *Synapse* 2006 Mar 1; **59**(3)**:** 173-176.

408. Zhang Y, James M, Middleton FA, Davis RL. Transcriptional analysis of multiple brain regions in Parkinson's disease supports the involvement of specific protein processing, energy metabolism, and signaling pathways, and suggests novel

disease mechanisms. *Am J Med Genet B Neuropsychiatr Genet* 2005 Aug 5; **137B**(1)**:** 5-16.

409. Kuhn A, Goldstein DR, Hodges A, Strand AD, Sengstag T, Kooperberg C *et al.* Mutant huntingtin's effects on striatal gene expression in mice recapitulate changes observed in human Huntington's disease brain and do not differ with mutant huntingtin length or wild-type huntingtin dosage. *Hum Mol Genet* 2007 Aug 1; **16**(15)**:** 1845-1861.

410. Guidotti A, Auta J, Davis JM, Di-Giorgi-Gerevini V, Dwivedi Y, Grayson DR *et al.* Decrease in reelin and glutamic acid decarboxylase67 (GAD67) expression in schizophrenia and bipolar disorder: a postmortem brain study. *Arch Gen Psychiatry* 2000 Nov; **57**(11)**:** 1061-1069.

411. Chin J, Massaro CM, Palop JJ, Thwin MT, Yu GQ, Bien-Ly N *et al.* Reelin depletion in the entorhinal cortex of human amyloid precursor protein transgenic mice and humans with Alzheimer's disease. *J Neurosci* 2007 Mar 14; **27**(11)**:** 2727-2733.

412. Botella-Lopez A, Burgaya F, Gavin R, Garcia-Ayllon MS, Gomez-Tortosa E, Pena-Casanova J *et al.* Reelin expression and glycosylation patterns are altered in Alzheimer's disease. *Proc Natl Acad Sci U S A* 2006 Apr 4; **103**(14)**:** 5573-5578.

413. Harrison PJ, Law AJ. Neuregulin 1 and schizophrenia: genetics, gene expression, and neurobiology. *Biol Psychiatry* 2006 Jul 15; **60**(2)**:** 132-140.

414. Bertram I, Bernstein HG, Lendeckel U, Bukowska A, Dobrowolny H, Keilhoff G *et al.* Immunohistochemical evidence for impaired neuregulin-1 signaling in the prefrontal cortex in schizophrenia and in unipolar depression. *Ann N Y Acad Sci* 2007 Jan; **1096:** 147-156.

415. Chong VZ, Thompson M, Beltaifa S, Webster MJ, Law AJ, Weickert CS. Elevated neuregulin-1 and ErbB4 protein in the prefrontal cortex of schizophrenic patients. *Schizophr Res* 2008 Mar; **100**(1-3)**:** 270-280.

416. Georgieva L, Dimitrova A, Ivanov D, Nikolov I, Williams NM, Grozeva D *et al.* Support for neuregulin 1 as a susceptibility gene for bipolar disorder and schizophrenia. *Biol Psychiatry* 2008 Sep 1; **64**(5)**:** 419-427.

417. Go RC, Perry RT, Wiener H, Bassett SS, Blacker D, Devlin B *et al.* Neuregulin-1 polymorphism in late onset Alzheimer's disease families with psychoses. *Am J Med Genet B Neuropsychiatr Genet* 2005 Nov 5; **139B**(1)**:** 28-32.

418. Pantazopoulos H, Stone D, Walsh J, Benes FM. Differences in the cellular distribution of D1 receptor mRNA in the hippocampus of bipolars and schizophrenics. *Synapse* 2004 Dec 1; **54**(3)**:** 147-155.

419. Ni X, Trakalo JM, Mundo E, Macciardi FM, Parikh S, Lee L *et al.* Linkage disequilibrium between dopamine D1 receptor gene (DRD1) and bipolar disorder. *Biol Psychiatry* 2002 Dec 15; **52**(12)**:** 1144-1150.

420. Craddock N, Jones L, Jones IR, Kirov G, Green EK, Grozeva D *et al.* Strong genetic evidence for a selective influence of GABA(A) receptors on a component of the bipolar disorder phenotype. *Mol Psychiatry* 2008 Jul 1.

421. Papadimitriou G, Dikeos D, Daskalopoulou E, Karadima G, Avramopoulos D, Contis C *et al.* Association between GABA-A receptor alpha 5 subunit gene locus and schizophrenia of a later age of onset. *Neuropsychobiology* 2001; **43**(3)**:** 141-144.

422. Mansour HA, Wood J, Logue T, Chowdari KV, Dayal M, Kupfer DJ *et al.* Association study of eight circadian genes with bipolar I disorder, schizoaffective disorder and schizophrenia. *Genes Brain Behav* 2006 Mar; **5**(2)**:** 150-157.

423. Benedetti F, Dallaspezia S, Colombo C, Pirovano A, Marino E, Smeraldi E. A length polymorphism in the circadian clock gene Per3 influences age at onset of bipolar disorder. *Neurosci Lett* 2008 Nov 14; **445**(2)**:** 184-187.

424. Le-Niculescu H, Patel SD, Bhat M, Kuczenski R, Faraone SV, Tsuang MT *et al.* Convergent functional genomics of genome-wide association data for bipolar disorder: comprehensive identification of candidate genes, pathways and mechanisms. *Am J Med Genet B Neuropsychiatr Genet* 2009 Mar 5; **150B**(2)**:** 155-181.